A Thesis submitted to The University of London for the degree of
Doctor of Philosophy

Expression Studies of Recombinant cAMP-specific Phosphodiesterase Type 4

Nadia Korniotis
School of Pharmacy
Department of Pharmaceutical and Biological Chemistry
29/ 39 Brunswick Square
London

January 2003

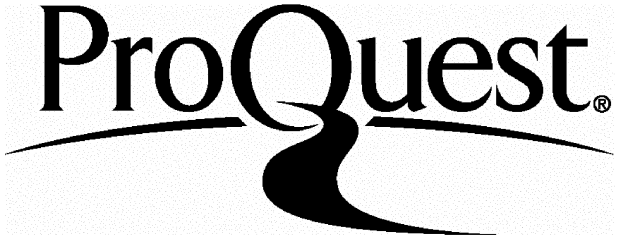

University of London

Abstract

Expression Studies of Recombinant cAMP-specific Phosphodiesterase Type 4

By Nadia Korniotis

Cyclic nucleotides (cAMP and cGMP) are second messenger molecules that play a key role in many physiological processes, cAMP in particular regulates cell growth, cell differentiation, inflammation and glycogen metabolism. cAMP is degraded by phosphodiesterase 3 (PDE3) and phosphodiesterase 4 (PDE4) which belong to a large family of PDEs consisting of 12 members. PDE4 isoenzymes which are highly specific for cAMP are most abundant in inflammatory cells making them good clinical targets for the therapy of asthma and other inflammatory disorders. The design of potential therapeutics will be helped by the structural analysis of PDE4.

To date, there have been limited reports on expression systems capable of producing milligram quantities of full length PDE4. This has been due to the protein's paucity and susceptibility to proteolysis. Although, the catalytic domain of PDE4 has been recently analysed by X-ray crystallography (Xu *et al.*, 2000), information regarding the regulation of the enzyme by its N-terminal regulatory domain and the binding of rolipram a PDE4 specific inhibitor is still poorly understood. Therefore, the main objective of this work was to establish a suitable expression system capable of expressing full length cAMP-specific phosphodiesterase 4 in quantities necessary to crystallise and analyze by X-ray crystallography. To achieve this objective Met^{26}RD1 clone (Shakur *et al.*, 1993) supplied by Professor Miles Houslay was used. This clone consisted of *rat brain cAMP-specific phosphodiesterase 4* gene which was cloned originally using *Drosophila dunce* gene as a probe hence the name RD1 (rat dunce 1). The *PDE4* gene consisted of both regulatory and catalytic domains but was missing the first 25 amino acids hence the name Met^{26} which helped solubilisation and prevented membrane attachment.

PDE gene *Met[26]RD1* was cloned and expressed in two systems, bacterial and mammalian. The bacterial system expressed Met[26]RD1 as a Glutathione S-transferase fusion protein in *Escherichia coli*. A substantial portion of phosphodiesterase expressed in bacteria was found to be inactive, insoluble and very highly degraded by proteolytic enzymes. Consequently, PDE4 expression in other systems was investigated. However, the insoluble protein produced was solubilised in urea and used to raise antibodies in rabbits as there were no commercial antibodies available against this protein.

Phosphodiesterase was also expressed in mammalian cells using Semliki Forest Virus (SFV) system. SFV system parameters were optimised for BHK-21 cells using *β-galactosidase* gene due to the ease in which cells expressing this gene could be assayed and analysed *in-situ* compared to cells expressing the *Met[26]RD1* gene. Semliki Forest viral particles carrying Met[26]RD1 mRNA were produced by co-transfection of BHK-21 cells with pSFV-1Met [26]RD1 mRNA and packaging-deficient helper RNA molecules at a ratio of 1:1. Met[26]RD1 was expressed by infecting BHK-21 cells with the recombinant virus at a multiplicity of infection of 0.5-1. This produced approximately 0.1-0.3 mg of Met[26]RD1 protein per 10^7 cells (75-90 ml) with K_m of 7.9 ± 0.86 μM and IC_{50} of 0.7 μM to rolipram (PDE4 selective inhibitor) consistent with previously published data for Met[26]RD1 (Shakur *et al.*, 1993). Preliminary purification strategy to purify Met[26]RD1 protein was developed using immunoaffinity column prepared from the antibody produced against the bacterial expressed Met[26]RD1 protein.

Acknowledgment

The work described here would not be made possible without the help and support of many people. However, my principle debt goes to my husband who showed me support, help and encouragement throughout the project and without whom this work would not be possible or worth doing.

I would like to thank my supervisor Dr Andy Wilderspin for giving me the chance to accomplish such an achievement and for providing me enough supervision and guidance to keep me on the right track.

Many thanks go to the many people that I had the opportunity of meeting over the last four years at the School of Pharmacy. In particular I wish to thank Pedro Baptisa, Bela Chopra, Liz Khatri and Seema Sharma for making the School of Pharmacy a happy and enjoyable environment to work in. My special thanks go to Lynda Hawkins for her technical help and support, to Jurgen for his assistance with DNA sequencing, and to Colin James for his computing expertise. I must also thank Kieran Brickley and Paul Chazot for their help and technical support with antibody production. To my colleagues, Adi Moloudi and Ravinda Sidhu go my best thanks for their help and support in the lab. and to whom I wish all the best for the future.

A word to my financial sponsors the BBSRC and to the Registrar Peggy Stone for her support and backing during the loss of my mother-in-law a year ago.... THANK YOU.

I would like to thank my current employers at GlaxoSmithKline and my future employer Novartis Institute of Medical Sciences for their help, support and patience through the past six months and through the coming months.

Finally I would like to thank my family for their encouragement and my cats Ebony and Ivory for keeping me sane throughout the duration of the writing period.

List of Abbreviations

~	Approximately
α	Alpha
Akt	Protein Kinase B
APC	Antigen presenting cells
APS	Ammonium persulphate
ATP	Adenosine triphosphate
β	Beta
β-gal	β-galactosidase
BHK	Baby hamster kidney
bp	Base pair
BSA	Bovine serum albumin
Ca^{2+}	Calcium ion
CaM	Calmodulin
cAMP	Cyclic adenosine 3', 5'-monophospate
cDNA	Complementary DNA
cGMP	Cyclic guanosine 3', 5'-monophosphate
CHO	Chinese hamster ovary
Chr	Chromosome
cpm	Counts per minute
C-terminal	Free carboxyl group of a protein
CREB	cAMP response element-binding protein
CRE	cAMP-response element
°C	Degrees centigrade
Da	Dalton
DAB	3', 3'-Diaminobenizine
DAG	Diacylglycerol
DNA	Deoxyribose nucleic acid
dATP	Deoxyadenosine triphosphate
dCTP	Deoxycytosine triphosphate
DEAE	Diethylaminoethyl-

DEPC	Diethyl pyrocarbonate
dGTP	Deoxyguanosine triphosphate
dhfr	dihydrofolate reductase
DMF	Dimethylformamide
DMSO	Dimethylsulphoxide
DMP	Dimethyl pimelimidate
dNTP	Deoxynucleotide triphosphate
DTT	Dithiothreitol
E. coli	*Escherichia coli*
EDTA	Ethylenediaminotetraacetic acid
EtBr	Ethidium bromide
ERK	Extracellular-signal-regulated kinase
Fab	Fragment antigen binding
Fc	Antibody fragment that is most readily crystallised
fmole	Femtomole, multiple of 10^{-15}
γ	Gamma
g	Gram
g	Acceleration due to gravity
GAF	cGMP-specific phophodiesterases, cyanobacterial *Anabaena* adenylyl cyclases, and *Escherichia coli* transcriptional regulator fh1A
GDP	Guanosine 5'-diphosphate
G_i	Inhibiting G-proteins
GMEM	Glasgow Minimal Essential Media
G_s	Activating G-proteins
GST	Glutathione S-Transferase
GTP	Guanosine 5'-triphosphate
H	Helix
^3H	Tritium
h	Hour
HBSS	Hanks' balanced salts
[^{3}H]-cAMP	Tritiated cyclic adenosine monophosphate
HCl	Hydrochloric acid

HRP	Horse Radish Peroxidase
HSL	Hormone-sensitive lipase
IBMX	3-isobutyl-1-methylxanthine
IgG	Immunoglobulin G
IL-2	Interleukin 2
IP3	Inositol triphosphate
IPTG	Isopropyl-β-D-thiogalactopyranoside
IRS-1	Insulin receptor substrate-1
kb or Kb	Kilobase pairs
kDa or KDa	KiloDalton
K_m	Michaelis-Menten constant
<	Less than
L	Litre
Lac Z	Reporter gene that encodes for β-galactosidase protein
LB	Luria-Bertani
LBA	Luria-Bertani Agar
M	Molar, moles per litre
mA	Milliamps
Me^{2+}	Divalent metal ion
MCS	Multiple cloning site
Mg^{2+}	Magnesium ion
µg	Microgram
ml	Millilitre
µl	Microlitre
µM	Micromolar
µmole	Micromole, multiple of 10^{-6}
MOPS	3-(N-Marpholino) propane sulphonic acid
mRNA	Messenger RNA
ng	Nanogramme
nm	Nanomitre
nmole	Nanomole, multiple of 10^{-9}
NO	Nitric oxide
NP-40	Nonidet P-40

N-terminal	Free α-amino group of a protein
OD	Optical density
ON or O/N	Overnight
Pi	Inorganic phosphate
PAGE	Polyacrylamide gel electrophoresis
PBS	Phosphate buffered saline
PDE	Phosphodiesterase
PEST	Proline, Glutamic acid, Serine, and Threonine amino acid sequence
pH	$-\log_{10}[H^+]$
PKA	Protein Kinase A
pKa	Dissociation constant, $-\log_{10}Ka$
PMSF	Phenylmethylsulphonylfluoride
PCR	Polymerase chain reaction
pmole	Picomole, multiple of 10^{-12}
RD1	Rat dunce 1
RNA	Ribonucleic acid
RNase A	Ribonuclease A
RNasin	Ribonuclease inhibitor
rNTP	Ribosomal nucleotide triphosphate
rpm	Revolutions per minute
SDS	Sodium dodecyl sulphate
SFV	Semliki forest virus
SH3	Src homology 3
Sj26	*Schistosoma japonicum* 26
SV	Sindbis virus
x	Times
TAE	Tris, Acetic acid, EDTA buffer
TEMED	N,N,N',N'-tetramethyethylethylenediamine
TLCK	Tosyllysine chloromethyl ketone
TPCK	Tosylphenylalanine chloromethyl ketone
Tris	Tris-(hydroxymethyl)amino-methane
Triton X-100	Triton X-100 (iso-octylphenoxy {poly} ethaxyethand,

	where 'poly' averages 10 ethaxyethenol moieties
TS	Tris saline buffer
V	Volt
V_H	Variable heavy chain
V_L	Variable light chain
V_{max}	Maximum velocity
vs	Versus
UCR	Upstream Conserved Region
UV	Ultraviolet light
(v/v)	Volume per volume
(w/v)	Weight per volume
X-gal	5-bromo-4-chloro-3-indolyl-β-D-galactopyranoside
Zn^{2+}	Zinc ion

Amino Acids and Their Symbols

Ala	Alanine
Cys	Cysteine
Asp	Aspartic acid
Glu	Glutamic acid
Phe	Phenylalanine
Gly	Glycine
His	Histidine
Ile	Isoleucine
Lys	Lysine
Leu	Leucine
Met	Methionine
Asn	Asparagine
Pro	Proline
Gln	Glutamine
Arg	Arginine
Ser	Serine
Thr	Threonine
Val	Valine
Trp	Tryptophan
Tyr	Tyrosine

Dedicated to my mother-in-law Chrissy Korniotis who sadly is not with us anymore and to my husband who believed in me

Table of Contents

List of Tables and Figures

Chapter 1

Chapter 2

Chapter 3

Chapter 4

Chapter 5

Chapter 6

Chapter 1

General Introduction

1.1 Intracellular Messenger Signalling Systems

Elaborate signalling systems have evolved in higher eukaryotes to enable cells to communicate with one another, so as to co-ordinate and control their behavior for the benefit of the whole organism. The importance of such systems has been apparent when these mechanisms fail, resulting in many serious diseases such as cancer.

Intracellular messages could be split into the following categories: 1) the generation of the signal; 2) the removal of the signal; 3) the direct mediators of the signal; and 4) the ultimate effects of the signal (Murray, 1992).

This introduction will give a general overview to the cAMP and cGMP second messenger system giving extra emphases to cAMP signalling pathways and Phosphodiesterase enzymes (PDE), in particular the cAMP-specific (PDE 4) members of the family.

1.1.1 Cyclic Nucleotides

One of the oldest and widest studied signals or so called second messengers are the 3',5' cyclic nucleotides, that include, adenosine 3',5' cyclic monophosphate (cAMP) and guanosine 3',5' cyclic monophosphate (cGMP). These molecules act as mediators relaying signals initiated by external first messenger molecules, for example hormones, to internal mediators leading to a certain cellular response.

1.1.1.1 cAMP

In the 1950s, Dr. Earl Sutherland performed some pioneering studies to understand how hormones act at the molecular level. These studies which had the aim of determining how

adrenalin and glucagon stimulate the breakdown of glycogen and the storage of glucose in the liver. It was found that these hormones elicit their effects by binding to receptors on the surface of the cell triggering the formation of cAMP which stimulates down stream effectors. As these hormones themselves, do not enter the cells, they have been given the name first messengers and consequently cAMP was called a second messenger. Similar experiments revealed that cAMP was present as a second messenger for many other hormones beside adrenalin and glucagon. For example, calcitonin, thyroid-stimulating hormone and noradrenalin.

cAMP has been reported to affect a wide range of cellular processes such as, the degradation of storage fuel, the secretion of acid by the gastric mucosa, dispersion of melanin pigment granules, aggregation of blood platelet (Sheth and Colman, 1995), and the opening of chloride channels (Light *et al.*, 1990; Lattore *et al.*, 1991).

The cAMP system is activated by seven helix membrane receptors such as β-adrenergic receptor following the binding of the hormone adrenalin also known as epinephrine. The hormone-receptor complex stimulate guanine nucleotide-binding proteins (G-proteins) leading to the activation of membrane bound enzymes called adenylate cyclases. The control of this enzyme is considered to be important as these enzymes have the sole responsibility of generating cAMP from ATP (Sutherland *et al.*, 1962). Control is performed by distinct heterotrimeric guanine regulatory proteins (G-proteins) that relay stimulatory (G_s) or inhibitory (G_i) signals through a sub-receptor complex (figure 1.1, Gilman, 1984; Krupinski, 1991).

cAMP, once formed, stimulates the phosphorylation of many target proteins by activating protein kinase A (PKA). This is performed by binding the cAMP to the regulatory domain of the PKA leading to the release of the catalytic domain which, in turn, phosphorylates specific serine or threonine residues on specific cellular target protein to regulate their activities (Nairn *et al.*, 1985). Proteins that are phophorylated using this mechanism for example are the transcriptional activator cAMP-response element binding protein (CREB) (Dwarki *et al.*, 1990). The phophorylation of these proteins leads to the expression of specific genes which are necessary for cell function.

The activation of the second messenger systems are abolished by the action of enzymes called phosphodiesterases (Butcher and Sutherland, 1962). These enzymes hydrolyse cAMP molecules converting them to their corresponding 5' monophosphates.

For cAMP molecules to function as intracellular mediators, their internal concentration, normally $< 10^{-7}$ M, must be able to change freely in accordance to stimulus activation (Schramm *et al.*, 1984). cAMP as mentioned before, is produced by adenylate cyclase from ATP, and is rapidly and continuously destroyed by phosphodiesterase by hydrolysing cAMP to 5'-monophosphate. The control of cAMP levels in cells is achieved by the regulation of these two enzymes and mostly by adenylate cyclase. The regulation of these two enzymes are achieved by the presence of particular isoforms with a certain level of activity, specific to certain types of cells.

Other signalling systems have an effect on controlling cAMP levels in cells. This is performed by directly regulating G-protein coupled receptors or adenylate cyclase or both. For example, IP3 signalling molecule which increases calcium ions and diacylglycerol (DAG) levels in cells, causes either, the reduction of cAMP production by the inhibitory action of protein kinase C (PKC) on certain G-protein coupled receptors and adenylate cyclase or, the increase in cAMP production by the stimulatory action of PKC on adenylate cyclase (Houslay, 1998).

1.1.1.2 cGMP

The cGMP system is activated directly by guanylate cyclases which apart from being the sole generators, of cGMP from GTP, are quite different from the adenylate cyclases. Adenylate cyclases are found exclusively bound to membranes whereas guanylate cyclases can be found both bound to membranes or soluble in the cytoplasm (Drewett and Garbers, 1994; Garbers and Lowe, 1994). Furthermore, it appears that guanylate cyclases are not regulated by G proteins (Drewett and Garbers, 1994).

The cGMP pathway has been reported to operate through a number of mechanisms involving the activation of cGMP-dependent protein kinases (Beebe and Corbin, 1986), a cGMP specific activator in visual transduction in retinal rod cells (Takemoto and

Cunnick, 1990; Stryer, 1991) and ion channel regulation (Light *et al.*, 1990; Lattore *et al.*, 1991).

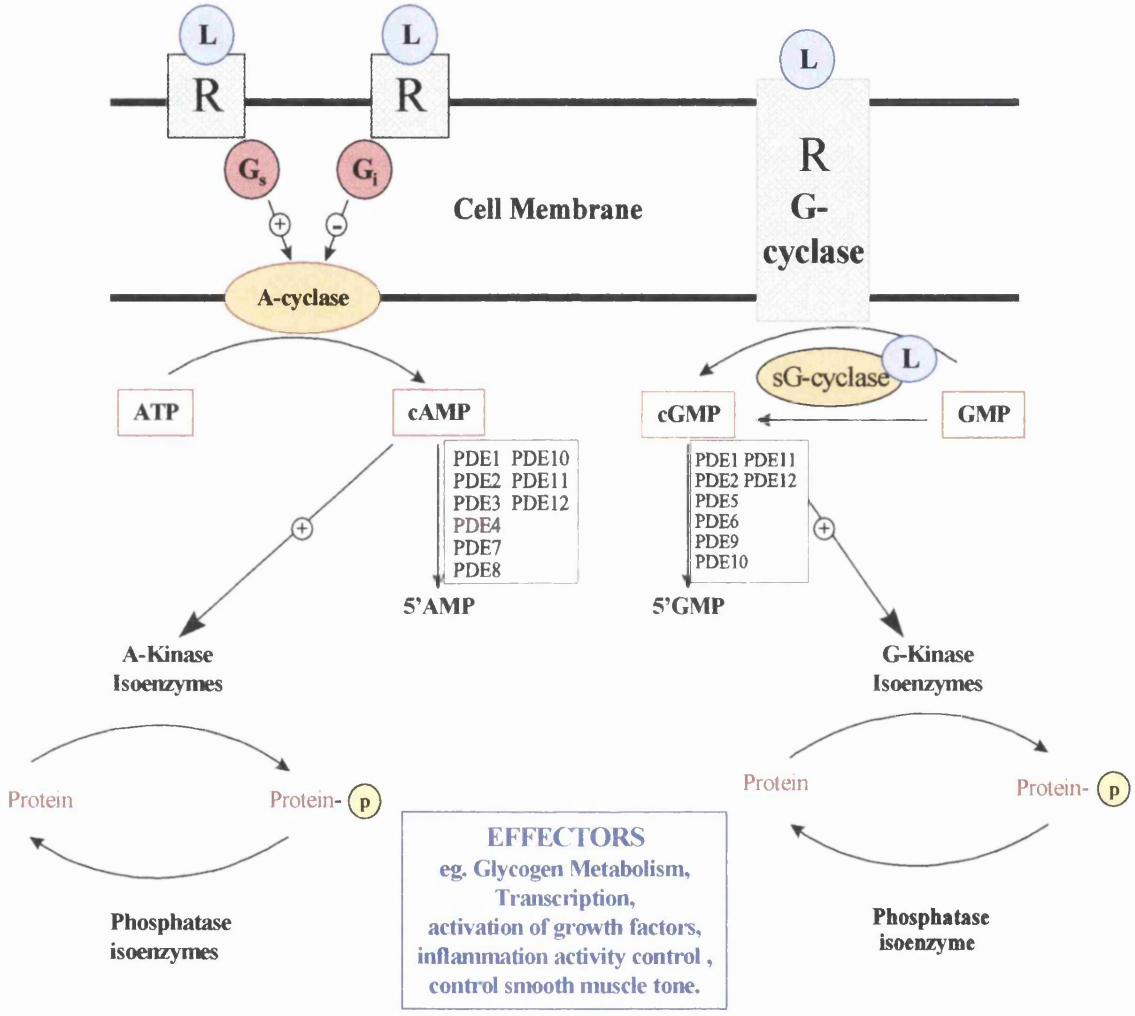

Figure 1.1 The signalling mechanism of second messenger systems. This simplistic scheme shows the signalling route of the second messenger systems known to date and does not imply that these routes are present in every cell. Abbreviations are: R for Receptor, L for Ligand, G_s for activating G-proteins, G_i for inhibiting G-proteins, A-cyclase for Adenylate cyclase, sG-cyclase for soluble Guanylate cyclase, A-Kinase for cAMP-dependent-protein Kinase, G-Kinase for cGMP-dependent-protein-Kinase, PDE for Phosphodiesterase Enzyme, ⊕ for activating reaction, ⊖ inhibiting reaction and (p) for phosphorylated.

1.2 Cyclic Nucleotide Phosphodiesterases

Phosphodiesterases (PDE) are a group of enzymes which were first discovered by Butcher and Sutherland in 1962 not long after the discovery of cyclic nucleotides. These enzymes played a vital role in characterising adenosine 3',5'-phosphate which lead to the discovery of the second messenger system.

PDEs have the important role of hydrolysing cyclic nucleotide second messengers to the corresponding, inactive 5'-monophosphate counterparts. The degradation of cyclic nucleotide via these enzymes represents the major route for termination of cyclic nucleotide action. Other routes for the removal of cyclic nucleotides are present, for example transport mechanisms that export cyclic nucleotides to the exterior of cells (Barber and Butcher, 1981). However, these mechanisms only account for a minor fraction of the total cyclic nucleotides present in cells (Barber and Butcher, 1980; Barber and Butcher, 1981).

PDEs have become more and more important after the discovery of PDE inhibitors which have been found to reduce or even relieve certain disease symptoms. Within only a few years, this field had expanded tremendously as more and more new isoforms have been found. To date twelve PDE families are known and each PDE family consisted of PDEs that originated from a subfamily of genes and alternative splice variants (Beavo, 1995).

Although all PDEs have the function of degrading cAMP, the different PDEs play different roles in regulating particular cellular processes. This was explained by the fact that PDEs from different families are different in tissue expression, localisation, substrate specificity, kinetic parameters, regulation and sensitivity to PDE inhibitors which, allowed tighter control of the physiological processes performed by particular members of each PDE superfamily. For example, the different K_m values that these PDEs possess for cAMP allowed them to have different performances which varied according to the prevailing cAMP concentration (Soderling and Beavo, 2000; Beavo, 1995; Manganiello *et al.*, 1995; Conti and Jin, 1999). This could be demonstrated by PDE7 and PDE 8, which have a K_m in the submicro-molar range to be involved in the regulation of the basal levels of cAMP when adenylate cyclase is not stimulated. However, when adenylate cyclase is activated

and levels of cAMP rise to 10-20 μM or higher, PDEs 3 and 4 were thought to be bought into action as their K_m values were in the micro-molar range. Extremely high cAMP levels were thought to be dealt with by PDE1 and PDE2 as their K_m lies in the tens of micro-molar range. The latter sets of enzymes were though to act to buffer cAMP concentration.

Different PDEs were also found to be expressed in particular cell types. For example PDE7A (a cAMP-specific PDE) was found to be expressed mainly in cells involved in the immune system and was found to be crucial in T cell activation (Li and Beavo, 1999) and, PDE5 (a cGMP-specific PDE) that was found to be expressed mainly in smooth muscles and was found to be important in the control of penile erection (Boolell *et al.*, 1996).

While PDEs were found to be differentially expressed amongst different cell types, they were also found to be differentially expressed at the cellular level. To best demonstrate this phenomena is to describe work performed by Beavo and co workers on the neuronal olfactory sensing cells present at the upper part of the respiratory tract (nasal epithelium, Juilfs *et al.*, 1997). Beavo described that in a single neuron cell, two PDE enzymes were expressed and located at different regions of the cell. While Ca^{2+}- sensitive PDE1 was found exclusively to the cilia at the ends of the neurites projecting out of the cavity, the Ca^{2+}-insensitive PDE4A was found exclusively to the cell body and neurites. This example demonstrates clearly that differential intracellular targeting of PDE isoenzymes to certain compartments of the cell which in turn allowed the control of distinct pools of cAMP in the cell. The compartmentalisation of PDE isoenzymes could also be seen in kidney cells. For example (Dousa, 1998; 1999) mesangial cells of the kidney glomeruli consist of two processes regulated by cAMP which in turn was regulated by distinct PDEs. The first process was the generation of superoxide during respiratory burst leading to pathogenesis of glomerulonephritis and the second was the mitogenic stimulation of DNA synthesis. It was found that rolipram (a PDE4 specific inhibitor) inhibited the regulation of the respiratory burst only, whereas cilostamide (a PDE3 specific inhibitor) exclusively inhibited the DNA synthesis process. This example also clearly showed that different PDEs regulate different pools of cAMP which appeared to regulate very different cellular processes in cells where more than one type of PDE was expressed.

Before the use of selective inhibitors such as the previously mentioned rolipram and cilostamide, non selective inhibitors such as methylxanthines firstly described by Sutherland and co workers (Sutherland and Rall, 1958; Butcher and Sutherland, 1962) were used to characterise PDEs. These inhibitors which included caffeine and theophylline and later IBMX (figure 1.2), show no preference to PDE isoenzymes and exhibited low inhibitory effects on PDEs. However, these inhibitors represent the first generation of PDE inhibitors without which none of the known selective inhibitors today would have been developed.

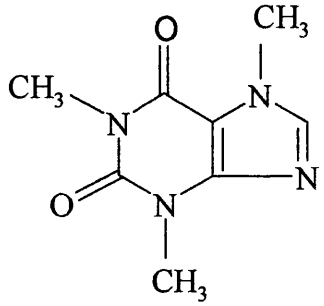

1, 3, 7 trimethylxanthine

(Caffeine)

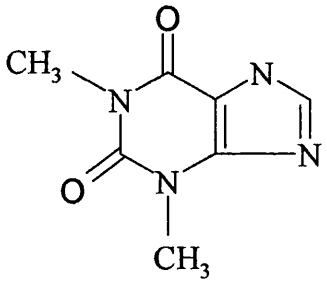

1, 3 dimethylxanthine

(Theophylline)

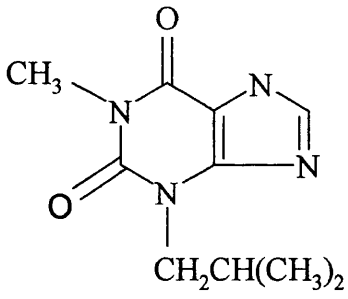

3-isobutyl-1-methylxanthine

(IBMX)

Figure 1.2 Structures of non-selective PDE inhibitors. 3-isobutyl-1-methylxanthine (IBMX) was used in this study.

1.2.1 Nomenclature

It has been increasingly difficult to name PDEs. This has been due to the multiple isoenzymes of PDEs being discovered through the years. Previously, workers have tended to number PDE isoenzymes according to their eluting order from an anion-exchange column. This was considered unsatisfactory, as the elution of the PDEs from the column depended on both the tissue type and the chromatographic conditions used, also each peak may contain more than one PDE isoenzyme. Many other procedures have been introduced to the fractionation mechanisms mentioned above to try and improve the identification of PDEs. These include the use of specific assay conditions which will identify fractions containing certain PDE isoenzymes, the use of selective inhibitors for each of the PDE isoenzymes, and the use of immunological identification methods to identify PDE isoenzymes (Beavo, 1988). These methods have not been widely used in the classification approaches because of their many potential pitfalls.

A more definitive approach has been proposed (Beavo,1988; Beavo and Reifsnyder, 1990). This approach classified the different PDE isoenzymes into families according to their similarity in protein sequence (i.e. both primary sequence and that deduced from cDNA), kinetic, regulatory, and physical properties (Beavo, 1988). Despite the fact, that this nomenclature cannot be completed due to new PDE isoenzymes being discovered, it classified five major families of PDE isoenzymes (Beavo and Houslay, 1990, Table 1.1). The naming of these families was represented by a descriptive name, a Roman numeral, and Arabic numerals which designate splice forms present in each family. In addition, Greek letters were used to designate individual subunits present in particular isoenzymes. It is important to mention that both the descriptive name and in particular the Roman numerals are arbitrary, so they did not necessarily denote the order of elution from DEAE-cellulose or any other fractionation column (Beavo and Houslay, 1990). As an example of this nomenclature system, light activated, cGMP-specific PDE present in rod photoreceptor outer segment would be called cGMP-specific PDE, $V_{B1\alpha}$ and the 61 kDa Ca^{2+}/ Calmodulin (CaM)-dependent PDE present in bovine brain would be called Ca^{2+}/ CaM-dependent PDE, I_{A2} (Beavo and Houslay, 1990).

Table 1.1 Nomenclature recommended by Beavo, 1988 and Beavo and Rifsnyder, 1990.

PDE Family	PDE Name	Splice Variant
Ca^{2+}/ Calmodulin-dependent	PDE I	7
cGMP-stimulated	PDE II	3
cGMP-inhibited	PDE III	4
cAMP-specific, low K_m	PDE IV	4
cGMP-specific, cGMP binding	PDE V	3

More recently, the 'diagnostic' system mentioned above was abandoned and naming of PDEs based upon gene families was adopted (Beavo *et al.* 1994). This method of naming provided a more rigorous assessment of family identity based upon primary sequence similarities. The names of entries assigned to the GenBank were similar to that previously described except for two main changes. The first was the addition of two letters at the beginning of the name to represent the species name and the second was the change of the Arabic numeral from being arbitrary to designate the PDE's gene family followed by a letter representing the individual gene product within the family. To demonstrate this description an example is shown below:

***HS*PDE8A2**

***Homo sapiens* (species)**

Gene Family (PDE + Arabic numeral)

Gene (Capital letter)

Splice variant

Entries for the Human Genome project lack the first two letters as all entries must be human sequences. Furthermore, an asterisk is included following the second Arabic number to represent alleles rather than splice variants. The latest updated nomenclature table is summarised in table 1.2.

Table 1.2 Nomenclature recommended by Beavo (1995).

PDE Family	Short Name	Genes	Splice variants
Ca^{2+} / calmodulin-stimulated	PDE 1	3	9+
cGMP-stimulated	PDE 2	1	2
cGMP-inhibited	PDE 3	2	2+
cAMP-specific, low K_m	PDE 4	4	15+
cGMP-specific, cGMP binding	PDE 5	2	2
Photoreceptor PDEs	PDE 6	3	3
High affinity cAMP-specific	PDE 7	3	1

Last updated by the Nomenclature committee on 30th July 1999.

Since 1995, new PDEs have been identified forming new PDE gene families PDE8, PDE9, PDE10, PDE11 and recently PDE12. However since the characteristics of their regulatory properties have not yet been fully elucidated, descriptive names representing their function have not yet been confirmed. The nomenclature shown in table 1.2 was adopted throughout this thesis.

1.2.2 Domain Organisation Of Cyclic Nucleotide Phosphodiesterase Enzymes

Sequence analyses and alignment studies revealed that nearly all mammalian PDEs known today share a conserved region of approximately 270 amino acids (Bentley and Beavo, 1992). This region which is near the carboxyl terminus of the enzyme was thought to contain the catalytic domain. The recent structural analysis (Xu *et al.*, 2000) confirmed the involvement of this region in the catalytic activity of the enzyme. Conserved histidine residues play an important role in chelating the tightly bound cations (Zn^{2+} and Mg^{2+}) that are found to be essential for the enzyme's catalytic activity (Francis *et al.*, 1994; Turko *et al.*, 1998; Omburo *et al.*, 1995; Omburo *et al.*, 1998; Zhang and Colman, 2000).

The regions which were found immediately at the N-terminus of the catalytic domain were found to be highly variable amongst the different families but similar within members of the same family. These regions were found to be involved in regulating the catalytic activity of PDEs as well as in some cases targeting the enzyme intracellularly. The domain organisation described is summarised in figure 1.3. In subsequent sections an in depth study of the most well-characterised PDEs will be discussed. These include PDE1, PDEs

containing cGMP-specific phophodiesterases, cyanobacterial *Anabaena* adenylyl cyclases, and *Escherichia coli* transcriptional regulator fh1A (GAF) domains (PDE2, PDE5, PDE6, PDE10 and PDE11) and PDE3. Very highly selective inhibitors have been developed for these PDEs creating the need to distinguish these PDEs from PDE4. Thus, information on localisation, domain organisation, regulation and inhibition of each of the above mentioned PDEs will be discussed.

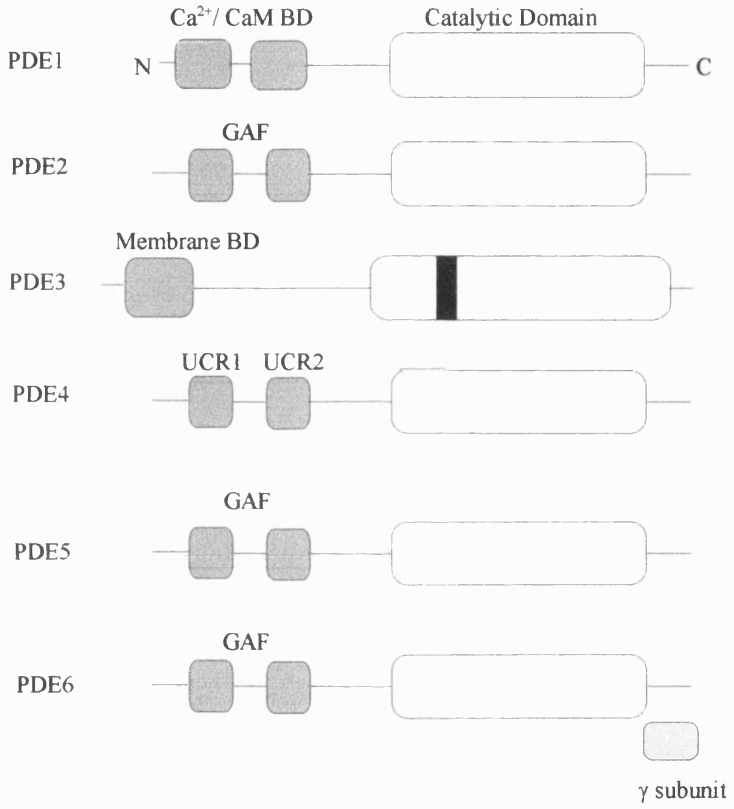

Figure 1.3 Domain organisation of cyclic nucleotide phosphodiesterase enzymes.This diagram is not to scale and is not an accurate reflection of size comparisons between members of the PDE family. Its propose is to show the different structural domains present in PDEs. Abbreviations are: Ca^{2+}/ CaM for Calcium ion/ Calmodulin, BD for Binding Domain, GAF for cGMP-specific phophodiesterases cyanobacterial *Anabaena* adenylate cyclases, and *Escherichia coli* transcriptional regulator fh1A, UCR for Upstream Conserved Region. The black region in the catalytic domain of PDE3 represents a 44 amino acid insertion. γ subunit represents the inhibitory PDE6 subunit (see section 1.4.3, page 16)

1.3 Calcium/Calmodulin-stimulated PDE 1

This family of PDEs are characterised and classified by their sensitively to stimulation by calcium and calmodulin allowing for 'cross-talk' between signalling pathways mediated between cyclic nucleotides (cAMP and cGMP) and signalling pathways mediated by calcium ions (Wang *et al.*, 1990). Generally, PDE1 isoenzymes hydrolyse both cAMP and cGMP. The rate at which these two cyclic nucleotides are hydrolysed are regulated by two Ca^{2+}/ calmodulin (Ca^{2+}/ CaM)-binding domains present at the N-terminus (regulatory domain) of PDE1 isoenzymes (Novack *et al.*, 1991; Sonnenburg *et al.*, 1995; Kincaid *et al.*, 1985; Charbonneau *et al.*, 1991).

To date, three genes encoding PDE1 have been identified. Using the nomenclature described in section 1.1.2, these genes were called PDE1A corresponding to bovine 61 kDa CaM-PDE, PDE1B corresponding to bovine 63 kDa CaM-PDE (Sharma *et al.*, 1980; 1984) and PDE1C possibly corresponding to an isoform identified in the rat testis (Rossi *et al.*, 1988). The diversity of PDE1s were further increased by 5' and 3' alternative splicing of each gene product resulting in the formation of splice variants (isoforms) that differ in their N and/ or C termini (Michibata *et al.*, 2001; Yan *et al.*, 1996; Sonnenburg *et al.*, 1995). The alternative 5' splicing generates isoforms that have different affinities to Ca^{2+}/ CaM due alteration of the Ca^{2+}/ CaM-binding domains. For example, PDE1C2 isoform has two of the Ca^{2+}/ CaM-binding domains intact whereas the rest of PDE1C isoforms (PDE1C1, 3, 4, and 5) have one of the two Ca^{2+}/ CaM domains spliced out making these isoforms less sensitive to Ca^{2+} when compared to PDE1C2 isoforms (Yan *et al.*, 1996).

CaM regulation of PDE1 is performed through the binding of four Ca^{2+} ions to calmodulin which in turn binds to the Ca^{2+}/ CaM-binding domain on the PDE1 isoenzyme causing activation of cyclic nucleotide hydrolysis (O'Neil and Degrado, 1985; Seeholzer *et al.*, 1986). The mechanism of PDE1 activation by CaM is thought to be induced by a conformational change in the tertiary structure of PDE1 caused by CaM binding (Charbonneau *et al.*, 1986). However, this assumption is very difficult to prove as no crystal data of PDE1 complexed with calmodulin is currently present.

Members of the PDE1 family are also regulated by phosphorylation. Generally phosphorylation occurs at the N-terminal regions of the PDE proteins by subtype specific kinases. For instance, PDE1A and PDE1C isoenzymes are phosphorylated by cAMP-dependent kinases whereas, PDE1B isoenzymes are phosphorylated by calmodulin-dependent kinase II (Sharma and Wang, 1986; Hashimoto *et al.*, 1989). The phosphorylation of PDE1 isoenzymes have been found to reduce the affinity of these enzymes to Ca^{2+}/ CaM (Beavo, 1995; Yan *et al.*, 1996). More recently, PDE1 isoenzymes have been reported to be regulated by degradation by m-calpain which are Ca^{2+}-dependent cysteine proteases through a PEST motif present in some PDE1 isoforms such as PDE1A2 (Kakkar *et al.*, 1999).

There are large and diverse compounds that are capable of inhibiting PDE1. These compounds have been divided into two categories according to their inhibiting effect on the enzyme. The first category included those inhibitors that acted on the enzyme's activity directly and the second included inhibitors that acted on the CaM stimulation of the enzyme. In this study Vinpocetine (figure 1.4), which is a potent vasodilating agent, was used (Hagiwara *et al.*, 1984). This inhibitor was found to act at the catalytic site of PDE1s. This inhibitor was found to be highly selective to PDE1 isoenzymes unlike other inhibitors of the same category for example, Zaprinast and 8-MOMX which were found to act on PDE5 with a similar potency to PDE1 (Ahn *et al.*, 1992).

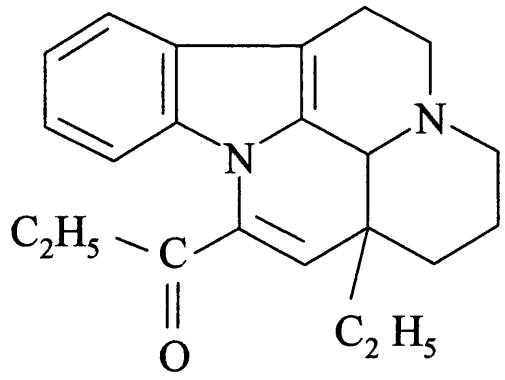

Figure 1.4 The structure of Vinpocetine PDE1 selective inhibitor.

1.4 PDE Families Containing GAF Domains

PDE2, PDE5, PDE6, PDE10 and the recently identified PDE11 have been identified to include a non-catalytic region at their N-terminus having high specificity to cGMP (Soderling and Beavo, 2000; Soderling *et al.*, 1999; Fawcett *et al.*, 2000; Mou *et al.*, 1999; Fujishige *et al.*, 1999; Fujishige *et al.*, 2000; Yuasa *et al.*, 2000). This domain (GAF), binds to cGMP and leads to an allosteric stimulation of the enzyme's activity (Granovsky *et al.*, 1998; Corbin and Francis, 1999; Tanaka *et al.*, 1991; Sonnenburg *et al.*, 1991). The acronym GAF is derived from the names of three proteins that contained this conserved sequence; cGMP-specific phophodiesterases, cyanobacterial *Anabaena* adenylyl cyclases, and *Escherichia coli* transcriptional regulator fhlA (Aravind and Ponting, 1997; Shabb and Corbin, 1992). Despite the conservation of this domain in the three proteins, the function of this domain it appears to be different in each of the three proteins.

1.4.1 cGMP-stimulated PDE2

To date there has been only one gene identified for this family of PDEs making them one of the smallest PDE families known. Two 5' splice variants have been identified which differ in their N-terminal regions (Rosman *et al.*, 1997). One of these isoforms has been found to be cytosolic and the other was found to be anchored to the plasma membrane by virtue of its N-terminal region as identified in hepatocytes (Marchmont and Houslay, 1980a). This intracellular targeting of these isoforms and their functional relevance is not yet fully understood. However, it supports the previous notion that intracellular distribution of PDEs in cells has fundamental importance.

PDE members of this family are capable of hydrolysing both cAMP and cGMP with slightly different affinities (K_m of ~ 30 μM for cAMP and K_m of ~ 15 μM for cGMP) (Martins *et al.*, 1982; Yamamoto *et al.*, 1983; Beavo, 1988; Murashima *et al.*, 1990). They have been implicated in the 'cross-talk' between several signalling pathways. PDE2 sensitivity to cGMP allowed for the 'cross-talk' between cAMP and cGMP signalling pathways. For example, nitric oxide (NO) mediated activation of guanylate cyclases (Koesling and Friebe, 1999) increases cGMP levels in the cell, leading to PDE2

stimulation and hydrolysis of cAMP. The decrease in cAMP levels may lead to deactivation of the cAMP signalling pathway. PDE2 isoenzymes present in particulate fractions have been shown to be phosphorylated by protein kinase C which is activated by Ca^{2+}. Furthermore, PDE2 isoenzymes have been shown to be involved in the 'cross-talk' between certain lipid signalling pathways (Geoffroy *et al.*, 1999).

1.4.2 cGMP-specific/ cGMP-binding PDE5

Until the cloning of cDNA for this isoenzyme (McAllister *et al.*, 1993), members of this family were thought to belong to the photoreceptor PDE6. This was due to similarity in their kinetics, cGMP-binding and size characteristics to members of PDE6 isoenzymes (Beavo, 1995). Sequence alignment studies revealed less than 60% identity between these two sets of isoenzymes (Beavo, 1995). Consequently members of PDE5 were placed in a separate family.

Only one gene product has been reported for this family and two splice variants have been identified with distinct N-terminal regions (Kotera *et al.*, 1998; Kotera *et al.*, 1999a). PDE5 isoenzymes are highly specific to cGMP hydrolysis with K_m values of approximately 5.6 μM and show no significant hydrolysis activity with cAMP (Thomas *et al.*, 1990a). cGMP has been found to bind to both the catalytic domain and to the two cGMP-binding (GAF) allosteric domains found at the N-terminal end of the proteins (Thomas *et al.*, 1990b; McAllister *et al.*, 1995).

The regulation of the catalytic activity of PDE5 is poorly understood however, there is evidence to suggest that the catalytic activity is influenced by elements in the regulatory domain (Lochhead *et al.*, 1997; Wyatt *et al.*, 1998). For instance, the binding of cGMP to the allosteric sites (GAF domain), have been found to induce a conformational change exposing serine residues at the surface of the protein (Tremblay *et al.*, 1985; MacPhee *et al.*, 1988) which, are phosphorylated by cGMP-dependent kinases (Thomas *et al.*, 1990a). This in turn caused an increase in PDE5 catalytic activity. The conformational change induced as a result of binding of cGMP to the GAF domains has been found to expose regions near the allosteric GAF domain that are implicated to the dimerisation of the

protein (Thomas *et al.*, 1990b). However, the function of this dimerisation is not well understood.

Recently there have been much interest in PDE5 due to the inhibition of these PDEs by Viagra which is used in the treatment of erectile dysfunction. Other PDE5 inhibitors are also available such as Zaprinast, MY 5445 and SK7F 96231 (Beavo and Reifsnyder, 1990; Nicholson *et al.*, 1991; Murray and England, 1992).

1.4.3 Photoreceptor PDE6

At present, there are at least three gene products described for this family of PDE6 (Hurwitz *et al.*, 1985), products of which are expressed exclusively in the rod and cone photoreceptors of the retina. These photoreceptors consist of PDE6 arranged as a multisubunit protein of two types of catalytic subunits α and β which are products of PDE6A and B genes respectively, bound to two inhibitory γ subunits. PDE6 isoenzymes are highly specific to cGMP hydrolysis and both the kinetic activity and subunit assembly are regulated by the presence of GAF domains at their N-terminus (Mou *et al.*, 1999). It has been described that the binding of cGMP to the GAF domain induces the dramatic increase in the affinity (300 fold) of PDE6 ($\alpha\beta$) to its inhibitory γ subunits (D'Amours and Cote, 1999).

The physiological function of the PDE6 family are the most well understood of any of the PDEs (Beavo, 1995). The visual transduction pathway is stimulated by the initial conformational change of rhodopsin, induced by light which in turn triggers the exchange of GDP to GTP by heterotrimeric G-protein transducin (Yarfitz and Hurley, 1994; Lagnado and Baylor, 1992). Following the binding of transducin to GTP, a conformational change is induced causing the release of the α subunit of the activated transducin which in turn binds to the PDE6 holoenzyme causing it to release its γ inhibitory domain. The release of the inhibitory domain of PDE6 allows the catalytic domain to hydrolyse cGMP causing the closure of cGMP-gated Ca^{2+} channels which in turn leads to the hyperpolarisation of the cell membrane and the decrease in neurotransmitter release.

1.4.4 PDE10

The PDE10 family represent one of the newly discovered groups so description names for these enzymes have not yet been assigned as little is known regarding their regulation and cellular targeting. At present products of one gene have been isolated from human fetal lung PDE10A1 and PDE10A2 (Fujishige *et al.*, 1999; Kotera *et al.*, 1999b). These isoforms have been found to hydrolyse both cAMP and cGMP with K_m values of 0.26 μM and 7.2 μM respectively, and V_{max} values for cGMP twice that of cAMP. Thus, these PDEs have exhibited properties similar to cAMP PDEs and cGMP inhibited PDEs (Fujishige *et al.*, 1999). Sequence alignment studies revealed similarity of PDE10A with both PDE2 and PDE5A. These similarities being at the catalytic domains and the GAF cGMP binding-domains (Fujishige *et al.*, 1999). However, the cAMP- and cGMP-dependent protein kinase phosphorylation sites present in PDE5, which are found to be important in the regulation of these PDEs, were absent in PDE10A. These have been found to be replaced by sites phosphorylated by protein kinase C suggesting regulation by this enzyme (Fujishige *et al.*, 1999).

1.4.5 PDE11

To date only one gene (PDE11A) has been identified for this family of PDEs. However, up to three splice variants (PDE11A 1, 3, and 4) have been reported (Yuasa *et al.*, 2000). These isoforms differ in their N-terminal regions, for instance, PDE11A4 consists of two complete GAF domains whereas PDE11A3 consist of one complete and one incomplete GAF domain (Yuasa *et al.*, 2000). On the other hand, PDE11A1 consists of an incomplete GAF domain, which lacks the N-terminal part of the GAF consensus sequence (Yuasa *et al.*, 2000). The exact function of the GAF domain present in these PDEs is not fully characterised. The catalytic domain of PDE11A has been identified to be highly homologous to that of PDE5A. However, although PDE5A is highly specific to cGMP, PDE11A has been found to hydrolyse both cAMP and cGMP with similar affinities (Yuasa *et al.*, 2000).

1.5 cGMP-inhibited PDE3

Two gene products have been identified to belong to the PDE 3 family (Meacci *et al.*, 1992; Taira *et al.*, 1993). Using the nomenclature described in section 1.1.2, these isoforms were called PDE3A and PDE3B. The first isoform PDE3A has been found to be abundantly expressed in smooth muscle, platelets, and cardiac tissues whereas, PDE3B isoforms have been shown to be expressed in adipocytes and liver (Beavo, 1995). Members of PDE3 are capable of hydrolysing both cAMP and cGMP with K_m values in the range of 0.1-0.8 μM and V_{max} for cAMP 4-10 times higher than that for cGMP therefore conveying specificity to cAMP (Degerman *et al.*, 1997; Beavo, 1995). Furthermore, cGMP has been found to bind at the catalytic domain and not at the N-terminal regulatory domains as in PDE2. Therefore, cGMP acts as a potent inhibitor for cAMP hydrolysed by PDE3 enzymes. The PDE3 'cross-talk' between cGMP mediated by nitrogen oxide (NO) stimulation of guanylate cyclase and cAMP signalling pathways is expected to increase cAMP levels due to the inhibitory effect of cGMP on the enzyme (Lugnier *et al.*, 1999).

The catalytic domain in PDE3 isoenzymes differ from the rest of the PDE families by an insertion of 44 amino acids (Degerman *et al.*, 1997). This insertion, which has distinguished the PDE3 catalytic domain from the rest of the PDE families, interrupts the first of the two putative Zn^{2+} binding domains that have been identified to be present in PDE catalytic domains (figure 1.3) (Degerman *et al.*, 1997; Francis *et al.*, 1994; Meacci *et al.*, 1992; Taira *et al.*, 1993). The presence of the 44 amino acid insertion in the catalytic domain of PDE3 has lead to assumption to the presence of subfamilies within PDE3 however the exact implication to substrate interactions as well as inhibitor interaction has yet to be elucidated (Degerman *et al.*, 1997).

The N-terminal portion of PDE3A and B isoenzymes have been found to be quite divergent (Degerman *et al.*, 1997). They have been mostly implicated in the cellular targeting of the enzyme. Two distinct hydrophobic regions present at their N-terminus form six transmembrane helices to help and integrate the isoenzyme to membranes (Shakur *et al.*, 2000). These hydrophobic region were absent in the cytosolic forms of the enzyme (Kenan *et al.*, 2000).

Using PDE3 selective inhibitors, PDE3 isoenzymes have been implicated in the regulation of key biological processes, such as lipolysis, glycogenolysis and cardiac contractility (Manganiello *et al.*, 1995; Beebe *et al.*, 1985). For example, PDE3B has been shown to mediate the inhibitory effect of insulin on lipolysis in adipocytes. This is performed by insulin activation of IRS-1, Phosphatidylinositol-3- kinase (PI3-kinase) and PDK signalling pathways and the final phosphorylation of PDE3B isoenzymes through PKB/ *Akt* (Ahmed *et al.*, 2000). The activation of PDE3B by phosphorylation causes the increase in cAMP hydrolysis leading to the fall in cAMP levels in the cell. This in turn reduces the activity of PKA which leads to the de-phophorylation and deactivation of hormone-sensitive lipase (HSL) and the consequence decrease in hydrolysis of stored triglyceride. Specific PDE3 inhibitors have found to induce mycocardial contractility, vascular and airway smooth muscle relaxation (Beavo and Reifsnyder, 1990; Weishaar *et al.*, 1987; Komas *et al.*, 1996; Manganiello *et al.*, 1995). PDE3 isoenzymes in these tissues have been shown to be phosphorylated via PKA *in vitro* however, the mechanism of regulation of these isoforms in intact cells is still poorly understood (Degerman *et al.*, 1997).

As a consequence of PDE3 involvement in myocardial contractility, several PDE3 selective inhibitors have been developed and are still in development. The first compound to be discovered were bipyridine and amrinone (figure 1.5) (Alousi *et al.*, 1979). These compounds, which caused a marked increase in cardiac contractility, were initially thought not to act on PDE3. This was due to the use of crude extracts to test for PDE response to these inhibitors and as PDE3 would be expected to have little contribution to the overall PDE activity, it wasn't surprising that it was missed. Subsequently an analog was developed called milrinone (Alousi *et al.*, 1983). Milrinone was found to be 10 to100 times more potent compared to amrinone, however, it was not proven at that time to have PDE inhibition as the mode of action (Alousi *et al.*, 1983). It was not until studies performed by Harrison *et al.*, 1986 and MacPhee *et al.*, 1986 using highly purified PDE3 enzyme that these isoenzymes were shown to be the direct target for these cardiotonic agents. Since 1986 more potent and selective inhibitors have been developed such as SK&F 94120 (Gristwood *et al.*, 1986) and bemoradan (Moore *et al.*, 1991).

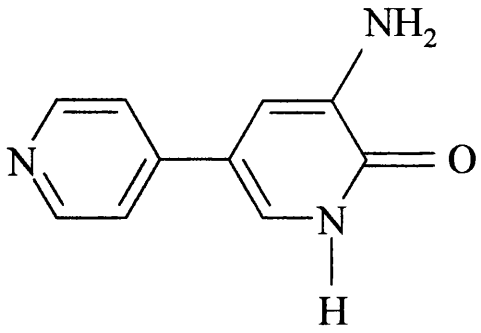

Figure 1.5 Structure of Amrinone PDE3 selective inhibitor.

1.6 cAMP-specific phosphodiesterase PDE4

The focus of this thesis is the study of cAMP-specific Phosphodiesterases. PDE4 isoenzymes are highly specific to cAMP, insensitive to cGMP and are also very highly sensitive to the anti-depressant drug rolipram (Yamamoto *et al.*, 1984). The PDE 4 family which, contribute to the 'low K_m' activity in many cells, have been found to be present in the brain where they are thought to contribute to the regulation of processes that control mood, emesis, and olfactory sensory transduction (De Mazancourt and Giudicelli, 1988; Davis, 1984). Members of PDE4 family have been found in the lung (Torphy and Cieslinski, 1990), tracheal smooth muscle (Shahid *et al.*, 1991) and macrophages (Barnes, 1995) it is likely that PDE4 may be involved in the regulation of inflammation. Indeed, PDE4 inhibitors have been found to suppress various functions of inflammatory cells (Torphy and Undem, 1991; Torphy *et al.*, 1994; Palfreyman and Souness, 1996). Therefore, there is the potential of utilising these PDE inhibitors in the therapy of asthma, allergy and other inflammatory diseases (Torphy and Undem, 1991).

Previous work on the *Drosophila dunce* gene mutant allowed the discovery of four mammalian subtypes belonging to cAMP-specific PDEs (Beavo and Relfsnyder, 1990; Beavo *et al.*, 1994). cDNA of four subtypes encoded by four genes (A, B, C, and D) have been cloned and expressed in various laboratories (Livi *et al.*, 1990; McLaughlin *et al.*, 1993; Engels *et al.*, 1995; Baecker *et al.*, 1994; Obernolte *et al.*, 1993; Bolger *et al.*, 1993; Wilson *et al.*, 1994; Amegadzie *et al.*, 1995; Wang *et al.*, 1997). Each subtype has been

found to produce at least six different splice variants arising from alternative mRNA splicing. PDE isoforms as well as their splice variants are regulated at several levels, including transcription, splicing, and in subcellular localisation (Bolger, 1994). It has been hypothesized that mRNA levels are transcriptionally regulated by cAMP via cAMP-response element (CRE) found in the promoter region of the gene. Moreover, differential splicing or degradation of mRNA is also regulated by cAMP. Recently Houslay and colleagues have found a splice variant encoded by rat PDE4A locus (RD1), to contain a membrane binding region (Shakur *et al.*, 1993). This finding demonstrates that differential splicing of PDE enzymes contribute to the regulation of the subcellular localisation of the enzyme (Bolger, 1994).

In this section members of PDE4 will be extensively reviewed giving extra emphases on their domain organisation, regulation as well as rolipram binding.

1.6.1 Genomic organisation

As mentioned previously, four PDE4 genes have been reported (PDE4A, B, C, and D). In humans, these genes are distributed on three different chromosomes: chr19p13.1 (PDE4A gene) (Sullivan *et al.*, 1998; Horton *et al.*, 1995), chr1 (PDE4B gene) (Szpirer *et al.*, 1995; Milatovich *et al.*, 1994), chr19p13.2 (PDE4C) (Sullivan *et al.*, 1999), and chr5 (PDE4D) (Milatovich *et al.*, 1994). These genes have been reported to be large approximately 50 kb in length and complex consisting of 18 or more exons at one instance (Sullivan *et al.*, 1998; Sullivan *et al.*, 1999).

The genomic organisation of rat PDE4 genes have been found to be similar to that in humans, suggesting ancestry links (Muller *et al.*, 1996). For instance, sequences of rat PDE4A , PDE4B and PDE4D have been shown to be highly conserved at the intron/ exon boundaries (Horton *et al.*, 1995; Monaco *et al.*, 1994). PDE4 genes have been defined in humans, rats and mice (Muller *et al.*, 1996).

1.6.2 Domain Organisation and the Generation of Splice Variants

Analysis performed on the amino acid sequences of the different PDE4 subtypes have revealed three distinct highly conserved regions. These being two 'upstream conserved regions' of 60 amino acids and 80 amino acids in length better known as UCR1 and UCR2 respectively located at the N-terminus of the isoenzymes, and the catalytic domain located near the carboxyl terminal which is conserved throughout all known PDE families. Highly variable regions called LR1 and LR2 were also identified. LR1 is localised between UCR1 and UCR2 whereas LR2 is localised between UCR2 and the catalytic domain. The function of these regions are thought to provide a subtype specific means of regulating the enzyme's activity by altering UCR1 and UCR2 interaction with the catalytic domain (Houslay, 1998).

Up to 18 different splice variants have been reported to be encoded by the four PDE4 genes. These splice variants have been characterised according to the presence or absence of UCR1 to form the long or the short isoforms respectively (Bolger, 1994; Bolger *et al.*, 1994) as well as the truncation of UCR2 to form supershort isoforms (Sullivan *et al.*, 1998) (figure 1.6). Recently, it has been suggested that N-terminal regions which include UCR1 and in a lesser extent UCR2, may be responsible for the localisation of PDE4 and for the regulation of the enzymatic activity (Muller *et al.*, 1996; Jacobitz *et al.*, 1996). In addition, it has been established that rolipram and cAMP do not bind to the same region in the PDE4 isoenzymes. Rolipram has been identified to interact within the region that lies amongst UCR1 and UCR2 whereas, cAMP has been found to interact exclusively with the catalytic domain (Jacobitz *et al.*, 1996). All PDE4 isoforms known to date are summarised in table 1.3 (Houslay, 2001).

Table 1.3 A summery of all known PDE4 isoforms.

Human	Rat	Isoform Type
4A1 (hRD1)	4A1(RD1)	Supershort
4A4B (pde46)	4A5 (rpde6)	Long
4A7 (2el)	4A7	catalytically inactive
4A8	4A8(rpde39)	Long
(TM3)	(TM3)	Long (putative)
4A10	4A10	Long
4B1	4B1 (DPD)	Long
4B2	4B2	Short
4B3	4B3	Long
4B4	4B4	Long
4C1	4C1	Long
4C2	4C2	Long
4C3	4C3	Long
4D1	4D1	Short
4D2	4D2	Supershort
4D3	4D3	Long
4D4	4D4	Long
4D5	4D5	Long

Adapted from Houslay, 2001.

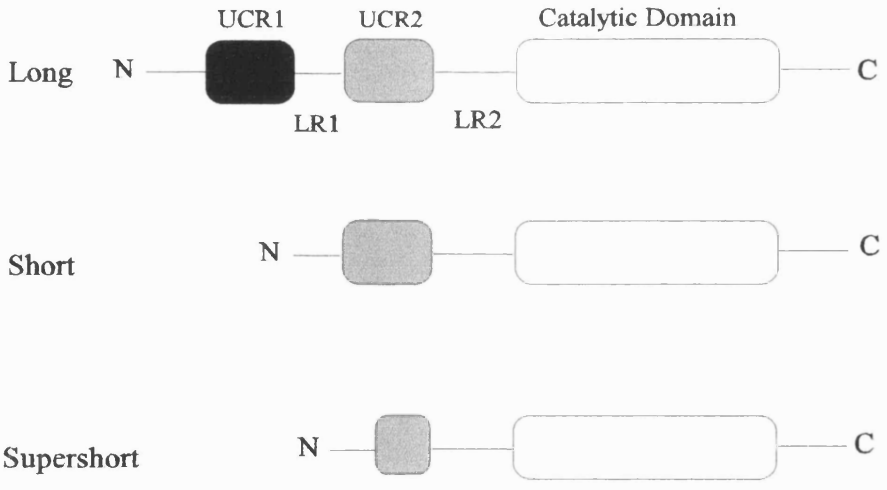

Figure 1.6 A schematic representation of the three forms of PDE4 isoenzymes.

1.6.3 Regulation

Regulation of PDE4 isoenzymes is found to be extremely complex. There does not appear to be endogenous allosterism or small regulator molecules that regulate PDE4 isoenzymes. However, PDE4 isoenzymes are found to be regulated at the transcription level as well as phosphorylation by a number of different types of protein kinases. In Sertoli cells, Conti and co-workers (Swinnen *et al.*, 1989b) have found a 100 fold increase in PDE4D2 mRNA following prolonged exposure to cAMP. More recently, the same group (Sette *et al.*, 1994b) have demonstrated that PDE4D3 are regulated by phosphorylation by protein kinase A. It has been suggested that transcriptional regulation provides a longer term response whereas, regulation by phosphorylation provides short term regulation (Beavo, 1995). It is not clear if both types of regulation are present in the same cell or even if it is the same PDE4 isoenzyme that is being regulated (Beavo, 1995). In Sertoli cells for example, it has been demonstrated that both types of PDE4 regulation are present (Beavo, 1995).

Recently, Houslay and co-workers have demonstrated using two hybrid analysis and pull down assays that UCR1 binds to UCR2 (Beard *et al.*, 2000). This supported the notion that UCR1 and UCR2 form some sort of regulatory module that can influence the structure and the function of the catalytic domain. The mapping for possible interaction sites was performed using several deletion studies. These identified two arginine residues (Arg 98 and Arg 101 in PDE4D3) present at the C-terminus of the UCR1 bound to negatively charged residues (Asp 149, Glu 147 and Glu 146 in PDE4D3) present at the N-terminus of UCR2 by ionic pair formation (Houslay *et al.*, 1998; Beard *et al.*, 2000). However, more interacting residues may be involved in the formation of the UCR1-UCR2 regulating module as it has been demonstrated that UCR1 can bind to a truncated UCR2-PDE4 catalytic unit complex (Beard *et al.*, 2000). Phosphorylation by protein kinase A, may change the conformation of this regulating module. Indeed phosphorylation of serine 54 (PDE4D3) in the motif Arg-Arg-Glu-Ser-Trp present in the UCR1 region or mutation of Ser 54 to Asp has been demonstrated to hinder UCR1-UCR2 interaction (Beard *et al.*, 2000).

A better understanding of the regulatory action of the UCR1-UCR2 regulator modules came about with the study of extracellular-signal-regulated kinase (ERK) phosphorylation of the PDE4 catalytic domain (MacKenzie *et al.*, 2000; Baillie *et al.*, 2000). These kinases which have been shown to play a key role in many physiological processes such as, those associated with cell activation, growth, survival, and differentiation appear to elicit different phosphorylation effects on different forms of PDE4 isoenzymes. It has been shown that ERK phosphorylation elicits activation of the short forms of PDE4 (e.g. PDE4D1 and PDE4B2) which lack the UCR1 region but elicit inhibitory effects of the long forms which contain both UCR1 and UCR2 regions (figure 1.6) (Baillie *et al.*, 2000). Thus it has been suggested that both UCR1 and UCR2 are responsible in orchestrating the functional consequence of the phosphorylation of the catalytic domain by ERK (MacKenzie *et al.*, 2000; Baillie *et al.*, 2000). Furthermore, the switching in the functional output performed by UCR1 and UCR2 were found to be operated by the N-terminal portion of UCR2 as the removal of this region in the supershort form PDE4D2 isoform, ablated the stimulatory effect of ERK phosphorylation, as seen in the short form (MacKenzie *et al.*, 2000; Baillie *et al.*, 2000).

1.6.4 Catalytic Unit

This region was initially identified as mentioned earlier according to sequence homologies between different PDE families. The importance of this region in activity was later confirmed as a single mutation caused the loss of activity (Jin *et al.*, 1992; Jacobitz *et al.*, 1996; Jacobitz *et al.*, 1997). Mutation studies also identified putative Me^{2+} binding sites which are considered to be important for catalysis (Omburo *et al.*, 1998; Jin *et al.*, 1992; Jacobitz *et al.*, 1997). The outer limits of the catalytic domain were identified using truncation analysis (Houslay *et al.*, 1998; Horton *et al.*, 1995; Jacobitz *et al.*, 1996; Owens *et al.*, 1997). For example, the catalytic domain in PDE4A4B was found to span from residues 332 or 365 to residue 680 (Houslay *et al.*, 1998).

The recent publication by Nolte and co-workers (Xu *et al.*, 2000) which described the three-dimensional structure of the catalytic domain of human PDE4B2 isoenzyme has changed our understanding of the catalytic domain of PDEs. In this study the three-dimensional structure solved by X-ray diffraction included residues 152-528 of *HS*PDE4B2

which is equivalent to residues 351-727 on PDE4A4B defined by truncation analyses. This structural analysis showed that the catalytic domain consisted of 17 α helices which subdivided to three sub-domains (figure 1.7). This sub-division of the catalytic domain has provided the possibility of adopting distinct conformational states and thus, explaining how different PDE4 isoforms exhibited different susceptibilities to inhibition by the PDE4-selective inhibitor rolipram when bound to other proteins (McPhee *et al.*, 1999; Yarwood *et al.*, 1999), or phosphorylated by PKA or ERK (Hoffmann *et al.*, 1998; Alvarez *et al.*, 1995), or bound to membranes (Huston *et al.*, 1996; Souness *et al.*, 1992). This supports the notion that different PDE4 conformers are present. The presence of the three sub-domains means that changing the orientation of one or more of the sub-domains to accommodate a certain conformation which is favorable for a particular function can be made easier. This could be achieved for example by changing the orientation of one of the domains in relation to another.

The first sub-domain was found to consist of a bundle of four helices (3, 5, 6, 7) with two short interconnecting helices (2 and 4) and two associated helices (1 and 0). The second domain was found to consist of two short helices (8 and 9) lying perpendicular to a pair of long antiparallel helices (10 and 11). Finally the third sub-domain was found to consist of five helices (12, 13, 14, 15, and 16) where a β-hairpin loop connects helices 12 and 13 (Xu *et al.*, 2000). cAMP was found to bind at a deep pocket of 440 Å in size lined by 21 residues of hydrophobic and negatively charged groups that are found to be conserved amongst all PDE families known to date. Two metal ions (Me^{2+}) have been found to bind at the bottom of the pocket to residues which have also found to be conserved amongst all PDE families (Xu *et al.*, 2000). Although the identities of the metal ions were not determined from the structure, it has been suggested that one of the two ions is Zn^{2+}. This suggestion was proposed due the existing biochemical evidence (Houslay, 1998; Londesbrough, 1985) and known high affinity of PDEs to zinc (Francis *et al.*, 1994). The second metal ion was thought to be Mg^{2+} (Wilson *et al.*, 1994). The motif of PDE was particularly similar to the active site of 3' ,5'-exonuclease of DNA polymerase I Klenow fragment which contained Zn^{2+} and Mg^{2+} ions with similar coordination spheres (Beese and Steitz, 1991).

Using the data provided by this crystal structure, a model was proposed for the binding of cAMP to the catalytic domain. This suggested that cAMP bound in an antiparallel conformation with the adenine base inserted into the lipophilic pocket formed from Leu 393 and Ile 396 present in between helices 13 and 14, Ile 410 and Phe 414 present in helix 14 and Phe 446 present in helix 15a (figure 1.7 and figure 1.9). This allowed the phosphate group to interact with the two Me^{2+} and the 1-N and 6-NH_2 groups to interact with Gln 443 in helix 15a through hydrogen bonding (Xu *et al.*, 2000).

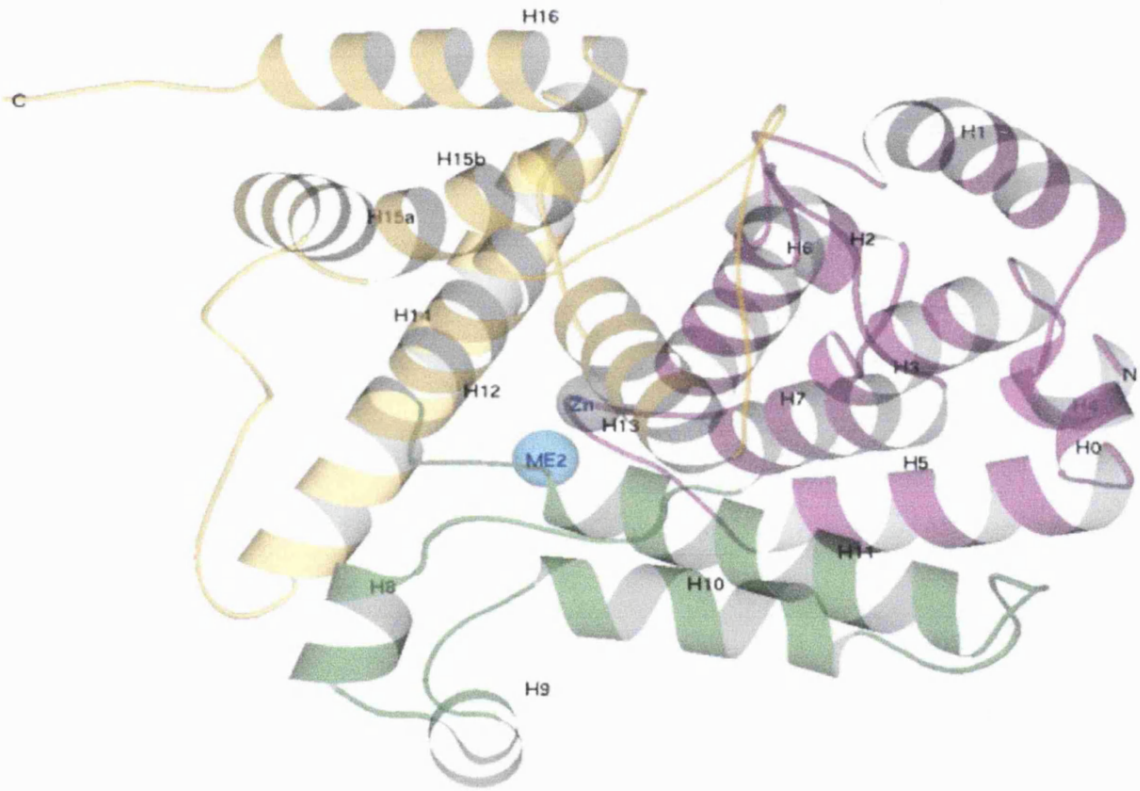

Figure 1.7 Ribbon diagram of PDE4B2B catalytic domain (residues 152 to 489). This diagram is based on information obtained from the crystal structure of PDE4B2 catalytic domain analysed by (Xu *et al.*, 2000) and drawn using the computer program MOLSCRIPT (Kraulis, 1991). ME1 is shown as a grey sphere reported to be occupied by a zinc ion (Xu *et al.*, 2000) and ME2 is shown as a blue sphere. The N-terminus sub-domain of the molecule (residues 152 to 274) is coloured pink, the mid sub-domain (residues 274 to 348) is coloured green and the C-terminus sub-domain (residues 348 to 489) is coloured yellow. H is an abbreviation for helix.

1.6.5 Rolipram Binding

Rolipram (figure 1.8) was originally developed as an anti-depressant. The clinical use of this prototypical PDE4 inhibitor and other analogs were limited due to its many side effects such as, nausea, emesis, gastric acid secretion, and central nervous system activation.

Very little was known on the binding mechanism of rolipram to PDE4 until recently. Rolipram bound to PDE4 isoenzymes with affinities which appear to be different. Originally it was hypothesised that rolipram binds in an allosteric fashion. Later experiments such as truncation of PDE4A (Jacobitz *et al.*, 1996) and proteolytic experiments of *HS*PDE4B2B (Racque *et al.*, 1996) revealed that the low affinity binding of rolipram was solely contained within the catalytic domain whereas, high-affinity binding of rolipram required residues within the catalytic domain and N– and/or C-terminal residues flanking the catalytic domain. It was therefore suggested that residues at the N– and/or C-terminus of PDE4 were required to assume a conformation that binds rolipram at high affinity (Jacobitz *et al.*, 1996). The notion that conformation states of the PDE4 isoenzyme determine the binding capacity to rolipram was strongly supported as factors that were thought to cause conformational change in PDE4 such as protein-protein binding did indeed cause a change in rolipram inhibition. For instance, rather different shifts in rolipram inhibition of PDE4A4 was achieved by complexing with SH3 domains (McPhee *et al.*, 1999). More recently and following the structural determination of the catalytic domain (Xu *et al.*, 2000), new information has given rise to clues to how these different conformational states might have formed. It was predicted that Me^{2+} ions were present in the catalytic domain and might play an important role in the formation of different conformers especially as these ions were in close contact with the three sub-domains. This was indeed confirmed by a study performed by Laliberte *et al.*, 2000 which revealed that Mg^{2+} was responsible for forming two coexisting conformers of PDE4 (apoenzyme: enzyme lacking Me^{2+} ions and holoenzyme: enzyme containing Me^{2+} ions) that bind similarly to cAMP but differently to rolipram. The holoenzyme active site was reported to be the high affinity rolipram binding site of PDE4 (Laliberte *et al.*, 2000). Regions in the catalytic domain that bound to rolipram were mapped. This was performed with the isolation of PDE4 mutants that are insensitive or show very low sensitivity to

rolipram from *S. cervisiae* using heat shock assays (Pilla *et al.*, 1993). These studies revealed that helices 14 and 15 play a key role in conferring sensitivity to rolipram.

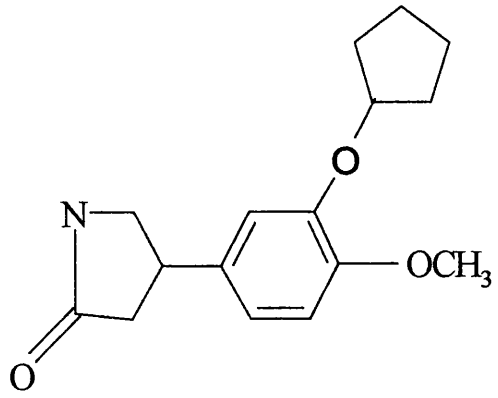

Figure 1.8 Structure of rolipram PDE4 selective inhibitor.

1.7 Rat PDE4A1(RD1)

1.7.1 Discovery

Studies performed by Davis and co-workers nearly 20 years ago on *Drosophila melanogaster,* in my opinion, signified the major starting point for the discoveries in field of PDE4 research. It was revealed that *Drosophila* contained two major forms of cyclic nucleotide PDE activities; one was Ca^{2+}-dependent PDE and the other was cAMP-specific PDE (Davis and Kauvar, 1984). Mutations in the *dunce* gene, which later was found to encoded for the cAMP-specific PDE, caused major deficiencies in learning and memory as well as female sterility (Davis, 1990). These observations prompted the use of the *dunce* gene as a probe to discover similar PDEs in other species. These include distinct cDNA isolated from rat brain (Davis *et al.*, 1989), testis (Swinnen *et al.*, 1989a), and Sertoli cell libraries (Colicelli *et al.*, 1989). The cDNA isolated from rat brain were later called rat *dunce* 1 (RD1), was expressed in yeast (Henkel-Tigges and Davis, 1989). This showed the cDNA to encode a low K_m cAMP-specific PDE with similar properties to that encoded by *Drosophila dunce* gene. However, unlike the *Drosophila dunce* gene, RD1 was inhibited by very low concentrations of rolipram. The response of the rat homologe RD1 to rolipram which is an anti-depressant drug and the specificity of RD1 expression to the brain

(Henkel-Tigges and Davis, 1989) lead to the prediction that RD1 could be involved in mood regulation similar to that reported earlier for *Drosophila dunce*.

Alignment studies revealed that RD1, which corresponded to PDE4A1 using recent nomenclature, shares great similarity (~ 76%), mostly present in the catalytic domain (Henkel-Tigges and Davis, 1989). These studies also revealed great differences in sequences at the N- and C-terminus, suggesting the presence of domains that define the regulation and cellular localisation of these isoenzymes. Indeed that was the case.

1.7.2 Intracellular Targeting

RD1 has been found to exist in the brain in a membrane bound form (Shakur *et al.*, 1995). The intracellular targeting of RD1 isoenzymes was thought to be attributed to unique regions at the N-terminus of the enzyme. This notion was later confirmed by studies performed by Houslay and co-workers on the supershort form rat PDE4A1 (RD1) isoenzyme (figure 1.5) (Shakur *et al.*, 1993; Shakur *et al.*, 1995; Scotland and Houslay, 1995; Smith *et al.*, 1996). These studies demonstrated that the intracellular targeting and membrane association of this isoform was entirely attributed to the unique 25 amino acids located at the N-terminus of the enzyme and not on truncation of the UCR2 or the catalytic region of the isoform as might have been imagined (Smith *et al.*, 1996). For instance, the removal of the first 25 amino acids in the engineered Met^{26}RD1 clone produced a fully functional and soluble enzyme (Shakur *et al.*, 1993; Shakur *et al.*, 1995). Expression studies have indicated that RD1 was not randomly distributed but specifically targeted to the Golgi complex (Shakur *et al.*, 1995; Pooly *et al.*, 1997). Furthermore, these studies showed that this isoform was restricted entirely to the brain (Davis *et al.*, 1989; Bolger *et al.*, 1994), suggesting the involvement of this enzyme in memory and learning as the *dunce* PDE. The three dimensional structure of this unique 25 amino acids has been characterised by ^1H NMR (Smith *et al.*, 1996). This region has been found to consist of two α helices joined by a mobile hinge. It has been found that membrane association was mediated in a Ca^{2+}-dependent fashion through exposing hydrophobic regions identified on the second α helix. Upon binding to Ca^{2+} a conformational change is induced exposing hydrophobic residues which in turn burrow into the lipid bilayer.

1.7.3 Alignment Studies

Figure 1.9 represents the alignment of the catalytic domains of PDE4B2 and Met^{26}RD1. This clearly shows the great similarity between these two isoforms suggesting that their catalytic domains might be assembled in a very similar fashion and probably subject to very similar control mechanisms. However, some differences were also identified which are thought to have some structural consequences on these particular regions in question. Most of the differences were identified between helices 0 and 5. For example, the presence of the proline in the middle of helix 0 in Met^{26}RD1 suggests the absence of this helix in Met^{26}RD1 isoenzyme as proline is likely to disrupt the formation of this helix. In helix 2, neutral amino acids in PDE4B2 are swapped for more charged amino acids in Met^{26}RD1 protein suggesting change in this region. In helix 3, there is a proline at the start of this helix in PDE4B2 which is absent in Met^{26}RD1 helix 3 suggesting structural differences in this region. Furthermore, there is a proline at the inter-region between helix 4 and 5 in Met^{26}RD1 and not in PDE4B2 again suggesting structural differences between the two isoenzymes at this particular region. Regions between helix 5 and 16 are generally found to be identical except for the present of a proline at the start of helix 14 in Met^{26}RD1 which might be of some importance in rolipram inhibition as this region as previously stated maps to the binding site for rolipram. Furthermore, there is a proline residue at the inter-region between helix 16 and 17 near the start of helix 17 in Met^{26}RD1 which is absent in PDE4B2. Some profound differences were also found between other members of the PDE4 family at this region suggesting that the structure of the catalytic domain could be rather different between the different members of the PDE4 family. This is predicted to have some functional differences as this region has been mapped to be the docking region for ERK (Phe-Gln-Phe amino acid sequence) and the region for possible phosphorylation at the serine in the amino acid sequence Gln-Ser-Pro. This region is also near helices 14 and 15a/b in which mutations in these helices have been found to abolish rolipram inhibition. Therefore it is fair to reiterate that those changes in the sub-domains between Met^{26}RD1 and PDE4B2 may contribute to alterations in the conformation of the enzyme which can cause differences in the level of rolipram inhibition and regulation by the regulatory domains.


PDE4B2B 69 SVSEMASNKFKRMLNRELTHLSEMSRSGNQVSEYISNTFLDKQNDVEIPSPTQKDREKK- 127
Met26RD1 26 ----------MLNRELTHLSEMSRSGNQVSEYISNTFLDKQNEVEIPSPTPRQRAFQQ 73
Helix-0
Helix-1
PDE4B2B ------KKQQLMTQISGVKKLMHSSSLNN--TSISRFGVNTENEDHLAKELEDLNKWGLN 179
Met26RD1 PPPSVLRQSQPMSQITGLKKLVHTGSLN---TNVPRFGVKTDQEDLLAQELENLSKWGLN 130
Helix-2
Helix-3
Helix-4
Helix-5
Helix-6
PDE4B2B IFNVAGYSHNRPLTCIMYAIFQERDLLKTFRISSDTFITYMMTLEDHY-HSDVAYHNSLH 238
Met26RD1 IFCVSEYAGGRSLSCIMYTIFQERDLLKKFHIPVDTMMMYMLTLEDHY-HADVAYHNSLH 189
Helix-6
Helix-7
Helix-8
Helix-9
PDE4B2B AADVAQSTHVLLSTPALDAVFTDLEILAAIFAAAIHDVDHPGVSNQFLINTNSELALMYN 298
Met26RD1 AADVLQSTHVLLATPALDAVFTDLEILAALFAAAIHDVDHPGVSNQFLINTNSELALMYN 249
Helix-10
Helix-11
Helix-12
PDE4B2B DESVLENHHLAVGFKLLQEEHCDIFMNLTKKQRQTLRKMVIDMVLATDMSKHMSLLADLK 358
Met26RD1 DESVLENHHLAVGFKLLQEENCDIFQNLSKRQRQSLRKMVIDMVLATDMSKHMTLLADLK 309
Helix-12
β-hairpin
Helix-13
Helix-14
PDE4B2B TMVETKKVTSSGVLLLDNYTDRIQVLRNMVHCADLSNPTKSLELYRQWTDRIMEEFFQQG 418
Met26RD1 TMVETKKVTSSGVLLLDNYSDRIQVLRNMVHCADLSNPTKPLELYRQWTDRIMAEFFQQG 369
Helix-14
Helix-15a
Helix-15b
Helix-16
PDE4B2B DKERERGMEISPMCDKHTASVEKSQVGFIDYIVHPLWETWADLVQPDAQDILDTLEDNRN 478
Met26RD1 DRERERGMEISPMCDKHTASVEKSQVGFIDYIVHPLWETWADLVHPDAQDILDTLEDNRD 429
Helix-16
Helix-17
PDE4B2B WYQSMIPQSPSPPLDEQ----NRDCQGLMEKFQFELTLDEEDSEGPEKEG 524 (40) 564
Met26RD1 WYHSAIRQSPSPPLEEEP--GGLGHPSLPDKFQFELTLEEEEEEDSLEVP 477 (133) 610

Figure 1.9 Alignment of catalytic domains of PDE4B2 (CN4B-Human) and $Met^{26}RD1$ (CN4Z -Rat). Underlined sequences represent position of the helixes. Alignment was performed using the computer program SRS Clustal-W. The dotted bold lines represent the boundaries of the region analysed structurally by (Xu *et al.*, 2000). Abbreviations are: (a) in red represents amino acids interacting with cAMP , (w) in blue represents amino acids interacting with water and (m) in green represents amino acids interacting with metal ions.

1.7.4 Aim of Study

It is clear from the discussion above, that PDE4 isoenzymes have been characterised biochemically and physiologically. However, despite the recent information provided by the crystal structure of the catalytic domain of PDE4B2, the precise nature by which these enzymes are regulated by the regulatory module, or by phosphorylation, and inhibition by rolipram are still not fully understood.

Thus, the main aim of this project is to express the full length of RD1 (Met^{26}RD1) in a system capable of producing stable, soluble and active enzyme in quantities necessary for X-ray crystallography. Met^{26}RD1 encodes for the supershort form of RD1 (PDE4A1) missing the first 25 amino acids. The removal of the first 25 amino acids was necessary to express the protein in a soluble form as these amino acids were found to attach the isoenzyme to membranes. The structural information obtained from this protein will provide vital clues into the mechanisms in which both the activity and inhibition are regulated in these enzymes.

This study will describe the cloning and expression of Met^{26}RD1 in two expression systems; bacterial and mammalian. The choice of expression system depended on the capability for expression and the potential for scale up. Scaling up of the expression system was important as the ultimate aim was to produce milligram quantities of the protein to enable crystallisation and structural analysis.

The first system to be described will be a bacterial system. Met^{26}RD1 will be expressed as a Glutathione S-transferase (GST) fusion protein in *Escerichia coli*. This study mainly focused on the optimisation of expression and purification of the protein using Glutathione affinity chromatography.

The insoluble Met^{26}RD1 fusion protein produced by expression in bacteria will be used to raise antibodies in rabbits. Antibody production is necessary due to the unavailability of commercial antibodies against this protein. The antibody will help to analyse the expressed recombinant protein in subsequent studies.

The second expression system that will be described is the Semliki Forest virus (SFV) system. This system will allow the expression of $Met^{26}RD1$ in mammalian cells using SFV viral replicon. Details of the system will be explained in individual chapters. Initial studies will focus on the optimisation of the system using *β-galactosidase* reporter gene. Subsequent studies will concentrate on obtaining heterologous $Met^{26}RD1$. This will involve the expression of $Met^{26}RD1$ in Baby Hamster Kidney cells (BHK-21) using recombinant SFV. Following expression of $Met^{26}RD1$, biochemical analyses will be performed to obtain, K_m, V_{max} and IC_{50}. A variety of inhibitors will be used to confirm the authenticity of the protein. Further, analyses on the molecular state of the protein and preliminary purification of $Met^{26}RD1$ using a column prepared from antibodies raised against the protein produced in bacteria will be also described.

Chapter 2

Materials And General Methods

This chapter consists of standard and general techniques used in the laboratory throughout the duration of the practical work. More specific techniques and methodologies that have been developed during this project are mentioned in other relevant chapters.

2.1 Materials

2.1.1 Reagents

2.1.1.1 Chemical Reagents

All chemical reagents used were AnalaR grade or Molecular biology grade purchased from either Sigma or BDH unless otherwise stated. Most solutions were prepared in distilled water. In experiments involving Molecular Biology, autoclaved distilled water purified using the Millipore Milli-Q system was used and in mRNA experiments Milli-Q water treated with diethyl pyrocarbonate (DEPC) was used. Solutions were sterilised by either autoclaving the solution for 20 minutes at 121°C or by passing the solution through a Millex-FG_{50} 0.22 μm membrane purchased from Millipore in a procedure called filter sterilisation. Solutions were stored at room temperature unless otherwise stated by manufacturer.

2.1.1.2 DNA Reagents

Bam HI and *Sma* 1 restriction enzymes, and *Taq* I polymerase were purchased from Promega, and *Spe* 1 restriction enzyme was purchased from Amersham Pharmacia, and Calf intestinal alkaline Phosphatase was purchased from Boehringer Mannheim.

PCR primers were synthesised by Oswel DNA service, University of Southampton. Sequencing primers were synthesised by Genset oligos, GENSET Corp, 505 Coast Blvd., South, La Jolla, CA 92037, USA.

The following vectors were used throughout this project:

pSVL*Met*^{26}*RD1* plasmid containing rat *dunce* Phosphodiesterase 4 gene cDNA was supplied kindly by Prof. Miles D. Houslay (Department of Biochemistry, University of Glasgow).

pSFV-3 mammalian expression vector containing *β-galactosidase* reporter gene and **pSFV-1** mammalian expression vector were both purchased from Gibco BRL Life Technologies.

Helper 2 vectors were kindly sent by Henrik Garof (Department of Molecular Biology, Karolinska Institute, 14137 Huddinge, Sweden).

pSV-*β*gal vector carrying the *β-galactosidase* reporter gene was purchased from Promega.

pGEX 3X vector carrying the gene for Glutathione S-transferase GST fusion protein was purchased from Pharmacia.

Maps of mentioned vectors are shown in relevant chapters.

1 Kb DNA Ladder DNA size markers were purchased from Gibco BRL with a concentration of 1.88 μg/μl. These markers contained 22 DNA fragments ranging in size from 75 bp to 12,216 bp.

2.1.1.3 mRNA Reagents

rNTP, RNasin, SP6 RNA Polymerase that comes with 100 mM DTT and its own buffer were purchased from Promega. DEPC was purchased from BDH.

mRNA size marker (7.5 single strand) and mRNA capping reagent were purchased from Gibco BRL.

2.1.1.4 Protein Reagents

PMSF, Benzamidine, TPCK, TLCK, Leupeptin, Pepstatin, BSA, SDS, β 2-Mercaptoethanol, DTT, bromophenol blue, Coomassie Blue R250, APS, TEMED, Protein-A Agarose, Protein-A Sepharose C12, and α-Chymotrypsin were from Sigma. Aprotinin was from Fluka. Bradford reagents were from BioRad. IPTG and X-gal were from Melfords.

The chromatography resin Q-Sepharose and Sephacryl S200HR were from Pharmacia.

Prestained protein size markers were purchased from BioLabs. These markers contained purified proteins covalently coupled to a blue dye that resolved into 8 bands of even intensity when electrophoresed. These bands represent MBP-β-galactosidase (*E.coli*) 175 KDa, MBP-paramyosin (*E.coli*) 83 KDa, Glutamic dehydrogenase (bovine liver) 62 KDa, Aldolase (rabbit muscle) 47 KDa, Triosephosphate isomerase (rabbit muscle) 32 KDa, β-Lactoglobulin A (bovine milk) 25 KDa, Lysozyme (chicken egg white) 16.5 KDa, Aprotinin (bovine lung) 6.5 KDa.

β-galactosidase 117 KDa, Bovine Serum Albumin (BSA) 66 KDa, and Ovalbumin 45 KDa purified single proteins were purchased from Sigma and used as protein size markers for SDS gels.

2.1.1.5 Phosphodiesterase Assay Reagents

Snake Venom, Dowex 1x 8 (100g mesh), cAMP, cGTP, Rolipram, and Vinpocetine were from Sigma. [^{3}H]-cAMP was purchased from Amersham Pharmacia.

2.1.1.6 Bacterial Growth Media

Luria Broth (LB) (Miller's Broth Base) was purchased from Gibco BRL.

2.1.1.7 Tissue Culture Cells and Reagents

All reagents were purchased from Sigma except for Fetal Calf/ Bovine serum was purchased from Gibco BRL.

Chinese Hamster Ovary (CHO, ECACC Number 85050302) and Baby Hamster Kidney (BHK-21; C13; ECACC Number 85011433) cells were purchased from the European Collection of Cell Cultures as frozen ampoules.

2.2 Methods

2.2.1 Bacterial Manipulation

2.2.1.1 Growth Media and Stock Solutions

1x Luria-Bertani (LB)

Growth media was prepared by suspending 25 g of Luria-Bertani (LB) (Miller's Broth Base) in 1L of distilled water to make a 1x stock. The mixture was autoclaved for 20 minutes at 121°C and stored at room temperature until used.

Ampicillin (50 mg/ml) Stock Solution

Ampicillin purchased from Sigma was dissolved in autoclaved Milli-Q water to form the concentration stated. The solution was filter sterilized into aliquots and stored at -20°C until used.

LBA Media (Luria-Bertani (LB) Supplemented with 50 μg/ml Ampicillin)

Following the preparation of 1x growth media as described above, ampicillin was added to a final concentration of 50 μg/ml.

LBA Plates (Luria-Bertani (LB) Agar Supplemented with 50 μg/ml Ampicillin)

25 g of Luria-Bertani (LB) was dissolved in 1 L Milli-Q water and 15 g of agar was added and autoclaved. The mixture was cooled to 50°C and ampicillin was added to a final concentration of 50 μg/ml. The mixture was divided between 40 petri plates. Plates were stored at 4°C for up to 2-3 weeks.

2.2.1.2 *E.coli* Strains used and Their Genotypes

DH5α *supE44Δ lacU169(ϕ80lacZΔM15) hsdR17 recA1 endA1 gyrA96 thi-1 relA1*

DH5α a recombinant-deficient suppressing strain was used for plating, plasmid propagation and cloning. The presence of *ϕ80lacZΔM15* gene allowed α-complementation with the amino terminus β-galactosidase encoded by some of the plasmids used in this project (e.g. pSFV3 *LacZ*). This ultimately helped in the cloning procedures performed at the beginning of the project. This bacterial strain was kindly provided by Dr Dean Nizetic based at The School of Pharmacy/University of London.

JM109(DE3) *recA1 supE44 endA1 hsdR17 gyrA96 relA1 thi Δ(lac-proAB) F'[traD36proAB+, lacI^q, lacZΔM15], (λcIts 857, indI, Sam 7, nin 5, Lac UV5-T7 gene1)*

This bacterial strain purchased from Promega was used to express GST- Met^{26}RD1 fusion protein described in chapter 3.

Stocks of these two strains of bacteria were prepared by mixing 600 μl of fresh overnight culture with 400 μl of sterile glycerol (sterilised by autoclaving) to make up a 40% mix, in a sterile 1.5 ml eppendorf tube. At least 5 samples were prepared at any given time and stored at -80°C. Stocks have been found to be stable for several months to one year. Each year, stocks were replaced by fresh stocks.

2.2.1.3 Preparation of Bacterial Competent Cells using Calcium Chloride

10 ml of LB medium was inoculated with a single colony of *E. coli* bacterial cells and incubated agitating at 200 rpm overnight at 37°C. 1ml of the overnight culture was used to inoculate 50 ml of LB medium in a 500 ml sterile conical flask. The mixture was incubated at 37°C agitating at 200 rpm until the OD_{600} reaches 0.5 (The OD was checked by transferring 1 ml sample into 1 ml cuvette and measuring the OD with a CECIL 2021 2000 series spectrophotometer hourly). Cells were centrifuged using a Sigma 6K10 benchtop centrifuge with swing out rotor (No 11162) set to centrifuge at 2400 *g* for 25 minutes at 4°C. Cells were re-suspended very gently in 25 ml of ice-cold 50 mM $CaCl_2$ and left on ice for 30 minutes. Pellets were collected as before and re-suspended in 2 ml of ice-cold 50 mM $CaCl_2$ containing 50 % sterile ice-cold glycerol. The cell suspension was mixed, aliquoted into 100 µl volumes and added to pre cooled 1.5 ml eppendorf tubes. Samples were frozen very rapidly in liquid nitrogen supplied by BOC and stored at -80°C until used. Both DH5α and JM109 (DE3) competent cells were prepared in this way and stored for up to one year with a loss of only 10% in competency.

2.2.1.4 Transformation of Competent Bacterial Cells

The cells used were made competent using $CaCl_2$. 100µl aliquot of competent cells was rapidly thawed and aliquoted into 20 µl volumes into pre-chilled 1.5 ml sterile microcentrifuge tubes. 1-10 ng of DNA or 10 µl of ligation mix was added to each aliquot and incubated on ice for 30 minutes. The cells were heat shocked by placing the tubes in a 42 °C water bath for 40 seconds. The tubes were placed on ice for 2 minutes and 80 µl of LB media was added to each tube. Cells were incubated agitating at 37°C for 1h and were plated without dilution on LBA plates. Plates were incubated inverted overnight at 37 °C.

2.2.2 DNA Manipulation

2.2.2.1 Plasmid Preparation

2.2.2.1.1 Small Scale Preparation (Miniprep)

This method was adopted when large number of transformants were being screened. Single colonies were picked using a sterile pipette tip and inoculated into 3 ml of LB containing the appropriate antibiotic. Cultures were incubated overnight at 37°C agitating at 200 rpm. 1.5 ml of the overnight culture was centrifuged using a 5415C eppendorf microcentrifuge set to centrifuge at 14 000 *g* for 1 minute. Cells were lysed and plasmids were purified as manufacturer's instructions using kits purchased from Promega. This method is based on the alkaline lysis method with a few modifications. Briefly, the medium was removed and the bacterial pellet was resuspended in 100 µl of chilled resuspension buffer (25 mM Tris-HCl pH 8.0, 10 mM EDTA, 50 mM glucose). The resuspension was incubated at room temperature for 5 minutes and 200 µl of lysis buffer (0.2 M NaOH, 1% SDS) was added and mixed by inverting 4-6 times. 150 µl of chilled neutralisation buffer (3.0 M potassium acetate pH 4.8) was added to neutralise the lysate. The solution was mixed by inversion and the mixture was incubated on ice for 5 minutes. Following the incubation period, the mixture was centrifuged using a 5415C eppendorf microcentrifuge set to centrifuge at 12 000 *g* for 5 minutes and the supernatant was added to a spin column provided by the Promega kit. The column was washed twice with 1 ml of wash buffer (190 mM potassium acetate, 20 mM Tris-HCl pH 7.5, 5 mM EDTA, 55% ethanol) to release any contaminating molecules (e.g. proteins) which might have bound to the column. Solutions were pushed through the column using 5 ml syringe. Plasmids were eluted in 50 µl of Milli-Q water (heated to 65°C) by placing the column in a 1.5 ml microcentrifuge tube and centrifuging using a 5415C eppendorf microcentrifuge set to spin at 14 000 *g* for 1 minute.

2.2.2.1.2 Large Scale Preparation (Midiprep and Maxiprep)

This method was used to prepare plasmid stocks for subsequent expression studies, cloning, or DNA sequencing. A single colony was picked and inoculated into 10 ml of LB containing

the appropriate antibiotic. The small culture was incubated for 7 to 8 hours at 37°C agitating at 300 rpm. 0.1 to 0.7 ml or 0.5 to 1 ml of small culture was inoculated into 100 ml (Midiprep) or 500 ml (Maxiprep) of LB media containing the appropriate antibiotic respectively. Cultures were incubated overnight at 37°C agitating at 300 rpm. Cells were harvested by centrifugation at 2500 *g* for 30 minutes at 4°C using a Sigma 6K10 benchtop centrifuge with fixed angle rotor (No 12500). Plasmids in each case were purified as manufacturer's instructions using kits purchased from Qiagen. This method is based on the alkaline lysis method with a few modifications. Briefly, the medium was removed and the bacterial pellet was resuspended in 4 ml (Midiprep) or 10 ml (Maxiprep) of chilled resuspension buffer (50 mM Tris-HCl pH 8.0, 10 mM EDTA, 100 μg/ml RNase A). 4 ml (Midiprep) or 10 ml (Maxiprep) of lysis buffer (200 mM NaOH, 1% SDS) was added to the resuspension and mixed thoroughly by inverting 4 to 6 times. The mixture was incubated at room temperature for 5 minutes or until the mixture appeared viscous. Following the incubation period, 4ml (Midiprep) or 10 ml (Maxiprep) of chilled neutralisation buffer (3 M potassium acetate pH 5.5) to neutralise the lysate. The solution was mixed by inversion and the mixture was incubated on ice for 15 minutes (Midiprep) or 20 minutes (Maxiprep). Following the incubation period, the mixture was centrifuged at 20 000 *g* using a Beckman centrifuge and a JA-20 rotor for 30 minutes at 4°C and the supernatant containing the plasmid DNA was removed promptly. The supernatant was applied to a pre-equilibrated QIAGEN-tip 100 (Midiprep) or QIAGEN-tip 500 (Maxiprep) with equilibration buffer (750 mM NaCl, 50 mM MOPS pH 7.0 15% isopropanol, 0.15% Triton X-100). The columns were washed twice with 10 ml (Midiprep) or 20 ml (Maxiprep) of wash buffer (1.0 M NaCl, 50 mM MOPS pH 7.0, 15% isopropanol) to release any contaminating molecules (e.g. proteins and carbohydrates) which might have bound to the column. DNA was eluted with 5 ml (Midiprep) or 15 ml (Maxiprep) of elution buffer (1.25 M NaCl, 50 mM Tris-HCl pH 8.5, 15% isopropanol). Following elution of the DNA molecules from the columns 3.5 ml (Midiprep) or 10.5 ml (Maxiprep) (0.7 volumes)of isopropanol was added and the solutions were mixed and centrifuged immediately at 15 000 *g* for 30 minutes at 4°C using a Beckman centrifuge and a JA-20 rotor. The supernatant was carefully decanted and the DNA pellet was resuspended in 2 ml (Midiprep) or 5 ml (Maxiprep) of 70% ethanol. The resuspension was centrifuged at 15 000 g for 10 minutes at 4°C using a Beckman centrifuge and a JA-20 rotor. The supernatant was carefully decanted without disturbing the pellet and the pellet was air dried for 30-60 minutes. The DNA pellet was resuspended in 250-500 μl of Milli Q water and stored at -20°C.

2.2.2.2 Digestion of DNA using Restriction Endonuclease Enzymes

Digestion reactions using endonuclease enzymes were used firstly to determine the identity of genes and plasmid DNA by restriction mapping and secondly to form sticky ends. 0.4-1 μg of plasmid DNA was digested in a 10-50 μl reaction containing 1-5 μl of 10x enzyme buffer, Milli Q water, and the restriction enzyme(s) prepared in such a way to give a ratio of 1 unit enzyme per 1 μg of DNA. Reactions were incubated for 1-18 hour at 37 °C using a fixed temperature program set up in a Biometra personal cycler (with heated lid) and were stored at -20°C until analysed. Generally restriction enzymes used were purchased from Promega or Gibco BRL. In most cases, buffers used were of that recommended and supplied by the manufacturer. But in the case of cloning (performed in this project) for example where two different restriction enzymes were needed to cut a single DNA sample simultaneously, a restriction enzyme buffer purchased from Promega called MultiCore was used. This buffer was found to be suitable for digesting the DNA with *Sma* 1 and *Bam* H1 restriction enzymes.

2.2.2.3 DNA Purification using Wizard™ DNA Clean-up Kit

DNA fragments that have undergone manipulations such as digestion or amplification were cleaned using Wizard™ DNA Clean-up System supplied by Promega which uses the alkaline lysis method to purify DNA but eliminating the need for organic extraction, gradient and differential precipitation by employing a proprietary silica-based resin (Wizard® DNA Clean-up resin) to bind to the plasmid DNA. The procedure followed instructions supplied by the manufacturers (Promega). Briefly, 1 ml of Wizard® DNA Clean-up resin was added to 1.5 ml microcentrifuge tube and 100 μl of DNA sample was added. Following gentle mixing the resin-DNA mixture was transferred to a 3 ml disposable syringe connected to a Wizard® Mini-column. The resin-DNA mixture was pushed into the Mini-column by attaching and pushing the syringe plunger. The DNA present in the Mini-column was then washed with 2 ml of 80% isopropanol and the Mini-column was detached from the syringe and placed in a 1.5 ml microcentrifuge tube. Access liquid in the column was removed by centrifugation at maximum speed (14 000 *g*) using a 5415C eppendorf microcentrifuge. The Mini-column was transferred to a clean microcentrifuge tube and DNA was eluted in 50 μl of Milli Q water by a 20 second centrifugation at maximum speed (14 000 *g*) using a 5415C eppendorf microcentrifuge.

2.2.2.4 DNA Sequencing

GST-Met^{26}RD1 and pSFV-1Met^{26}RD1constructs were sequenced in house in both directions using an ABI PRISM 310 with Integrated Thermal Cycler manufactured by PE Applied Biosystems. The sequencing method employed was based on the chain-terminator technique using four distinct fluorophore tags attached to the four chain-terminator nucleotides. The products of the four chain-terminator reaction were electrophoresed through a thin polymer where they passed a detector allowing the nucleotides to be scanned in an automated fashion.

Sequencing reactions were prepared to contain 300 ng of double stranded GST- Met^{26}RD1 or pSFV-1Met^{26}RD1 constructs, 3.2 pmole of sequencing primer, 8 µl of terminator ready reaction mix and water to bring the reaction up to 20 µl.

The sequencing primers used were:

Forward primers

S1F 5'-ATATAACAGTGGTGGAAGTGGCAGAG-3'
RD1f 5'- ATATAGGATCTAAGCCGCCACCATGGTGAACCGTGAGCTCAC-3'

Reverse Primers

S1B 5'-TATATGTCCTCTTGATCTGTCTTGAC-3'
RD1b 5'-ATATGAATTCCCCGGGTCAGGATCAGGCAGGGTCTCCGC-3'

Using these four primers, the majority of the *Met^{26}RD1* gene cloned into either pGEX-3X and pSFV-1 plasmids was sequenced as up to 700 bp were produced per sequencing primer per sequencing reaction. Regions sequenced and annealing positions of these primers are shown in Appendix 2.

2.2.2.5 Agarose Gel Electrophoresis for DNA Analysis

50x TAE electrophoresis buffer	242 g Tris base, 57.1 ml Glacial Acetic Acid, 37.2 g $Na_2EDTA.2H_2O$ were mixed in 1 L of distilled water. The solution was autoclaved and stored at room temperature for up to one year without any change in consistency.
Ethidium bromide solution	10 mg/ml stock solution stored at 4°C was purchased from Sigma.
10x Loading buffer	20 % glycerol, 0.1 M Na_2EDTA pH 8.0, 1 % SDS, 0.25 % Bromophenol Blue were mixed in distilled water and was stored at room temperature.

DNA was analysed on 0.8 % (w/v) of agarose gels. Agarose was dissolved in 1x TAE buffer by boiling in a microwave oven. Once the gel cooled down to about 45°C, ethidium bromide (EtBr, 10 mg/ml stock solution) was added to a final concentration of 5 μg/ml to stain DNA fragments as they run through the agarose gel. The molten gel was poured into a horizontal gel mould and 8 or 15 well comb was placed on one side of the cast about 1 cm from the edge. The gel was left to set for 10 minutes at room temperature and placed in a BioRad/ Mini Sub DNA Cell electrophoresis tank containing 1x TAE buffer supplemented with EtBr to a final concentration of 5 μg/ml. The comb was removed and DNA samples mixed with a fifth of their volume with loading buffer, were loaded into the wells. 0.1 μg of 1Kb DNA ladder (Gibco BRL) was loaded into one of the wells and was used as a molecular size marker. The gel was run at 60 V for ~ 45 minutes or until the blue dye front had migrated about three quarters of the gel. DNA bands were visualised using a LKB 2011 Macrowview UV transillumenator and were photographed using a black and white Polaroid camera type 667 film.

2.2.3 Protein Manipulation

2.2.3.1 Concentration of Protein Samples Using Chloroform/Methanol Method

This method was based on the approach introduced by Cik *et al*, 1993. The method was used to concentrate protein samples prior to analysis using SDS polyacrylamide gel electrophoresis (PAGE). 150 µl of protein sample was transferred into a 1.5 ml eppendorf tube and 4 volumes (i.e. 600 µl) of methanol, 1 volume of chloroform, and 3 volumes of Milli Q water were added sequentially. The protein sample was mixed by vortex for 2 seconds after each addition and pulse centrifuged at maximum speed 14 000 *g* in a 5415C eppendorf microcentrifuge to spin down any droplets formed as a result of the vortex. The mixture turned a cloudy white colour following the addition of water. This was due to the precipitation of the proteins present in the sample. This precipitant appeared at the interface between the organic bottom layer and the aqueous top layer once centrifuged for 1 minute at maximum speed 14 000 *g* in a 5415C eppendorf microcentrifuge. The top layer was removed carefully so as not to disturb the white interface and 1 volume of methanol was added. The sample was mixed by vortex for 2 seconds and centrifuged for 4 minutes at maximum speed 14 000 *g* in a 5415C eppendorf microcentrifuge to pellet the precipitated proteins. The liquid around the pellet was removed and pellet was dried under vacuum for ~ 30 minutes. 15 µl of 1x SDS (1:5 dilution of 5x SDS loading buffer see section 2.2.3.2) loading buffer was added and mixed by vortexing. Samples were boiled using a boiling bath for 5 minutes, centrifuged at 14 000 *g* for 3 seconds using a 5415C eppendorf microcentrifuge and either stored at - 20°C or loaded directly onto polyacrylamide gels after the addition of DTT to a final concentration of 100 mM.

2.2.3.2 Protein Analysis by SDS PAGE

Stock Solutions used were stored at room temperature and were stable between to 1-2 years.

2x SDS loading buffer 0.3 M Tris pH 6.8, 2 % SDS (w/v), 20 % glycerol (w/v), 0.01% bromophenol blue (w/v).

5x SDS loading buffer	0.3 M Tris pH 6.8, 5 % SDS (w/v), 20 % glycerol (w/v), 0.01% bromophenol blue (w/v).
Protogel	30 % acrylamide (w/v), 0.8 % bisacrylamide (w/v) purchased from National Diagnosis.
10x running buffer	144 g Glycine, 30.3 g Tris, and 10 g SDS dissolved in 1 L of distilled water.

The method used was based on the method introduced by Laemmli (1970). Sodium dodecyl sulphate (SDS), a detergent used in protein analysis as it binds to most proteins at a ratio of approximately of one SDS molecule to two amino acid groups causing the proteins to assume a rod-like shape. The strong negative charge of the SDS molecules masks the intrinsic charge of the proteins so that SDS treated proteins have similar shapes and equal charge to mass ratios. Therefore, the electrophoresis of proteins in SDS containing polyacrylamide gels would separate proteins according to their molecular mass due to its filtration effect.

SDS PAGE was performed in a Hoeffer Mighty small II SE250 mini gel protein apparatus. 7.5-10 % resolving gel was prepared as shown in table 2.1 and was overlaid firstly with gel buffer to keep the surface area even while it polymerises and secondly with stacking gel prepared as in table 2.1. The percentage resolving gel used was adequate to resolve proteins of sizes ranging between 100-60 kDa. The resolving gel prepared was left to polymerise for approximately 1 hour at room temperature and the stacking gel was left to polymerise at room temperature for about 15 minutes after inserting a 10 or 15 well comb.

Meanwhile, protein samples to be loaded on the gels were prepared. Protein samples were either concentrated using Chloroform/Methanol method as described in section 2.2.3.1. or loaded directly on gels after being mixed with 5x SDS loading buffer to a final 1x solution. DTT was added to a final concentration of 100 mM to reduce the disulphide bonds present in proteins so that all of the constituent polypeptides in multisubunit molecules can be analysed separately. Samples were boiled for 10 minutes using the thermocycler and were loaded on the gels.

After the stacking gel had set, it was placed in 1x running buffer vertically and the comb was removed. The wells were cleaned using running buffer to remove traces of acrylamide that might have been present. Protein samples were loaded and gels were run initially at 60 V, 20 mA until samples run into the resolving gel and at 110 V, 30 mA until dye front reaches about 1-2 mm from the bottom of the gel. Protein gels were stained with either Coomassie Brilliant Blue R-250, Silver stain or both to visualise the protein bands.

Table 2.1 Components of SDS Polyacrylamide gels.

	Stacking Gel	**10% Resolving Gel**	**7.5% Resolving Gel**
Autoclaved Milli Q water	2.75 ml	3.75 ml	8.4 ml
1 M Tris pH 8.8	----------	6 ml	11.2 ml
1 M Tris pH 6.8	0.676 ml	----------	----------
Protogel (Page 48)	0.867 ml	5 ml	7.5 ml
10 % SDS	52 µl	120 µl	0.3 ml
TEMED	5.2 µl	12 µl	10 µl
10 % APS	52 µl	120 µl	100 µl

Volumes shown for the stacking gel and the 10 % resolving gel were enough to prepare 2 mini gels. Volumes shown for the 7.5 % resolving gel were enough to prepare about 5 mini gels.

2.2.3.3 Staining of SDS polyacrylamide Gels

Once the polyacrylamide gels were run the gels were stained to visualise the protein bands. Two staining methods were used during this project. Each of which had different sensitivities to the protein staining. Coomassie Brilliant Blue R-250 stained proteins blue and detected proteins in microgram quantities. Gels containing less than this amount of protein were detected using silver stain, which was approximately 50 times more sensitive but was more difficult to apply. Most gels were stained with Coomassie stain first and then stained with silver stain if the Coomassie failed to visualise the desired protein bands. Gels following silver stain were kept in 5% acetic acid in the dark overnight at 4°C and washed with water and

preserved by drying under vacuum onto Whatman 3MM paper using a Howe GELVAC slab dryer.

2.2.3.3.1 Coomassie Brilliant Blue Stain

Coomassie Brilliant Blue Stain	0.2% Coomassie Brilliant Blue R-250 (w/v), 30% Methanol (v/v), 10% Acetic Acid (v/v). Filtered through Whatman filter paper and stored at 4°C.
Destain solution	30% Methanol (v/v) and 10 % Acetic Acid (v/v). Stored at room temperature in a sealed container.

Gels were soaked rocking in a small container containing Coomassie Brilliant blue s for 30 minutes at room temperature. This fixed the proteins in the gel by denaturing them and allowed the dye to complex with the proteins. The Coomassie stain was removed and retained for reuse. Excess dye was washed away by many changes of destain solution until protein bands were apparent. Once protein bands were visible, the destain solution was discarded and background stain minimised. Gels were stored in distilled water at 4°C until dried.

2.2.3.3.2 Silver Stain

All solutions were prepared prior to use and were made up in Milli Q water.

Fixing Solution	10 % glutaraldehyde (v/v).
Silver stain	0.5 % Silver Nitrate (w/v).
Developer	3 % Na_2CO_3 (w/v), 0.01 % Formaldehyde (v/v).

For best results gels were stained with Coomassie stain and destained completely before silver staining. This helped to fix the protein bands before silver staining. Gels were treated with glutaraldehyde for 30 minutes and washed with Milli Q water several times before leaving the gels to soak in Milli Q water overnight to remove excess glutaraldehyde. Gels were then

submerged in silver stain for 1 hour and rinsed with Milli Q water twice before being treated with developer until protein bands were visible. Developer was removed and gels were rinsed with Milli Q water which stopped the developing reaction. Gels were submerged in 5 % Acetic Acid for about 1 hour at room temperature and were then stored at 4°C in the dark until dried.

2.2.3.4 Protein Analysis by Immunoblotting

Solutions were made fresh prior to the blotting procedure.

Transfer buffer	2.42 g Tris-base, 11.52 g Glycine, 160 ml Methanol, 640 ml Milli Q water
Tris Saline (TS) buffer	10 mM Tris pH 7, 150 mM NaCl
Blocking solution	0.5 g BSA (Sigma), 50 ml TS buffer This solution was mixed gently to prevent frothing

Immunoblotting also known as 'Western blotting' (Burnette, 1981) was used to transfer proteins separated by electrophoresis from the polyacrylamide gel to a medium on which they can be further analysed by specific antibodies.

Proteins separated on SDS PAGE as previously described were blotted using a BioRad TransferBlot tank. The sandwich arrangement shown in figure 2.1 consisting of four sheets of 3MM Whatman filter paper, gel, nitrocellulose membrane, and two support pads was prepared after each component being pre-soaked in transfer buffer for about five minutes. This sandwich was placed in a support cassette that was placed in the transfer tank, with the nitrocellulose membrane nearest to the Anode electrode as shown in figure 2.1. The transfer was performed at 150 mA constant current for 1 hour and 50 minutes or 10 mA when transferred overnight. An external ice block was used to prevent over heating caused by the rapid electrophoretic transfer which required a high current. In the case of the overnight transfer, the electrophoretic transfer was performed in a cold room (4°C).

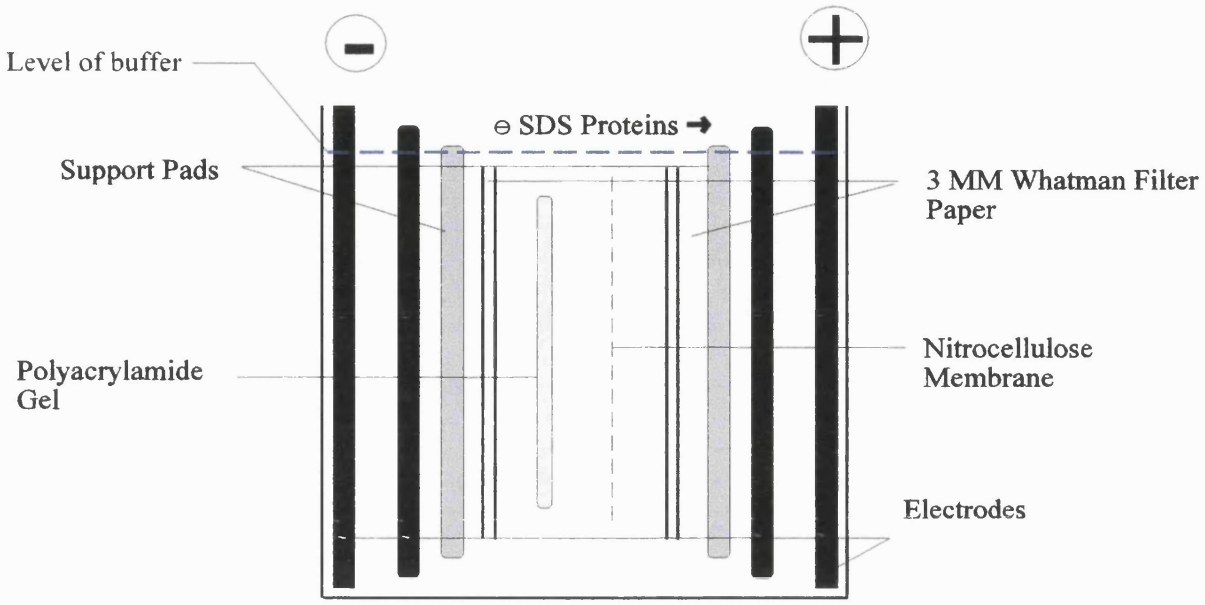

Figure 2.1 The arrangement of the blotting sandwich in the transfer tank.

Once the electrotransfer was complete, the nitrocellulose membrane was removed and soaked in 1% BSA blocking solution for one hour at room temperature to block the unoccupied binding sites on the nitrocellulose and hence, preventing the nonspecific adsorption of the antibodies. The blot was treated with 1% BSA blocking solution containing 0.05 % Nonidet p-40 (NP- 40) nonionic detergent and 1/500 - 1/2000 diluted primary antibody for 18 hours (overnight) when incubated at 4°C or for two hours when incubated at room temperature.

The primary antibody was carefully removed and stored at 4°C to be reused. The blot was then washed at room temperature with TS buffer for 10 minutes followed by two washes with TS buffer containing 0.05 % NP- 40 detergent for 10 minutes followed by a final TS wash for 10 minutes. This ensures the removal of any unbound primary antibody. The membrane was drained and treated with 1% BSA blocking solution containing 0.05% NP-40 detergent containing 1/1000 - 1/2000 diluted secondary antibody for two hours at room temperature. After the incubation period, the secondary antibody was removed and stored at 4°C to be reused at a later date. It has been found that the secondary antibody could be reused for up to 3x.

After washing away excess unbound secondary antibody as before, Horse Radish Peroxidase (HRP) an enzyme covalently bound to the secondary antibody was visualised using two different substrates causing bands to appear on the nitrocellulose membrane where the protein of interest was bound. Initially the blots were developed using Sigma Fast 3', 3'-Diaminobenzidine (DAB) substrate kit. DAB reacted with the Horse Radish Peroxidase found on the secondary antibodies resulting in the production of an insoluble brown coloured end product. This insoluble end product caused the staining and the visualisation of the bands on the nitrocellulose membrane. The staining was performed as stated by the manufacturer Sigma briefly, one tablet of DAB and one tablet of urea was dissolved in water and the mixture was added to the blot. The DAB solution was stopped once the bands started to appear by washing the DAB solution with water. The blots were then allowed to dry and covered with clean film.

Later in the project, a more sensitive detection system was used which was capable of detecting picogram of protein. This system was based on chemiluminescence which is a chemical reaction that resulted in light emission. The kit used was the ECL kit purchased from Amersham. Band visualisation using this system was produced by luminol reacting with HRP in the presence of hydrogen peroxide causing the production of a flash of light that was detected by photographic ECL Hyperfilm purchased from Amersham.

2.2.3.5 Determination of Protein Concentration

There were many methods available to determine the concentration of proteins. Generally two methods were used in this project. The type of method chosen depended on the availability of the sample, the concentration of the sample, the composition of the sample, and the degree of accuracy required.

2.2.3.5.1 Bradford Assay

This method used a commercial kit purchased from Bio-Rad based on the Bradford assay introduced by Bradford (1976). This method involved the binding of a Coomassie Brilliant Blue dye to proteins. Coomassie Brilliant Blue was dissolved in acid at a pH below 1 which turned the Coomassie Brilliant Blue to a brown colour. But once the dye was added to a protein sample the colour of the dye changed to a blue colour. This was due to a shift in the

pKa of the bound Coomassie dye. The absorbence of the protein samples was measured at 595 nm and was used with reference to a BSA standard curve to estimate the concentrations of the protein samples.

2.2.3.5.2 Ultraviolet Absorption

This method of measuring protein concentration was based on the findings of Warburg and Christian (1941) which were that nucleic acids and nucleotides absorb light at wavelengths of 260 nm and 280 nm respectively.

Proteins in particular can absorb at a wavelength of 280 nm due to the presence of the aromatic amino acids tyrosine and tryptophan. Since the content of these amino acids varies enormously between different proteins, the absorption at 280 nm varied considerably between different proteins. Proteins also absorbed at the far-UV region ranging from 192 nm-220 nm. This absorption was contributed to the absorption of the peptide bonds found in proteins (Goldfarb *et al*, 1951).

Although, measuring the far-UV absorbance of protein was more sensitive than 280 nm absorption and was less affected by the protein amino acid composition, most reagents used in this project absorbed strongly at this region masking the absorbance by the protein's peptide bonds. For this reason protein concentrations were estimated using absorbance readings measured at 280 nm. This was performed by firstly, diluting the protein sample when necessary and blanking the protein sample against a suitable blank followed by performing a spectroscopic scan from 200-350 nm using a CECIL 2021 2000 series spectrophotometer. As the absorbance coefficient for PDE4 was not known and as each of the analysed protein samples consisted of many different proteins with different absorbance coefficient, an average absorbance coefficient of 1 mg/ml/cm was used.

2.2.3.6 Activity Assay of Phosphodiesterase using the One-Step Method

This method of detecting the activity of Phosphodiesterase (PDE) enzyme introduced by Thompson and Appleman *et al.* (1971) and later modified by Thompson *et al.* (1979) was adopted throughout this project.

In this assay, two consecutive reactions were performed in the same 1.5 ml eppendorf tube hence the name One-Step. The first reaction converted cyclic adenosine 3',5'-monophosphate (cAMP) to 5' adenosine monophosphate (5'-AMP) by the action of the PDE enzyme. The second reaction converted the 5'-AMP to adenine and inorganic phosphate by the action of a nucleotidase enzyme present in snake venom (figure 2.2). The uncharged nucleoside (adenine) was separated from the charged nucleotides (cAMP and 5'-AMP) using an anion-exchange resin called Dowex.

2.2.3.6.1 Preparation of 10x Assay Buffer

20 mls of 10x assay mix was prepared. This mixture contained 100 mg of crude rattle snake venom dissolved in 7.94 ml of Milli Q water, 0.4 M Tris-HCl pH 8, 0.2 M $MgCl_2$, and 60 µl of β-mercaptoethanol. The assay mixture was aliquoted into 1 ml aliquotes and stored at -80°C until used. This mixture was enough to perform 800 assay points.

2.2.3.6.2 Preparation of Dowex

100 g of Dowex resin was washed sequentially with 1 L of the following: 0.5 M HCl (1x), distilled water (2x), 0.5 M NaCl (1x), distilled water (2x), 0.5 M HCl (1x) and several washes of distilled water until pH > 5 allowing the resin a period of 30 minutes to settle after each wash. 400 ml of distilled water was added to the resin to make up a 1:4 slurry. The pH of the slurry was adjusted to pH 7 to 7.4 using 5 M NaOH and was stored at room temperature until used.

2.2.3.6.3 Assay

Each reaction mixture, of a final volume of 200 µl was prepared to contain, 165.5 µl Milli Q water, 20.5 µl of 10x assay buffer, 4.35 µl of 10 µM cAMP (cAMP stock prepared in Milli Q water), 33 nM [^{3}H] cAMP. The final concentration of cAMP substrate which includes hot and cold ligand was 0.25 µM. Following equilibration at 30°C for 5-10 minutes, the reactions were sequentially initiated with the addition of 10 µl of PDE enzyme preparation at 20-30 seconds intervals. Enzyme preparations used in the assay were adjusted to produce activities below the maximum of the assay which was around 20 000 cpm. Samples were diluted in 50 mM Tris-HCl pH 8, 0.1 % BSA just before use, if enzyme activity exceeded the above value. In addition to reactions containing PDE, a 'blank' containing no PDE (replaced by buffer or water) was included to calculate the amount of hydrolysis that was not catalysed by PDE activity. The reaction was incubated at 30°C for 15 minutes in the linear range of the reaction see figure 2.3 and terminated by the addition of 20 µl of 10 % SDS.

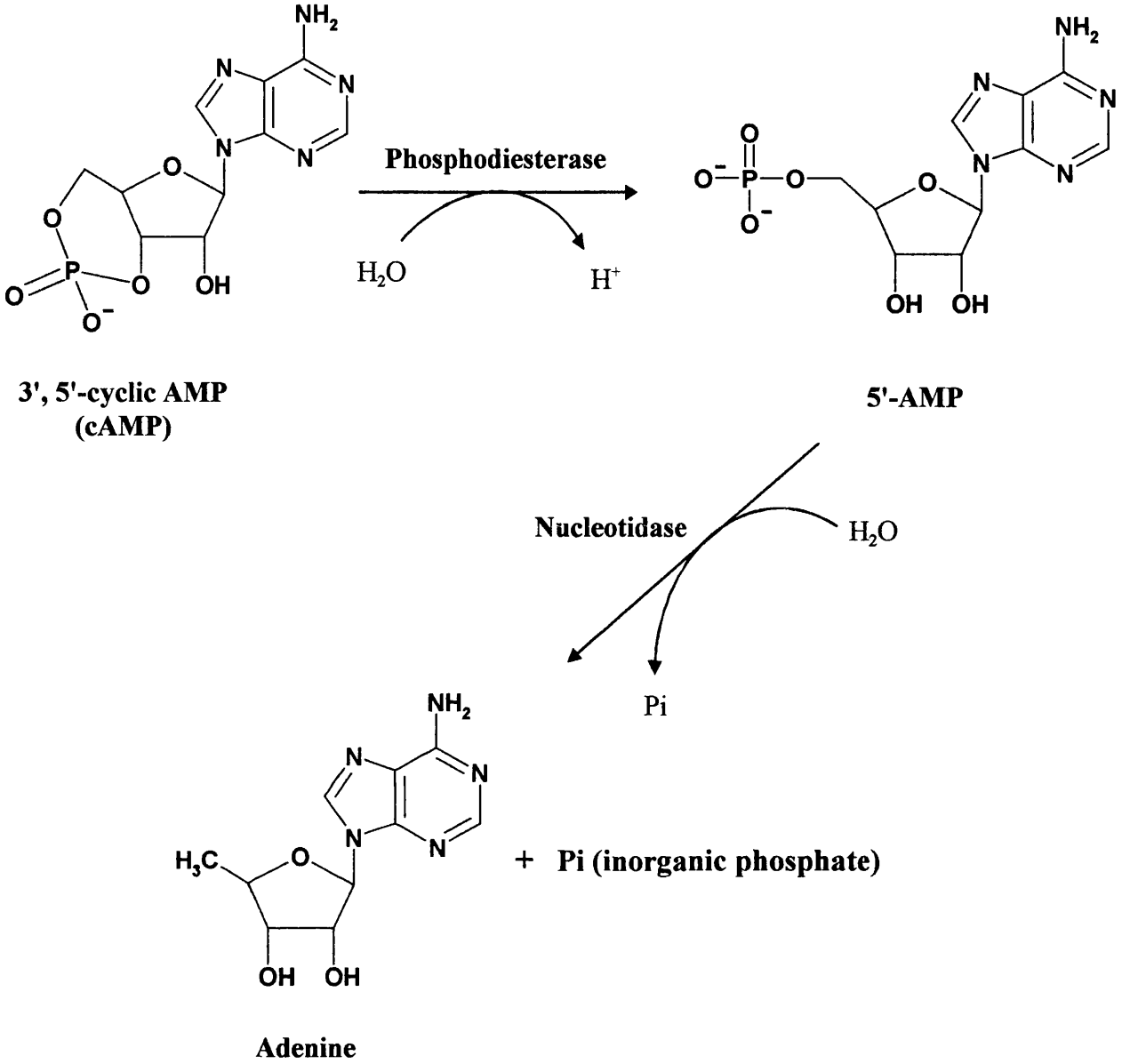

Figure 2.2 Structural representation of one-step PDE assay.

1 ml of 1:4 Dowex slurry prepared as previously described was added to the reaction mixture and incubated for 20 minutes shaking at room temperature. The sample was centrifuged for 5 minutes at maximum speed 14 000 *g* using a 5415C eppendorf microcentrifuge to spin down the resin. 0.5 ml of supernatant was added to 4.5 ml of scintillation fluid. The scintillation fluid which consists of solvent, an emulsion and fluor helps to convert the beta particle energy emitted during the redioactive decay process to light which is detected by the liquid scintillation counter (Beckman model 5000 CE). Total cpm in 0.5 ml samples was counted

by replacing Dowex with water and background cpm was counted by replacing the enzyme sample with water.

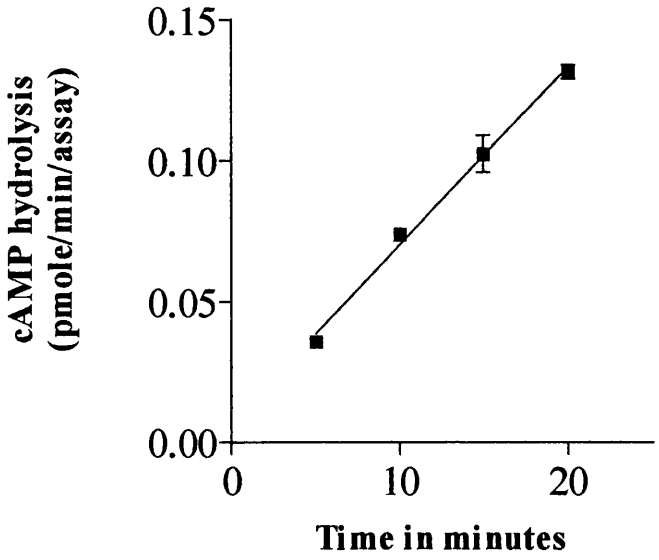

Figure 2.3 The rate at which PDE4 (Met^{26}RD1) hydrolyses cAMP. The assay was performed using 0.25 μM cAMP at various incubation times and Met^{26}RD1 samples prepared in BHK-21 cells as described in Chapter 6.

2.2.4 Tissue Culture

2.2.4.1 Resuscitation Of Cells From Gaseous Phase Liquid Nitrogen

Both CHO and BHK-21 cells were received as frozen ampoules from the European Collection of Cell Cultures. To resuscitate the cells, ampoules were incubated at 37°C for 2 minutes to thaw the cells. Cells were then transferred to 10 ml of fresh media (Hams F-12 for CHO cells and GMEM for BHK-21 cells) supplemented with 10% FCS, 2 mM glutamine and 5% Tryptose phosphate Broth (the later only added to GMEM). Each cell suspension was centrifuged using a Sigma 6K10 benchtop centrifuge with swing out rotor (No 11162) set to centrifuge at 400 *g* for5 minutes at 20°C to pellet the cells. Cells were then resuspended in 15 ml of media with all supplements (media relevant to cell line in use) and transferred to 75 cm^2 tissue culture flask and placed in a LEEC Research CO_2 incubator model GA3010 at

37°C supplemented with 5% CO_2 and maximum humidity.

2.2.4.2 Culturing Cells

CHO cells were cultured in Ham's F12 (Sigma) supplemented with 2mM glutamine and 10% Fetal Calf serum (FCS) and BHK-21 cells were cultured in Glasgow minimal essential medium (GMEM) (Sigma) supplemented with 2mM glutamine, 10%(FCS) and 5% Tryptose phosphate Broth (Sigma).

Cells were subcultured once they reached confluency. Old media was discarded and cells were washed twice with 1x PBS (2.6 mM KCl, 1.4 mM K_2PO_4, 0.1369 M NaCl, 8.1 mM Na_2PO_4) and then treated with 1 ml of 1x Trypsin/ EDTA (Sigma) for 3-5 minutes at 37°C. Fresh media was added to flasks and cells were distributed between a number of new flasks. Generally CHO cells were split 1:3 every 2-3 days and BHK-21 cells were split 1:6 or 1:10 every 2-3 days.

2.2.4.3 Storage

For long term storage, 10^6 cells (cells counted as described below in section 2.2.4.4) were suspended in 1ml of freezing solution consisting of 70% of either Hams F-12 medium (if CHO cells were used) or GMEM medium (if BHK-21 cells were used), 20% of FCS, 5% glutamine and 7.5% DMSO. The cells were cooled very slowly by placing them in a tissue culture freezing box containing isopropanol and incubated at -80°C for 24 hours. The frozen ampoules (1.5 ml Nunc cryo-vials) were then placed in liquid nitrogen.

2.2.4.4 Trypan Blue Test and Cell Counting

Trypan Blue stain purchased from GIBCO BRL was used for counting of viable cells via dye exclusion procedure which was based on the principle that live (viable) cells do not take up the dye, whereas dead (non viable) cells do.

0.5 ml of 0.4% Trypan Blue solution (w/v) was mixed with 0.3 ml HBSS and 0.2 ml of cell suspension prepared following the addition of 1 ml 1x Trypsin/EDTA solution and incubation for 3-5 minutes (See section 2.2.4.2). Solutions were mixed and left to stand for 15 minutes

at room temperature. Following the preparation of the WEBER England hemacytometer and with the cover slip in place, 20 µl of Trypan Blue cell suspension was transferred to both chambers by carefully touching the edges of the cover slip with the tip of the pipette and allowing the chamber to fill up by capillary action. Blue cells (non viable cells) as well as the non coloured cells present in the 1 mm centre square of each chamber were counted as shown in figure 2.4.

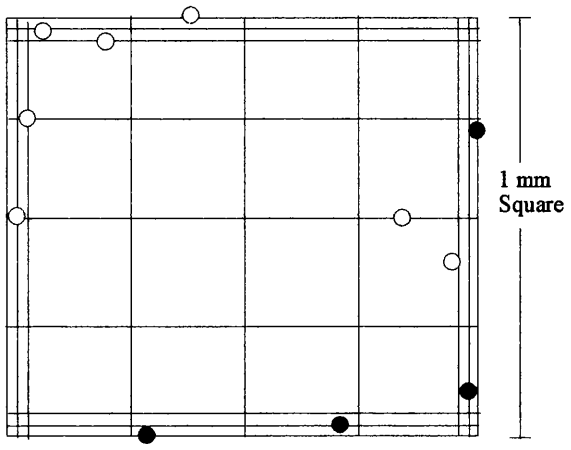

Figure 2.4 A simplified diagram representing the central square of a hemacytometer (WEBER England) at approximately 100x light microscope magnification. To count the cells, cells represented by white circles present in middle squares as well as those at the top and left touching the middle line on the edge were counted, whereas cells represented by black circles were not.

To count cells a WEBER England hemacytometer was used. Each square (large squares only) of the hemacytometer with the cover slip in place consisted of a total volume of 0.1 mm^3 or 10^{-4} cm^3 and since 1 cm^3 was equivalent to 1 ml, cell concentration (i.e. cell count) calculated was per 1 ml. This was determined using the following calculation:

Cells per ml: average count per square x dilution x 10^4

Total cells: Cells per ml x the original volume of cell suspension

Cell viability: total viable cells(non stained cells) ÷ total cells (stained and unstained cells)x 100

Chapter 3

Bacterial Expression of GST-Met^{26}RD1 Fusion Protein

3.1 Introduction

Over the past decades there have been numerous experimental procedures that have revolutionised science and allowed the introduction of new research areas such as molecular biology and biotechnology. Biological techniques such as PCR, cloning and recombinant protein expression were established which simplified analytical studies of several proteins and enzymes. Many vectors were constructed and designed not only to allow efficient expression of proteins but to also allow the efficient purification of the recombinant protein from the host proteins. Furthermore, this technology also made it possible to express proteins in several biological systems such as bacterial, mammalian, yeast and insect cells.

Bacterial expression systems using *Escherichia coli* (*E. coli*) are most commonly and routinely used in the production of heterologous gene products from both prokaryotic and eukaryotic origins. This is due to the organisms ease of growth and manipulation using available laboratory equipment, to its well characterised genetics and physiology, to the availability of many commercial vectors and bacterial strains that have been developed to maximise expression. Furthermore, large amounts of protein could be produced rapidly and quickly for example, milligram quantities of some proteins can be expressed in less than two weeks.

3.1.1 Glutathione S-transferase (GST) Gene Fusion System

The pGEX vectors constructed by Smith *et al.*, 1988 (figure 3.1) allowed the expression of protein as C-terminal fusions with Sj26. The presence of the Sj26 protein which is a 26kDa Glutathione S-transferase (GST) protein encoded by the parasitic helminth *Schistosoma japonicum* (Smith *et al.*, 1988) allowed the purification of the fusion proteins immobilised on glutathione columns by simple non-denaturing conditions. Several fusion

proteins could be purified in parallel by easy batch washing procedures and the GST carrier on the purified protein could be cleaved by proteases such as thrombin or factor X (depending which pGEX vector used) recognising sequences introduced to the C-terminus of the Sj26 protein. These vectors (figure 3.1) also contain the over-expressed *lacI*^{q} allele of the *lac* repressor allowing the repression of the GST fusion protein until the induction with Isopropyl-β-D-thiogalactopytanoside (IPTG), regardless of the state of the *lacI*^{q} present in bacterial cells. Furthermore, these vectors allow high levels of expression of GST fusion protein with the presence of *tac* promoter which is reported to be a strong promoter.

In general GST expression systems have been reported to be used in the generation of PDE antibodies but nevertheless, there have been numerous attempts to use *E. coli* in the expression of active rolipram-sensitive PDE4 (Swinnen *et al.*, 1989; Jin *et al.*, 1992) since the first reports of cloning PDE4 in the late 1980s. These attempts revealed that expression of PDE4 using bacterial systems can produce active protein which retain properties similar to that of native PDE4 proteins (K_m 1-4 μM). For example, rat PDE4D1/2 expressed in this system had a K_m value of 2 μM and an IC_{50} of 0.5 μM for rolipram (Swinnen *et al.*, 1989; Jin *et al.*, 1992). Kovala *et al.*, 1997 reported the expression of active PDE4D1 as a Glutathione S-transferase (GST) fusion protein with a specific activity of 0.9 nmol/min/mg when using 5μM cAMP and an IC_{50} of 0.4 μM when treated with rolipram (PDE4 specific inhibitor). This specific activity was considered to be low when compared to the estimated specific activity of the native PDE4 protein of 1.8 μmol/min/mg reported by Thompson *et al.*, 1988 and 1-2 μmol/min/mg using 1 μM cAMP reported by Conti *et al.*, 1995. Furthermore, subsequent experiments revealed some solubility problems especially when expressing large GST fusion proteins (Kovala *et al.*, 1997) and extensive degradation products before and after GST purification (Jin *et al.*, 1992; Kovala *et al.*, 1997). These degradation products were predicted to cause problems in the determination of parameters needed to study the kinetics of the expressed PDE fusion proteins as some of these short species may possess activity. In addition, the presence of the degradation products were suggested to be the cause of the low activities observed by Kovala *et al.*, 1997.

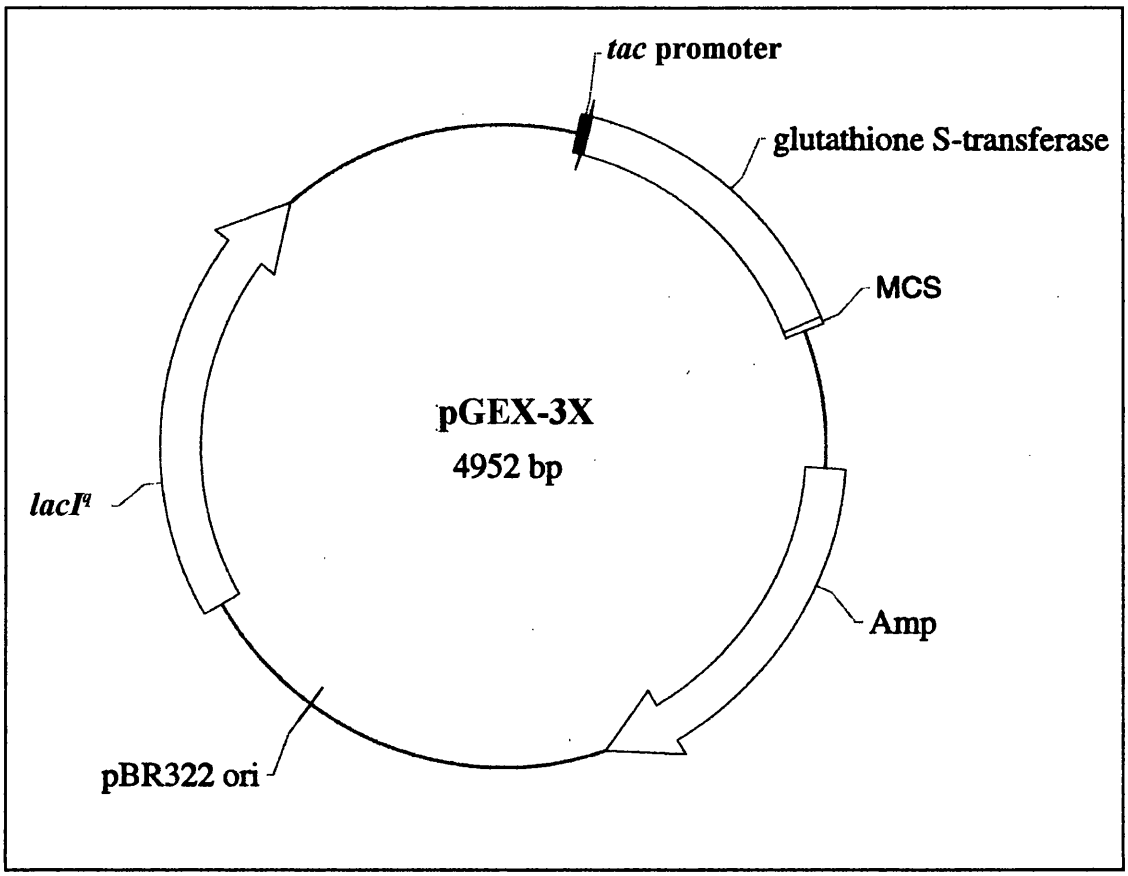

Multiple Cloning Site (MCS)

Ile	Glu	Gly	Arg	Gly	Ile	Pro	Gly	Asn	Ser	Ser		
ATC	GAA	GGT	CGT	GGG	ATC	CCC	GGG	AAT	TCA	TCG	TGA	CTG A CT GAC
Factor Xa				*Bam* HI		*Sma* I		*Eco* RI			Stop Codons	

Figure 3.1 A schematic map of pGEX-3X vector and the multiple cloning site.

3.1.2 Recombinant Protein Extraction from Bacteria

The introduction of over-expression of recombinant protein in bacteria and DNA technologies over 20 years ago lead to the rise of many new problems. One of these problems was the extraction of recombinant proteins from bacterial cells. Some expression systems excrete the recombinant protein into the growth media therefore eliminating the need to lyse the bacterial cells. However, the majority of the expression systems available require the lysis of the bacterial cell wall to release the proteins from the bacterial cell cytoplasm. There are a number of methods available to lyse the bacterial cell wall, the choice of method depends on the nature of protein in question and the scale of the process (Cull and McHenry, 1990). For PDE proteins expressed in bacteria, the method used in majority of the reported preparation was based on the use of enzymatic and mechanical means (Kovala *et al.*, 1997; Swinnen *et al.*, 1989). The enzymatic methods used lysozyme activity to cleave the glucosidic linkages found in the bacterial cell-wall polysaccharides and the mechanical methods using sonicators were used to disrupt the inner cytoplasmic membrane.

Another problem frequently encountered during protein over-expression in bacteria was the formation of insoluble protein aggregates called inclusion bodies which appear as cytoplasmic granules under the light microscope (Kane and Hartly, 1989). These inclusion bodies can contain most of the protein of interest and hence require further extraction. Numerous methods have been reported to reduce the accumulation of the protein in the inclusion body fraction and increase their solubility. Expression of protein in the form of fusion proteins for example as glutathione S-transferase or thioredoxin fusion protein has been proven to increase the solubility of the expressed proteins in bacteria (Smith and Johnson, 1988; LaVallie *et al.*, 1993). Growth temperature, host strain and media composition have also been found to have an effect on the solubility of the recombinant proteins (Schein and Noteborn, 1988). Theoretically reducing the growth temperature during induction of protein expression improves the solubility of the fusion protein by reducing the rate at which proteins are synthesised in the bacterial cytoplasm, allowing enough time for the protein to fold into its correct conformation.

Most of the available bacterial expression systems use bacterial cells derived from the K12 strain of *E.coli* to express recombinant proteins. This is due to the extensive genetic analysis of the strain compared to any other, leading to a better understanding of the organism. *E.coli* K12 derivatives are unable to colonise in humans and satisfies the governmental guide-lines and regulations set out for recombinant DNA work in which the organism used should be well characterised and non-pathogenic.

3.1.3 Aim

In order to undergo structural studies, there was the requirement to produce correctly folded, highly pure, and active PDE 4 protein in milligram quantities. The difficulty in isolating PDE enzymes is predominantly caused by the low expression levels of these enzymes in cells (estimated 1: 100,000 of the cell protein) and their instability during and after purification from natural sources (Thompson *et al.*, 1988; Conti *et al.*, 1995). Heterogenous over expression of the PDE 4 in its native or non native form will alleviate the need to isolate it from its natural source, leading to the possible production of milligram quantities for structural studies.

The major studies performed in this chapter described expression of Met^{26}RD1 clone in *E.coli* as a glutathione S-transferase fusion protein and the purification of this protein using glutathione affinity column. This was performed with the aim of producing pure and active protein possessing the correct kinetic characteristics of PDE4 published data (Kovala *et al.*, 1997; Jin *et al.*, 1992; Swinnen *et al.*, 1989). Trial procedures were performed on the small scale with the intention of scale up once a method was achieved.

3.2 Methods

3.2.1 Construction of GST-Met^{26}RD1 (PDE4A1)

The bacterial expression vector pGEX-3X purchased from Pharmacia was used to create the glutathione S-transferase (GST) fusion clones. *Met^{26}RD1* gene which encodes for rat Phosphodiesterase 4A1 (PDE4A1) enzyme was amplified using polymerase chain reaction

(PCR) and inserted into pGEX-3X vector to create GST-Met^{26}RD1 construct.

3.2.1.1 Polymerase Chain Reaction of *Met^{26}RD1*

Met^{26}RD1 contained in pSVL plasmid kindly provided by Professor Miles Houslay was amplified as a 1.7 kb fragment using RD1f and RD1b primers shown in figure 3.2. 100 µl PCR reaction was set up to consist of 10 % *Taq* DNA polymerase 10 x reaction buffer (500 mM KCl, 100 mM Tris-HCl pH 9, 1% Triton X-100 and 15 mM $MgCl_2$), 8 µl of deoxynucleotide triphosphate (dNTP 100 mM final concentration, Gibco BRL), 1ng/µl or 10 ng/µl of DNA template and 50 pmole of forward and reverse primers. The PCR reactions were heated to 94°C for 45 seconds at which point 5 units of *Taq* DNA polymerase was added. The reaction mixtures were heated to 94 °C for 45 seconds, 61 °C for1 min and 72 °C for 1.45 minutes sequentially for 30 cycles. Finally the reactions were heated to 72 °C for 10 minutes and stored at 4°C until analysed. The repeated temperature cycles were performed using the Biometra personal cycler (with heated lid).

RD1f

5'-ATATA-GGATCC-TAA-GCCGCCACC-ATGGTGAACCGTGAGCTCAC-3'

Bam HI Stop codon Kozak sequence *Met^{26}RD1* gene

RD1b

5'-ATAT-GAATTC-CCCGGG-TCA-GGATCAGGCAGGGTCTCCGC-3'

Eco RI *Sma* I Stop codon *Met^{26}RD1* gene

Figure 3.2 Primer sequences used in PCR reactions. RD1f (forward) primer consisted of 42 nucleotides with a *Bam* HI restriction enzyme site on its 5' end to aid cloning down stream of *GST* gene and a Kozak sequence (Kozak, 1992) to allow efficient expression of the *Met^{26}RD1* gene in mammalian systems when cloned into Semliki forest virus vectors (see Chapter 6) and to add a 3 amino acid linker to the GST fusion protein. RD1b (reverse)

primer consisted of 39 nucleotides with two restriction enzymes *Sma* I and *Eco* RI at its 5' end and a stop codon TCA.

3.2.1.2 Frame Shift Mutation

In order to generate a frame shifted mutation, 10 μg of 2a (see results 3.3.1 and figure 3.3) clone (DNA) was digested with *Bam* HI in a 40 μl reaction and 1 μl of the reaction was analysed on a 0.8% agarose gel following the method described in section 2.2.2.5 to confirm linearisation by *Bam* HI restriction enzyme. The rest of the reaction (39 μl) was used in the filling-in reaction performed by Klenow enzyme containing 2 μl of 1 mM dNTP, and 12 Units of Klenow enzyme (Amersham). The filling-in reaction was incubated at 22°C (room temperature) for 15 minutes and stopped by heating to 75°C for 10 minutes.

Following the filling-in procedure, Milli Q water was added to the samples to bring their volumes up to 100 μl. Samples were cleaned from any contaminating enzymes and/or unwanted salts by the Wizard clean-up kit purchased from Promega following method described in section 2.2.2.3.

3.2.1.3 Ligation Reaction of pGEX-3X-Met^{26}RD1

10 μl ligation reactions were set up to contain 1, 2, 3, and 4 μl of the cut DNA. Each of which were incubated at 4°C for 8 hours and 15°C for 17 hours. Generally the ligation reactions were set up over the weekend to incubate at 15°C to allow efficient ligation to take place. Ligation reactions were transformed into JM109 (DE3) competent cells prepared by $CaCl_2$ method as described in section 2.2.1.3. DNA from positive clones was isolated using Promega kits following protocol described in section 2.2.2.1.1 and 5' ends of clones were sequenced by ABI sequencer as described in section 2.2.2.4 and sequence data are shown in Appendix 2.

3.2.2 Initial Expression Studies of GST-Met^{26}RD1 Fusion Protein

The method used was based on the method reported by Kovala *et al.*, 1997.

3.2.2.1 Time Course of GST-Met^{26}RD1 Fusion Protein Expression

Following transformation of JM109(DE3) competent cells with *C17* (see results 3.3.1), a single colony was inoculated into 5 ml of Luria Broth (LB) supplemented with 50μg/ml of ampicillin (LBA). Cultures were incubated overnight at 37°C shaking at 200 rpm. 1 ml of the overnight cultures was inoculated into 50ml LBA and cells were grown to an optical density of 600 (OD_{600}) = 0.3. The OD was checked by transferring 1 ml sample into 1 ml cuvette and measuring the OD with a CECIL 2021 2000 series spectrophotometer hourly. A 1ml sample was removed at time point zero and IPTG was added to a final concentration of 2 mM to induce expression of GST-Met^{26}RD1 protein. Bacterial cells were left to grow for about 4 hours following the addition of IPTG and 1ml samples were collected at regular 1 hour intervals. The remainder of the bacterial cultures were centrifuged using a Sigma 6K10 benchtop centrifuge with a swing out rotor (No 11162) set to centrifuge at 2400 *g* for 25 minutes at 4°C and cell pellets were stored at -20°C until used. All 1ml samples were centrifuged for 1 minute at 14 000 *g* using a 5415C eppendorf microcentrifuge to spin down the cells. Cell pellets were stored at -20°C for 24 hours.

Cells were disrupted in 10 ml of lysis buffer (10 mM Tris pH 8, 1 mM EDTA, 0.1 M NaCl, 1 mM DTT, 1 mM PMSF, 20 μM TPCK and 8 μg/ml leupeptin) by the freeze/thaw method which involved flash freezing of the cells in liquid nitrogen followed by thawing in a 42°C water bath for about 3 minutes. This was repeated twice until a viscus texture was achieved which was indicative of bacterial genomic DNA release caused by lysis of the cells. Samples were centrifuged at 14 000 *g* for 5 minutes using a 5415C eppendorf microcentrifuge placed at 4°C to separate the supernatant from the cell debris. Assays were performed on the supernatant samples using 0.25 μM of cAMP substrate as described in section 2.2.3.6.3.

3.2.2.2 Induction at Different Growth Temperatures

The growth temperatures of the bacterial cultures were reduced to ambient temperatures ranging between 21-24°C and the expression levels of GST-Met^{26}RD1 soluble protein was tested by PDE assays using expression at 37°C as a control.

Expression was performed as described in section 3.2.2.1 with minor alteration for ambient temperature expression. 10 ml of overnight cultures were inoculated into 40 ml LB media supplemented with 50 μg/ml ampicillin and cultures were incubated at room temperature shaking until the OD_{600} reached 0.3 using a Luckham orbital shaker. IPTG was added to a final concentration of 2 mM and cultures were incubated until OD_{600} reached 1.6-1.9 at which point samples were collected by centrifugation using a Sigma 6K10 benchtop centrifuge with a swing out rotor (No 11162) set to centrifuge at 2400 *g* for 25 minutes at 4°C and lysed using a method introduced by Marston *et al.*, 1984 with a few modifications. Cell pellets were thawed at room temperature and mixed with lysis buffer (10 mM Tris pH 8, 1 mM EDTA, 0.1 M NaCl, 1 mM DTT, 1 mM PMSF, 20 μM TPCK and 8 μg/ml leupeptin) at a ratio of 3 ml of lysis buffer per 1 g of pellet. A fresh stock of Lysozyme of 10 mg/ml was prepared and added to the mixture at a ratio of 80 μl per 1 g of bacterial pellet. Samples were incubated on ice for 30 minutes and sonicated on ice at three 20 second intervals using the MSE Soniprep 150 sonicator and centrifuged using a Beckman L8 ultracentrifuge set to centrifuge at 40 000 *g* for 30 minutes at 4°C. Supernatants were analysed by PDE assays, shown in figure 3.7(a). Bacterial samples for SDS PAGE and Western blot analysis were collected before IPTG induction and post IPTG induction OD_{600} of 1.7. Samples were centrifuged using a 5415C eppendorf microcentrifuge set to centrifuge at 14 000 *g* for 2 minutes and pellets were resuspended with 40 μl of 1x SDS loading buffer containing 1 mM DTT. Samples were boiled for 5 minutes and 8 μl were loaded on 10 % SDS gels.

3.2.2.3 Induction at Different Points of the Bacterial Growth Phase

The expression and lysis methods used, were similar to the methods described in section 3.3.1 with minor alterations. The cultures were induced with 2 mM IPTG (final

concentration) at different points in their growth. These points were measured according to the optical density at 600nm (OD_{600}) of the bacterial culture. Cultures were induced at OD_{600} of 0.3 and 1 which are at mid-exponential phase and at late exponential-phase respectively. Cultures were grown until OD_{600} reached 1.7-1.9 at which point cells were collected and lysed as described in section 3.3.1. Supernatants were assayed for PDE activity and shown in figure 3.8.

3.2.3 Expression of GST-Met^{26}RD1 Fusion Protein

Cells were induced for expression using optimised parameters described previously and following the method described in section 3.2.2.1. Cells were collected by centrifugation and pellets were weighed and washed twice with 10 ml of freshly made 1x phosphate buffer saline (PBS) (2.6 mM KCl, 1.4 mM K_2PO_4, 0.1369 M NaCl, 8.1 mM Na_2PO_4) using a Janke & Kunkle Ultra-Turrax T25 homogeniser set at a 6000 rpm. A 10 L fermenter (Electrolab 10 L fermenter with pH, temperature and oxygen control modules) was also used to express GST-Met^{26}RD1 fusion protein using the parameters optimised previously. Small samples equivalent to the 50 ml cultures (equivalence in pellet wet weight) were collected and washed twice with 10 ml 1x PBS. All pellets were lysed using the method described in section 3.2.2.1

3.2.4 Purification of GST-Met^{26}RD1 Fusion Protein using Glutathione Agarose

Most of the purification procedures described in this section were either performed at 4°C or on ice to reduce proteolytic cleavage unless otherwise state. Soluble fractions prepared from 0.5 g of bacterial pellet by lysis using the method mentioned in section 3.2.2.1 were mixed with 2 ml (bed volume) of reduced glutathione, immobilized on Agarose CL-4B purchased from Sigma at 4°C for 60 minutes to allow batch binding. The protein resin complex was washed with 20 ml of freshly made 1x PBS using a Sigma 6K10 benchtop centrifuge with a swing out rotor (No 11162) set to centrifuge at 500 *g* for 5 minutes at 18°C. PDE fusion protein, was eluted with 2 ml of elution buffer (50 mM Tris pH 8, 0.2 mM NaCl, 1 mM DTT and 0.01 % Triton X-100) containing 10 mM glutathione at room temperature for 30 minutes and the suspension was collected by centrifugation. This

procedure was repeated three times and all eluates were pooled and concentrated using centricon-30 purchased from Amicon and analysed for PDE activity, SDS PAGE and Western blotting. The concentration of the eluted samples using centricon-30 was as follows. 7 ml of eluted samples were concentrated to 0.7 ml by centrifugation using a Sigma 6K10 benchtop centrifuge with a swing out rotor (No 11162) set to centrifuge at 2 000 *g* for 60 minutes at 4°C. Centrifugation allowed the buffer as well as protein molecules smaller than 30 kDa in size to diffuse through the centricon's filter which has a pore size of 30 kDa allowing the larger proteins present in the preparation to be more concentrated in the tube. Centricons were washed with 1 ml of autoclaved water after being used and 2 mls of storage buffer (50 mM Tris pH 7.4, 0.1% NaN_3) was added and the centricons were stored at room temperature.

3.3 Results

3.3.1 Cloning of *Met[26]RD1* into pGEX-3X Plasmid

The 1.7 kb *Met[26]RD1* gene was amplified by polymerase chain reaction using primers shown in figure 3.2. The amplified fragment was cut with *Bam* HI and *Sma* I ligated into pGEX-3X expression vector (Pharmacia). These two restriction enzymes are present in the multiple cloning site of the vector (see figure 3.1) allowing the *PDE* gene to be preceded by a *Glutathione S-transferase* (GST) gene. Both genes were under the control of the *tac* promoter which allowed the expression to be induced by the addition of IPTG to the growth media.

Following the transformation of JM109 (DE3) bacterial cells with the ligation reactions, screening for potential clones took place. This was performed by cutting with *Bam* HI and *Sma* I restriction enzymes and analysing the results on 0.8% agarose gel. This revealed a clone (named 2a) showing the right profile on agarose gel (data not shown). Sequencing the 5' ends of the inserted gene (clone 2a) revealed that the ATG start codon was out of frame (Figure 3.3). To correct the reading frame, 2a clone was digested with *Bam* HI and the 5' sticky ends produced were filled by Klenow DNA polymerase. This procedure was necessary to shift the reading frame by four nucleotides (figure 3.3) to bring the PDE

codon to the correct reading frame, to enable expression of *Met*^{26}*RD1* gene in subsequent experiments.

Recombinants were screened using small-scale preparations of DNA (Promega mini-preps kit) from 18 colonies. Positive clones by searching for clones with modified *Bam* HI site. This was performed by digesting all clones with *Bam* HI restriction enzyme. This method of screening (figure 3.4) revealed 16 out of 18 selected colonies that did not response to *Bam* HI digestion signalling the modification of the *Bam* HI restriction site. DNA minipreps of two of these positive clones (*C10* and *C17*) were initially sequenced by automated fluorescent sequencing using ABI sequencer using sequencing primers shown in section 2.2.2.4 to confirm that the PDE codon ATG was in the correct reading frame. This showed that the *Bam* HI site was filled-in correctly and the start codon was in the correct reading frame (figure 3.3). These two clones (*C10* and *C17*) were subsequently sequenced as described in section 2.2.2.4 and shown in Appendix 2 and were used in expression of *Met*^{26}*RD1* gene in *E.coli.*

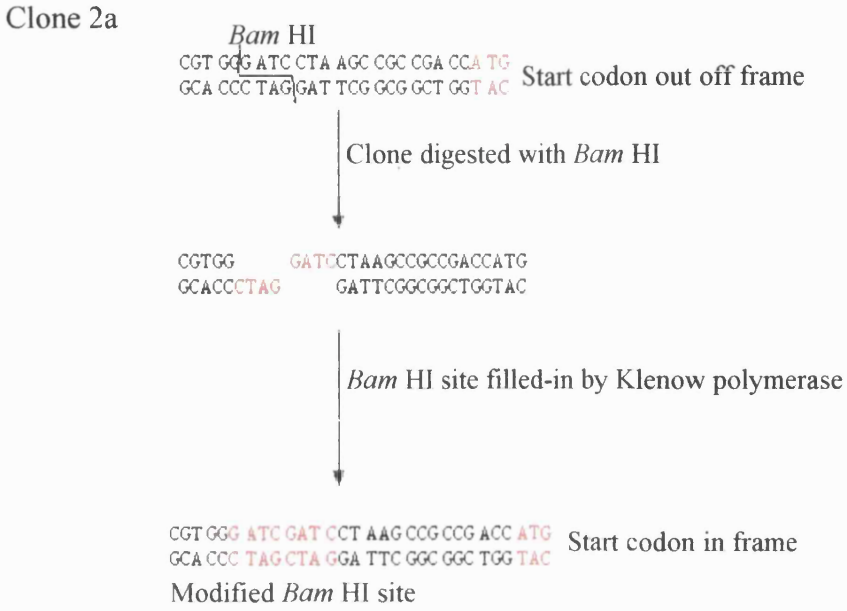

Figure 3.3 A schematic diagram to show the cloning of *Met*^{26}*RD1* gene into pGEX-3X vector. 5' end DNA sequence of 2a clone (clone consisted of the *Met*^{26}*RD1* gene cloned into pGEX-3X vector) sequenced using automated fluorescence ABI sequencer, showed that the *Met*^{26}*RD1* gene was in the wrong reading frame due to the length of the Kozak sequence. To bring the gene into the right reading frame, 4 nucleotides were added by filling-in the *Bam* HI restriction site. *Met*^{26}*RD1* gene start codon, *Bam* HI sticky ends and modified *Bam* HI site are indicated in red.

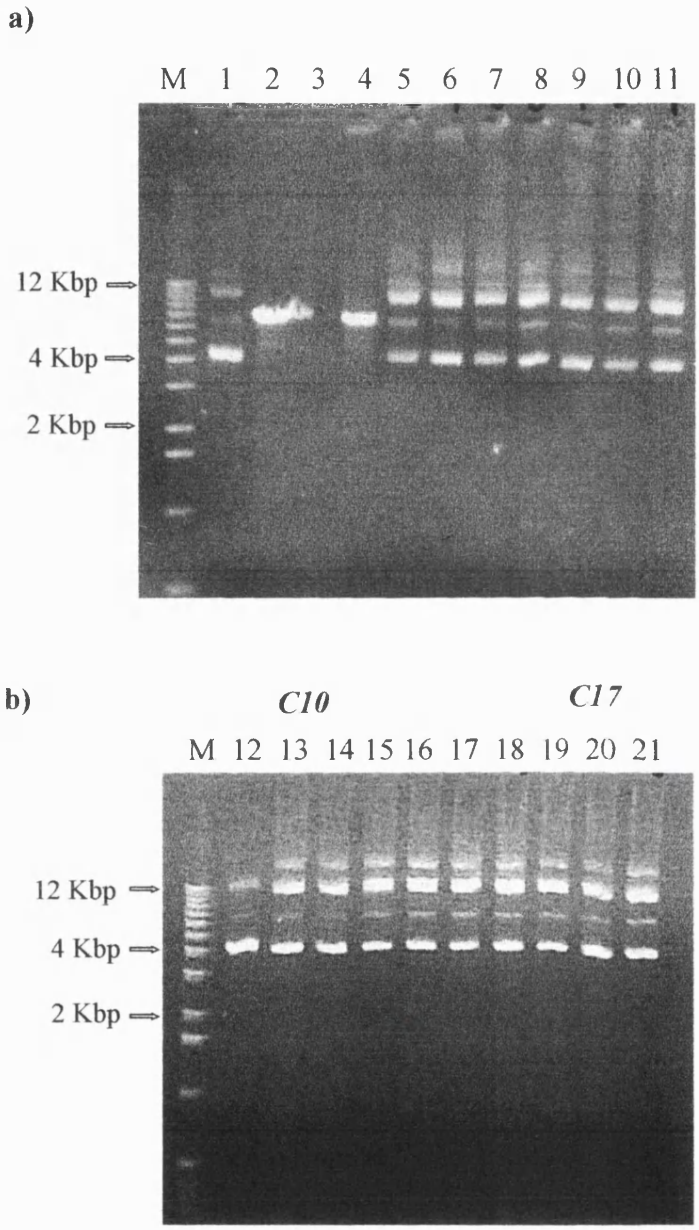

Figure 3.4 Agarose gel analysis of mini-preps that have been digested with *Bam* HI restriction enzyme. 100 ng of DNA size markers (1 Kb DNA ladder) and 400 ng of digested and undigested DNA samples were loaded on 0.8% agarose gel. Electrophoresis, gel staining and gel visualisation were performed as described in section 2.2.2.4. The Lanes in panel **a)** are: (M) DNA molecular size marker, (1) Clone 2a undigested sample used as a control, (2) Clone 2a digested with *Bam* HI and (3-10) Mini-preps digested with *Bam* HI and in Panel **b)** are: (M) DNA molecular size marker, (12-21) Mini-preps digested with *Bam* HI. Abbreviations: *C10* and *C17* represent clones 10 and 17 respectively.

3.3.2 Optimisation Of Expression Parameters Of GST-Met^{26}RD1

To determine the optimal parameters for maximum expression of GST-Met^{26}RD1 construct, the first step was to determine the time allowed for maximum expression. Bacterial cells were incubated for different periods following induction with IPTG. PDE assays performed on collected bacterial lysates (figure 3.5) showed that the maximum PDE activity was recorded at around 5 hours after induction. The drop in PDE activity recorded after 2 hours was probably due to poor lysis rather than low levels of PDE expression. Supernatants and pellets were analysed by SDS PAGE and Western blotting (figure 3.6). These gels showed that PDE fusion protein was expressed with the correct molecular weight of around 92 kDa. The intensity of this band in the supernatant samples increased with time (post-induction) up to 5 hours, then decreased. Whereas, the intensity of the band in the pellet samples increased throughout the induction procedure. This suggested that the levels of recombinant protein expressed reached a maximum at 5 hours post-induction after which point levels of the soluble protein started to fall due to their precipitation in the form of inclusion bodies. This could explain the rapid decline in PDE activity after 5 hours IPTG induction observed in PDE assays (figure 3.5).

Following the establishment of the optimum incubation time for maximum PDE expression, bacterial cells were grown at ambient temperature as well as 37°C to discover whether a decrease in temperature would increase PDE activity detected in the supernatant fraction. The decrease in growth temperature was predicted to allow better folding of expressed proteins in bacteria. Therefore, this should decrease the insoluble Met^{26}RD1 present in the pellet fraction and increase the soluble and active enzyme in the supernatant fraction. However, the results presented in figure 3.7 showed that the activity observed in PDE assays, was higher at 37°C growth temperature compared to expression at ambient temperature. In fact the activity was approximately 2x higher at 37°C induction compared to ambient temperature induction. These results were confirmed by band intensities on SDS PAGE and Western Blot analysis.

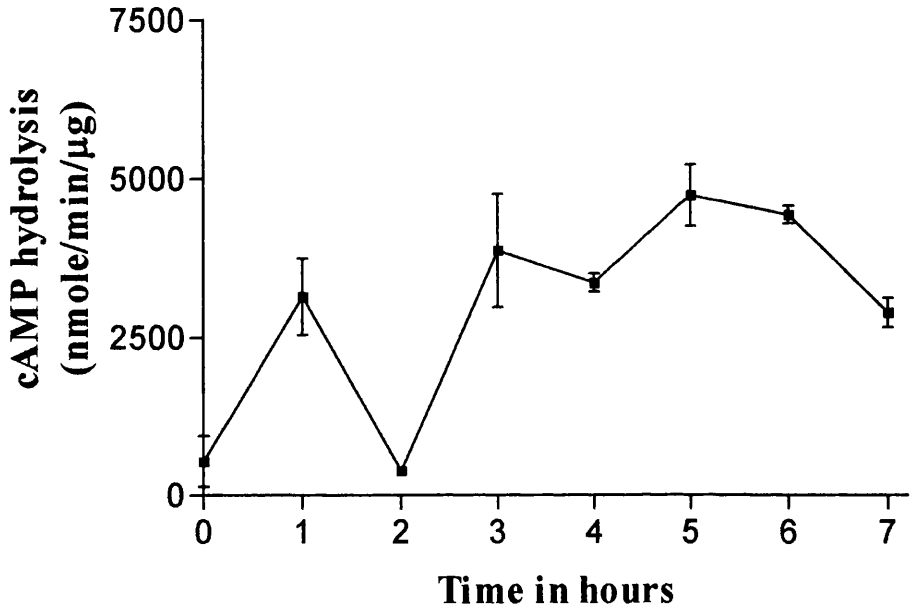

Figure 3.5 The induction profile of GST-Met^{26}RD1 fusion protein expression. The assay using 0.25µM cAMP as a substrate as described in section 2.2.3.6.3 was performed in duplicates on supernatants from two separate preparations. The counts per minute (cpm) in the graph were blanked against water and plotted against time post IPTG induction. The error bars represent the deviation of the values from the mean.

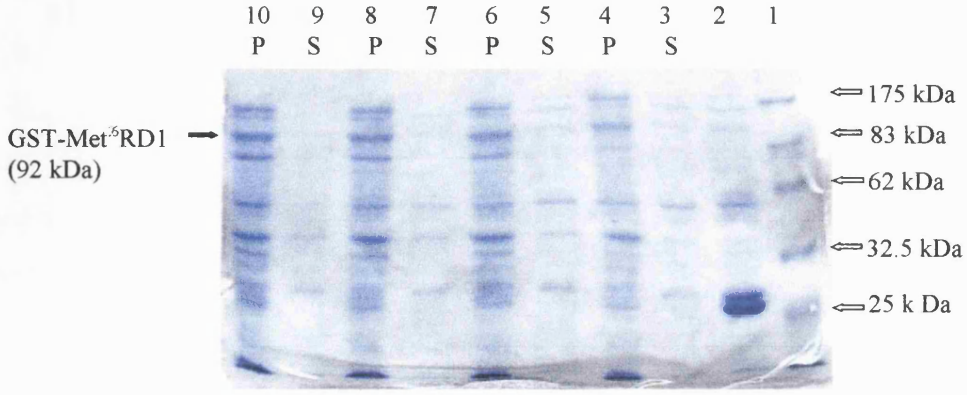

Coomassie Brilliant blue Stained Gel

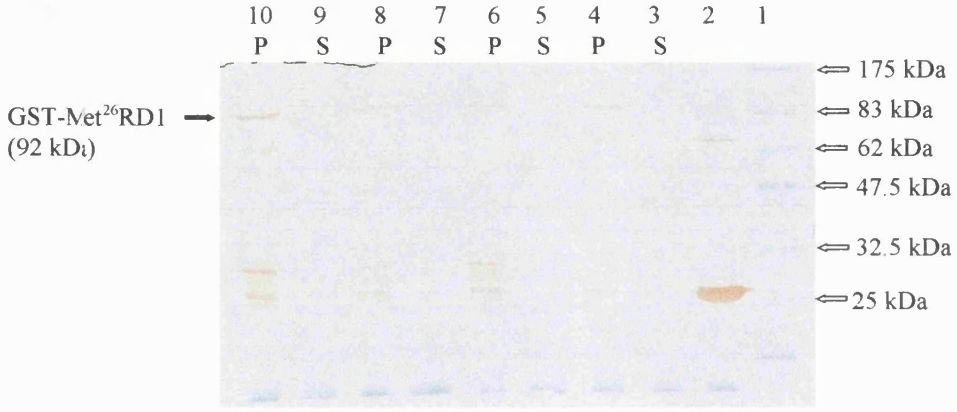

Anti GST antibody

Figure 3.6 SDS PAGE and Western blot of GST-Met[26]RD1 time course expression. Panel (a) shows a Coomassie Brilliant blue stained 10% SDS PAGE gel, while panel (b) shows a replica gel that has been blotted and probed with an anti-GST antibody and stained with DAB as described in section 2.2.3.4. The lanes in both panels are (1) Molecular size markers. (2) control pGEX-3X GST expression and lanes (3-10) represent samples of supernatant (S) and pellet (P) for 1, 2, 5, and 7 hours post IPTG induction. Supernatant gel samples were prepared by mixing 32 µl of lysates with 8 µl of 5x SDS loading buffer and pellet samples were prepared by mixing pellets with 100 µl of 1x SDS loading buffer. Following boiling of gel samples for 10 minutes, 6 µl of each sample was loaded on gel.

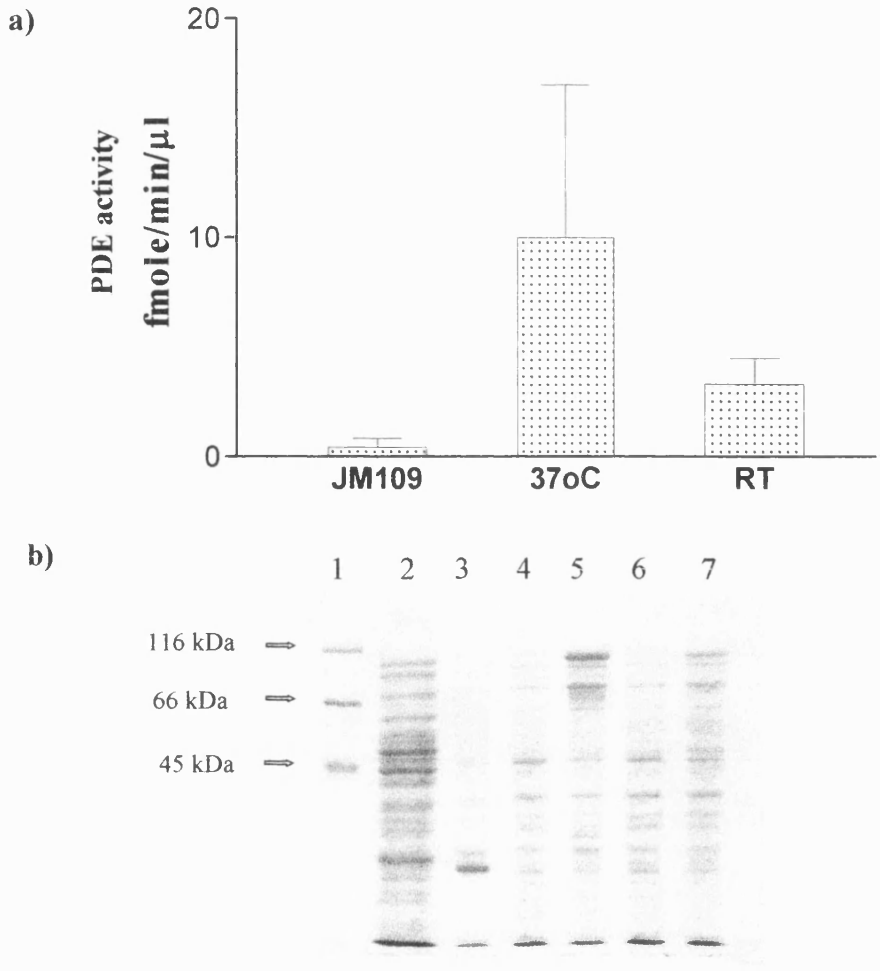

Figure 3.7 Effect of changing the growth temperature of the bacterial culture on expression of GST-Met[26]RD1 fusion protein. Panel (a) shows supernatants assayed for PDE activity using 0.25 µM cAMP as substrate. Panel (b) represents Coomassie stained 10 % SDS gel of bacterial samples collected before IPTG induction and after IPTG induction of bacterial cells grown at both 37°C and ambient temperature. Lanes in panels (b) are: (1) 0.6 µg Molecular size markers. (2) 10 µg bacterial lysate. (3) 10 µg bacteria lysates transformed with pGEX-3X plasmid. (4)10 µg bacteria transformed with pGEX-3X Met[26]RD1 construct before IPTG induction/ 37°C. (5) 10 µg of bacterial lysate transformed with pGEX-3X Met[26]RD1 construct after IPTG induction/ 37°C. (6) 10 µg of bacterial lysate transformed with pGEX-3X Met[26]RD1 construct before IPTG induction/ ambient temperature. (8) JM109 (DE3) bacteria carrying pGEX-3X Met[26]RD1 construct after IPTG induction/ ambient temperature.

Finally, the last parameter to be optimised was the time of induction with IPTG. Expression levels shown in figure 3.8 were the highest in bacterial cells induced at an OD_{600} of 0.3 and the lowest in bacterial cells not induced with IPTG. Also, expressed protein from an OD_{600} of 0.3 induction, responded to rolipram inhibitor the most compared to other parameters used. Consequently, GST-Met^{26}RD1 protein was expressed by inducing bacteria at OD_{600} of 0.3 in future experiments. Results shown in figure 3.8 indicated that IPTG induction was necessary to express the maximum amounts of active GST-Met^{26}RD1 protein. Further more, induction was the highest when cultures were induced at mid-exponential phase of the bacterial growth.

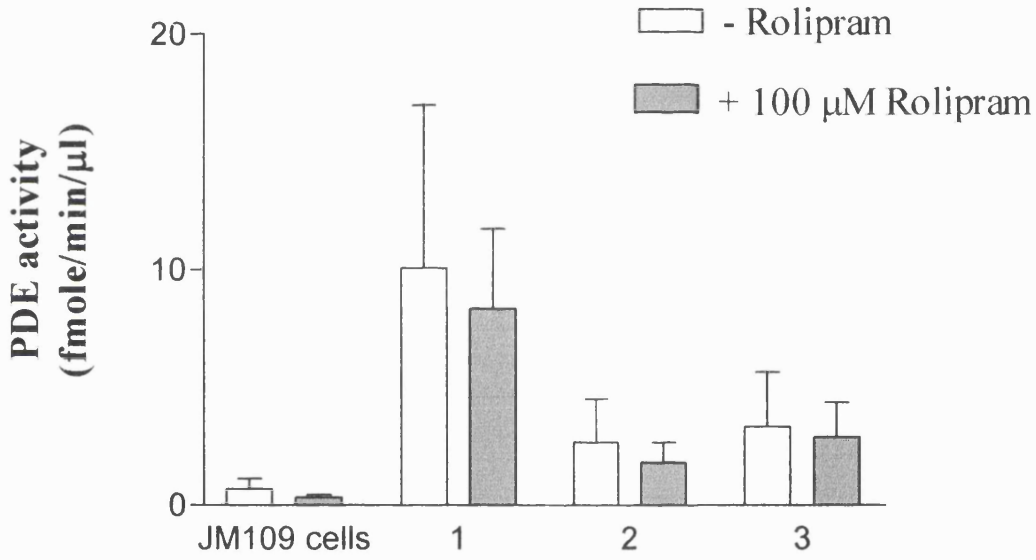

Figure 3.8 Effect of IPTG induction at different points in the growth phase of the bacterial cells on the expression of GST-Met^{26}RD1 fusion protein. The assay using 0.25 μM cAMP as a substrate was performed in triplicates on supernatants from two separate preparations. Samples were also treated with 100 μM of Rolipram a PDE 4 specific inhibitor. The activity was calculated from dpm of the sample minus dpm for water blank. The error bars represent standard deviation from the mean value. *JM109* represents bacterial (JM109 (DE3)) cells with no plasmid as control. Sample (1) represents cultures induced at OD_{600} of 0.3. Sample (2) represents cultures induced at OD_{600} of 1. Sample (3) represents cultures not induced with IPTG.

3.3.3 Analysis And Purification Of GST-Met^{26}RD1 Protein

Following the pilot studies described in section 3.3.2, expression studies of GST-Met^{26}RD1 were performed using those optimised parameters to analyse the behaviour of this expressed recombinant protein regarding activity and response to rolipram (PDE4 specific inhibitor).

Table 3.1 Expression and purification of GST-Met^{26}RD1 fusion protein.

Sample	Total protein (mg)	Protein concentration (mg/ ml)	PDE activity (pmol/min/mg)	100 μM Rolipram (pmol/min/mg)
JM109(DE3) soluble	**55**	**11**	**0.068 ± 0.004**	**0.067 ± 0.02**
JM109 (DE3) pGEX-3X soluble	**45**	**9**	**0.061 ± 0.01**	**ND**
GST-Met^{26}RD1 Total	**453.4**	**90.7**	**0.12 ± 0.0036**	**0.03 ± 0.003**
GST-Met^{26}RD1 soluble	**82.8**	**16.6**	**0.67 ± 0.01**	**0.34 ± 0.1**
GST-Met^{26}RD1 pellet	**333.8**	**66.8**	**0.06 ± 0.014**	**0.02 ± 0.005**
Glutathione purification	**1.2**	**0.12**	**4.56 ± 0.7333**	**1.38 ± 0.1**

Data are mean values of two to three preparations with standard deviation. All cultures have equivalent pellet wet-weight of 0.5g. PDE activity assays were determined by using 0.25μM cAMP following method described in section 2.2.3.5. Protein concentrations were determined by Bradford assays described in section 2.2.3.4.1. ND= Not determined.

Analysis of the soluble fractions by PDE activity assays revealed that GST-Met^{26}RD1 fusion protein exhibited a ten-fold increase beyond that of *E. coli* carrying pGEX-3X plasmid (0.67 ± 0.01 pmol/min/mg vs 0.06 ± 0.003 pmol/min/mg) when cultured. A substantial portion of the expressed GST-Met^{26}RD1 fusion protein was found to be insoluble (lane 4 in figure 3.9) with low PDE activity (Table 3.1) suggesting that most of the insoluble PDE was probably in the form of inclusion bodies. Furthermore, the expressed GST-Met^{26}RD1 showed response to inhibition by 100 μM rolipram (Table 3.1) a PDE4 specific inhibitor of 50%.

Purification data revealed that virtually all of the GST-Met^{26}RD1 protein bound to the glutathione agarose (figure 3.10) and approximately 50% of the bound PDE was eluted

with 10 mM glutathione. However, Western blot analysis of the eluted sample gave two major bands of 92 kDa (size of the full length GST-Met^{26}RD1 protein) and a band of approximately 62 kDa in size as well as several other minor bands 32 to 26 kDa in size (figure 3.10/b). These bands were thought to result from proteolytic cleavage of GST-Met^{26}RD1 protein. SDS gels stained with Coomassie (shown in figure 3.10/a) revealed many other protein bands that were not recognised by anti-GST antibody. These bands were thought to be a result of non-specific binding of proteins to the glutathione-agarose beads. The addition of Triton X-100 before purification failed to reduce the non-specific binding.

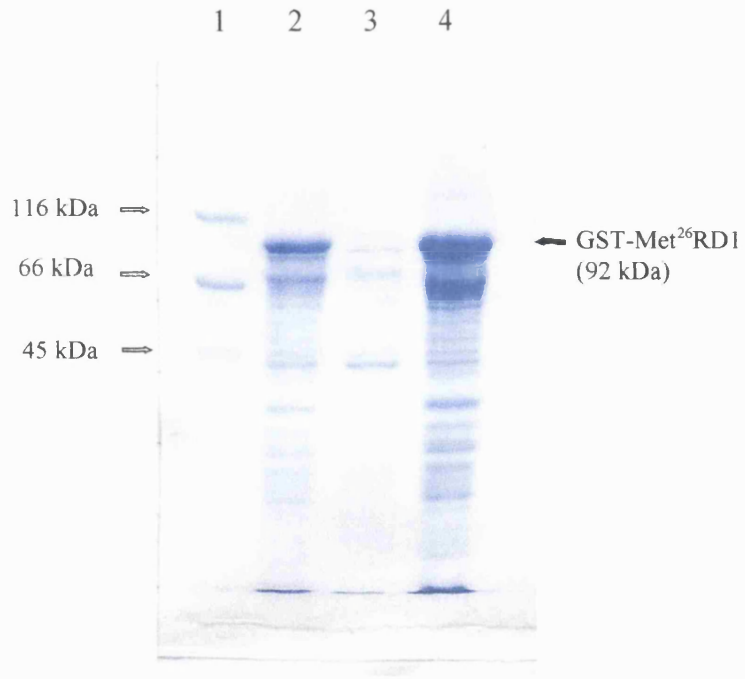

Figure 3.9 SDS PAGE of GST-Met^{26}RD1 expression studies. This figure represents a Coomassie Brilliant blue stained 10% SDS PAGE gel of bacterial lysates collected from 10 L after 5.30 h post induction for protein expression with IPTG. Following the lysis procedure, samples were centrifuged at 30 000 *g* for 30 minutes at 4°C using a Beckman L8 ultracentrifuge and prepared for SDS PAGE analysis as described in section 2.2.3.3. The lanes are: (1) Molecular size markers containing 0.6 µg of *β*-galactosidase, BSA and Ovalbumin. (2) 5 µg of total cell lysate. (3) 1 µg of soluble fraction. (4)10 µg insoluble fraction.

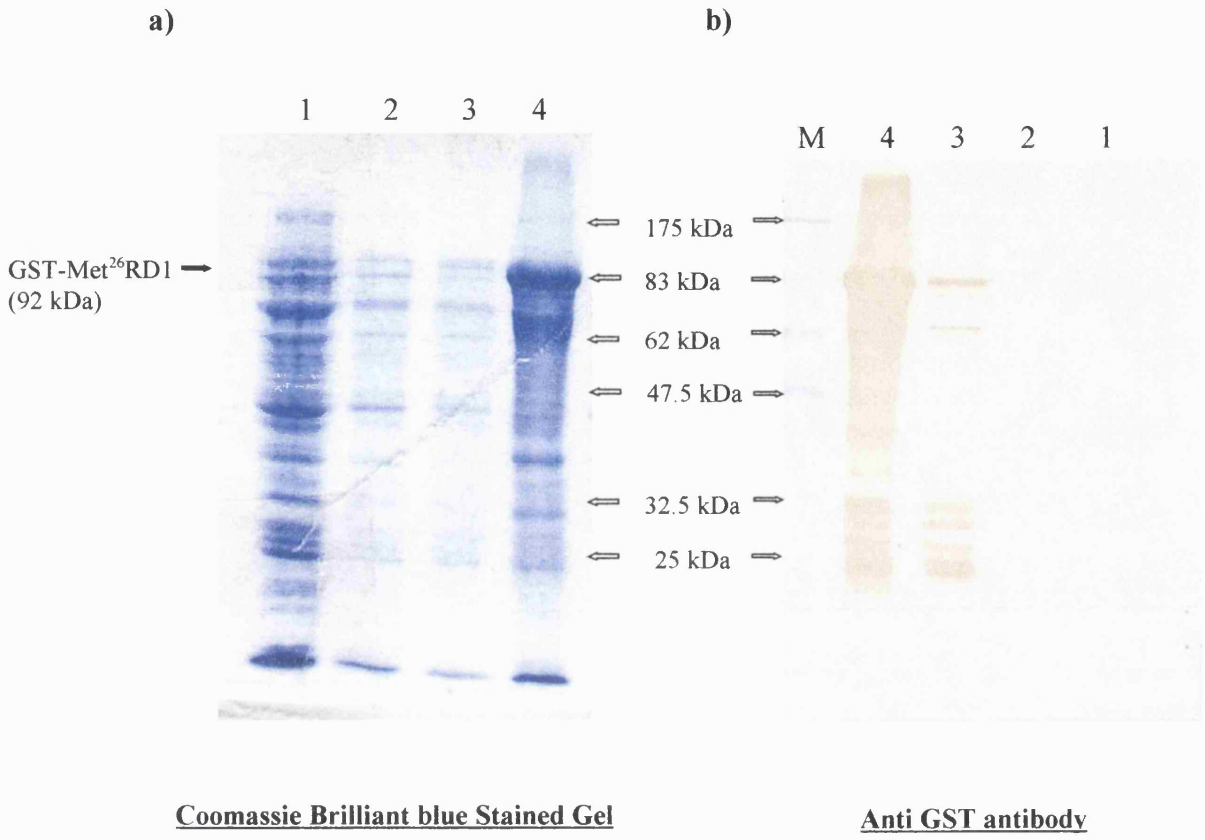

Figure 3.10 SDS PAGE and Western Blot analysis of Glutathione Affinity Column Purification. Panel (a) shows a Coomassie Brilliant blue stained 10% SDS gel, whilst panel (b) shows a replica gel that has been blotted onto nitrocellulose membrane and probed with anti-GST antibody. The lanes in both panels are: (M) Pre stained molecular size markers. (1) unbound material. (2) Column wash material. (3) Glutathione eluate. (4) Inclusion body fraction as control. Samples (except for the inclusion body sample) were concentrated 10x using methanol/ chloroform method as described in section 2.2.3.1 prior to loading onto SDS gel.

3.4 Discussion

The main objective of the work described in this chapter is to determine the methods to express the full length Met[26]RD1 as a glutathione S-transferase (GST) fusion protein in *E.coli* in a soluble form with activities similar to those reported in the literature (Swinnen *et al.*, 1989; Jin *et al.*, 1992; Kovala *et al.*, 1997), and to purify the recombinant GST protein to homogeneity using non denaturant conditions with the intention of scale-up to produce adequate amounts of protein to perform crystallisation and structural analysis.

At the beginning trial studies were performed at a small scale to determine the methods necessary to express GST-Met[26]RD1 fusion protein in bacteria and to purify the recombinant protein using glutathione affinity columns. Since different recombinant proteins possess different characteristics that could affect optimum expression, there was the need to determine the expression parameters that would give maximum expression of GST-Met[26]RD1 fusion protein. Although the specific activity of previously mentioned protein was low, parameters optimised in this project were time of expression, growth temperature and time of IPTG induction. JM109 (DE3) bacterial cells transformed with *C17* recombinant plasmid that directed the synthesis of GST-Met[26]RD1 protein, were induced to express GST-Met[26]RD1 protein using the *tac* promoter. Following protein induction, a band appeared on SDS gels with a molecular weight similar to that predicted for GST-Met[26]RD1(figure 3.6) accounting for approximatly10% of total cell protein. Western blot analysis revealed that this new protein was recognised by anti-GST antibody identifying the protein as GST-Met[26]RD1. However, the majority of the expressed GST-Met[26]RD1 fusion protein was found to be insoluble even when expressed at ambient temperature (figure 3.7). This was in agreement with other reports of full length PDE4D expression performed by Kovala *et al.* 1997. PDE activity assays performed on these samples detected low activities suggesting that most of insoluble PDE was inactive, due to the possible precipitation of the PDE proteins in inclusion bodies.

Most of the PDE activity detected was in the supernatant fraction. This activity was in the range of 0.67 ± 0.01 pmole/min/mg which was low compared to 0.4-0.9 nmole/ min/ mg activities reported for crude PDE recombinant preparations in bacteria (Swinnen *et al.*,

1989; Jin *et al.*, 1992; Kovala *et al.*, 1997) and lower than native activities of 1-2 μmole/ min/ mg for PDE4 isoenzymes (Conti *et al.*, 1995). Furthermore, the expressed protein showed 50% inhibition with 100 μM rolipram using 0.25 μM cAMP which was much lower than expected since IC_{50} of PDE4 recombinant protein expressed in bacteria have been reported to be in the range of 0.3 to 0.4 μM using 1 μM cAMP substrate (Jin *et al.*, 1992; Kovala *et al.*, 1997). The poor activity and inhibition of the recombinant GST-Met^{26}RD1 could be attributed to the misfolding of the protein lowering its binding to both cAMP and rolipram hence the given different kinetic characteristics. Indeed, this could be the case as GST-Met^{26}RD1 fusion protein failed to bind to Cibacron blue resin during dye affinity chromatography (data not shown) confirming the assertion that GST-Met^{26}RD1 fusion was misfolded as the Cibacron blue resin will only bind to correctly folded proteins with intact nucleotide binding region.

GST-Met^{26}RD1 recombinant protein was found to bind to the glutathione resin with high affinity and was found to elute with 10 mM glutathione. The elution of GST-Met^{26}RD1 fusion protein from glutathione agarose beads gave an activity of 4.56 pmol/min/mg and an inhibition of 70% when treated with 100 μM rolipram (Table 3.1). Although, purification improved the recombinant protein's susceptibility to rolipram, GST-Met^{26}RD1 still showed low activity. Furthermore, extensive degradation products were observed before and after purification.

A prediction of possible proteolytic sites can be proposed using the sizes of the proteolytic fragments observed on the Western blot (figure 3.10/b). As GST is fused to the Met^{26}RD1 at the N-terminus of the protein and as the antibody used in the Western blot analysis probed to the GST protein, fragments observed on the blot must contain the GST protein. Therefore, it is proposed that GST-Met^{26}RD1 fusion protein may be cleaved at two locations, one between GST and Met^{26}RD1 proteins to form small proteolytic fragments of 32-26 kDa and the second approximately 30 kDa from the C-terminus of the Met^{26}RD1 protein to form the larger proteolytic fragments of 62 kDa (figure 3.11). The second cleavage site was considered to have structural consequences which were predicted to have drastic activity affects as this cleavage site could be located to the hairpin region on Met^{26}RD1 connecting α helix 12 and 13 (see full protein sequence of Met^{26}RD1 in

Appendix 1 and figure 1.9). Thus proteolytic cleavage at this site would cause structural disturbance and removal of helices 13 onwards which have been found to bind to cAMP leading to lowered cAMP hydrolysis. Furthermore, as mentioned earlier in Chapter 1, these regions are important for rolipram binding hence the removal of these regions could abolish or reduce binding to rolipram which could explain the low inhibition of GST-Met[26]RD1 by rolipram.

While cleavage in the catalytic domain has kinetic consequences, the cleavage site estimated to be in the region between the GST and Met[26]RD1 proteins possibly located at amino acids 30-40 of Met[26]RD1 protein (Figure 3.11, Appendix 1), is important in the regulation of the protein as discussed in Chapter 1. Therefore, it is important to isolate the full length Met[26]RD1 without any contamination by these proteolytic fragments to properly analyse the protein kinetically and physically. Further purification of the glutathione GST-Met[26]RD1 eluate using standard purification methods may succeed in removing some of these products if not all. One way to achieve this is to mutate these cleavage sites to prevent cleavage by proteolytic enzymes. However, as one of these sites is present at the catalytic domain, mutation at this position is likely to affect catalysis.

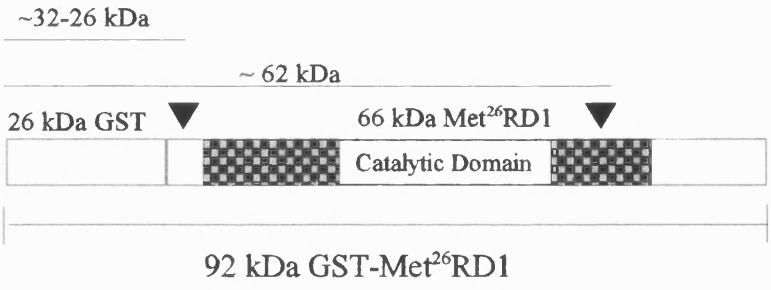

Figure 3.11 Schematic representation of possible proteolytic sites on GST-Met[26]RD1. Back boxes represent proteolytic sites. Checked box represent position of catalytic domain mapped according to structural analysis of PDE4B2 (Xu *et al.*, 2000). Black triangles represent possible proteolytic cleavage sites.

The heavy degradation of the protein caused difficulty in calculating specific activities due to difficulty in estimating the concentration of the active species of the enzyme. Thus, direct activity comparisons with the literature were not made.

In conclusion, it was found that Met^{26}RD1 was expressed successfully as a GST fusion protein in bacteria. However, it was observed that Met^{26}RD1 was highly insoluble, unstable and very susceptible to proteolytic cleavage even with the presence of protease inhibitors. The presence of proteolytic products as well as other contaminating proteins (figure 3.10) made purification of the Met^{26}RD1 recombinant protein difficult. As a consequence, expression of Met^{26}RD1 protein using bacteria was superceded by mammalian expression due to the failure to fulfil the objectives set out at the beginning of this chapter.

Chapter 4

Generation Of Polyclonal Antibody Against GST-Met^{26}RD1 Fusion Protein

4.1 Introduction

Antibodies have represented powerful analytical tools used in many fields of biochemical research for decades. This is due to their specificity and to the ease in which they can be labelled making them valuable in detecting and identifying antigens in many complex mixtures.

The development of immunological approaches to study proteins in 1975 by Kohler and Milstein allowed the production of highly specific probes to study PDE isozymes in impure systems. These probes were subsequently used for the isolation and purification of unique PDE isozyme from crude extracts using techniques such as immunoprecipitation and affinity chromatography (Hurwitz *et al.*, 1984). However, following cloning of PDEs and the development of recombinant DNA expression technologies in the early 1990s, antibodies were used to a lesser extent in the isolation and purification of PDE but more particularly in the immunological characterisation of the expressed recombinant PDEs.

This chapter gives an overview of the factors affecting antibody response in animals and thetechniques used to achieve optimum immunological response. In order to appreciate theimportance of the different steps adopted to produce antibodies both generally and in this work it is important to understand the different processes and interactions that occur during an immune response. A general overview will be given on the interactions and reactions that occur in a typical immune response giving extra focus on antibody production.

4.1.1 Immune Response System

The immune response is made of two cellular systems: The humoral or circulating antibody system and the cell mediated system. Both of which recognise and identify antigens such as foreign proteins or polysaccharides as part of the virus, bacterium or as degraded byproducts. The humoral antibody system produces antibodies via B-cells that recognise and bind to antigens leading to antigen destruction. These antibodies are found either bound to B-cell membranes or free in the serum and lymph. The cell mediated system, on the other hand, acts on antigens appearing on the surface of individual cells called antigen presenting cells (APC). T-cells then recognise these antigens via T-cell receptors leading to a series of processes and cell interactions causing ultimately, the destruction of cells containing the antigen. These two systems are summarised in figure 4.1.

4.1.1.1 Antibody Production

Antibodies are defined as groups of proteins that belong to a family of molecules called immunoglobulins. Immunoglobulins shown in figure 4.2 have the common structure of four polypeptide chains: two identical heavy chains and two identical light chains. The two heavy chains are joined to each other by two disulphide bonds, and each of the light chains are joined to the heavy chain by one disulphide bond. Both the light and heavy chains consist of constant, variable and hypervariable regions within their amino acid sequences. Five major groups of immunoglubulin have been identified: IgG, IgA, IgM, IgD and IgE with the most common being IgG. These groups have been classified according to their heavy chain component.

Antibodies are produced by B lymphocytes or B cells. Each B lymphocyte produces a distinct antibody molecule (Ig) which binds to two antigens at one given time. The antibody response to an antigen begins with the engulfment of the foreign body by the process of phagocytosis. This is performed nonspecifically by antigen presenting cells (APC) which include macrophages and other cells such as Langerhans cells found in the skin, lymph nodes, dendritic cells found in the spleen, and monocytes found in the blood.

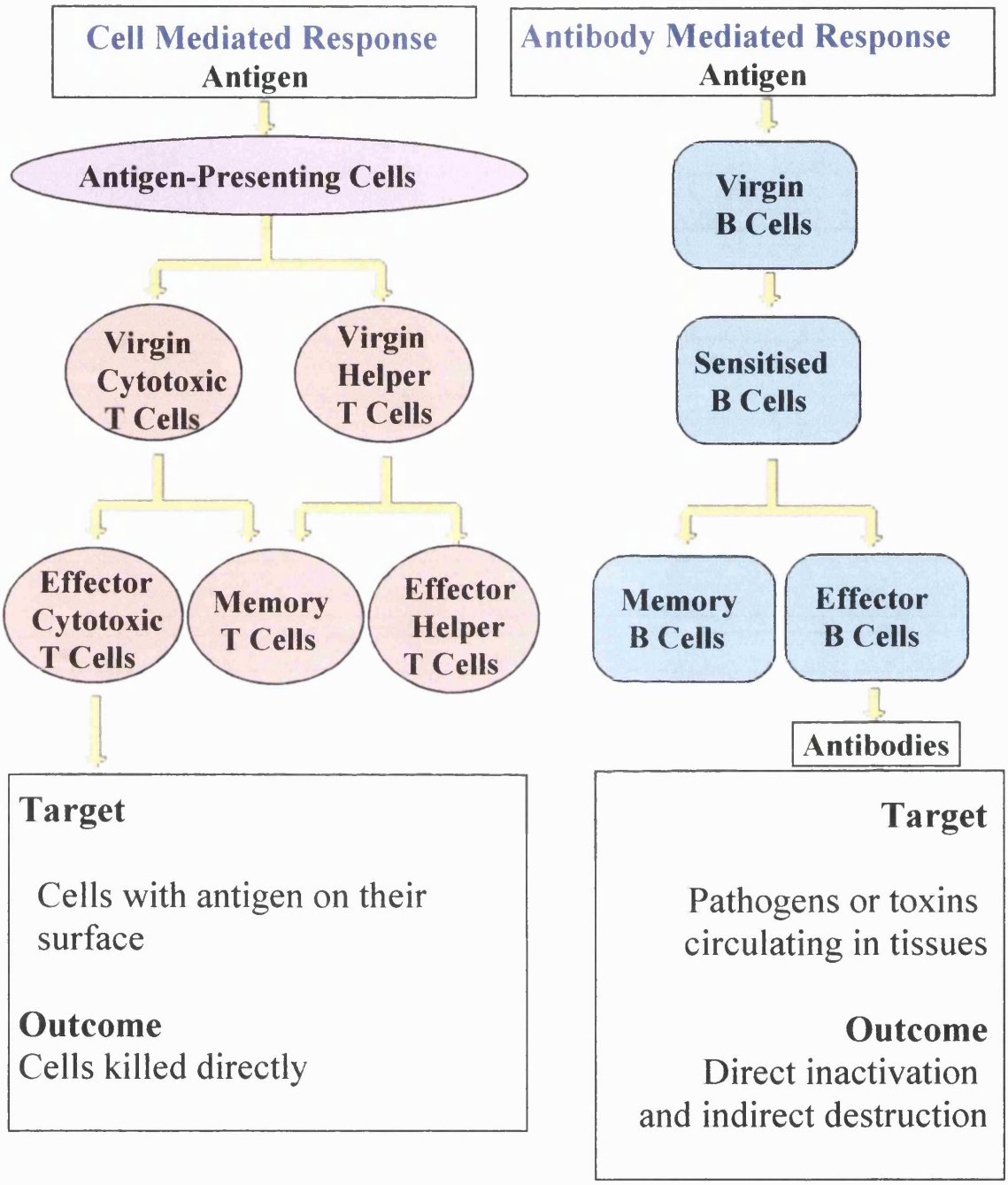

Figure 4.1 A schematic representation of immune response represented by the humoral system and the cell mediated system.

Following antigen degradation, byproducts are displayed on the surface these cells via cell-surface glycoprotein called MHC (major histocompatibility complex) class II. The APC interacts with the helper T-cells by binding antigen fragment-class II protein complexes with the T-cell receptors. A soluble polypeptide called Interleukin 1 (IL-1) is released by APC upon binding to the helper T-cells. This interaction leads to the activation, proliferation and differentiation of the helper T-cells, which is maintained by the release of a second polypeptide called interleukin 2 (IL-2) and the synthesis of IL-2 receptors by the T-cells.

While helper T-cells are proliferating, virgin B cells are stimulated by antigen binding to free antibodies present on their surface. The antigen-antibody complex is then internalised and the antigen is degraded and antigen fragments are displayed on the surface the cells by MHC class II complexes similar to those in APC. The proliferating helper T-cells stimulated by APC now bind to the B-cell. This interaction is an absolute requirement of antibody production because it leads to B cells' division and proliferation and the start of antibody production. The binding of B-cells to helper T-cells causes the synthesis of Interleukin 4 receptors. These receptors bind to Interleukin 4 molecules secreted by activated helper T-cells and stimulate the B cells to synthesise receptors that bind the differentiation factor Interleukin 10 (IL-10) which is also secreted by the activated Helper T cells. The interaction of both IL-10 as well as other factors (not well understood) induces the differentiation of the dividing B cells into plasma cells and memory cells. The plasma B cells specialise in the production large amounts of antibodies. In fact 40% of total protein synthesised by these cells are antibodies. These cells are short lived (3-4 days) and are found in the lymphoid organs. In contrast memory B cells are long-lived cells that do not secrete antibodies but do retain antibodies on their cell surface which have high affinities to exposed antigens.

The majority of the antibodies produced belong to the IgM class of immunoglobulins. These antibodies, which are found to peak around 7-10 days after the initial immunisation take part in the removal and clearance of the antigen. Antibody response has been found to decline if no more antigens are introduced due to the decline of plasma cells. However, helper T-cells and B-cell memory cells remain in circulation. So if a second dose of the same antigen were injected into the animal, a second response would develop using the

same pathway as the primary response described. This second response is found to occur faster and the majority of the antibodies produced are found to be of the IgG class which have higher affinities to the antigen compared to IgM class mentioned previously. These increased affinities of IgG antibodies to the antigen are mainly produced by somatic mutation of the variable region of the heavy and light chains of the B cells during their differentiation. Some mutation may yield affinities higher than the original B clone. B cells carrying antibodies with high affinity to the antigen are selected for proliferation and division as they will bind more efficiently to the antigen.

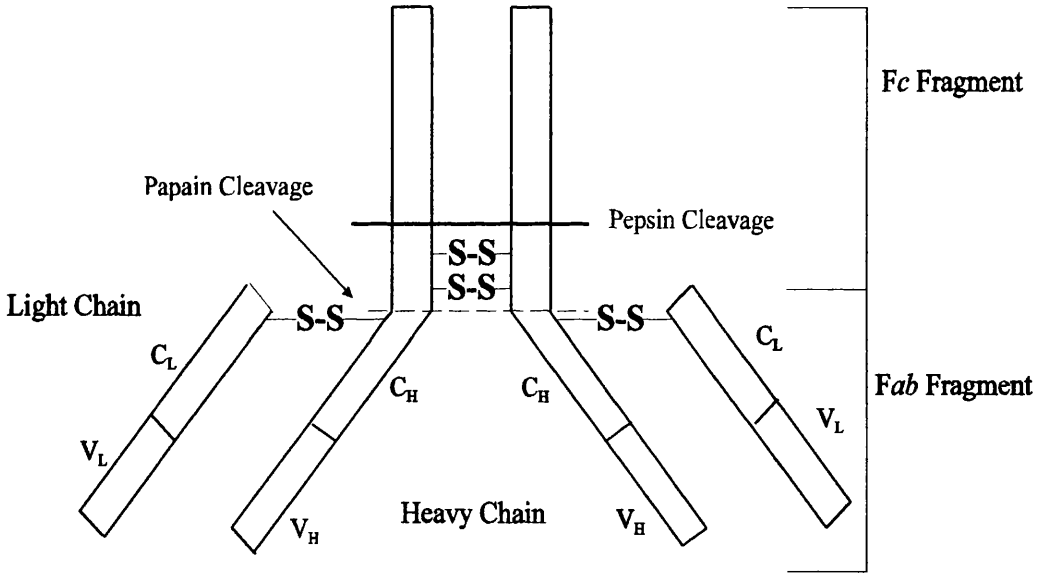

Figure 4.2 Basic structure of Immunoglobulin proteins. The bold line shows the proteolytic cleavage with pepsin into two molecules: one F(ab)$_2$ and sub-fragments of Fc. The dotted line shows the proteolytic cleavage with papain into three ~50 kDa fragments: two identical Fab fragments and one Fc fragment. Abbreviations: C_L represents constant light chain, C_H represents constant heavy chain, V_L represents variable light chain, V_H represents variable heavy chain, Fab represents fragment antigen binding and Fc called that as it is the fragment that is most readily crystallised.

4.1.2 Choice Of Antigen Preparation

In light of the processes that occur during the antibody response described previously, antigen preparation must be given a large amount of attention. It has been documented that over-expression in bacteria is considered to be one of the most excellent sources for antigens when antibodies are needed against cloned genes (Marston *et al.*, 1984). In the case of PDE antibody production, the most commonly used vectors that express protein in bacteria are those producing tryptophan (trpE) or Glutathione S-transferase (GST) fusion proteins (Kovala *et al.*, 1997; Huston *et al.*, 1996), the later system being the most common. Generally antigens were prepared using a method described by Huston *et al.*, 1996. In this method soluble protein purified to homogeneity using Glutathione affinity columns were used in the generation of the polyclonal antibodies. However, purification using glutathione columns did not always produce pure proteins due to the non specific binding of some proteins. Furthermore, it has been reported that particulates are found to be better immunogens than soluble molecules.

Generally, soluble fractions of many proteins induce poor antibody response whereas aggregates of the same proteins were found to induce good antibody responses (Harlow and Lane, 1988). This is found to be due to the ease in which particulates are taken up compared to soluble proteins by the antigen presenting cells (APC) described in section 4.1.1.1 by the process of phagocytosis. Consequently we decided to use GST-Met^{26}RD1 found in inclusion bodies in the generation of Met^{26}RD1 antibodies.

The intended use of the resulting antibody also had an impact in deciding on the type of preparation of the antigen. In this project the intended antibody was needed to be highly specific and to recognise Met^{26}RD1 PDE4 with high affinity in Western blot analysis. Therefore, purification of the antigen was found to be necessary in reaching this goal. The GST-Met^{26}RD1 antigen was purified using polyacrylamide gel rather than conventional chromatography methods. This is because antigens purified with this method are generally denatured resulting in the generation of antibodies that are useful for techniques that need denaturation-specific antibodies (Harlow and Lane, 1988).

Following sample separation using polyacrylamide gel electrophoresis, the protein band

of interest was isolated. This was performed by cutting strips from the edge of the polyacrylamide gel and staining them with Coomassie stain. This staining method was chosen to avoid excessive fixation of the proteins in the gel matrix.

Many approaches have been reported to process the gel slice ready for injection. These approaches depended on the type of animal injected. Generally gel slices can be injected directly into large animals such as rabbits after being fragmented prior to injection. Whereas, proteins for injection into small animals such as mice should be electro-eluted or electrophoresed onto suitable membranes before injection. However, in this project GST-Met^{26}RD1 protein separated using polyacrylamide gel electrophoresis was electro-eluted prior to injection into rabbits. This was performed to reduce severity of the injection on the animals.

4.1.3 Choice Of Animal

The choice of animals used in an immunisation procedure depends on how much serum is required, how much antigen is available, which species the antigen is isolated from and whether a monoclonal or a polyclonal antibody is required. Animals used routinely for antibody production in the laboratory are rabbits, mice, rats, hamsters and guinea pigs. These animals allowed the collections of adequate amounts of serum ranging from 25 ml from rabbits to 1-2 ml from rats, hamsters and guinea pigs. Larger animals such as sheep, goat, donkey and pigs can be used to produce larger volumes of serum.

Rabbits are reported to be especially good for polyclonal antibody production even when the amount of antigen is limited. These animals are easy to keep, to handle and can be bled safely when test bleeds are required. Furthermore, antibodies produced by rabbits are easily characterised which can make purification of the antibodies efficient and quick. In addition, adequate volumes of serum can be collected, volumes totalling 500 ml could be collected sequentially from a single rabbit if the rabbit is looked after carefully. Little is known about the genetics of the immune response in rabbits due to the outbreeding of most rabbits used for practical purposes. This outbreeding of rabbits causes the formation of a wide range of class II proteins capable of responding to many antigens. However, outbreeding of rabbits will cause different antibody responses to a single preparation of

antigens. Therefore, if the amount of the antigen is not limited a minimum of two rabbits should be immunised and the serum from each rabbit should be screened separately. In contrast to rabbits, mice are mostly inbred and the genetic bases of their immune response are intensively studied. These animals require small quantities of antigen and they produce small amounts of serum which can be collected at a given time. These characteristics make these animals ideal for monoclonal antibody production.

Another very important criteria that should be taken into account, when choosing the type of animal used for immunisation is the characteristic of self-tolerance. Self-tolerance is found in all immune systems and it occurs as consequence of the removal of the thymus, T-cells which possess receptors that react to internal components via a procedure which is poorly understood. Therefore, protecting the animal against damage from its own immune system. So to get a good immune response, antigens immunised into animals should be of different species. For example, antigens prepared from proteins that are isolated from rats should not be injected into rats but injected into rabbits instead as rats and rabbits are evolutionary distinct from each other.

4.1.4 Immunisation of Animals

Not only will the form and type of antigen preparation have an effect on antibody response but the choice of injection sites and the use of adjuvant will also have some affect. Both aspects work by optimising immunisation by increasing the efficiency of phagocytosis. Antigens are generally injected into sites that are rich in antigen presenting cells (APC) and low in processes that degrade the antigen. The most common routes of injection are subcutaneous, intradermal, intramuscular, intraperitoneal and intravenous (Harlow and Lane, 1988). Adjuvants on the other hand, help to protect the antigen from rapid degradation initiated by the body, and also stimulate factors that recruit macrophages to the site of the antigen leading to increased phagocytosis. The most common adjuvant used in research is the Freund's adjuvant which consists of a mix of water in oil prepared from a non metabolised oil (Freund and McDermott, 1942; Freund, 1956). Complete adjuvant contains killed *M. Tuberculosis* whereas incomplete adjuvant does not. Freund's adjuvant is characterised as the best adjuvant due to its capability to elicit a strong prolonged immune response. However, it is found to be very aggressive and can cause persistent

granulomas. Therefore, it is recommended that only the primary injection should contain the complete adjuvant whereas all subsequent boosts are given with the incomplete adjuvant. Animals need to be continuously monitored during the antibody production process to ensure they remain healthy.

The proper dose of the antigen given to animals depends on type of animal, the site of injection and the adjuvant used. Antigens once injected are susceptible to degradation by the body eliminating most of the antigens before reaching appropriate type of cells. To overcome this, adequate amounts of the antigen needs to be injected into the animal. It is reported that 50-100 μg of the antigen is often adequate in producing reasonable antibody response in rabbits. These amounts are reduced by 10 fold in mice and rats. Traditionally, the first dose given is two to three times bigger than the subsequent boosters. This has been found to produced adequate amounts of antibodies. In the literature, successfully produced antibodies against PDE protein either in the form of polyclonal or monoclonal suggested that PDE proteins have been good immunogens (MacPhee *et al.*, 1986; Hurwitz *et al.*, 1984; Kovala *et al.*, 1997; Huston *et al.*, 1996) . Consequently, this information was used to determine a minimal dose when injecting rabbits.

4.1.5 Antibody Purification

The purification of IgG is considered to be important for many reasons. The degree of purification were determined by the purpose for which the final preparation is intended. For example, if the antibody was used for an assay as part of a large system then removing contaminants that may interfere with this assay would be considered to be important. But on the other hand if the antibody was used for analytical reasons and needs to be stored for long periods, then purification is considered to be important to remove contaminating proteolytic activity to maintain the immunoreactivity of the antibody.

Many purification methods have been reported to purify monoclonal and polyclonal antibodies raised against GST-PDE4 immunogens. These methods ranged from the use of GST affinity columns (Kovala *et al.*, 1997) to protein-A affinity columns. The later method is considered to be the most common and routinely used technique in the purification of antibodies in particularly polyclonal antibodies generated from rabbits,

human, pig, guinea pig, dog or cats (Harlow and Lane, 1988). This is due the efficient binding of protein-A to antibodies produced by these animals. Protein-A which is produced using a specific strain of *Staphylococcus aureus* (Staph A) has six different binding sites to IgG. Five of these show high affinity to the Fc region of the IgG molecule and four out the five show some affinity to the F*ab* region of the IgG molecule.

4.1.6 Aim

The main object of the work described in this chapter was to produce an antibody against GST-Met^{26}RD1 fusion protein. Although some difficulty was faced with the expression of Met^{26} RD1 gene in bacterial cells (Chapter 3), the gene was successfully expressed in mammalian cells (Chapter 6). However the lack of a commercially available antibody against this recombinant protein would have made it difficult to identify and characterise this protein when expressed in mammalian cells. Therefore, the objective was to produce an antibody that would be able to recognise Met^{26}RD1 protein expressed in mammalian cells.

4.2 Methods And Results

4.2.1 Preparation of GST-Met^{26}RD1 Antigen using Electro-elution

GST-Met^{26}RD1 inclusion bodies were treated with the aim of producing soluble protein. The solubilisation was achieved by denaturing the protein using urea followed by refolding of the protein by the gradual removal of the denaturant by dilution.

8 g of the bacterial cell pellet was lysed initially by freezing the sample in -80°C freezer ON followed by thawing the sample at room temperature for a few hours. This procedure was repeated three times. The pellet was then resuspended in 80 ml of homogenisation buffer (50 mM Tris pH 8, 1 mM EDTA, 50 mM NaCl) and homogenised for 1 minute at room temperature using a Janke & Kunkle Ultra-Turrax T25 homogeniser set at 6000 rpm. Lysozyme freshly prepared as a 10 mg/ml stock in distilled water was added to the homogenate to a final concentration of 200 μg/ml and the mixture was incubated on ice

for 30 minutes whilst homogenising every 10 minutes using a Janke & Kunkle Ultra-Turrax T25 homogeniser set at 6000 rpm. 5% sodium deoxycolate (w/v) prepared in distilled water was added to the homogenate to a final concentration of 0.1 % and the mixture was incubated at room temperature for 30 minutes whilst again homogenising every 10 minutes using a Janke & Kunkle Ultra-Turrax T25 homogeniser set at 6000 rpm. The mixture was centrifuged at 3600 *g* for 60 minutes at 4°C using a Sigma 6K10 benchtop centrifuge with a fixed angle rotor (No 12500). The supernatant, which had a yellow colour, was removed and retained for future analysis. The pellet which had a mucus texture and brown/ yellow in colour was resuspended in 80 ml of homogenisation buffer containing 0.5% Triton-X 100 using a Janke & Kunkle Ultra-Turrax T25 homogeniser set at 6000 rpm. The mixture was centrifuged at 3600 *g* for 60 minutes at 4°C using a Sigma 6K10 benchtop centrifuge with a fixed angle rotor (No 12500) and the pellet was washed with Triton twice more or until the pellet was white and chalky in texture. Following the Triton washes, the mixture was divided into two 50 ml falcon tubes and centrifuged at 3600 *g* for 60 minutes at 4°C using a Sigma 6K10 benchtop centrifuge with a fixed angle rotor (No 12500). Half of the mixture was solubilised by resuspending the pellet with 50 ml denaturation buffer (50 mM Tris pH 8, 8 M deionised urea purchased from Sigma, 5 mM EDTA, 50 mM NaCl) using a Janke & Kunkle Ultra-Turrax T25 homogeniser set at 6000 rpm. The homogenate was left to incubate at room temperature for 2-3 h and half the mixture was re-natured by diluting the mixture 1 in 5 in re-naturation buffer (20 mM Tris pH 7.4, 1 mM EDTA, 20 mM $MgCl_2$) at room temperature using a Pharmacia P1 pump set at 6 ml/h.

188 µl of the solubilised sample was loaded into a single large well of 10% SDS-polyacrylamide gel. The SDS gel was prepared and run as described in section 2.2.3.2. The gel was washed with an elution buffer (25 mM Tris base, 192 mM Glycine, 0.05% SDS) and edges of the large well were cut and stained with Coomassie Brilliant blue for 5-10 minutes and destained for a further 5-10 minutes to identify the band of interest. The stained edges were aligned with the rest of the gel to identify the wanted band. The band of interest was excised and cut into smaller pieces to allow maximum protein elution from the gel. 5 cm length dialysis tube (with a size cut-off range of 14 kDa) soaked in distilled water was clipped on one side and 1 ml of elution buffer (25 mM Tris base, 192 mM Glycine, 0.05% SDS) was added. The small gel pieces were transferred into the dialysis

tubing which was then sealed with another clip after removing excess elution buffer. Generally 0.5 ml was enough to cover the gel pieces. The dialysis tubing was placed in a Western blotting tank purchased from BioRad. The elution buffer was added so it just covered the bag. The proteins were eluted out of the SDS-polyacrylamide gels using 100 mA constant current set for 3 to 4 hours, the current was then reversed for 2 to 5 minutes to detach the eluted protein off the dialysis membrane. Following electro-elution, gel slices were removed from the bag and were stained with Coomassie Brilliant blue to check that the protein of intrest has eluted. The eluted protein was analysed by SDS PAGE and Western blots to check the authenticity of the protein. Figure 4.3 showed that the electro-eluted protein migrated to the correct molecular size and that it was recognised with anti-GST antibody.

The eluted protein was quantified by running known amounts of protein size markers beside the eluted protein and comparing the intensities of the markers with the intensity of the eluted proteins. 1mg/ml stock solutions of bovine serum albumin (66 kDa) and β-galactosidase (116 kDa) were prepared. 2 μg and 4 μg of each marker were run on 10% SDS PAGE beside 2 μl of the eluted protein, the gel is shown in figure 4.4. The intensity of the eluted protein was mostly compared to the band intensity of β-galactosidase protein band due to the band size similarity between the GST-Met^{26}RD1 and β-galactosidase (92 kDa and 116 kDa respectively) making the band staining with Coomassie Brilliant blue comparable. Figure 4.4 showed that the intensity of GST-Met^{26}RD1 was similar to β-galactosidase protein band resulted from loading 2 μg of sample suggesting that the concentration to be approximately 0.5-1 μg/μl.

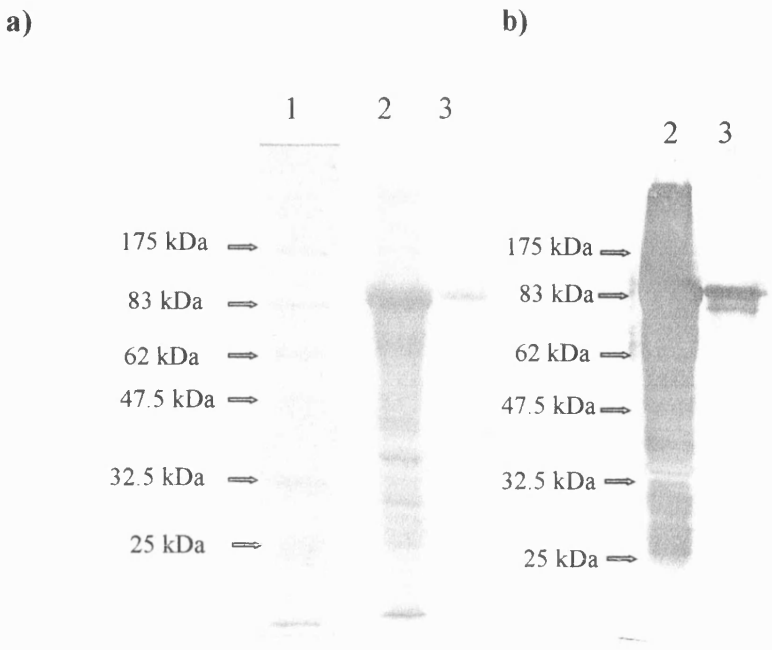

Figure 4.3 SDS PAGE and Western Blot analysis of electro-eluted GST-Met^{26}RD1 fusion protein. Panel **(a)** shows a Coomassie Brilliant blue stained 10% SDS gel, whilst panel **(b)** shows a similar gel that has been transferred onto nitrocellulose membrane and probed with anti GST antibody at a 1 in 1000 dilution. Bands were visualised using 3', 3'-Diaminobenizine (DAB) staining described in section 2.2.3.4. The lanes in panel (a) are: (1) Pre stained molecular size markers. (2) Inclusion body solubilised with 8 M urea. (3) Electro-eluted GST-Met^{26}RD1 protein. Lanes in panel (b) are: (2) Inclusion body solubilised with 8 M urea. (3) Electro-eluted GST-Met^{26}RD1 protein.

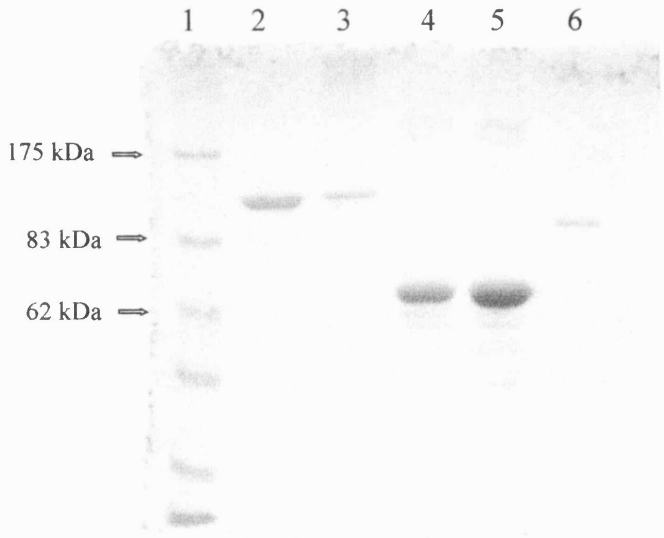

Figure 4.4 Quantification of the electro-eluted GST-Met^{26}RD1 protein using Coomassie Brilliant blue stained 10% SDS-polyacrylamide gel. The lanes are: (1) Pre stained molecular size markers (BioLabs). (2) 4μg β-galactosidase (116 kDa). (3) 2 μg β-galactosidase. (4) 2 μg Bovine Serum Albumin (BSA 66 kDa). (5) 4 μg BSA. (6) 2 μl of electro-eluted GST-Met^{26}RD1 protein.

4.2.2 Production of Met^{26}RD1 Polyclonal Antibody in Rabbits

Animal procedures described in this section 4.2.2 were according to project licence number 70/5185 and were performed by Kieran Brickley (a personal licence holder). General assistance maintaining and testing of bleeds was by the author.

4.2.2.1 Injection of GST-Met^{26}RD1 Antigen into Rabbits

360 μl (0.5 μg/μl) of electro-eluted GST-Met^{26}RD1 fusion protein prepared as described in section 4.2.1 was mixed with 700 μl of Freunds Adjuvant/Complete (Sigma) by

repetitive sucking and releasing the mixture using a 1 ml syringe until the mixture became thick and milky (for about 15 minutes at room temperature). Two black and white rabbits (labelled LZ72 and LZ77) were injected subcutaneously with half of the mixture (approximately 500 μl) at two positions situated at the rear on both legs using a 25-gauge needle. The injection was performed following the administration of EMLA cream (Astra) as a local anaesthetic.

Following injection of the antigen in two rabbits, ulcers formed at the two sites of injection within a week. The presence of these ulcers did not have an effect on the health of the rabbits. These ulcers eventually disappeared and there was no re-occurrence when antigen was injected again when boosters were given.

4.2.2.2 Boosts of Immunological Response to GST-Met^{26}RD1 Antigen

A month after the primary injection of GST-Met^{26}RD1 antigen, each rabbit was injected with 400 μl of a mix containing 700 μl Freund Adjuvant/Incomplete (Sigma), 180 μl (0.5 μg/μl) GST-Met^{26}RD1 electro-eluted protein and 180 μl 1x PBS, to boost the immuno-response to GST-Met^{26}RD1.

4.2.2.3 Collection of Test Bleeds

At seven days and at three weeks after the second injection (booster), test bleeds were performed to check the production of anti GST-Met^{26}RD1 antibodies. EMLA cream was applied on the inner edge of the rabbits' ears and left for approximately 20 minutes to take affect. Rabbits were wrapped in a restraining towel and blood was collected by making an incision through the marginal vein found on the inner edge of the ears. 1-2 ml of blood were collected from one ear by allowing the blood to fall drop wise into a clean test tube. The blood flow was stopped by applying pressure on the incision for 10-20 seconds.

4.2.3 Serum Preparation

4.2.3.1 Test Preliminary Bleeds

The blood samples collected previously in section 4.2.2.3 were allowed to clot at room temperature for about 1 hour. The serum was separated from the clot by centrifugation at 400 *g* for 3 minutes at 4°C using a Sigma 6K10 benchtop centrifuge with a swing out rotor (No 11162). The bleeds were tested for antibody production by Western blotting and results are shown in Figure 4.5. Results showed that serums collected from both rabbits recognised both the GST-Met^{26}RD1 protein used to inject the rabbits and the protein expressed in mammalian cells with similar specificity. Therefore, serum obtained from LZ77 rabbit was used in all future Western blot analysis requiring the use of Met^{26}RD1 antibody. The response was detected even when diluting the antibody 1000 fold suggesting that a high affinity antibody has been produced.

4.2.3.2 Testing Final Bleeds

The final blood sample was collected by cardiac puncture under terminal anaesthesia using a sub-lethal dose of general anaesthetic with death by exsanguination. 45-50 ml of blood was collected per rabbit. The serum obtained was approximately 50% of the total volume. The serum was obtained as described in section 4.2.3.1 except in this case blood samples were incubated overnight at 4°C to allow efficient clotting to occur. Serum obtained from the final bleeds were tested for the presence of anti GST-Met^{26}RD1 antibodies by Western blot analysis. Figure 4.6 showed the crude sera obtained from the final bleeds to recognise the Met^{26}RD1 recombinant protein produced in mammalian cells in a specific fashion similar to the results obtained for the preliminary test bleeds.

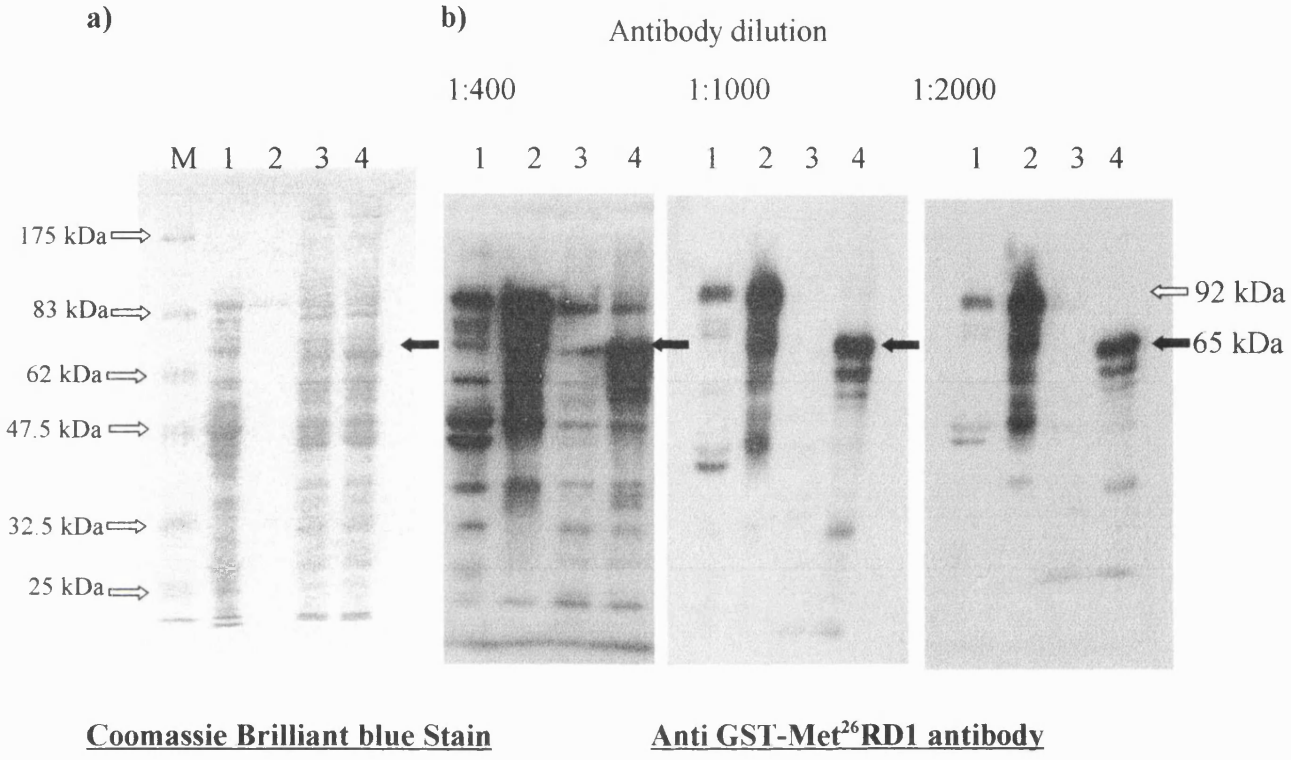

Figure 4.5 SDS PAGE analysis and Western blot analysis of test bleeds. Panel **(a)** shows a 10% SDS gel stained with Coomassie Brilliant blue stain. Panel **(b)** shows similar gels transferred onto nitrocellulose membrane and probed with crude serum of anti GST-Met^{26}RD1 antibody test samples collected from both rabbits diluted 1:400, 1:1000 and 1:2000. Bands on the nitrocellulose membranes post transfer were visualised using ECL substrates as described in section 2.2.3.4. The lanes are: (M) Pre-stained markers (BioLabs). (1) 10 µg JM109 (DE3) lysate. (2) 2 µg GST-Met^{26}RD1 antigen. (3) 10 µg Baby Hamster Kidney cells (BHK). (4) 10 µg Met^{26}RD1 recombinant protein expressed BHK (Chapter 6). The black arrow indicates the position of the 65 kDa Met^{26}RD1 protein expressed in BHK-21 cells.

4.2.4 Purification of The Polyclonal Antibody

Antibodies produced against GST-Met^{26}RD1 from the final bleeds were batch purified using protein-A agarose. 0.5 ml of protein-A agarose (wet bed volume) was washed 2-3 times with freshly made 1x PBS (2.6 mM KCl, 1.4 mM K_2PO_4, 0.1369 M NaCl, 8.1 mM Na_2PO_4) and bound to 20 mg of crude serum (LZ77) by overnight incubation at 4°C with gentle rocking. Following the overnight incubation the GST-Met^{26}RD1 antibody resin complex was washed three times with 1.5 ml of fresh 1x PBS (2.6 mM KCl, 1.4 mM K_2PO_4, 0.1369 M NaCl, 8.1 mM Na_2PO_4) by mixing and resin sedimentation under gravity. The antibody was eluted three times with 0.3 ml of 0.2 M fresh glycine pH 2 which was immediately neutralised by the addition of 30 µl of 1 M Tris pH 10. The three eluates were pooled and transferred into a dialysis tubing (14 kDa cut off pore size) pre soaked in distilled water. The sample was dialysed overnight at 4°C against 500 ml of 1x PBS (2.6 mM KCl, 1.4 mM K_2PO_4, 0.1369 M NaCl, 8.1 mM Na_2PO_4) to remove the glycine. The absorption at 280 nm of the dialysed sample was measured and the concentration of the IgG was calculated using the relationship 1 OD_{280} equals 1.26 mg/ml of protein. The majority of the polyclonal antibody in the rabbit serum bound to the resin and approximately 80 % of the original protein concentration eluted with glycine. Figure 4.7 indicates that a band with a molecular weight of 66 kDa was present in the eluted sample. This band was suggested to be serum albumin.

4.2.5 Preparation of Antibody affinity column

Purified GST-Met^{26}RD1 antibodies were coupled to protein-A Sepharose using a general room temperature method described by Harlow and Lane, (1988). Briefly, 2 mg of GST-Met^{26}RD1 polyclonal antibody prepared as described in section 4.2.3.2 and purified as described in section 4.2.4 was added to 1 ml bed volume of protein-A Sepharose (Sigma) contained in a 10 ml loose slurry for 1 hour at room temperature. The beads were then washed 3x with 10 volumes of 0.2 M sodium borate pH 9 (solution was prepared by dissolving 0.2 M boric acid in water and adjusting the pH to 9 with 1 M NaOH) by centrifugation using a Sigma 6K10 benchtop centrifuge with a swing out rotor (No 11162) set to centrifuge at 910 rpm for 5 minutes at 18°C. The beads were suspended in 10

volumes of 0.2 M sodium borate pH 9 and 100 µl was removed for SDS PAGE analysis. 20 mM final concentration of dimethyl pimelimidate DMP (Sigma) was added to the beads. Beads were incubated with gentle mixing at room temperature for 30 minutes. Again 100 µl of the coupled beads were removed for SDS PAGE analysis. The coupling reaction was stopped by washing the beads once with 0.2 M ethanolamine pH 8 and then incubating with 0.2 M ethanolamine for 2 hours at room temperature with gentle mixing. The beads were finally washed once with fresh 1x PBS (2.6 mM KCl, 1.4 mM K_2PO_4, 0.1369 M NaCl, 8.1 mM Na_2PO_4) and stored in 1x PBS supplemented with 0.04% NaN_3 at 4°C. The efficiency of the coupling was checked by boiling the samples of beads collected before and after coupling in protein sample buffer (section 2.2.2.3). 1 and 9 µl of beads were loaded on 10% SDS polyacrylamide gel (section 2.2.2.3).

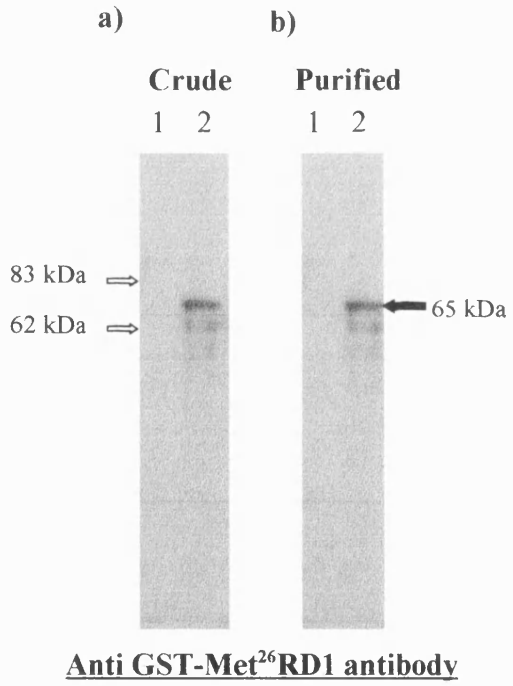

Figure 4.6 Western blot analysis using crude and purified serum. Panel (a) shows a blot probed with crude GST-Met^{26}RD1 anti-sera. Panel (b) shows a replica blot probed with purified GST-Met^{26}RD1 anti-sera using Protein-A agarose. Bands in both blots were visualised using ECL substrate as described in section 2.2.3.4. Lanes are: (1) 10 µg of untransfected BHK-21 cell lysates. (2) 10 µg pSFV-1-Met^{26}RD1 transfected BHK-21 cell lysates. The black arrow indicates the position of the 65 kDa Met^{26}RD1 protein expressed in BHK-21 cells.

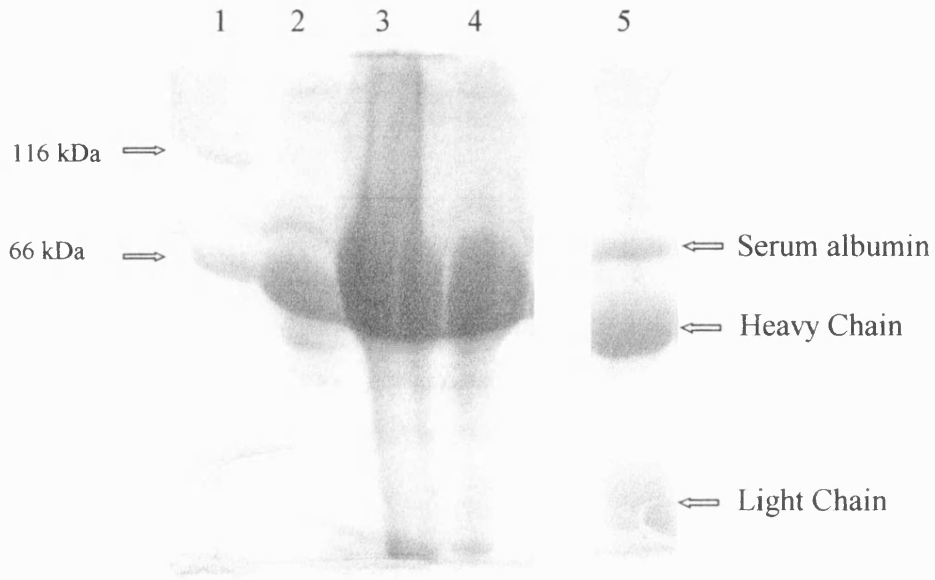

Coomassie Brilliant blue Stain

Figure 4.7 SDS PAGE analysis of Protein-A agarose purification of GST-Met^{26}RD1 IgG. This figure shows a Coomassie Brilliant blue stained 10% SDS. The lanes are: (1) Molecular size markers β-galactosidase (116 kDa), BSA (66 kDa). (2) 10 µl original material. (3) 10 µl unbound material. (4) 10 µl Wash material. (5) 10 µl IgG eluate.

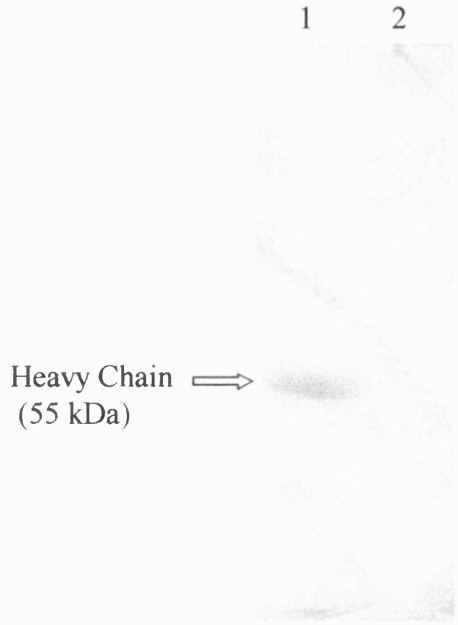

Figure 4.8 SDS PAGE of cross-linking of GST-Met^{26}RD1 antibody to Protein-A Sepharose. This figure shows a Coomassie Brilliant blue stained 10% SDS gel. Lanes are: (1) 9 µl of cross-linking reaction before addition of DMP. (2) 9 µl of cross-linking reaction after addition of 20 mM final concentration of DMP.

4.3 Discussion

The main aim of the work discussed in this chapter was to produce an antibody capable of recognising the mammalian expressed Met^{26}RD1 (Chapter 6) as well as the original antigen GST-Met^{26}RD1 on Western blots. In the absence of a commercial antibody the production of this antibody provided a useful tool to enable the identification and characterisation Met^{26}RD1 when expressed in mammalian cells using the Semliki Forest virus system (described in Chapter 6).

The immunogen used in this work was previously expressed as a GST-Met^{26}RD1 fusion protein in bacteria (described in Chapter 3). To recap, this protein was found to accumulate in an insoluble form thought to be inclusion bodies. These inclusion bodies

provided adequate amounts of protein for antibody production. Following the separation and detection of the fusion protein on SDS PAGE gels (figure 4.3), the band identified as the fusion protein was cut and the gel slice was either lyophilysed (freeze dried) or crushed (data not shown). SDS gel analysis as well as western blot analysis showed that the protein was not recovered by these two methods. Consequently, another method was employed to prepare the antigen. The method chosen was electro-elution, in which the protein in question was eluted from the polyacrylamide gel slice by electrophoresis. Separating contaminating polyacrylamide from the protein was important since it could be toxic for the animals. Western blot analysis of the eluted protein using anti GST antibody probe (figure 4.3) showed that the eluted protein migrated the same distance as the protein in the original sample suggesting that the correct band was eluted. However, only half of the original protein was recovered. In an attempt to increase the amount of protein eluted, the protein was eluted for increased or decreased periods of time. These experiments failed to increase the amounts of protein recovered (data not shown).

The primary injection of the antigen caused the formation of an ulcer at the site of injection. This was thought to occur as a result of the rabbit's reaction to the Freund's complete adjuvant as no reaction was observed when incomplete Freund's adjuvant was used. Freund's complete adjuvant as mentioned earlier can cause granuloma due to the presence of the killed *M. Tuberculosis*. This toxin activates the phagocytes at the site of injection causing inflammation.

The antisera collected from both rabbits at the first test bleed, were screened separately. Both antisera detected both the GST-Met^{26}RD1 antigen and the Met^{26}RD1 protein expressed by the BHK cells (figure 4.5) with similar affinities. Although the exact titres were not identified, the anti sera detected the two mentioned proteins with high efficiency even when diluted up to a 1000 fold, suggesting that the GST-Met^{26}RD1 antibody was produced in high affinity (figure 4.5). The purification of the crude serum was not successful in reducing the background as no difference was observed between the purified and non purified sera (figure 4.6). Nevertheless, diluting the primary antibody to 2000 times was found to be effective in reducing the background in Western blot analysis. Therefore, all subsequence Western blots using GST-Met^{26}RD1 antibody were performed using crude sera diluted 2000 fold.

SDS PAGE analysis (figure 4.7) of the purification procedure of the crude antisera using Protein-A agarose showed the presence of a protein which was suspected to be albumin due to similarity in size. Further purification of the antibody to remove this contaminant was found unnecessary as albumin was used in all Western blot analysis as a blocking reagent.

Western blot analysis in figure 4.5 lane 5 showed that the antisera detected several bands beside the 65 kDa Met^{26}RD1. These bands were thought to be a result of probable proteolysis of the Met^{26}RD1 protein as these bands did not appear in Baby Hamster Kidney cell (BHK) lysates not expressing Met^{26}RD1 protein. The antiserum also detected a second protein in the bacterial lysate of a similar size as the GST-Met^{26}RD1 fusion protein(figure 4.5 lane 2). The presence of this protein can be explained by the fact that this protein could have co-eluted with the GST-Met^{26}RD1 fusion protein during antigen preparation and was consequently, injected with the fusion protein into the rabbits. Therefore, antibodies were raised against this protein as well as the GST fusion protein. The presence of antibodies against this bacterial protein was not considered to be a problem since this antibody was mainly used to detect Met^{26}RD1 recombinant protein expressed in mammalian rather than bacterial cells. Although the antisera was raised against the bacterial fusion protein GST-Met^{26}RD1 , the high specificity for the mammalian expressed Met^{26}RD1 protein, enabled an immuno-affinity column to be prepared. The immuno-affinity column allowed the purification of Met^{26}RD1 protein in the later stages of the project. Preparation of the immuno-affinity column was performed by binding the purified IgG antibodies to protein-A Sepharose and cross-linking the two proteins with dimethyl pimelimidate (DMP). Successful cross-linking was achieved using DMP reagent as shown by the disappearance of the heavy chain from solution following the addition of DMP in figure 4.8.

To conclude, an antibody was produced from the inoculation of GST-Met^{26}RD1 protein previously prepared from *E. coli*. This antibody was found to be highly specific to the mammalian expressed Met^{26}RD1 protein providing an analytical tool for Met^{26}RD1 protein in later stages of the project. Furthermore, the specificity of the antibody to Met^{26}RD1 protein made it possible to produce an antibody affinity column which would enable the purification of Met^{26}RD1 protein to homogeneity (Chapter 6).

Chapter 5

Optimisation Of Semliki Forest Virus Mammalian Expression System

5.1 Introduction

Some recombinant proteins can be difficult to express due to their topology, folding requirements, and post-translational modifications. Although many non-mammalian expression systems such as bacteria and insect cells have a good reputation in expressing milligram quantities of proteins, they have different post-translational modifications compared to mammalian cells which may affect folding and enzyme activity. Therefore it is advantageous to express mammalian genes in mammalian cells as physiological conditions will be provided for the recombinant protein to fold correctly and function actively and similarly to its native counterparts.

Numerous expression systems have been developed to express heterologous DNA sequences in animal cells in large amounts. Previously, stable expression technologies, based on chromosome integrated plasmid sequences, were routinely used for large-scale expression of proteins. This was due to their capability of producing milligram or even kilogram amounts of complex proteins (Wurm and Bernard, 1999). However, the development of these technologies have been reported to be considerably expensive, time consuming, and labour intensive.

Since the development of better transfection methods, transient expression systems in mammalian cells have been explored beyond the laboratory scale. Large scale transient expression, have been reported to be mediated via plasmid vectors or virus vectors (Wurm and Bernard, 1999; Bernard and Blasey, 1999). Although, DNA vector mediated, expressions have been successfully scaled-up (Blasey *et al.*, 1996), they suffer limitations such as the requirement for large quantities of DNA and large scale transfection procedures (Blasey *et al.*, 2000). On the other hand, viral mediated transient expressions are characterised to be capable of high levels of expression and efficient delivery of cloned

genes into host cells (Liljestrom and Garoff, 1993). Therefore, it is not surprising that viral-based expression systems are widely used amongst many researchers.

About a decade ago, Liljestrom and Garoff, 1991 developed a mammalian expression system based on Semliki Forest Virus (SFV). This system since its development has been used to express a large number of recombinant proteins (Table 5.1) which made it one of the most widely used expression systems to date. SFV has the distinct advantage over other viral based mammalian expression systems with respect to speed and expression levels. The high levels of expression accomplished, have been reported to be due to the SFV extremely efficient 26S promoter and to the high number of RNA copies (200.000) per infected cell which ultimately leads to high levels of expression (Wurm and Bernard, 1999). Furthermore, SFV can virtually infect most mammalian, insect, amphibian cell types allowing the expression of the heterologous gene in the optimum cell type. The recent publication by Blasey *et al.*, 2000 reported the use of this system for scale up expression using bioreactors. This would ultimately help with the production of milligram quantities of protein which is needed for structural studies. Therefore, the work described in this chapter describes the optimisation of the system using pSFV-3 as recommended by the manufacturer (Gibco BRL) with the aim of using this system to express phosphodiesterase 4 (Met^{26}RD1). β-galactosidase is a tetrameric protein (4 identical 116 kDa Subunits) which catalyse the hydrolysis of various β-galactosides one of which is 5-bromo-4-chloro-3-indolyl-β-D-galactoside (X-gal). X-gal is suitable for staining fixed mammalian cells (i.e. *in situ* staining) expressing β-galactosidase allowing the determination of the transfection efficiency which in turn allowed the determination of the viral titres as will be described in this chapter's material and methods. The hydrolysis reaction catalysed by β-galactosidase using X-gal as substrate is as follows:

5-bromo-4-chloro-3-indolyl-β-D-galactoside + H_2O ⟹ galactose + blue insoluble indolyl
(X-gal) derivative

Table 5.1 Proteins expressed from SFV vectors.

Enzymes	
β-gal	Liljestrom and Garoff, 1991
Mouse dehydrofolate reductase	Liljestrom and Garoff, 1991
Chicken lysozyme	Liljestrom and Garoff, 1991
Terminal deoxynucleotide transferase	Ciccarone *et al.*, 1993
Caspase-2 (Nedd-2)	Allet *et al.*, 1996
Human cyclooxygenase-2	Blasey *et al.*, 1997
Rat and human catechol O-methyltransferase	Ulmanen *et al.*, 1997
Thyroid peroxidase	Bikker *et al.*, 1997
Receptors	
Human transferin receptor	Liljestrom and Garoff, 1991
Mouse 5-HT3 receptor	Werner *et al.*, 1994
Human neurokinin receptor-1	Lundstrom *et al.*, 1994
Dopamine receptor 3	Lundstrom *et al.*, 1995
Human neurokinin receptor-2	Lundstrom *et al.*, 1995
Adenosin A3 receptor	Patel *et al.*, 1997
Human postaglandin receptor EP-4	Marschall *et al.*, 1997
Human 5-HT1 alpha receptor	Stables *et al.*, 1997
Human Purinergic Receptor (P2X) P2X1, rat P2X2, rat P2X3, and rat P2X4	Lundstrom *et al.*, 1997
GABAA alpha and beta 2 subunits	Gorri *et al.*, 1997
Metabotropic glutamate receptor 8	Malherbe *et al.*, 1999
Opioid receptor	Lundstrom, 1999
Galanin receptor	Lundstrom, 1999
Histamin recptor	Lundstrom, 1999
Odorant receptors: rat 17 and OR5 and Caenorhabditis elegans odr-10	Minastyrskaia *et al.*, 1999
Gα: Gq, Gi, Go, Gs, G16	Lundstrom, 1999
α1b-adrenergic receptor, Gαq, Gγ2, Gβ2	Scheer *et al.*, 1999

Adapted from Blasey *et al.*, 2000

5.1.1 Semliki Forest Virus Vectors

The SFV vectors (pSFV-1 and pSFV-3) (figure 5.1/a) were developed by inserting the genomic SFV cDNA into a plasmid containing SP6 promoter. The SFV structural genes were removed to another SP6 plasmid which formed the SFV Helper vectors figure 5.1/b). The separation of the SFV genome in this way was found to be necessary to make SFV vectors safe to use. By separating the structural genes from the non structural gene, only the recombinant RNA molecules should be packaged into SFV particles. Therefore, once these viral particles infect host cells no further viral production can be performed.

5.1.2 Production Of Semliki Forest Virus

To make virus in SFV expression system, *in vitro* synthetic recombinant and helper capped (+) RNA are co-transfected into mammalian cells using standard transfection methods. The procedure presented in figure 5.2 starts by the translation of RNA replicase encoded by non structural proteins (nsP1-4) genes using the host cell's machineries and synthesis of the complementary (-) strands of both incoming RNA species are then performed by the replicase. The reverse reaction (i.e. (-) strand as template and (+) as product) is also catalysed by the replicase allowing the massive amplification of both (+) and (-) RNA strands. However, once the (-) RNA strands are synthesised, the replicase binds to the subgenomic promoter (26S promoter) and the (+) RNA strand is synthesised. This allows the translation of both the recombinant gene and the structural proteins (capsid, E3/E2 (p62), E1, and 6K) using again the host cell's machineries. The capsid forms the nucleocapsid around the (+) RNA strand and self cleaves from the rest of polypeptide and diffuses to the cell surface. Meanwhile, the rest of the polypeptide is processed to form the spike proteins by transporting the polypeptide through firstly the endoplasmic reticulum (ER) where it is cleaved into p62 (E3-E2 fusion), 6K, and E1 and secondly through the Golgi apparatus where the p62 and E1 proteins are heterodimerised via the E3 domain. Normally in the wild type virus the p62 precursor protein would cleave to form E3 and E2

proteins which in turn would lead to the formation of a mature spike protein by the dimerisation of three E1-E2 proteins. However, to make the SFV system extra safe, the cleavage sites between E3 and E2 have been changed by three amino acids (pSFV Helper 2) so that activation of the virus could only be performed by treatment with α-chymotrypsin (Berglund *et al.*, 1993). Once the glycoproteins reach the cell surface, both the nucleocapsid and the glycoproteins bud out the cell to form SFV via membrane permeability of unknown mechanism by 6K protein.

a)

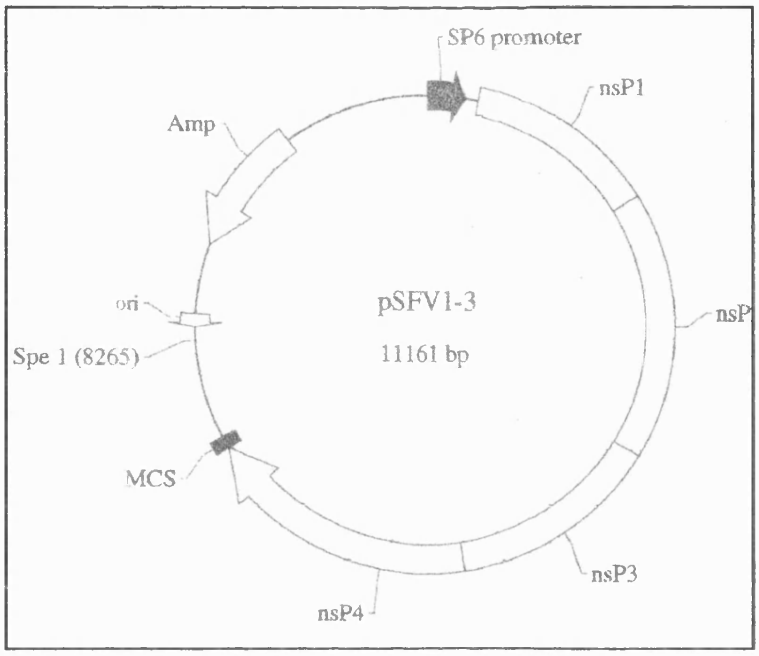

Multiple Cloning Site (MCS)

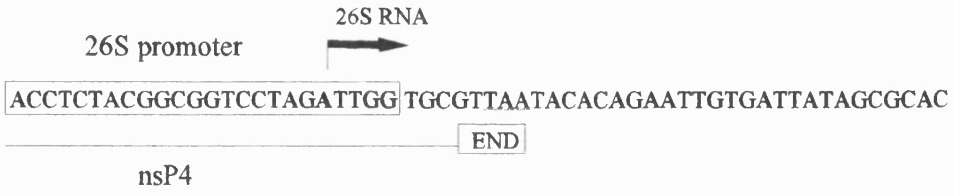

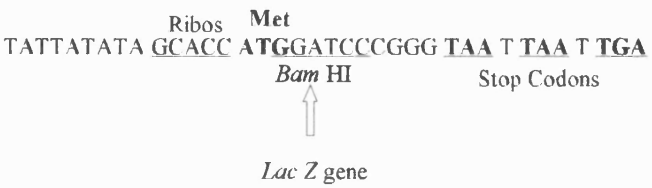

b)

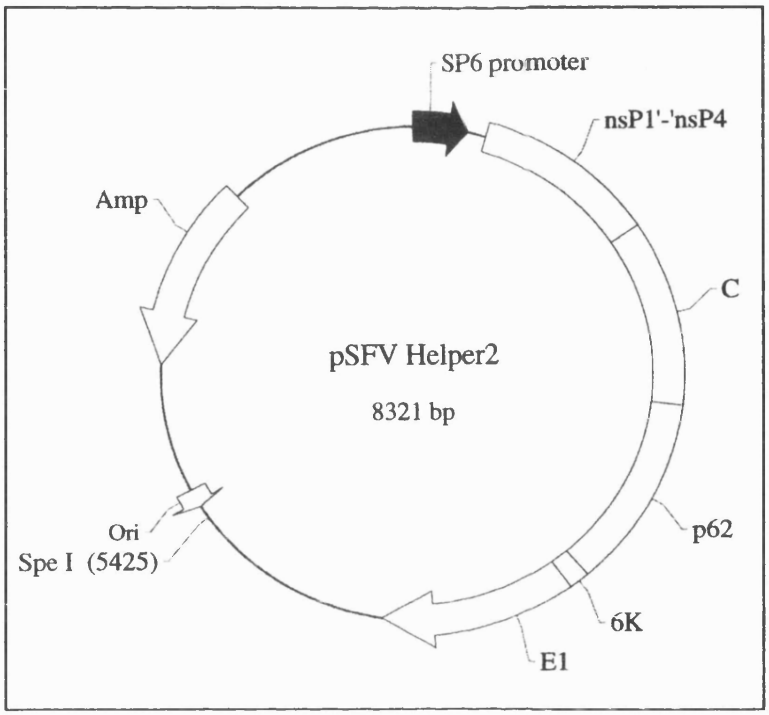

c)

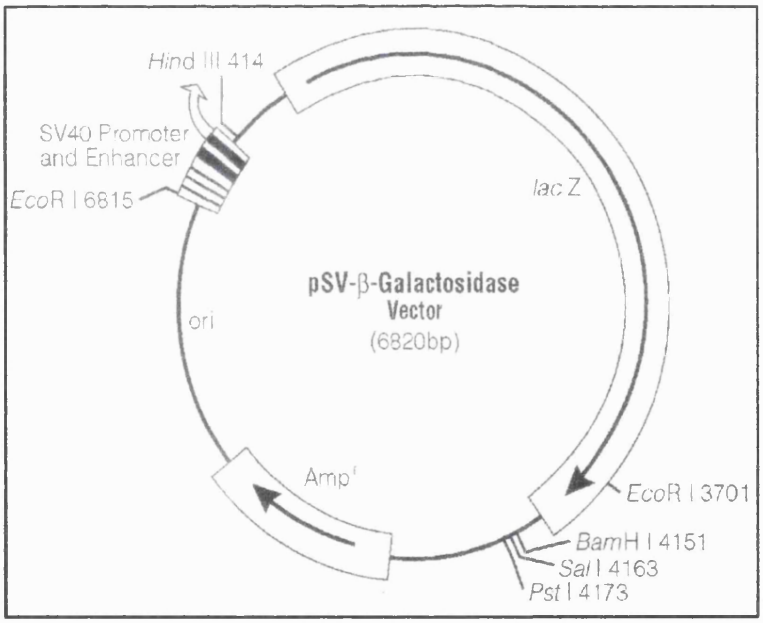

Figure 5.1 Circular maps of pSFV-3, Helper 2 and pSV-βgal plasmids. The multiple cloning site of pSFV-3 shown in panel (a) indicates the position of the subgenomic 26S RNA (boxed) and the first nucleotide to be *in vivo* transcribed by the replicase indicated by the arrow. The *lacZ* gene was inserted into pSFV-3 via the *Bam* HI restriction site which is followed by three stop codons.

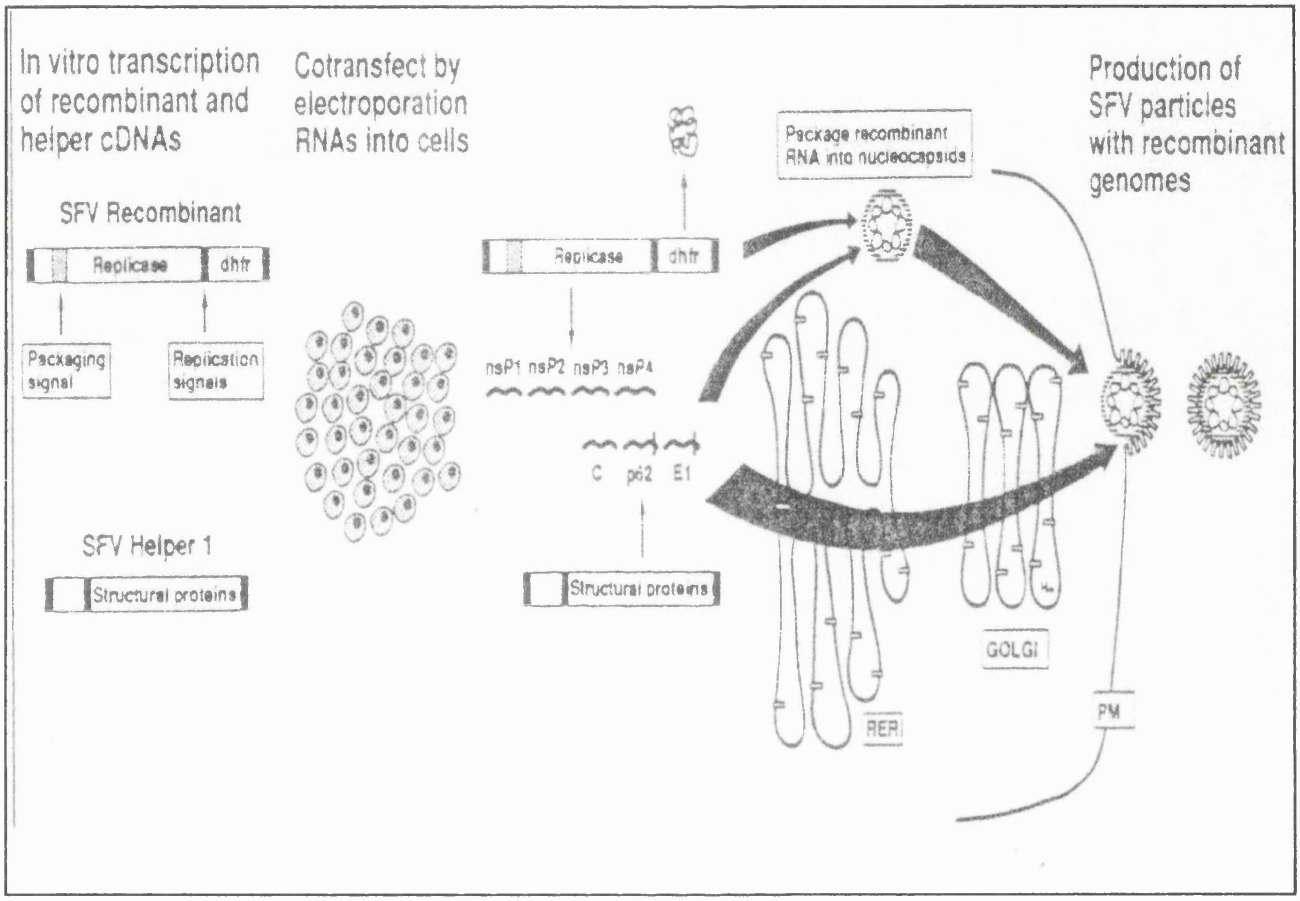

Figure 5.2 A schematic presentation adapted from Liljestrom and Garoff, 1991 of the *in vivo* packaging of pSFV-1-mouse dihydrofolate reductase (dhfr) mRNA into viral particles.

5.1.3 Semliki Forest Virus Infection

Enveloped RNA SFV infect cells via endocytotic pathways which require binding of the virus to the plasma membrane, uptake into endocytotic versicles, and low pH for the fusion of the viral membrane with the endosomal membrane (Helenius *et al.*, 1980).

Cell surface binding of alphaviruses have been studied extensively using radiolabelled viruses added to cells at 4°C. These studies found the virus binding to the proteinaceous sites on the microvilli of the cell via their spike protein described earlier (Kielian, 1995). Different receptors found on the surface of different hosts and tissues have been found to serve in binding to the alphaviruses. The idea that a diverse range of protein could be involved in binding to these viruses has come about due to their wide host range and their different protease sensitivity in different host cells (Marsh and Helenius, 1989). Early studies have implicated the class I major histocompatibility antigens in SFV binding to cells (Helenius *et al.*, 1980) however, cells not expressing this protein were found to also be infected with the virus suggesting, again, the involvement of multiple receptors in binding to alphaviruses. Recently, the high-affinity laminin receptor whose function is to bind to the basement membrane laminin in mammalian cells has be shown to bind to Sindbis virus (SV, Kielian, 1995). The laminin receptor is highly conserved in Baby Hamster Kidney cells (BHK), a common host cell line which is used in this study, as well as other mammalian cells (Kielian, 1995). Furthermore, the expression levels of this receptor has been found to correlate with infection levels of host cells to SV suggesting the possibility that the alphaviruses (that include SFV and SV) bind to this protein (Kielian, 1995). However, direct binding of the virus to the laminin receptor has not yet been demonstrated.

Following binding of the SFV to receptors on the plasma membrane, SFV is taken up into the cell by cellular pathways of receptor-mediated endocytosis (Kielian, 1995; Helenius *et al.*, 1980; Marsh and Helenius, 1980). The virus is translocated along clathrin-coated pits whose function is to invaginate and pinch off to form coated vesicles. The initial vesicles which are relatively neutral in pH, rapidly uncoated releasing their content to the

early endosomes (Schmid *et al.*, 1989). The pH is gradually lowered with the early, peripheral endosomes having a pH approximately 6.2 and 5.3 respectively and later, perinuclear endosomes having a pH lower than 5.3 (Schmid *et al.*, 1989). The exposure of the SFV spike proteins to low pH causes the induction of a conformational change leading to the virus membrane fusion with the endosome membrane and the release of the viral nucleocapsid into the cytoplasm (Kielian, 1995). The released nucleocapsid is rapidly uncoated, and the viral replication pathway takes place as described in section 5.1.2. The non-fused viruses and spike proteins remaining in the endosome membrane are transported via the endocytic pathway to the lysosome compartment, where they are degraded.

5.1.4 Aim

As described in the previous sections Semliki Forest Virus system represents an efficient method of expression in mammalian cells capable of scale up. This feature is important as the general aim is to produce $Met^{26}RD1$ in large quantities for crystallisation and the eventual structural evaluation. However, before embarking in $Met^{26}RD1$ expression using this system, the SFV system needed to be optimised. This chapter describes the optimisation of the SFV expression system using the reporter β-galactosidase gene present in pSFV-3 plasmid DNA. This system was optimised using this reporter gene rather than the PDE4 gene due to the ease of use of β-galactosidase and its ability to be assayed with methods that are easily detected by eye.

5.2 Material And Methods

5.2.1 Transient Transfection

All procedures described in this section were performed in a sterile tissue culture hood unless other wise stated. In this section a few transfection methods were tried and transfection efficiencies were tested using both pSV-βgal DNA plasmid (Promega) and pSFV-3 mRNA transcripts containing *β-galactosidase*. The Map of pSFV3 plasmid is shown in figure 5.1.

5.2.1.1 Transient Transfection using Chemical Methods

5.2.1.1.1 SuperFect Transfection

SuperFect transformations were performed according to manufacturers' instruction (Qiagen). In brief, Baby Hamster Kidney clone-21 (BHK-21) cells were seeded in 3.5 cm^2 plates at a cell density of 4 x 10^5 cells per 5 ml of Glasgow Minimal Essential Media (GMEM) complete media, the day before transfection. The cells were incubated for 24 hours in a LEEC Research CO_2 tissue culture incubator model number GA3010 set at 37°C, 5% CO_2 and maximum humidity. 2 µg of DNA or 5 µg of mRNA transcripts were diluted in 100 µl serum free GMEM. The mixture was firstly mixed by pipetting up and down five times and secondly centrifuged for few seconds to bring the droplets down. 10 µl of SuperFect reagent purchased from Qiagen was added and the solution was mixed by pipetting up and down five times and secondly centrifuged for a few seconds to bring the droplets down. The solution was then incubated at room temperature for 10 minutes. Meanwhile, the growth media of previously seeded BHK cells were removed and cells were washed twice with freshly made 1x PBS (2.6 mM KCl, 1.4 mM K_2PO_4, 0.1369 M NaCl, 8.1 mM Na_2PO_4). 600 µl of GMEM/complete medium (i.e. containing fetal calf serum) was added to the transfection solution and mixed twice as previously. The mixture was then added to the pre washed BHK cells and cells were incubated with the mixture for 3 hours in a tissue culture incubator set with the same settings as previously mentioned. Following the 3 hours incubation the media was removed and cells were washed once with 1x PBS. 1 ml of fresh GMEM/complete medium was added and cells were incubated for 18 hours if transfected with mRNA and 24 hours if transfected with DNA. Following the incubation period, cells were analysed for β-galactosidase expression.

5.2.1.1.2 Liposome Transfection

Transfection described in this section were performed following manufacturers' instructions. However, the general method will be described briefly. Two 24-well tissue culture plates were used in this experiment. Liposomes used were purchased from Gibco

BRL.

BHK-21 cells were seeded at a density of 5 x 10^4 cells per well in 1 ml of complete media in one of the two 24-well plates. The cells were incubated in a tissue culture incubator until cells reached a confluency of 60-80% which usually took about 24 hours. In the second 24-well plate 600 µl of serum free media was added to well 1 A-D and 300 ml was added to rest of the wells. Liposomes were added in the following order: 10 µl of Lipofectin to well A1, 15 µl of Lipofectamine to well B1, 10 µl of Cellfectin to well C1 and 10 µl of Dmrie-C to well D1. Following mixing of each type of liposome with the growth media, the mixtures were incubated at room temperature for 30 minutes. 10 µg of pSFV-3 mRNA was added to each well A1-D1 and mixed thoroughly by swirling gently. The lipid:RNA complex was serially diluted by transferring 300 µl of well A1 to A2, mixed and 300 µl was transferred to A3. This was continued to well A6 where the final 300 µl was discarded. This procedure was repeated to all other rows (B, C, and D). Meanwhile the complete media was removed from the cells and cells were washed once with serum free media. The lipid: RNA mixture prepared were added to the corresponding well of the cell plate and cells were incubated for 5 hours in the tissue culture incubator. The lipid: RNA in each well was replaced by 1 ml of complete media and cells were incubated for 18-20 hours and cells were analysed for β-galactosidase expression.

5.2.1.2 Transient Transfection using Electroporation

The method used was based on the methods introduced by Liljestrom and Garoff 1991 and DiCiommo and Bremner, 1998 with some modifications. The optimisation procedures discussed in this section were performed using pSV-βgal DNA plasmid as well as pSFV-3 mRNA.

Cells were cultured in 75 cm^2 flasks as described in section 2.2.4.2 to achieve a cell confluency of 60-80% on the day of transfection. The medium was removed and cells were washed twice with 1x PBS and trypsinised to detach using the method described in section 2.2.4.2. Cells were pelleted by low speed centrifugation using a Sigma 6K10 benchtop

centrifuge with a swing out rotor (No 11162) set to centrifuge at 400 *g* for 3 minutes at 18°C and washed once with 4 ml of serum free media supplemented with 2 mM glutamine and once with 4 ml of ice-cold 1x PBS. The final cell pellet was resuspended in fresh 1x PBS (room temperature) to achieve a cell density of 1.47 x 10^6 cells /ml of 1x PBS. 0.75 ml of the cell suspension (i.e. 1.1 x 10^6 cells) was mixed with pSV-βgal DNA or pSFV-3 mRNA and the mixture was transferred quickly to an electroporation cuvette with an electrode 4 mm (Flowgen) and cells were electroporated with an EasyJect electroporator purchased from Flowgen. Generally one 75 cm^2 flask yielded cells to enable to perform two electroporations. Following the electroporation procedure, the cells were diluted with 4 ml of growth media supplemented with 10% fetal calf serum using a plastic pipette.The electroporation chamber (i.e. cuvette) was rinsed with 1 ml of extra complete media. Cells were transferred to 3.5 cm^2 plates and incubated for 24 hours in a 37°C incubator supplemented with 5% CO_2 and maximum humidity. Cells were analysed for β-galactosidase expression.

To optimise the electroporation procedure to achieve maximum transfection efficiencies, many factors were considered. The type of cell line has a large effect on the transfection efficiency as some cell lines have poor capacity for transfection. The majority of the published experimental procedures using Semliki Forest Virus system used BHK-21 cells and CHO cells. Therefore, these two cell types were used in the optimisation procedures. Other factors reported to affect transfection were found to be linked to the amount of plasmid DNA electroporated into the transfected cells. DNA amounts ranging from 5 μg to 20 μg were used to transfect cultured cells. In electroporations performed using mRNA, the same procedure was followed except after electroporation cells were incubated for 18 hours rather than 24 hours.

5.2.1.3 *In Situ* Staining of Cells for β-galactosidase Activity

Procedures described here were performed on the bench and not in the tissue culture hood. Initially the X-gal (5-bromo-4-chloro-3-indolyl-β-D-galactoside) was dissolved in DMF to produce a 2% stock solution. The X-gal stock was aliquoted into 1 ml samples

contained in 1.5 ml centrifuge tubes which were wrapped in aluminum foil to protect them from light and were stored at -20°C until used. $K_4Fe(CN)_6 .3H_2O$ and $K_3Fe(CN)_6$ were prepared as 0.1 M stock solutions in water. Both stocks were filtered through 0.2 μm filter and stored at room temperature in a dark place for up to a year.

The transfected cells were washed twice with 1x PBS and fixed with the addition of 1 ml of 0.25% glutaraldehyde per 3.5 cm^2 plates. Cells were incubated at room temperature for 15 minutes and washed 3x with 1x PBS to remove small traces of glutaraldehyde. 0.5 ml of X-gal solution (0.2 % X-gal, 2 mM $MgCl_2$, 5 mM $K_4Fe(CN)_6 .3H_2O$, 5 mM $K_3Fe(CN)_6$) was added to the cells and then were incubated for 1-2 hours at 37°C for efficient staining. Following the 37°C incubation cells were washed twice with 1x PBS and visualised under the light microscope. Cells were counted in 3-5 random fields and the transfection efficiencies were calculated using the following formula:

Average number of Blue cells ÷ Average number of total cells x 100

For long-term storage (weeks or months), cells were stored in 70% glycerol at 4°C.

5.2.2 *In vitro* Transcription of mRNA

To inactivate contaminating RNase, Milli Q water and all containers used in this section were treated with 0.1% DEPC overnight at 37°C and were then autoclaved for 30 minutes to remove traces of the DEPC. All solutions were prepared in with DEPC treated water.

pSFV-3 and Helper 2 plasmids were prepared using maxipreps described in section 2.2.2.1.2. 60 μg of each plasmid were cleaved to linearise them in a final volume of 100 μl with 24-27 units of *Spe* I restriction endonuclease for 18 hours at 37°C. This was necessary to generate 3' terminus transcripts that can support the viral RNA replication process. *In vitro* transcripts were prepared in 1.5 ml microcentrifuge tubes containing 5μg of linearized plasmids (pSFV-3 and Helper 2), 1 mM $m^7G(5')ppp(5')G$ (Gibco BRL) capping reagent, 5 mM dithiothreiol (DTT), rNTP mix (1 mM rATP, 1 mM rCTP, 1 mM

rUTP and 0.5 mM rGTP) (Promega), 50 units RNasin (Promega) and 38 units SP6 RNA polymerase (Promega) (Lusa *et al.*, 1991). The mixture was incubated for 3 hours at 42°C using a hot block (Stuart Scientific SHT2D). Both *Spe* I reactions and run-off transcripts were analysed by agarose gel electrophoresis as described in section 2.2.2.5.

5.2.3 Quantification of the Run-off Transcripts

To quantify the transcripts prepared in the previous section, transcripts of known volumes were loaded onto 0.5-0.8% agarose gels prepared in 1x TAE as described in section 2.2.2.5, next to a single banded mRNA marker of known size and concentration. The band intensities were compared and the concentration of transcripts were estimated. Band intensities were compared digitally using a Kodak DC120 digital camera with UV filter and the Kodak digital Science™ 1D image analysis software.

5.2.4 Generation Of Semliki Forest Virus (SFV) Containing pSFV-3

Once transfection parameters were established using pSV-βgal plasmid, the same parameters were used to transfect pSFV-3 mRNA transcripts. This was performed to confirm and to ensure that the optimised electroporation parameters worked with a similar transfection efficiency with mRNA as with DNA. mRNA electroporation followed the same method described in section 5.2.1.2.

To produce virus, BHK-21 cells were electroporated with both pSFV-3 and Helper 2 mRNA transcripts using the method described in section 5.2.1.2. To produce optimum viral titre, (In duplicate experiments) 1.1 x 10^6 BHK-21 cells were electroporated with pSFV-3 and Helper 2 mRNA at volume ratios of 1:0.5, 1:1 and 1:2 respectively. Cells were added to 2 ml of GMEM complete growth media and incubated for 24 hours at 37°C, 5% CO_2 and maximum humidity. The SFV present in the media was collected and cell debris was separated by centrifugation using a Sigma 6K10 benchtop centrifuge with a swing out rotor (No 11162) set to centrifuge at 2000 rpm for 10 minutes at 4°C. The virus suspension was aliquoted into 200 µl samples and stored at -80°C until used.

5.2.5 Preparation of BHK-21 Cells For Viral Infection

For optimisation experiments, 3 x 10^5 cells were plated on 25 cm^2 flasks the day before infection. For 75 cm^2 flasks, 6 x 10^5 of BHK-21 cells were plated the day before infection. Plating cells at this cell density produces cells with confluency of 40-60% on the day of infection. This density has been reported to be the best for cell infectability (DiCiommo, 1998).

5.2.6 Preparation of Virus For Infection

The method used in this section were based on methods described by both Berglund, 1993 and DiCiommo, 1998. α-Chymotrypsin was prepared as a 1 mg/ml stock in filter sterilised 1x PBS buffer supplemented with 10 mM $MgCl_2$ and 20 mM $CaCl_2$. Stocks were stored at -70°C and thawed only once. Aprotinin was prepared as a 10 mg/ml stock in 0.01 M HEPES buffer which has been previously filter sterilised.

To produce the virus with optimum activity, SFV was treated with 50 μg/ml, 100 μg/ml, 200 μg/ml, 300 μg/ml and 400 μg/ml of α-chymotrypsin. Following incubation at room temperature (22-25°C) for 45 minutes, chymotrypsin was inactivated by the addition of aprotinin to a final concentration of 0.67 mg/ml and incubation at room temperature for 5 minutes.

5.2.7 Infection of Cells

GMEM complete media was removed from BHK-21 cells about to be infected. Cells were washed twice with 1x PBS and were infected with activated SFV prepared in as described in section 5.2.6. In duplicate experiments, activated virus of three different volumes 12, 25 and 50 μl were diluted in 1 ml of GMEM complete media. The dilution of viral stock was necessary to achieve about 40-50% infection efficiency to enable titre determination of virus stock as described later (section 5.2.8). Cells were incubated with the virus for 45

minutes in humidified atmosphere of 5% CO_2 in air. The media containing the virus was removed at the end of the incubation period and fresh GMEM complete media was added. Cells were incubated for 18 hours at 37°C in a humidified atmosphere of 5% CO_2 in air.

5.2.8 Viral Titre Determination

Following the 18 hour incubation after infection, cells were stained *in situ* for β-galactosidase activity as described in section 5.2.1.3 to determine the virus titre using method described by DiCiommo, 1998. To determine the viral titre in terms of infectious units / ml (IU / ml), the following formula was used:

(area of plate) / (area of field) x (Xgal % staining) = stained cells/ plate x [1000 / (volume of virus added in μl)]

area of field = 0.13 cm^2

5.3 Results

5.3.1 *In vitro* mRNA Synthesis

mRNA synthesised from pSFV-3 and Helper 2 plasmid was analysed by agarose gel electrophoresis (figure 5.3). Both *in vitro* transcribed species migrated as distinct bands on agarose gels. Gel electrophoresis was also used to quantify the mRNA produced from each *in vitro* transcription reaction. This was achieved using a digital camera which took the photo of the agarose gel and band intensities of mRNA transcripts were compared by image analysis to the intensity of a single mRNA marker with known concentration. mRNA concentration determined using this method was in the range of 0.5-1 μg/ml. Generally, approximately 25-50 μg of mRNA was produced from a single transcription reaction.

5.3.2 Transfection of BHK-21 Cells Using SuperFect

SuperFect was successful in transfecting BHK-21 cells with pSV-βgal plasmid. Transfection efficiencies of up to 67.5% were achieved. These transfection efficiencies were found to decrease the longer the Superfect was stored. This was thought to occur due to the degradation of the SuperFect with time. However, SuperFect was not able to transfect mRNA at all as X-gal staining of transfected cells revealed no blue cells (Table 5.2).

5.3.3 Transfection Of BHK-21 Cells Using Liposomes

The highest level of pSFV-3 mRNA transfection was achieved when using Lipofectamine and DMRIE-C. Both liposomes gave transfection efficiencies of 24% and 22% respectively. Results of the transfection efficiencies were calculated as described in section 5.2.1.3 and shown in Table 5.2. Cells transfected with liposomes were found to lift off the flasks and plates. The exact cause of this observation was not determined, however it was thought to be due to a toxic effect caused by the liposomes. Nevertheless, serial dilution of the liposomes did not alleviate this problem.

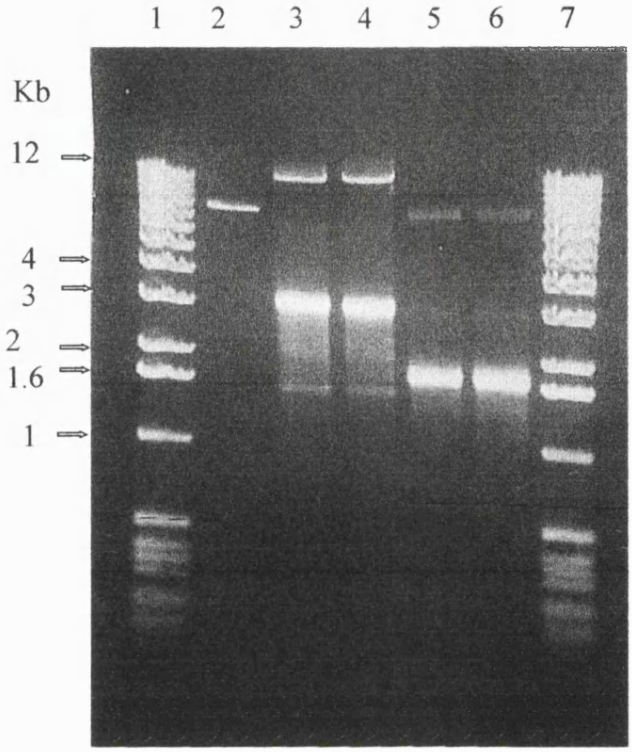

Figure 5.3 Ethidium bromide stained agarose gel analysis of pSFV-3 and Helper 2 mRNA transcribed *in vitro*. 1 µl of the in vitro transcription reaction underwent electrophoresis on 0.8% agarose gel prepared as described in section 2.2.2.5. Lane 1 and 7: 1 Kb DNA ladder. Lane 2: Supercoiled pSFV-3 plasmid. Lanes 3 and 4: Duplicates pSFV-3 mRNAs. Lanes 5 and 6: Duplicate Helper 2 mRNAs.

Table 5.2 Transfection efficiencies resulting from transfection of BHK-21 cells with either SuperFect or Liposomes.

Transfection Method	Transfection Efficiency %	
	pSV-βgal plasmid	pSFV-3 mRNA
SuperFect	67.5	0
Liposomes:		
Lipofectin	ND	2.9
LipofectAmine	ND	24.2
CELLFACTIN	ND	2.1
DMRIE-C	ND	22

Data are mean values of two preparations. BHK-21 cells were transfected using methods described in in sections 5.2.1.1.1 and 5.2.1.1.2. Transfected cells were stained with X-gal and transfection efficiencies were determined using method described in section 5.2.1.3

5.3.4 Transfection Of BHK-21 Cells Using Electroporation

Electroporation resulted in higher transfection efficiencies compared to other transfection methods used. It has been noted that different cell types have different degree of transfectability therefore, the effects of cell type on the transfection efficiency were initially tested. As most of the cells types described in publications using Semliki Forest Virus system were BHK-21 and CHO cells, electroporations were performed using these two cell types. The transfection efficiencies in BHK-21 cells were found to be higher compared to observed transfection efficiencies in CHO cells (figure 5.4). BHK-21 cells electroporated with no pSV-βgal plasmids or pSFV-3 transcripts showed no staining with X-gal confirming the absence of endogenous β–galactosidase activity in these type of cell lines (data not shown).

Electroporation conditions were tested using parameters reported by both Liljestrom, 1991 and DiCiommo, 1998. Using 1.5kV and a capacitance of 25 μF (Liljestrom, 1991) produced transfection efficiencies of 1.22%, whereas using 350V and 1500 μF

(DiCiommo, 1998) produced transfection efficiencies of up to 97%. To optimise the amount of nucleic acids added to the cells during the electroporation, both DNA and mRNA were varied. Transfection with 20 μg of DNA produced transfection efficiencies of 74.7 ± 14.2% (figure 5.5). These transfection efficiencies were low compared to transfection efficiencies produced when pSFV-3 mRNA was used. Figure 5.5 showed transfection efficiency as high as 95.7 ± 0.6% were achieved. Furthermore, smaller amounts of mRNA (10 μg) were needed to achieve these high transfection efficiencies.

However, despite the high transfection efficiencies achieved, large number of BHK-21 cells were found floating as clumps in the medium the day after each electroporation. The majority of the floating cells were found to be dead when tested with Trypan blue as described in section 2.2.4.4. The few cells adhering to the tissue culture flasks looked healthy. The low numbers of BHK-21 cells surviving the electroporation procedure were thought to cause a problem in later stages of the SFV expression system (see later). To increase the percentage of cell survival, the time allowed for the trypsinisation of BHK-21 cells during cells preparation were varied and the voltage used during electroporation was reduced. Increase exposure to trypsin causes the degradation of membrane protein making the cell's membrane more flexible and allowing the cell's pores to close more easily following electroporation. However, only a marginal increase in cell survival (~0.1%) was observed when cells were exposed to trypsin for 10 minutes (figure 5.6). So for convenience, cells were exposed to trypsin for 3 minutes during subsequent cell preparations. The electroporation parameters used so far in this work were 350 V and 1500 μF capacity as described by DiCiommo, 1998. The reduction in the voltage used during electroporation, was thought to reduce cell damage and hence yield an increase in cell survival. However, this reduction in the voltage used, had no effect on the number of cells surviving the electroporation procedure (figure 5.7) but, had a marked reduction in transfection efficiency instead. Therefore, a voltage of 350 V was used in subsequent experiments.

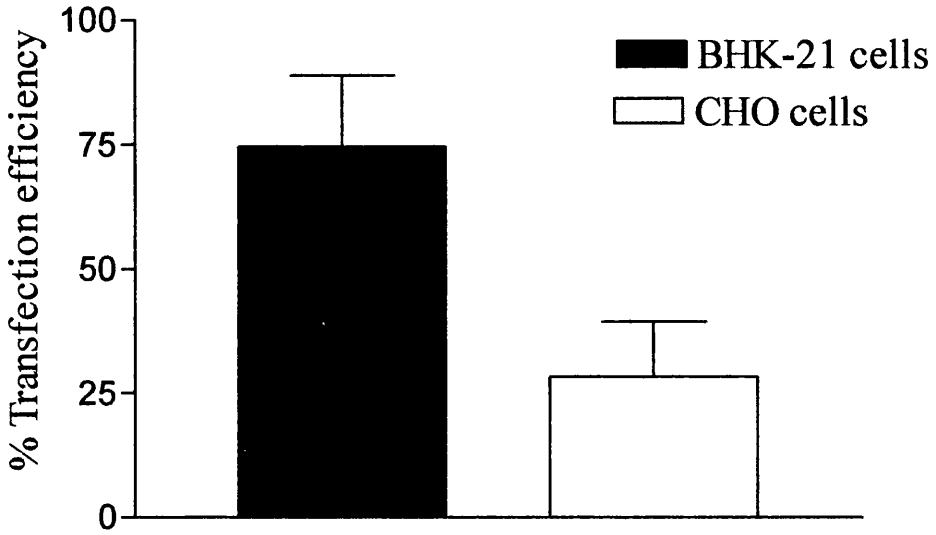

Figure 5.4 Effects of type of cell line on the transfection efficiency using electroporation. 1.1 x 10^6 BHK-21 cells and CHO cells underwent electroporation with 10 μg of pSV-βgal plasmid DNA and β-galactosidase expression was determined 24 hours after electroporation using β–galactosidase *in-situ* staining described in section 5.2.1.3.

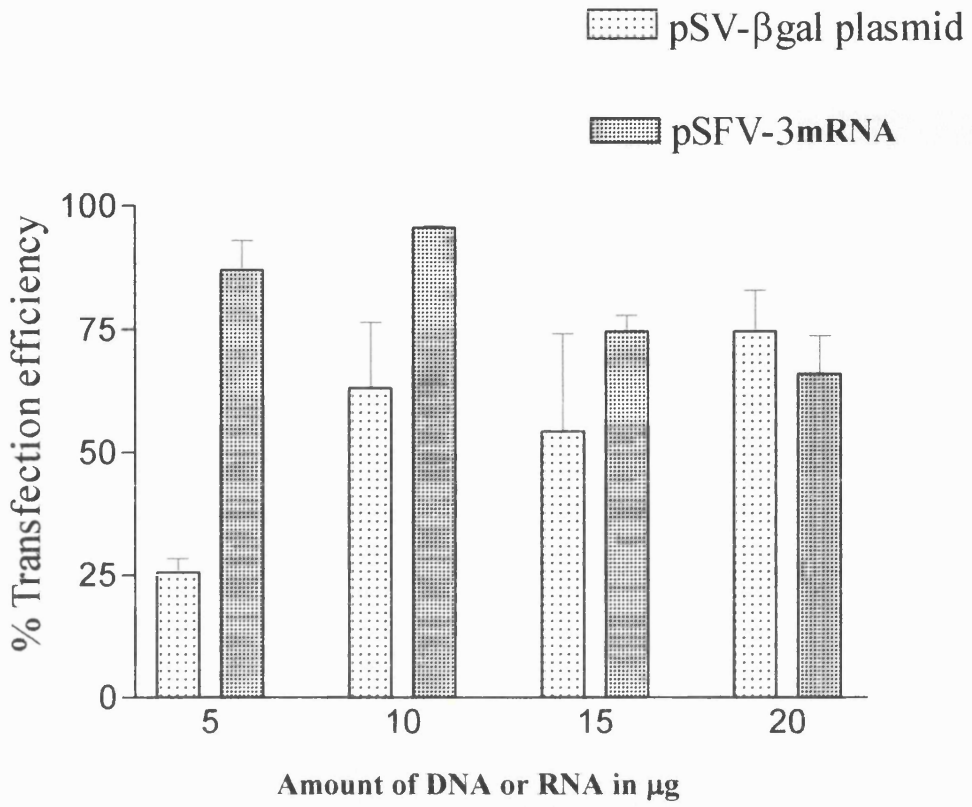

Figure 5.5 Effects of changing the amounts of pSV-βgal plasmid and pSFV-3 mRNA on the transfection efficiency of BHK-21 cells transfected by electroporation. 1.1. x 10^6 BHK-21 cells were electroporated with the indicated amounts of pSV-βgal plasmid DNA or pSFV-3 mRNA transcripts. β-galactosidase expression was determined 24 hours after electroporation using β-galactosidase *in-situ* staining described in section 5.2.1.3.

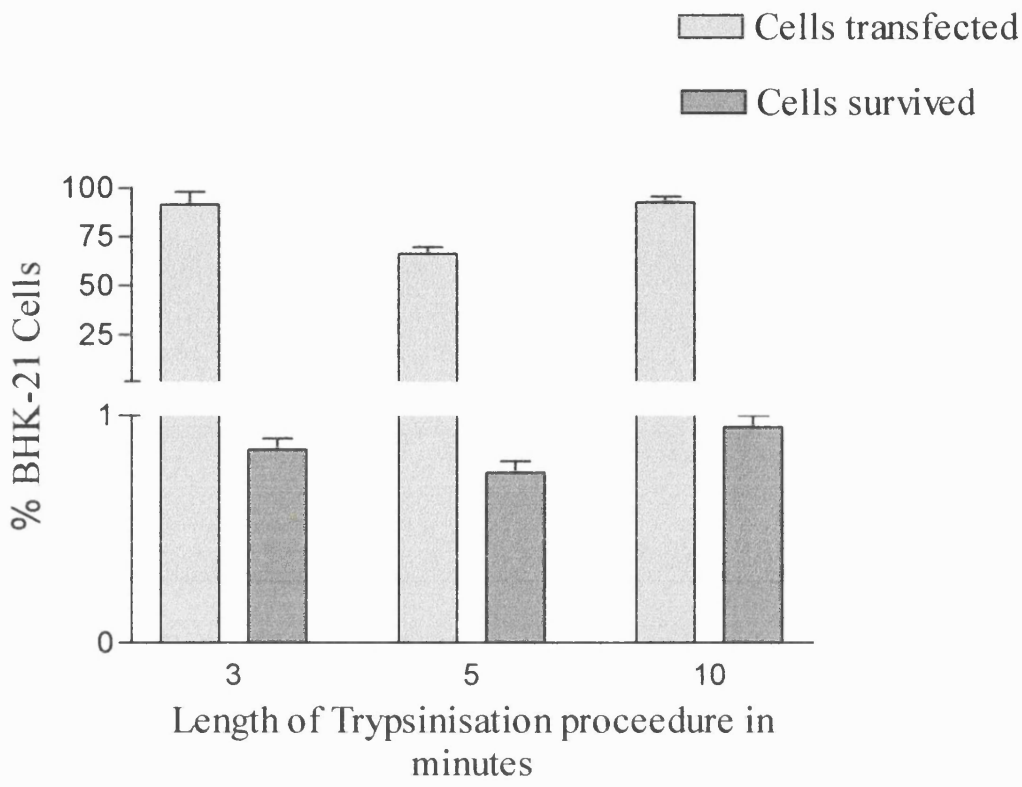

Figure 5.6 Effects of trypsinisation on the transfection efficiency and BHK-21 cells survival. BHK-21 cells were incubated with trypsin at the above indicated times. 1.1 x 10^6 BHK-21 cells were electroporated with 10 μg of pSFV-3 mRNA and β-galactosidase expression was determined 18 hours after electroporation using β-galactosidase *in-situ* staining described in section 5.2.1.3.

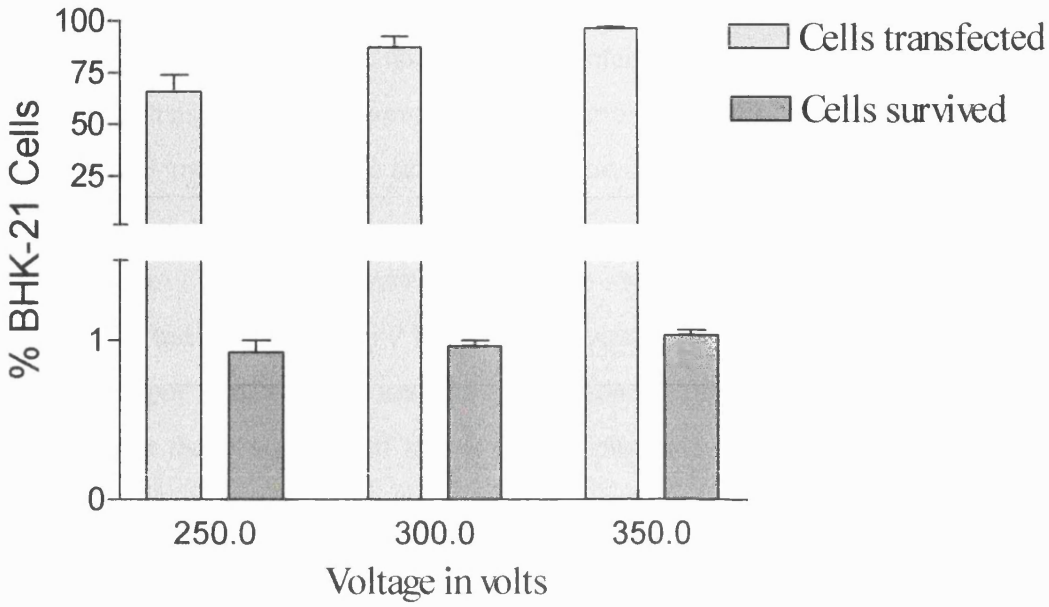

Figure 5.7 Effects of voltage on the transfection efficiency and survival of BHK-21 cells transfected by electroporation. 1.1 x 10^6 BHK-21 cells were electroporated at voltage settings indicated above with 10 μg of pSFV-3 mRNA. β-galactosidase expression was determined 18 hours after electroporation using β-galactosidase *in-situ* staining described in section 5.2.1.3.

5.3.5 Generation of Semliki Forest Virus Infectious Particles

The Helper 2 mRNA contains the sequence at either end of the SFV genome which mediates the amplification of the non structural proteins (nsPs), but lacks the packaging signal located in nsP2 gene (DiCiommo, 1998). Therefore, to allow for the amplification of the Helper 2 message as well as the transcription of the subgenomic message and translation of the structural proteins, the Helper 2 mRNA was cotransfected with the pSFV3- replicon mRNA (DiCiommo, 1998). The structural proteins will package the replicon RNA, but not the Helper 2 RNA and the viral particles were then released into the media. Helper 2 mRNA also contains a mutation at the p62 structural protein gene which prevents the processing of the p62 spike protein into E2 and E3 protein and therefore inhibiting viral infection. To activate the virus, the virus needs to be treated with α-chymotrypsin (Berglund *et al.*, 1993).

To generate infectious viral particles, pSFV-3 and Helper 2 mRNA transcripts were co-transfected into BHK-21 cells with three volume ratios 1:0.5, 1:1, 1:2 as described in section 5.2.4. Virus was collected after 24 hours, activated with α-chymotrypsin, applied to fresh BHK-21 cells and titre was determined as described in section 5.2.6. The highest titre obtained was when BHK-21 cells were cotransfected with pSFV-3 and Helper 2 mRNA at a volume ratio of 1:1, followed by 1:2 and 1:0.5 (figure 5.8).

To obtain viruses with maximum infectability, the virus was treated with α-chymotrypsin at various concentrations. Maximum infectability was achieved with 200 μg of α-chymotrypsin per ml of virus (figure 5.9). The viruses taken from the same batch were found to be inconsistent in their infectability of BHK-21 cells as 1 out of 4 infection experiments failed. This problem was thought to be due to poor viral activation as a result of incomplete α-chymotrypsin cleavage of the infectious proteins. α-Chymotrypsin has been reported to be heat sensitive and pH sensitive. The optimum temperature for this enzyme is 25°C and the optimum pH is between 7 and 8. Thus, care was taken in providing these parameters for efficient enzyme activity in subsequent experiments. This lead to more consistent infections.

From a single electroporation using 1.1 x 10^6 BHK-21 cells with 1% survival rate (1.1 x 10^4), 1.2 x 10^7 infectious units were obtained. The virus needs the cells' machinery to replicate and multiply, so only live cells were thought to be capable of virus production. Therefore, the amount of virus produced was calculated to be a 1000 fold higher than the number of transfected cells. For infection of 1.2 x 10^6 BHK-21 cells with 100% efficiency, 2.8 x 10^5 particles were needed, so the total virus produced from this single electroporation was able to infect 5 x 10^7 BHK-21 cells. These experiments described so far were to optimise the viral titres however, to produce virus stocks. The number of BHK-21 cells used in the electroporation were increased to 1 x 10^7, these cells produced 1 x 10^7 IU/ml which were capable of infecting 5-2.5 x 10^7 (depending viral titre of batch) of BHK-21 cells. Infections were performed at multiplicity of infection (m.o.i) of 0.5-1. Virus was found to be stable when stored at -80°C or 4°C without a significant reduction in infectability (Table 5.3). For convenience porposes, all viral stocks were stored at -80°C

Table 5.3 Viral Stock Storage Conditions (conditions were performed for 48 hours).

Titre before storage (IU/ml)	Virus stored at 4°C (IU/ml)	Virus stored at -80°C (IU/ml)
6.25 x 10^6	5.7 x 10^6	6.2 x 10^6

Data are mean values of two preparations. Virus was generated as described in section 5.2.4. BHK-21cells were infected with virus and cells were stained with X-gal and viral titres were determined using method described in section 5.2.7.

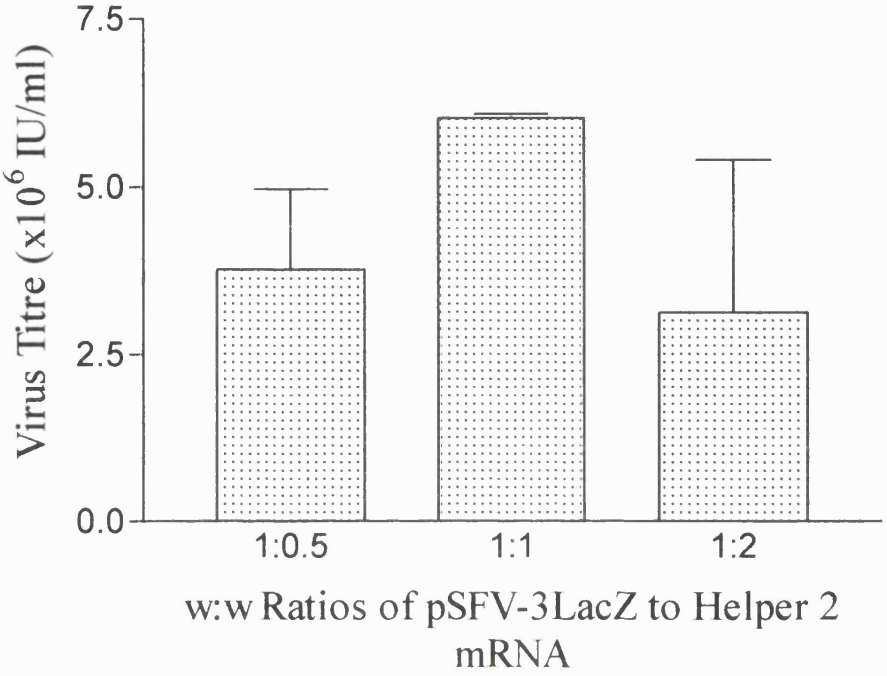

Figure 5.8 Effects of the ratio of mRNA species transfected into BHK-21 cells on the SFV titre production. 1.1 x 10^6 BHK-21 cells were transfected with pSFV-3 and Helper 2 mRNA transcripts as indicated above. Virus was collected 24 hours after transfection and titres was assessed 18 hours after infection using β-galactosidase *in-situ* staining described in section 5.2.1.3.

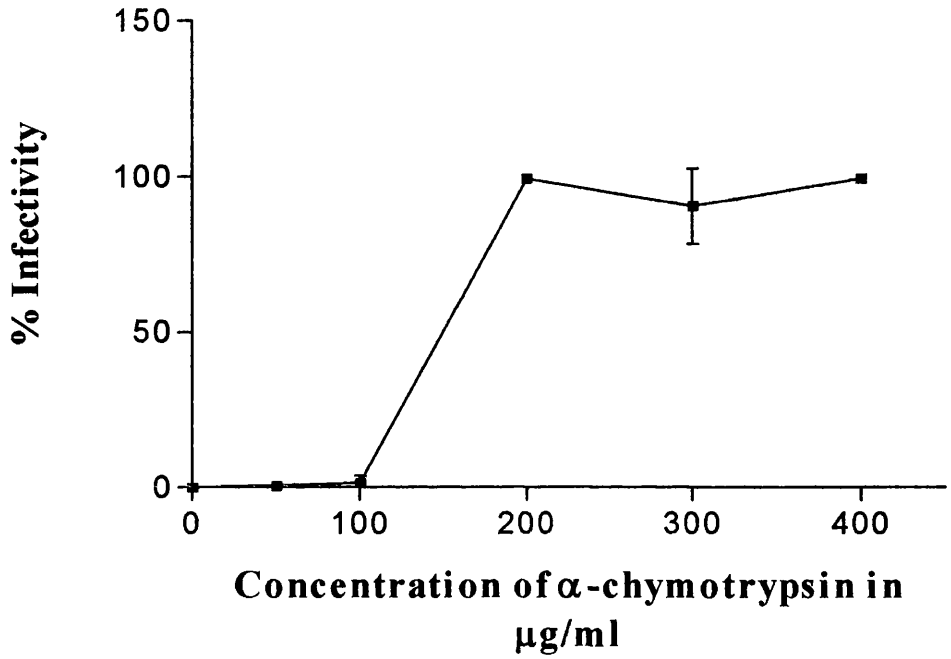

Figure 5.9 Effects of changing α-chymotrypsin on the infectability of SFV. 6 x 10^5 BHK-21 cells were infected with virus incubated with α-chymotrypsin at concentrations of 0, 150, 200, 300, and 400 μg/ml. β-galactosidase expression was determined 18 hours after electroporation using β-galactosidase *in-situ* staining described in section 5.2.1.3 and the percentage of infection was calculated according to percentage of cells expressing β-gal enzyme.

5.4 Discussion

The primary aim of the work described in this chapter was to set up and optimise the Semliki Forest Virus expression system with the aim of using this system to express $Met^{26}RD1$ clone in the future. To achieve this, preliminary experiments were performed to determine the most appropriate transfection methodology and transfection parameters that would allow for maximum viral production.

5.4.1 Assessment Of Transfection Methods

The most commonly and traditionally used methods of transfecting mammalian cells with nucleic acids has been calcium phosphate precipitation (Graham *et al.*, 1973) or treatment with DEAE-dextran (McCutchan and Pagano, 1968). However, these methods of transfection have been reported to yield low transfection efficiencies (Liljestrom *et al.*, 1991). For maximal protein production, transfection efficiencies as high as 90% were needed. This was to prevent the outgrowth of the transfected cells by the untransfected cells due to their higher rate of cell division. Therefore, other methods such as cationic dendrimers (SuperFect) and cationic lipids (LIPOFECTIN, LIPOFECTAMINE, CELLFECTIN and DMRIE-C) were used.

Transfections performed using SuperFect and cationic lipids failed in achieving the high transfection efficiencies needed. In fact SuperFect in particular failed to transfect BHK-21 cells with mRNA. This method of transfection was considered to be unsatisfactory as SFV expression system depended upon RNA transfection (Liljestrom and Garoff, 1991). Consequently, we focussed our attention on electroporation as another method of transfection. Electroporation has increased in popularity in the transfection of both eukaryotic and prokaryotic cells with nucleic acids and proteins due to the high transfection efficiencies achieved using this method. In addition, the majority of the publications on the SFV system reported by Liljestrom and Garoff (founders of SFV system) used this method of transfection (Liljestrom and Garoff, 1991; Liljestrom *et al.*, 1991; Liljestrom and Garoff, 1993; Berglund *et al.*, 1993).

Electroporation conditions used initially were as reported by Liljestrom and Garoff, 1991. These experiments yielded transfection efficiencies of 1.22%. These transfection efficiencies were unsatisfactory as described earlier. A DNA base SFV system was reported by DiCiommo and Bremner, 1998. Although the DNA-based vectors described in this publication were not used, electroporation parameters (350 V and 1500 μF capacity) similar to those reported were used. By optimising the amounts of mRNA used in the electroporation procedure, transfection efficiencies as high as 97% were obtained (figure 5.3). However, high cell death was observed as a result of the electroporation procedure and only 1% of the cells survived the voltage used. Specific reasons for the high percentage of cell death were not known as no previous reports were found making this observation. However, the voltage used, was predicted to be the major cause for the massive numbers of cell death. Attempts in reducing the voltage used during electroporations failed to reduce the numbers of cell death. In addition extending the trypsinisation periods which was thought to make the cells' plasma membrane more flexible and therefore preventing cell collapse due to electric field also failed to reduce the of percentage cell death. Using lower capacities ranging between 1500 and 500 μF might result in the reduction in cell death and the production of adequate transfection efficiencies. These experiments were not performed.

5.4.2 Generation of β-galactosidase recombinant Semliki Forest Virus

The cotransfection of Helper 2 and pSFV-3 transcripts at a ratio of 1:1 generated viral stocks with titres in the range of 10^8 IU/ml. These generated titres were found to be 10-fold lower than those reported by Liljestrom and Garoff, 1991 (titres of 10^9). Generally Semliki Forest viruses need the cells' machinery to replicate (i.e. ribosomes) therefore, it was predicted that only living cells were producing viruses. As only 1% of cells survived the transfection procedure, it was estimated that cells were producing viruses at factor of 100 (1×10^5 cells produced 10^8 IU/ml) which were in accordance with the data published by Liljestrom, 1991 (1×10^7 cells produced 10^9 IU/ml). Therefore, viral titre could be improved by increasing the number of cells electroporated by a factor of 10 however, to eliminate this problem, further work needs to be performed to optimise the electroporation

conditions to minimise the percentage cell death.

The low titres observed could be due to discrepancies with X-gal staining as some groups (Couffinhal *et al.*, 1997) have reported that X-gal method of staining underestimates the number of β-galactosidase positive cells. However, as concentrations of β-galactosidase produced per infection were not determined, the occurrence of any discrepancies cannot be confirmed.

Virus stocks produced during this project used Helper 2 vectors. These viral stocks were conditionally infectious due to a mutation introduced to the structural protein p62 at the junction between E2 and E3 of the spike protein (Berglund *et al.*, 1993). As previously described, this modification reduced the chances of recombination between replicon and helper RNA to form wild-type virus which require the reversion or suppression of the mutation (DiCiommo and Bremner, 1998). To activate the virus produced by this method, the virus stock was treated with a-chymotrypsin which cleaved p62 precursor protein to E2 and E3 membrane proteins. Full infectability was achieved generally by treatment with 200 μg/ml (final concentration) of α-chymotrypsin. This concentration varied between 200-300 μg/ml with different stocks of viruses produced therefore, the optimal amounts of enzyme needed for full infectability were determined for different viral stocks produced. These concentrations were similar to previously published data which reported optimum infectability with final concentrations ranging from 100 μg/ml (Berglund *et al.*, 1993) to 200 μg/ml (Blasey *et al.*, 2000).

Chapter 6

The Expression Of *Met*^{26}*RD1* Gene In Mammalian Cells Using Semliki Forest Virus Expression System

6.1 Introduction

Very little structural and functional information was available on phosphodiesterase enzymes type 4 about a decade ago which made this set of enzymes one of the most poorly characterised biophysically and biochemically until the recent structural evaluation of the catalytic domain of human PDE 4B by Xu *et al.*, 2000. This has been mainly due to the small expression levels in cells and the susceptibility of the enzyme to proteolysis. Consequently, attempts to purify these enzymes from these native sources have been extremely difficult (Yamamoto *et al.*, 1984; Weishaar *et al.*, 1987; Tenor *et al.*, 1987; Fougier *et al.*, 1986; Giorgi *et al.*, 1992). However, advances in cloning and expression of PDE 4 reported by many research groups has enabled the over-expression of different mammalian PDE 4 isoforms leading to some successful purification providing adequate protein for better functional and structural investigations.

At the start of this project Recque *et al.*, 1997 reported the first expression of milligram quantities of human recombinant rolipram-sensitive cAMP phosphodiesterase (HSPDE4B2B residues 81-564 and 152-528) using a baculovirus expression system. The group also reported the purification of the protein to homogeneity.The success of this expression system prompted other groups to use this expression system to produce many other PDE 4 isoforms (Table 6.1). Despite the success of baculovirus system in expression of PDE4 isoenzymes, this system had its own problems. For example Conti and co workers (Sette *et al.*, 1996) have noted partial inactivation of the enzyme expressed in insect cells. Reasons for this were not clear however, they observed that PDE4 isoenzymes expressed in Sf9 cells (insect cells) by baculovirus system tended to aggregate which might be involved in the partial inactivation of the enzyme. Baculovirus can only be used to infect

insect cells which are known to differ from mammalian cells in their post-translational modification of proteins. They are found to over glycosylate proteins following translation. Problems associated with baculovirus systems as well as other systems for example yeast which also differ from mammalian cells in their post-translational modification of proteins inspired us to look at systems which would allow the expression of Met^{26}RD1 (PDE4A1) in mammalian cells.

Mammalian cell expression was considered to be the most optimal expression system for PDE expression because it recovers PDE proteins with properties very similar or identical to those of native proteins (Thompson *et al.*, 1988; Conti *et al.*, 1995). Different PDE 4 isoforms have been expressed in mammalian cells either transiently or in a stable format (Swinnen *et al.*, 1991; Pooley *et al.*, 1997). In transient expression many different cell lines were used. For example COS1 cells which were mainly used by Houslay's group to express RD1 and *Met^{26}RD1* clones (Shakur *et al.*, 1993), COS7 (Houston *et al.*, 1996), and MA-10 cells (Jin *et al.*, 1992). Expression in mammalian cells have been problematic due to the poor transfectability of mammalian cells and low levels of expression. As the main objective of this project was to express Met^{26}RD1 for structural analysis, the production of milligram quantities of the protein was considered vital. To achieve both expression in mammalian cells and produce high quantities of the protein lead us to use Semliki Forest Virus (SFV) expression system. This system as described in Chapter 5 represented not only a novel method of expressing PDE 4 as no other group has used this system previously but also allowed transfection into animal cells with efficiencies of approximately100% and possible scale up to > 10 L bioreactors (Basley *et al.*, 2000).

In this chapter, the molecular cloning of *Met^{26}RD1* gene which encodes for the rat type 4 Phosphodiesterase enzyme into pSFV-1 vector and the expression of the gene in mammalian cells using SFV system will be described. Kinetic analysis, including inhibitory response will be also discussed with comparisons with kinetic activities of previously expressed Met^{26}RD1 in mammalian cells (Shakur *et al.*, 1993). Preliminary attempts to purify the recombinant Met^{26}RD1 protein by immunoaffinity chromatography using GST-Met^{26}RD1 antibody columns prepared 'in-house' will be discussed.

Table 6.1 Properties of PDE4 recombinant proteins produced from mammalian and insect cells.

Clone Name	Host	K_m (μM)	Specific Activity Crude (nmol/min/mg)	Specific Activity Purified (V_{max}, μmol/min/mg)	Reference
Native PDE4					
Dog heart				1.8	Thompson *et al.*, 1988
rat Sertoli cell				1-2	Conti *et al.*, 1995
Mammalian cell Expression					
ratPDE4A1(RD1)	COS1 cells	3.8	-	-	Shakur *et al.*, 1993
ratPDE4A1(met^{26}RD1)	COS1 cells	5.3	-	-	Shakur *et al.*, 1993
ratPDE4A1(RD1)	FTC133 cells	-	0.027	-	Pooley *et al.*, 1997
ratPDE4A1(RD1)	FTC133A cells	-	0.018	-	Pooley *et al.*, 1997
ratPDE4A1(RD1)	FTC133G cells	-	0.028	-	Pooley *et al.*, 1997
humPDE4A4	COS7 cells	2.6	8-12	-	Huston *et al.*, 1996
ratPDE4D1	MA-10 cells	2	0.65	-	Jin *et al.*, 1992
Insect cell Expression					
humPDE4A	Sf9 cells	5.2		0.057	Wang *et al.*, 1997
humPDE4A(330-723)	Sf9 cells	2	0.02	8.8	Lario *et al.*, 2001
humPDE4A(201-886)	Sf9 cells	3.3	57.4	-	Amegadzie *et al.*, 1995
humPDE4B2(81-564)	Sf9 cells	4	70	40	Rocque *et al.*, 1997
humPDE4B	Sf9 cells	4.7	-	0.132	Wang *et al.*, 1997
humPDE4C	Sf9 cells	1.7	-	0.308	Wang *et al.*, 1997
humPDE4D3	Sf9 cells	1.2	-	0.027	Wang *et al.*, 1997

6.2 Methods

6.2.1 Construction and *In Vitro* Transcription of pSFV-1Met^{26}RD1

The *Met^{26}RD1* gene was amplified as a *Bam* HI and *Sma* I fragment using polymerase chain reaction (PCR) as described in section 3.2.1.1. The PCR product was subcloned into *Bam* HI and *Sma* I sites of the polylinker region of the pSFV-1 vector (figure 6.1) and was subjected to nucleotide sequence determination as described in section 2.2.2.4.

pSFV-1Met^{26}RD1 clones containing the *Met^{26}RD1* gene in the right orientation to the SFV 26S promoter (figure 6.1), were linearised with *Spe* I and run off transcripts of these clones as well as Helper 2 vectors were synthesised using protocol described in section 5.2.2.

6.2.2 Transfection And Expression of pSFV-1Met^{26}RD1 Construct in BHK-21 Cells

BHK-21 cells were prepared for electroporation using protocol described in section 5.2.1.2. BHK-21 cells (2.5×10^6) were mixed with 10 μg of pSFV-1Met^{26}RD1 mRNA and electroporated at 350 V and 1500 μF capacity. Cells were diluted into 5 ml of pre warmed GMEM complete media and converted into 60 mm tissue culture plates. Cells were then incubated at 37°C supplemented with 5% CO_2 and maximum humidity for 24 hours. Following the incubation, cells were washed twice with freshly made 1x PBS and 400 μl of buffer A with protease inhibitors (50 mM Tris pH 8, 20 mM $MgCl_2$, 1 mM DTT, 1 mM EDTA, 0.1 % Triton X-100, 100 μM PMSF, 10 μg/ml aprotinin, 5 μg/ml pepstatin, 10 μM TLCK and 20 μM TPCK) was added. Cells were incubated on ice for 10-15 minutes and cell lysate generated was transferred into 1.5 ml eppendorf tubes. The tubes were centrifuged at maximum speed (14 000 *g*) for 2 minutes using a 5415C eppendorf microcentrifuge placed in the cold room (4°C). Supernatants were assayed for PDE activity and analysed by SDS PAGE. Results are shown in figure 6.3.

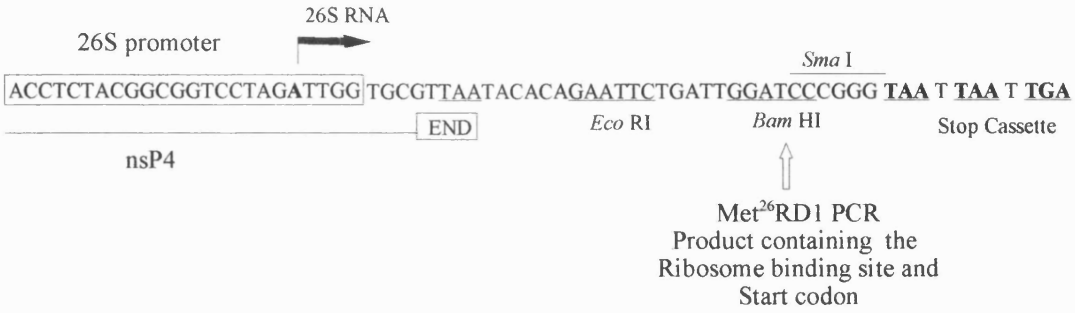

Figure 6.1 Polylinker region of the pSFV-1 vector. The position of the 26S promoter is boxed and the first nucleotides to be transcribed *in vivo* are indicated by the arrow. The *Bam* HI site and *Sma* I site which are 31 bases and 35 bases downstream of the transcription initiation site are shown. Three stop codons in all three reading frames are underlined and in bold.

6.2.3 Generation Of pSFV-1Met^{26}RD1 recombinant SFV

10 µl of *in vitro* RNA transcripts prepared from pSFV-1Met^{26}RD1 and Helper 2 vectors were cotransfected into 1 x 10^7 BHK-21 cells at a ratio of 1:1 (v:v) by electroporation at 350 V and 1500 µF (optimised parameters from Chapter 5, section 5.2.4). Virus stocks were collected 24 hours after electroporation and stored at -80°C after removing cell debris by centrifugation (10 minutes, 4°C, 2000 rpm). Two viral stocks were prepared for the duration of this project. Recombinant virus stocks produced were non infectious due to the use of pSFV-Helper 2 as discussed earlier in chapter 5 (Berglund *et al.*, 1993). In order to establish optimum activation of virus, 35 µl of each stock were treated with 50, 100, 200, 300 and 400 µg of α-chymotrypsin per milliliter of virus stock as described in section 5.2.6. Results are shown in figure 6.4.

6.2.4 Viral Infection

For small scale infections , 6 x 10^5 BHK-21 cells were prepared for infection as described in section 5.2.5. In duplicate experiments, 55 µl of activated virus (virus prepared from

different stocks) was mixed with 1 ml of GMEM complete medium and added to pre washed BHK-21 cells. Cells were incubated with the viral mixture for 45 minutes at 37°C and 5% CO_2 with maximum humidity. Following the incubation, the viral mixture was removed and fresh GMEM complete medium was added. Cells were incubated for 3, 6, 9, 18, 24 and 48 hours at 37°C and 5% CO_2 with maximum humidity and then lysed using the method previously described in section 6.2.2. Supernatants were assayed for PDE activity as described in section 2.2.3.5. Results are shown in figure 6.5.

For large scale infections, 1.2 x 10^6 BHK-21 cells were seeded in 75 cm^2 tissue culture flasks and incubated for 24 hours in the tissue culture incubator set to incubate at 37°C and supplemented with 5% CO_2 and maximum humidity. Following the incubation, cells were infected with 100-200 µl of activated pSFV-1Met^{26}RD1 recombinant virus for 45 minutes in the tissue culture incubator. The viral mixture was removed and 15 ml GMEM complete media was added and cells were incubated for 24 hours in the tissue culture incubator. The cells were then lysed using the method described in section 6.2.2 with some modifications. The volume of buffer A used was adjusted to 3 ml and the final centrifugation step was performed at a speed of 15000 rpm for 30 minutes at 4°C using a Beckman centrifuge with a JA20 rotor. The supernatant was collected, aliquoted and stored at -80°C until analysed. On average the expression procedures performed during this project consisted of infections of 5-6x 75 cm^2 tissue culture flasks.

6.2.5 Ion-Exchange Chromatography

Two types of ion exchange columns were used during this project, the Q columns supplied by Viva Sciences which consisted of charged particles fixed on 10 filters and the more conventional resin Q-Sepharose.

6.2.5.1 Q-columns

The columns which had a maximum binding capacity of 2 mg of protein were washed and eluted via centrifugation using a 5415C eppendorf microcentrifugate at room temperature and a speed of 4000-6000 rpm.

Before use, columns were washed twice with 0.5 ml of Milli Q autoclaved water to remove any preservatives present on the filters. 284 µl of Met^{26}RD1 sample (lysate of small scale infection) was diluted 1:3 with buffer A with 100 µM PMSF to a final volume of 0.5 ml. The sample was then loaded onto the column three times to ensure adequate binding of proteins to the column. The column was then washed 4x with buffer A and proteins were eluted with 0.5 ml of buffer A containing an increasing concentration of NaCl (0.1-1 M). Samples were stored at -20°C until analysed by PDE assays, SDS PAGE and Immunoblotting.

6.2.5.2 Q-Sepharose

Purification described in this section was performed in a fridge cooled to 4-5°C. 5 ml (bed volume) of Q-Sepharose fast flow resin purchased from Pharmacia Biotech was washed 3x in 100 mM Tris pH 8 and degassed in a 50 ml conical flask. The resin was transferred into 20 ml plastic column (BioRad) and buffer A (50 mM Tris pH8, 20 mM $MgCl_2$, 1 mM EDTA and 1 mM DTT) was run through via gravity (~ 50 ml) until the resin was fully packed and equilibrated. 400µl of Met^{26}RD1 sample (lysate of small scale infection) was diluted 1:5 with lysis buffer and loaded onto the column. The column was washed with 20 ml of lysis buffer under gravity and proteins were eluted with lysis buffer containing an increasing concentration of NaCl (0.2 -0.6 M). 5 ml fractions were collected and assayed for PDE activity immediately and analysed by SDS PAGE and Immunoblotting 24 hours later after storing the samples at -20°C.

For purification of large scale infections (5-6x 75 cm^2), lysates from 5 to 6 flasks were pooled and loaded on pre equilibrated column (2 ml bed volume) with buffer A via gravity. The column was washed with five times the column volume of lysis buffer and recombinant Met^{26}RD1 protein was eluted with lysis buffer containing 0.4 M NaCl at flow rate of 0.1 ml/ minute. 20x 1ml fractions were collected and soon after collection, a cocktail of protease inhibitors containing final concentrations of 10 µg/ml of pepstatin, 10 µg/ml aprotinin, 10 µM leupeptin,10 µM TLCK and 20 µM TPCK was added. Fractions were stored at 4°C until assayed for PDE activity which was generally performed within 24 hours of purification and analysed by SDS PAGE and Western blotting.

Columns were regenerated for further use by washing for 30 minutes at a flow rate of 0.4 ml/minute with 1x PBS, 1x PBS + 2 M NaCl and 1x PBS sequentially. The column was then equilibrated with buffer in use for 1 hour using the same flow rate as previously mentioned.

6.2.8 Biochemical Analysis of mammalian Expressed Met^{26}RD1 Protein

6.2.8.1 Estimation of molecular weight by Gel Filtration Chromatography

The native molecular weight of Met^{26}RD1 recombinant protein was determined using S200 HR Sephacryl resin purchased from Pharmacia Biotech. The resin was degassed and poured into a 30 x 1.5 cm glass column and left to level out by gravity at 4°C. The column was then packed overnight at a flow rate of 0.45 ml/minute using GF buffer (50 mM Tris pH 7.5, 20 mM $MgCl_2$, 2 mM EDTA and 0.2 M NaCl) and calibrated using the molecular weight markers bovine serum albumin (66 kDa), carbonic anhydrase (20 kDa) and vitamin B_{12} (6 kDa) at a lower flow rate of 0.09 ml /minute.

1 ml Q-Sepharose eluate was then applied to the column, and 60 x 1 ml samples were collected at the same flow rate as the previously described for the calibration markers. The column was stored at 4°C containing GF buffer supplemented with 0.4 % NaN_3. The void volume (V_o) was determined using 1 mg of Blue dextran (Sigma) dissolved in GF buffer.

6.2.8.2 PDE Activity Analysis

The assay used was as described in section 2.2.3.6 with modifications described in the following sections.

6.2.8.2.1 K_m, V_{max} and IC_{50}

Increasing volumes (10 µl) of pSFV-1Met^{26}RD1-transfected BHK-21 cells lysates were run on 10 % polyacrylamide gel and transferred onto nitrocellulose membrane and analysed by Western blotting using GST-Met^{26}RD1 antisera prepared as described in chapter 4. The

resultant bands' intensities were compared to the intensity of a known amount (μg) of GST-Met^{26}RD1 electro-eluted protein (preparation described in section 4.2.1). This method determined approximately, protein concentrations of Met^{26}RD1 recombinant protein used in the determination of the K_m and V_{max} of the protein. PDE activity was defined as moles of cyclic nucleotide hydrolysed per minute per mg. This was calculated as follows:

[(moles cyclic nucleotide per assay ÷ Total dpm) x (dpm - dpm blank)] ÷ 15 min ÷ mg or ml in assay

To determine K_m and V_{max}, the concentration of cAMP substrate in the assays was varied (0.025-100 μM). The amount of [^{3}H]-labeled cyclic nucleotide per assay was kept constant. Estimates of K_m and V_{max} values were determined graphically by plotting the data as direct linear plot using the graphic computer program Grafit 4.

Following the determination of the K_m value, cAMP concentration identical to K_m value was used to determine the inhibition response of Met^{26}RD1 recombinant protein towards known PDE inhibitors. Assays were performed in the presence of increasing concentrations of PDE inhibitors, Rolipram. Inhibition data were analysed graphically using the computer Microsoft Excel and concentration of PDE inhibitors that elicited a 50% reduction in PDE activity (IC_{50}) was estimated.

6.2.9 Immunoaffinity Chromatography

6.2.9.1 Purification Using GST-Met^{26}RD1 antibody column

Procedures described in this section were performed at 4°C. The GST-Met^{26}RD1 antibody coupled to protein A Sepharose as described previously (Chapter 4) was packed in a 2 ml plastic column purchased from BioRad. The column was washed with fresh 1x PBS for 1 hour at 0.4 ml/minute flow-rate to remove preservative, and was equilibrated with buffer A for 30 minutes using the same flow rate. Meanwhile, fractions 2 and 5 of Q-Sepharose elutes were dialysed in buffer A containing 0.4 M NaCl to remove DTT. The dialysed

fractions were applied by continuous cycling through the column at a constant flow rate of 15 ml/h overnight. The column was then washed with buffer A containing 0.4 M NaCl for 2 hours at 25 ml/minute flow rate. Proteins were eluted at a flow rate of 10 ml/h sequentially with 10 ml of each of the following elution buffers: (a) aminocaproic acid pH 10.5, 1 mM EDTA and 1% glycerol; (b) diethylamine pH 11.5, 20 mM $MgCl_2$ and 1 mM EDTA; and (c) 3.5 M $MgCl_2$, 50 mM Tris pH 7.4, 1 mM EDTA and 1% Triton X-100. These buffers were used to establish optimal elution conditions. The column was washed with buffer A between elution 1 and 2 and washed with fresh 1x PBS between elutions 2 and 3. 1 ml fractions were collected using the fraction collector and fractions were assayed immediately for PDE activity and analysed by immunoblotting 24 hours later.

To regenerate the antibody column, the column was washed with 10 ml of 3.5 M $MgCl_2$ elution buffer followed by 1x PBS at a flow rate of 10 ml/h prior to use.

6.3 Results

6.3.1 Cloning and Expression of pSFV-1Met^{26}RD1 Construct

The rat PDE4 (*Met^{26}RD1* clone) was subcloned into pSFV-1 at *Bam* HI and *Sma* I sites following amplification by PCR using primers shown in section 3.2.1.1. To ensure that *Met^{26}RD1* gene was cloned in the right reading frame and orientation, 5' and 3' ends were sequenced using ABI sequencer as described in section 2.2.2.4. In all clones sequenced, there was no change identified compared to published sequence (Davis *et al.*, 1989; EMBL/GenBank data base Accession no. J04554).

Before embarking on the production of recombinant pSFV-1Met^{26}RD1 protein using Semliki Forest Virus system, the expression of *Met^{26}RD1* gene using pSFV-1 vector in BHK-21 cells was evaluated. In order to perform this, mRNAs of pSFV-1Met^{26}RD1 synthesised *in vitro* (figure 6.2) were electroporated into BHK-21 cells. The cells were collected 24 hours post electroporation and lysed following method described in section 6.2.2. Supernatant samples were tested for PDE activity and analysed by Western blot (figure 6.3).

This experiment showed a significance increase in PDE activity in cells transfected with pSFV-1Met^{26}RD1 construct. Furthermore the activity (13.7 ± 5.5 pmole/min/assay) was inhibited by more than 96% when treated with 100 μM rolipram a PDE 4 specific inhibitor (figure 6.3/b). Also, endogenous PDE activity of 0.07 pmole/min/assay responded to inhibition by rolipram indicating that the endogenous PDE activity may originate from type 4 phosphodiesterase enzymes (figure 6.3/b).

Polyclonal antibody GST-Met^{26}RD1 produced in house (Chapter 4) was used to analyse the expression of *Met^{26}RD1* gene by Western blotting. The antibody detected a number of bands of approximately 65, 64 and 62 kDa in size in crude samples of BHK-21 cells transfected with pSFV-1Met^{26}RD1 construct (figure 6.3/a). These bands were not observed in lysates not expressing the *PDE* gene suggesting that they could be a result of proteolytic cleavage of Met^{26}RD1 recombinant protein expressed in BHK-21 cells.

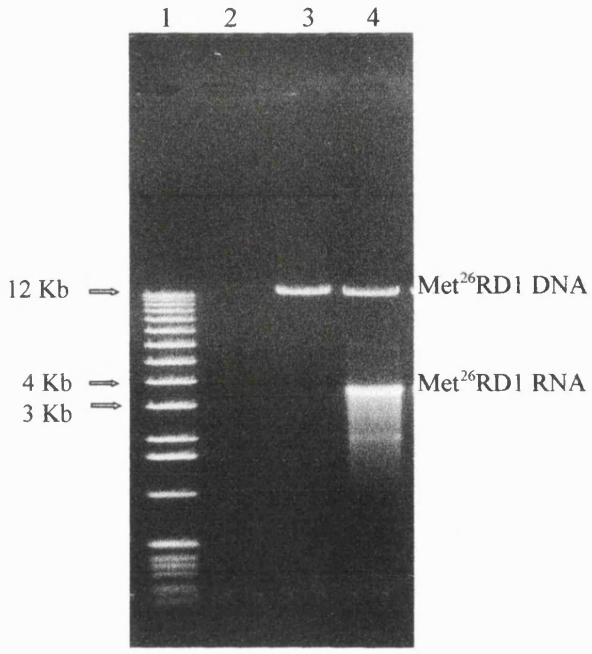

Figure 6.2 Agarose gel analysis of pSFV1-Met^{26}RD1 RNA transcribed *in vitro*. 1 µl of the *in vitro* transcription reaction was electrophoresed on 0.5% (w/v) agarose gel containing ethidium bromide. Lane 1: 1 kb DNA ladder. Lane 2: Transcription reaction minus DNA template. Lane 3: Transcription reaction minus RNA polymerase. Lane 4: Complete transcription reaction.

a)

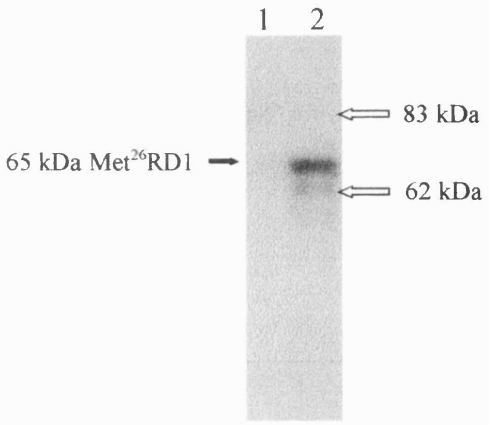

b)

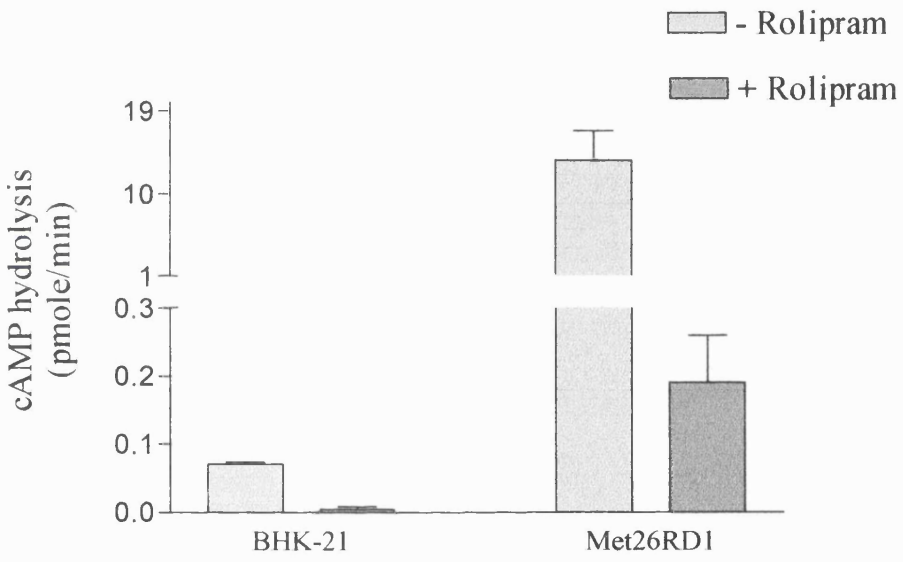

Figure 6.3 Western blot analysis and PDE activity assay of pSFV-1Met[26]RD1 expressed in BHK-21 cells. 2.5 x 10^6 BHK-21 cells were electroporated with 10 µl of pSFV-1Met[26]RD1 mRNA at 350 V and 1500 µF. The cells were incubated for 24 hours in a tissue culture incubator and lysed as described in section 6.2.2. Panel **(a)** represents supernatant of both BHK-21 lysates of cells non-expressing (Lane 1) and expressing pSFV-1Met[26]RD1 (Lane 2), run on 10% SDS PAGE gel and transferred onto a nitrocellulose membrane. The membrane was then probed with GST-Met[26]RD1 antibody. Panel **(b)** represents PDE activity assays using 0.25 µM cAMP in the absence and presence of 100 µM Rolipram. Assays were performed in triplicates from samples of a single preparation and the error bars represent the standard deviation.

6.3.2 Generation of Met^{26}RD1 Virus stock

In order to produce Met^{26}RD1 recombinant virus, BHK-21 cells were coelectroporated with transcripts of pSFV-1Met^{26}RD1 and Helper 2 using parameters optimised in chapter 5. Briefly, in these applications as described previously in chapter 5, RNA species of both transcripts would be amplified in the BHK-21 cells but only recombinant RNA molecules carrying the packaging signal (i.e. pSFV-1Met^{26}RD1) (Liljestrom and Garoff, 1991) would be selectively packaged into virus particles (Lundstrom *et al.*, 1994).

300 μg/ml concentration of α-chymotrypsin was estimated to be the maximum concentration needed for maximum pSFV-1Met^{26}RD1viral activation (figure 6.4) which was similar to the previously estimated α-chymotrypsin concentration needed for maximum pSFV-3 viral activation.

6.3.3 Expression of pSFV-1Met^{26}RD1 Construct using Semliki Forest Virus System

To determine the optimum expression levels of SFV-1Met^{26}RD1 construct, PDE assays of three separate preparations were carried out in duplicates after 3, 6, 8, 18, 24, 36 and 48 hours post infection using BHK-21 cells. To ensure 100% infectability of cells, a multiplicity of infection (m.o.i) of 5 was used.

The highest activity was observed after 24 hours of SFV infection this was followed by a sharp decline in activity recorded after 36 and 48 hours of infection (shown in figure 6.5). Infections with virus containing pSFV-1 vector only, showed very little activity that declined to negligible amounts after 24 hours of infection (figure 6.5). Furthermore, PDE activity observed after 24 hours of SFV infection was found mainly in the supernatant fraction with < 0.2% of the total activity present in the pellet fraction (figure 6.6/a). This observation was also later confirmed by Western blot analysis (figure 6.6/b).

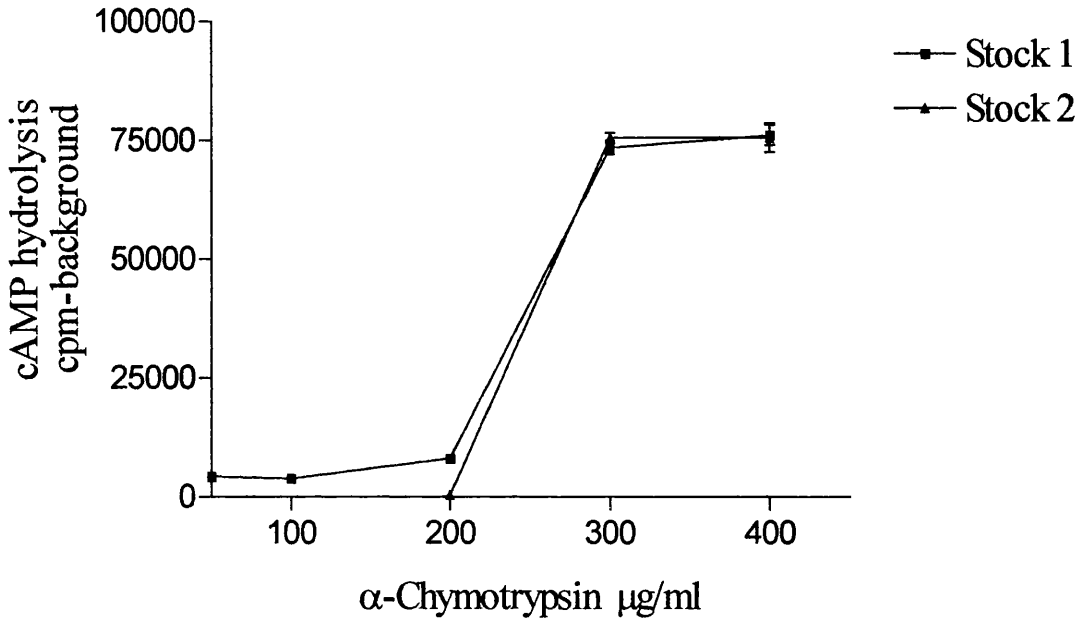

Figure 6.4 Activation of two recombinant $Met^{26}RD1$ viral stocks by α-chymotrypsin at different concentrations. 35 μl of two viral stocks (prepared as in section 6.2.3) collected 24 hours after co-electroporation of pSFV-1$Met^{26}RD1$ and helper 2 were treated with α-chymotrypsin concentrations of 50, 100, 200, 300 and 400 μg/ml of following the method described in section 5.2.6. The activated virus stocks were then mixed with 1 ml of GMEM complete medium and added to 6 x 10^5 BHK-21 cells seeded the day before in 25 cm^2 flasks. Cells were lysed using method described in section 6.2.2 20 hours post infection and supernatant samples were collected and diluted 1/50 with dilution buffer (0.1% BSA, 50 mM Tris pH 8) and assayed for PDE activity using 0.25 μM cAMP substrate. Assays were performed in duplicates so error bars represent the values deviation from the mean.

Following the establishment of the optimum time needed for Met^{26}RD1 expression in BHK-21 cells, the expression procedure was performed on a larger scale. 5-6x 75 cm^2 tissue culture flasks containing adherent BHK-21 cells were infected, incubated for 24 hours and collected for lysis. Lysates expressing Met^{26}RD1 tested for PDE activity revealed an increase of approximately 99% in PDE activity over background (Table 6.2). Typically, between 0.1 and 0.3 mg of Met^{26}RD1 protein was produced per 10^7 transfected BHK-21 cells. The expressed Met^{26}RD1 showed a specific activity of 45.6 nmol/min/mg (Table 6.2 n=2). Enzymatic studies were performed on the crude sample of expressed Met^{26}RD1protein to determine the protein's specificity to cAMP and inhibition by type 4 PDE-specific inhibitor Rolipram. The K_m and V_{max} values (for cAMP hydrolysis) were estimated graphically, by the direct linear plot of velocities against substrate concentration using the computer programme Grafit 4. Figures 6.7 and 6.8 shows that the K_m was 7 ± 0.6 μM and the V_{max} was 0.214 μmole/min/mg.

Analysis of inhibition was performed at the K_m value of 7 μM previously determined for the recombinant Met^{26}RD1. The ranges of concentration employed were 0.001- 200 mM for Rolipram, Amrinone, IBMX and Vinpocetine. PDE activity was also studied with the addition of 2 μM of cGMP. Similar inhibition studies were performed on lysates of BHK-21 cells infected with virus carrying pSFV-1 construct with no *Met^{26}RD1* gene. The expressed Met^{26}RD1 was observed to show great specificity to rolipram (a PDE 4 specific inhibitor) with an IC_{50} values of 0.7 μM which was found to be consistent with Shakur *et al.*, 1993 findings for Met^{26}RD1 (Table 6.3). It was observed that the protein showed a weak response (only 30% reduction in activity, Table 6.3) to high levels (100 μM) of both Amrinone and Vinpocetine which are PDE3 and PDE1 specific inhibitors respectively and a relatively high response (approximately 70% reduction in activity) to 100 μM IBMX PDE non selective inhibitor. In BHK-21 transfected with pSFV-1 mRNA, the endogenous PDE activity was inhibited completely with 100 μM Rolipram and inhibited by 87 % with IBMX but showed very little response to Amrinone (a PDE 3 specific inhibitor) and to Vinpocetine (a PDE 1 specific inhibitor).

Table 6.2 Large scale expression of Met[26]RD1 in BHK-21 cells using SFV system.

Source	Protein mg/ml	Activity nmole/min/mg	Specific activity nmole/min/mg PDE
BHK-21	3.3	0.003	ND
BHK-21-pSFV-1	2.48	0.003	ND
BHK-21-pSFV-1Met[26]RD1	2.4	0.2	45.6

Data represent mean values of two separate preparations. PDE assays as described in section 2.2.3.6, protein concentrations were determined by Ultraviolet Absorption as described in section 2.2.3.5.2. For specific activity determination, protein concentration of PDE were determined by Western blotting as described in section 6.2.8.2.1. ND= Not Determined.

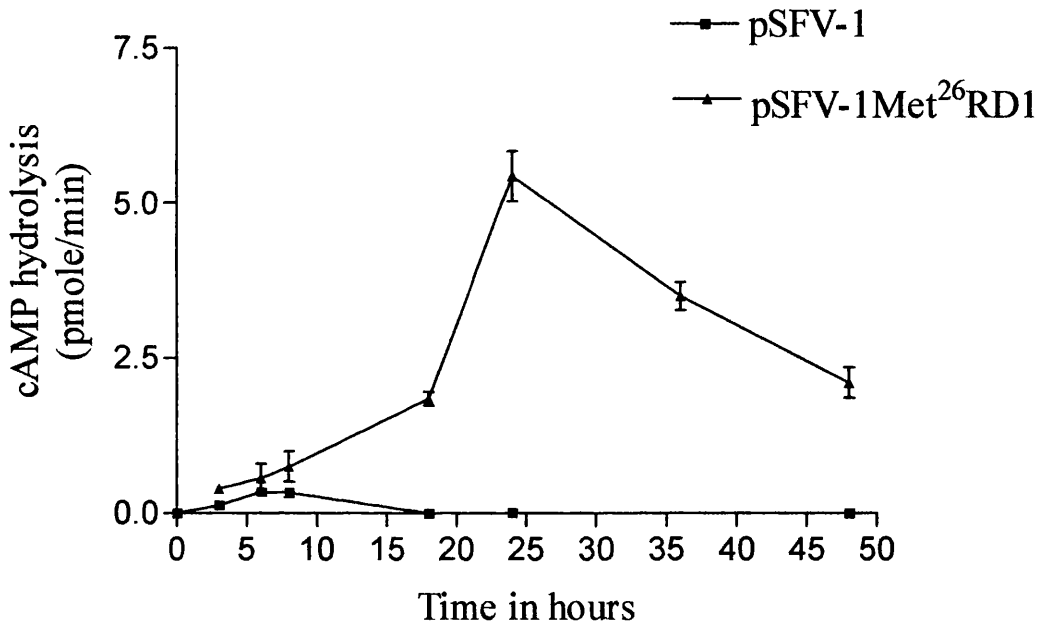

Figure 6.5 Time course of pSFV-1Met[26]RD1 construct expression in BHK-21 cells infected with recombinant Semliki Forest virus. 3 x 10^5 BHK-21 cells plated on 25 cm^2 flasks 24 hours previously, were infected with 55 µl of the virus stock carrying pSFV-1Met[26]RD1 construct. Cells were collected for lysis and assayed for PDE activity using 0.25 µM cAMP substrate at the indicated times.

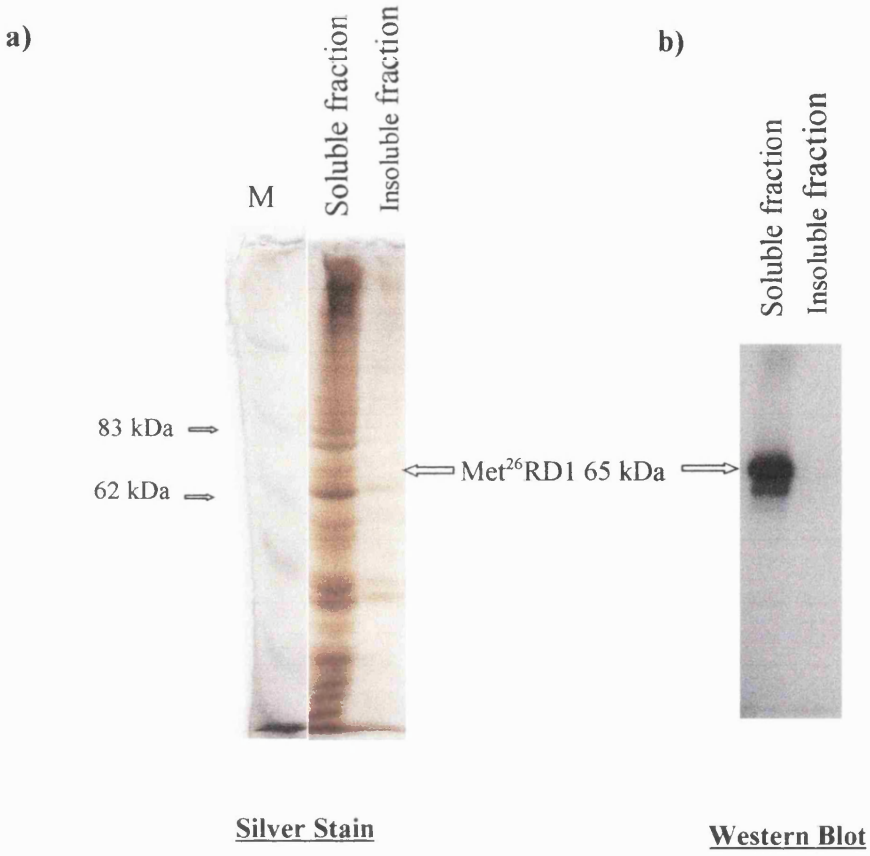

Figure 6.6 Intracellular distribution of the *Met[26]RD1* gene product expressed in BHK-21 cells. 6 x 10^5 BHK-21 cells were infected with virus carrying pSFV-1Met[26]RD1 vector using method described in section 6.2.4. The cells were then incubated for 24 hours in a tissue culture incubator maintained at 37°C, 5% CO_2 and maximum humidity. The cells were harvested and lysed in 400 µl of lysis buffer containing 0.1% Triton X-100. Lysates were centrifuged for 2 minutes at 4°C at maximum speed (14 000 *g*) using a 5415C eppendorf microcentrifuge to separate the soluble fraction from insoluble fraction. 10µl of each fraction was loaded on 10% SDS polyacrylamide gel. Panel **(a)** shows the SDS gel stained with silver and Panel **(b)** shows a similar gel transferred onto nitrocellulose membrane and probed with GST-Met[26]RD1 polyclonal antibody produced in house to recognise Met[26]RD1 protein (described previously in Chapter 4).

c)

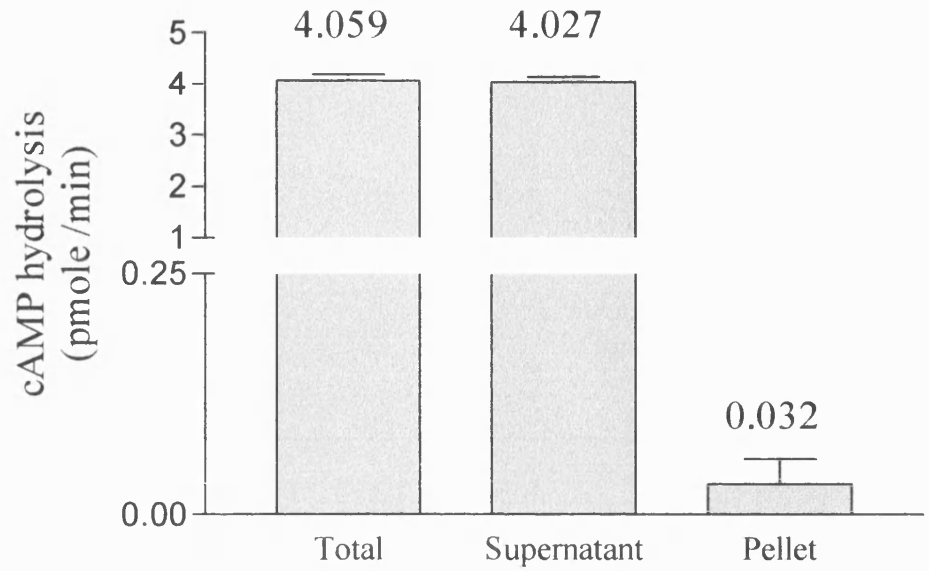

Figure 6.6/C Intracellular distribution of the *Met*^{26}*RD1* gene product expressed in BHK-21 cells. 6 x 10^5 BHK-21 cells were infected with virus carrying pSFV-1Met^{26}RD1 vector using method described in section 6.2.4. The cells were then incubated for 24 hours in a tissue culture incubator maintained at 37°C, 5% CO_2 and maximum humidity. The cells were harvested and lysed in 400 µl of lysis buffer containing 0.1% Triton X-100. Lysates were centrifuged for 2 minutes at 4°C at maximum speed (14 000 *g*) using a 5415C eppendorf microcentrifuge to separate the soluble fraction from insoluble fraction. Panel **(c)** represents PDE activity assays using 10 µl samples collected from the lysis procedure stated above. The assay was performed in triplicates and error bars represents standard deviation.

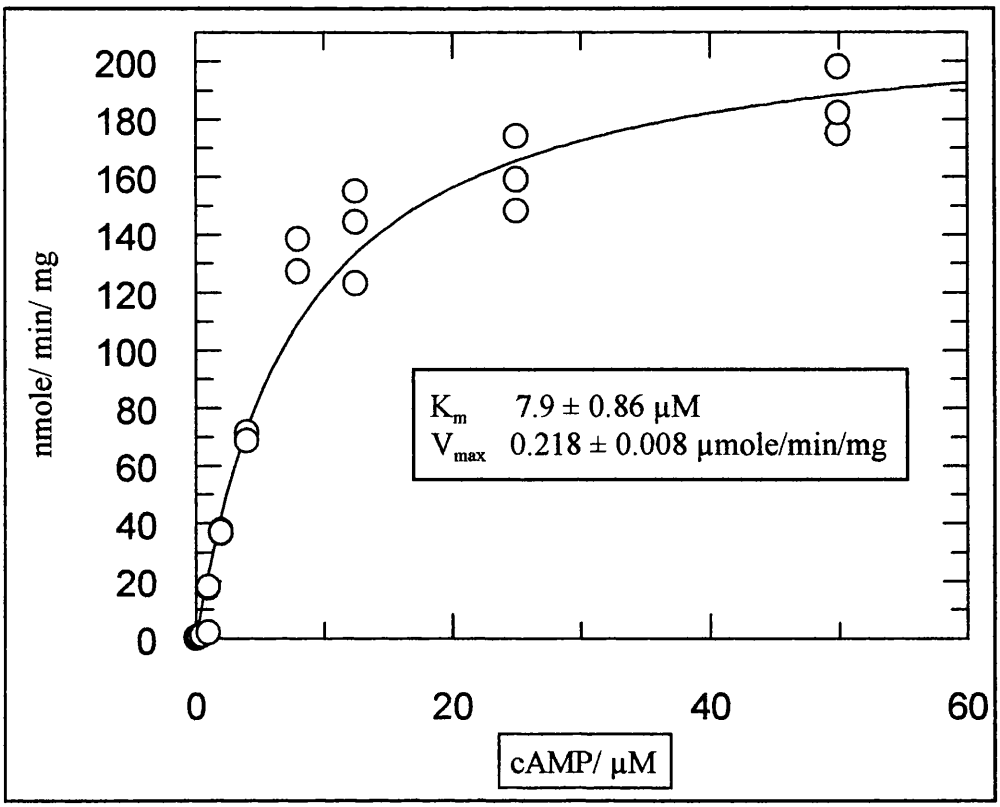

Figure 6.7 Kinetic characterisation of $Met^{26}RD1$ protein expressed in BHK-21 cells. The graph represents the direct linear plot of PDE activity against cAMP substrate concentrations. 10 µl (24 µg total protein) of BHK-21 cell extracts containing expressed $Met^{26}RD1$ protein were assayed for PDE activity with cAMP concentrations ranging from 0.025 to 50 µM. Assays were performed in triplicates using cell extracts from one expression study.

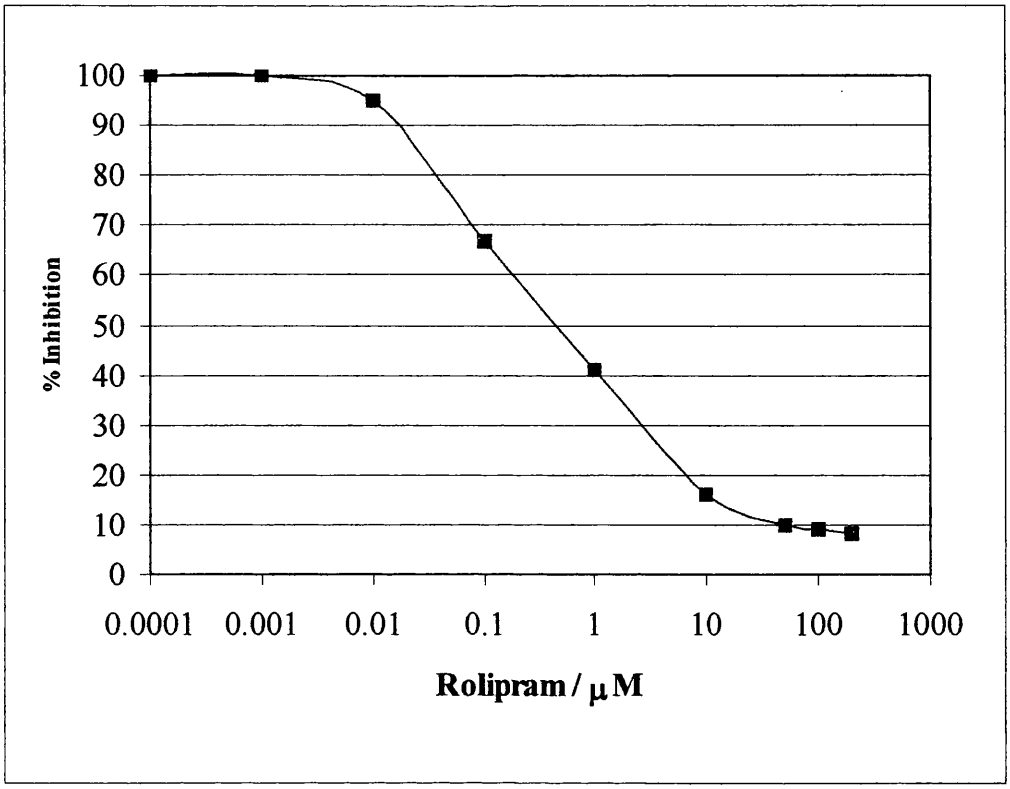

Figure 6.8 The action of Rolipram a PDE 4 specific inhibitor on expressed $Met^{26}RD1$. The degree of $Met^{26}RD1$ inhibition was analysed using 10 μl of BHK-21 cell extracts containing expressed $Met^{26}RD1$ protein (24 μg of total protein). The cAMP substrate concentration was set at 7 μM, the K_m of $Met^{26}RD1$.

Table 6.3 Pharmacological properties of recombinant $Met^{26}RD1$ and endogenous PDE (pSFV-1 transfected BHK-21 cells) expressed using SFV system.

Property	$Met^{26}RD1$	Endogenous PDE
K_m (μM)	7.9 ± 0.86	NT
V_{max} (nmole/min/mg)	218 ± 8	NT
IC_{50} or % inhibition with 100 μM		
IBMX (non Selective)	66.5%	87%
Rolipram (PDE 4)	0.7	100%
Amrinone (PDE 3)	30%	No change
Vinpocetine (PDE 1)	35%	20%
Specific Activity (nmole/min/mg)	45.6	NT
cGMP (2 μM)	<30%	NT

Assays were performed using crude lysates of BHK-21 cells infected with virus carrying either pSFV-1$Met^{26}RD1$ or pSFV-1 in the case of endogenous PDE. IC_{50} and inhibitions studies, assays were performed using 7μM cAMP. Values presented were either mean values of two separate studies or mean values with standard deviation of three separate studies. Abbreviation NT represents not tested conditions.

6.3.4 Ion-Exchange Purification of expressed pSFV-1$Met^{26}RD1$ Construct

The nucleic acid sequence for *$Met^{26}RD1$* gene was determined by deleting the first 75 base pairs from RD1 published sequence (Davis *et al.*, 1989; EMBL/GenBank data base Accession no. J04554) (see Appendix 1). The pI value was found to be 5.75 hence, anion exchanges were used in this purification procedure.

Initially, a small scale (0.5 ml) trial was performed to determine approximate salt concentration needed to elute the $Met^{26}RD1$ protein. 0.5 ml BHK-21 lysate of cells infected with SFV carrying pSFV-1$Met^{26}RD1$ construct, were loaded onto Q- columns supplied by Viva sciences. PDE activity was eluted by using a salt gradient ranging between 0.1- 1 M. Majority of the PDE activity eluted at 0.4 M salt (figure 6.9/a) and Western blot analysis later confirmed the presence of $Met^{26}RD1$ protein in this fraction (figure 6.9/b).

Following the trial determination, larger scale expressions (5-6x 75 cm^2 flasks) were

loaded onto 2 ml (bed volume) Q-Sepharose column. The column was washed with 10 ml of lysis buffer and PDE activity was eluted with 0.4 M NaCl.

Table 6.4 Q-Sepharose purification of $Met^{26}RD1$.

Fraction	Total Volume ml	Total Protein mg	Activity nmole/min/ml	Total activity nmole/min/total volume
Homogenate	15	36	0.445	6.67
Flow through	15	2.27	ND	0.03
Wash	10	5.562	0.002	0.024
Bound		28.168		6.616
QS elute				
Fraction 2	2	2.84	0.5	1
Fraction 3	2	2.368	3	0.3
Fraction 4	2	1	0.115	0.023
Fraction 5	2	1	0.025	0.005
Eluted		7.208		1.328

Data are mean values of two different preparations. PDE activities and protein concentrations were determined as described in section 2.2.3.6 and 2.2.3.5.2 respectively. QS= Q-Sepharose.

The binding efficiency of Q-Sepharose was estimated crudely by measuring the total protein content and total PDE activity in the starting material (homogenate) and subtracting protein and PDE activity present in both the flow through and wash samples. This method although relative in its estimation, found that 60 % of the proteins bound to the resin and virtually all of the PDE activity was retained by the resin (Table 6.4). The eluting efficiency of Q-Sepharose was estimated in a similar way and it was found that only 20% of PDE activity was eluted (Table 6.4). This was considered to be low and further optimisation would be needed to be performed if this method should be used as a purification step in the future. Q-Sepharose chromatography was used as a cleaning up step prior to molecular mass determination using Gel Filtration chromatography and immunoaffinity chromatography using columns prepared from polyclonal antibodies raised against GST-$Met^{26}RD1$ previously described in Chapter 4.

a)

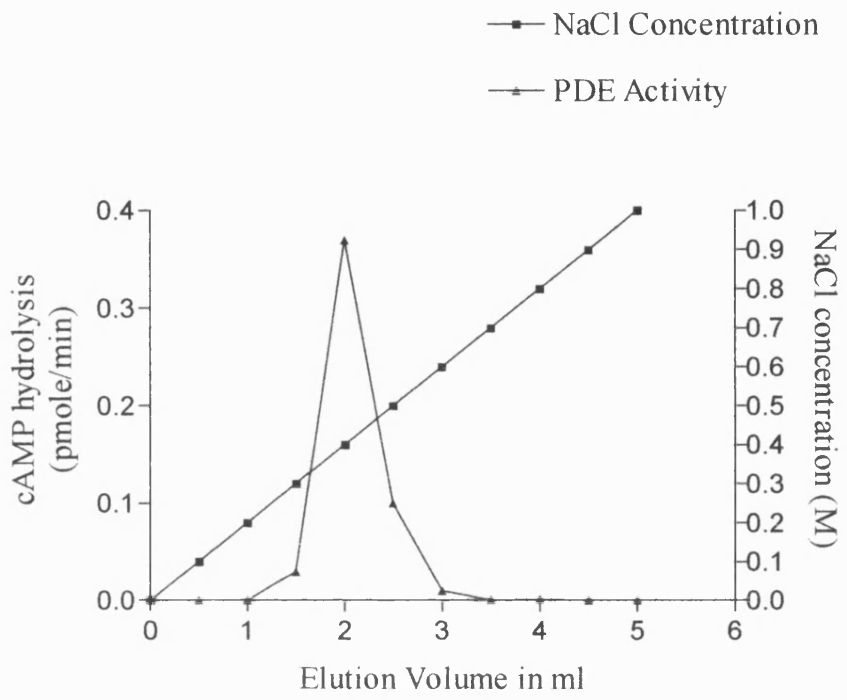

b)

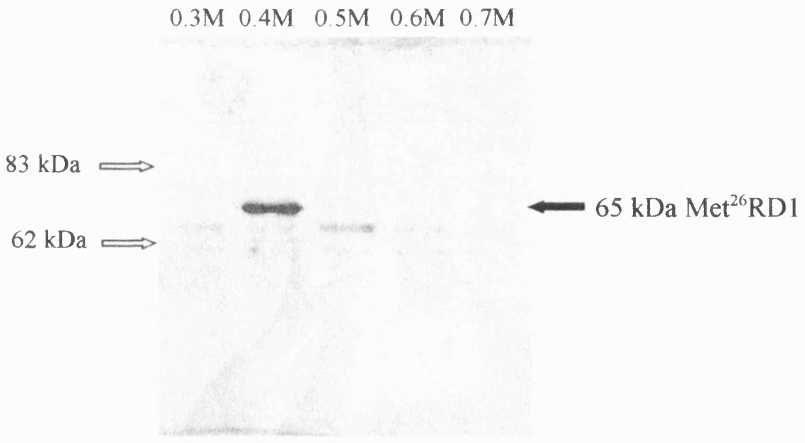

Figure 6.9 Q-Sepharose elution profile. 15 ml of crude homogenate was loaded onto 2 ml bed volumes of Q-Sepharose resin. Panel **(a)** shows PDE activity eluted at 0.1 ml/min with linear NaCl (0-1M) gradient. Panel **(b)** shows the Western blot of the eluted fractions using GST-Met^{26}RD1 antibody as the primary antibody. The lanes represent fractions eluted with 0.3-0.7 M salt. 150 µl of each fraction was concentrated to 10 µl by methanol/ chloroform method as described in section 2.2.3.1 was loaded on 10% SDS gel.

6.3.5 Native Molecular Weight Determination of Recombinant Met^{26}RD1 Protein

To determine the molecular weight of the native Met^{26}RD1 recombinant protein and its association state, half of the sample eluted from the Q-Sepharose column was applied on S200 HR Sephacryl Gel Filtration column (30 x 1.5 ml glass column). The protein eluted from the sizing column as a broad peak with a relative molecular weight of about 66 kDa (figure 6.10), which suggested that the protein existed as a monomer.

6.3.6 Purification of Met^{26}RD1 Using Immunoaffinity Chromatography

Preliminary studies to purify Met^{26}RD1 recombinant protein to homogeneity was performed using a GST-Met^{26}RD1 antibody column prepared in Chapter 4. These studies were performed to attain information about the binding properties and the elution properties of the expressed protein. The sample eluted from Q-Sepharose was applied on 0.75 ml (bed volume) antibody column by continuous cycling to ensure maximum binding to column. Met^{26}RD1 was eluted using three different eluting buffers. Met^{26}RD1 bound completely to the GST-Met^{26}RD1 polyclonal antibody column and approximately 70% of the bound PDE activity was eluted exclusively with $MgCl_2$ rather than high pH (figure 6.11/a). Elution using low pH buffer was not performed as addition of acid to PDE assays to lower the pH to 2.5, was found to abolish the PDE activity. This observation could help to separate the 65 kDa Met^{26}RD1 from its proteolytic species. Polyacrylamide gel analysis of the eluted fractions showed the elution of three proteins with molecular weights ranging from 65 kDa to 62 kDa (figure 6.11/a). These protein bands were detected by anti-Met^{26}RD1 antibody (GST-Met^{26}RD1 antibody) confirming the identity of these bands to the recombinant Met^{26}RD1 protein (figure 6.11/b).Western blots of the eluted fractions revealed the elution of protein bands approximately 62 kDa in size which were thought to be present as a result of proteolytic cleavage of the full length Met^{26}RD1. Western blot analysis of resin samples collected before and after PDE protein elution with $MgCl_2$ showed the elution of the 65 kDa protein as well as proteins approximately 62 to 63 kDa in size. These smaller proteins were thought to be a result of proteolysis of the full length

Met[26]RD1.

a)

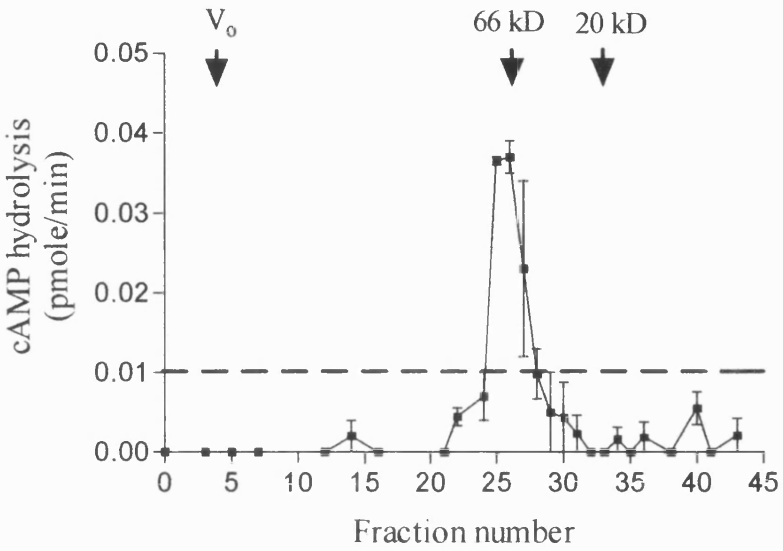

b)

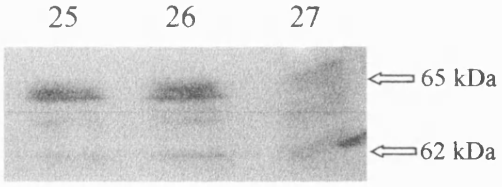

Anti GST-Met[26]RD1 antibody

Figure 6.10 Molecular weight estimation of Met[26]RD1 protein expressed in BHK-21 cells by Gel Filtration chromatography. 1 ml of Q-Sepharose elute containing approximately 1 mg of total protein was loaded onto 30 x 1.5 cm S200 HR column. 1 ml fractions were collected at a flow rate of 0.09 ml/ minute and assayed for PDE activity (Panel a). The dotted line represents the baseline of the PDE assay. The elution volumes of Bovine serum albumin 66 kDa and Carbonic anhydrase 20 kDa were indicated as arrows. V_o represent void volume. 10 µl of fractions 25, 26 and 27 were analysed by Western blots (Panel b) using polyclonal antibody GST-Met[26]RD1 (produced in house Chapter 4)as the probe.

a)

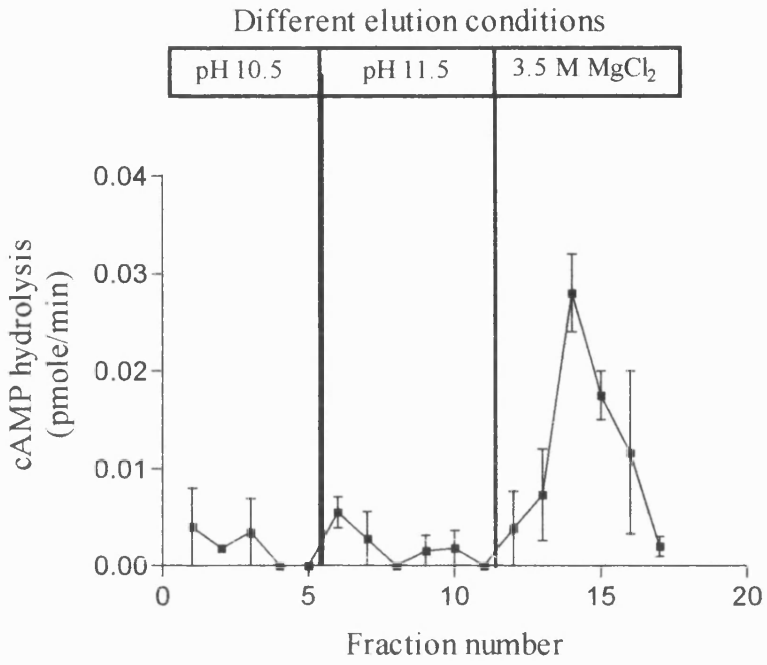

b)

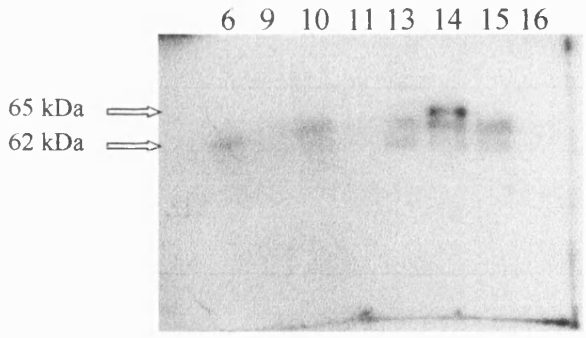

Figure 6.11 The elution profile of Met[26]RD1 using immunoaffinity chromatography. 0.4 ml of Q-Sepharose elute was loaded onto 0.75 ml (bed volume) of GST-Met[26]RD1 polyclonal antibody (produced in house Chapter 4) immobilised on protein A Sepharose. PDE activity was eluted with three different elution buffers (boxed in panel a) at the flow rate of 0.17 ml/ minute. Panel **(a)** shows PDE activity using 0.25 μM cAMP of the fractions collected. Panel **(b)** shows Western Blot analysis of fractions 6, 9, 10, 11, 13, 14, 15 and 16 using GST-Met[26]RD1 antibody as the probe.

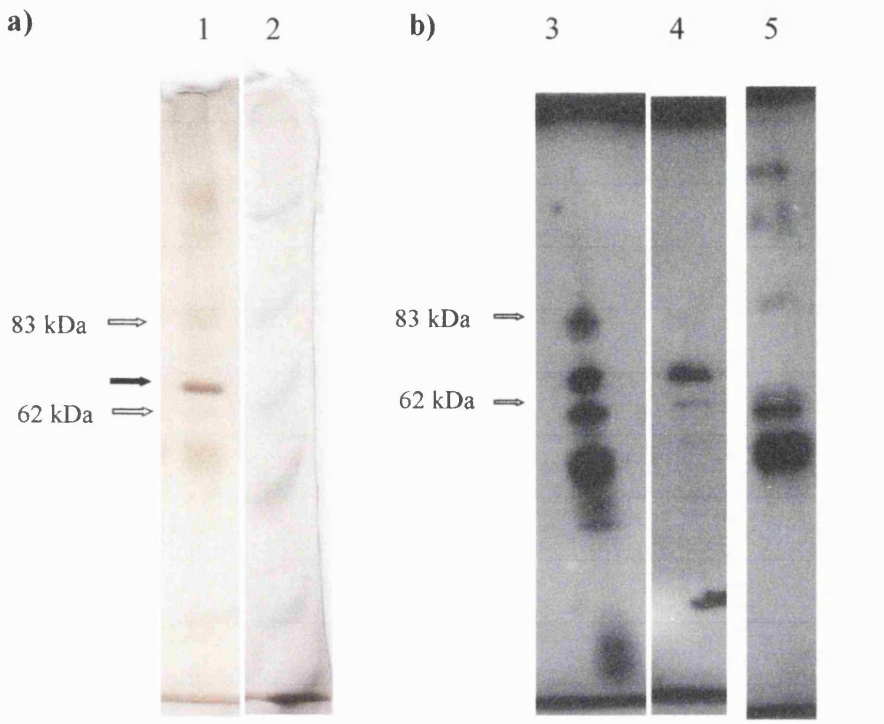

Figure 6.12 Polyacrylamide gel and Western blot analysis of fraction 14 purified by immunoaffinity chromatography. Panel (a) shows silver stain of 10% SDS polyacrylamide gel of eluted fraction 14 (Lane 1) and pre stained molecular weight markers (Lane 2). Panel (b) shows Western blot analysis of 10 µl of sample taken from top of column before $MgCl_2$ elution (Lane 3), 10 µl (1 µg of $Met^{26}RD1$ protein) of fraction eluted with $MgCl_2$ (Lane 4), and 10 µl sample taken from top of column after elution with $MgCl_2$ (Lane 5) using the antiserum GST-$Met^{26}RD1$ as the probe (Chapter 4). Black arrow indicates the location of the band that corresponded to $Met^{26}RD1$ protein 65 kDa in size.

Table 6.5 Purification of $Met^{26}RD1$ using immunoaffinity column prepared from anti GST-$Met^{26}RD1$ antibody.

Fraction	PDE Activity pmol/min/ml
QS eluate	95.4
unbound	0.1
Bound	95.3
eluate	
Fraction 2	4.1
Fraction 3	9.9
Fraction 4	8.6
Fraction 5	8.4
Fraction 6	8.2
Fraction 7	11.65
Fraction 8	13.10
Fraction 9	7.8
Fraction 10	2.7
Eluted	74.35

Data are values of one preparation. PDE activity was determined using 0.25 μM cAMP using method described in section 2.2.3.6. QS= Q Sepharose eluate.

Following the trial purification described previously, 1 ml Q-Sepharose eluate was loaded onto 0.75 ml (bed volume) of a GST-$Met^{26}RD1$ antibody column, the same column used for the trial purification. The column was washed with buffer A, and PDE activity was eluted with buffer A containing 3.5 M $MgCl_2$. The binding efficiency of the antibody column was estimated as previously described in section 6.3.4. Table 6.5 showed that nearly all of the PDE activity detected in starting material was retained by the column and total PDE activity eluted from the column was found to be approximately 78% of the bound activity. PDE assays performed on resin samples taken from the top of the column before and after elution with $MgCl_2$, revealed decrease in PDE activity from 0.1 pmole/min/assay to 0.0066 pmole/min/assay respectively. Although these figures cannot be compared directly as the volumes collected were not directly comparable, the values do suggest the elution of majority of the bound protein. Figure 6.12 showed the elution of 65 kDa $Met^{26}RD1$ with $MgCl_2$, but retention of other proteolytic fragments. This purification method could be used to separate the different proteolytic fragments from the full length protein.

Following the purification procedure described above, eluates were dialysed several times to remove $MgCl_2$. The dialysed sample was then concentrated using centroprep-10 with a 10 kDa cut off membrane. Assays performed on the concentrated samples revealed a loss of PDE activity, this was explained by the loss of the protein shown by polyacrylamide gels and Western blot (gels not shown). Since the activity eluted from Q-Sepharose was lost during the concentration procedure, all of the kinetic studies described in this chapter were performed using crude lysates.

6.4 Discussion

The main objective of this work was to express *Met[26]RD1* gene in mammalian cells using Semliki Forest virus system in an active and soluble form.

The fist step taken to achieve this goal was to test the expression of the gene in the cell types used in the SFV system by evaluating the expressed protein by Western blot analyses using GST-Met[26]RD1 a polyclonal antibody produced in-house (see chapter 4) and the protein's response to rolipram which is a well documented PDE 4 specific inhibitor. BHK-21 cells transfected with Semliki Forest Virus mRNA (pSFV-1) containing the *Met[26]RD1* gene showed elevated PDE activity (figure 6.3/b) (99% over background with transfected cells with pSFV-1 mRNA alone). The activity was found to be inhibited by rolipram suggesting that the activity may originate from type 4 PDEs. Western blot analysis of these samples revealed a protein band of the appropriate size of 65 kDa, which was recognised by the polyclonal antibody raised against GST-Met[26]RD1 fusion protein produced in *E. coli* (Chapter 4). Since no bands were detected with mock transfected cells or with cells transfected with pSFV-1 alone (figure 6.3/a) using this antiserum, it appears that the antiserum had no cross reactivity to the endogenous PDE which was also found to be responsive to rolipram (figure 6.3/b).

The majority of the PDE activity was found in the cytosol of BHK-21 cells with < 0.2 % of the total activity in the pellet. These observations were later confirmed by Western blot analysis using GST-Met[26]RD1 antiserum (figure 6.6). The distribution of expressed

Met^{26}RD1 protein was in agreement with the published data by Shakur *et al.*, 1993 which reported the presence of the Met^{26}RD1 protein exclusively in the cytosol compared to the full length protein (RD1) that was presence associated with the plasma membrane.

Following these trial experiments to establish the capability of BHK-21 cells in expressing the *PDE* gene, Semliki Forest virus carrying the *Met^{26}RD1* gene was produced by co transfecting BHK-21 cells with both pSFV-1Met^{26}RD1 and Helper 2 mRNA. The titre of SFV-Met^{26}RD1 virus stock was not determined directly. This was due to unavailability of the commercial antibodies against the SFV structural proteins which were required to perform immuno-fluorescence to enable the visualisation of cells infected with the virus. Although an antibody against Met^{26}RD1 was available, this antibody was not fluorescently labelled and consequently was not used in SFV titre determination. However, since both pSFV-3 and pSFV-1Met^{26}RD1 were packaged in parallel experiments and the same concentration of α-chymotrypsin was required to activate both viral stocks, it was assumed that the viral titre for both viral stocks were similar. The SFV titre using pSFV-3 mRNA (previously discussed in Chapter 5) was found to be approximately 1 x 10^8 infectious units per millilitre, the SFV titre using pSFV-1Met^{26}RD1 mRNA hence was estimated to be a similar value.

Following the trial expression studies described previously, larger scale expressions using infections by SFV carrying the *Met^{26}RD1* gene were performed. These expression studies produced Met^{26}RD1 protein, approximately, between 0.1 mg and 0.3 mg of PDE per 10^7 cells. The amounts of protein produced were slightly less than the amounts of lac Z of 0.8 mg per 10^7 reported previously by Liljestrom and Garoff, 1991. This was as expected as the expression of PDE could be potentially more toxic to cells than β-galactosidase expression and therefore, cells would most likely express β-galactosidase protein in higher levels compared to expression of PDE protein. However, the low amounts of protein produced here were thought to be not as problematic as initially thought due to the potential of Semliki Forest Virus expression system to be scaled up to > 10 L using bioreactors (Blasey *et al.*, 2000). This would allow for the production of some milligram amounts of PDE protein which inturn would allow for possible structural analysis of the

protein in the future.

The enzyme produced was highly active with specific activities of 45.6 nmole/min/mg which was higher than previously reported values for crude PDE 4 from mammalian recombinant sources 8-12 nmole/min/mg (Huston *et al.*, 1996). The enzyme showed a normal Michaelis-Menten kinetics (figure 6.7) with a K_m value for cAMP of 7.9 ± 0.86 μM which was similar to the previously reported K_m value of 5 ± 3 μM for $Met^{26}RD1$ recombinant protein (Shakur *et al.*, 1993). In addition, the V_{max} was found to be 0.218 ± 0.008 μmole/min/mg which was found to be 10 fold lower than the range of 1-2 μmole/ min/ mg reported by Thompson *et al.*, 1988 and Conti *et al.*, 1995 for native PDE 4 using 1 μM cAMP. This reduction in V_{max} could be explained by a number of factors including the fact the samples analysed were crude lysates of the expressed protein which means that some proteins in the extract may have interfered with the recombinant PDE protein causing the observed reduction in the maximum velocity.

Inhibitory studies were performed and found that $Met^{26}RD1$ expressed here was potently inhibited by the type 4 specific inhibitor rolipram with an IC_{50} of 0.7 μM (figure 6.8, Table 6.3) which was close to be reported value of 0.6 ± 0.2 μM by Shakur *et al.*, 1993. Additionally, it was found that the enzyme was potently inhibited by the non-selective PDE inhibitor IBMX, but was insensitive to type 3 PDE inhibitor Amrinone and showed little change to type 1 PDE inhibitor Vinpocetine. The enzyme also showed very little change to low concentrations of cGMP again indicating no PDE3 activity. All studies described confirmed the authenticity of $Met^{26}RD1$ protein and showed that the protein expressed here had characteristics of typical members of the rolipram-sensitive subset of type 4 PDE activity as reported by both Shakur *et al.*, 1993 and Beavo, 1990. However lysates of BHK-21 cells transfected with pSFV-1 mRNA missing the *$Met^{26}RD1$* gene showed 100% inhibition with 100 μM Rolipram and little inhibition with100 μM Amrinone and Vinpocetine suggesting that majority of the endogenous PDE may also belong to the type 4 PDEs. This endogenous activity although found to be a PDE 4 was 2 folds below the activity detected when $Met^{26}RD1$ was expressed. Furthermore, this endogenous PDE could be separated from $Met^{26}RD1$ protein by immunoaffinity chromatography (described later

in this section) using columns prepared from polyclonal antibodies raised against the GST-Met[26]RD1 fusion protein expressed in bacteria (Chapter 4).

Table 6.6 Comparisons of pharmacological and biochemical properties of Met[26]RD1 from this work with other type 4 PDE reported by other studies.

Property	PDE $4_{(1)}$	Rat Met[26]$RD1_{(2)}$
MW SDS PAGE (kDa)		65
Native State	Monomer/ Dimer	Monomer
K_m (μM)	5.3 ± 3 (*)	7.9 ± 0.86
V_{max} (μmole/min/mg)	6-30 (‡)	0.218 ± 0.008
IC_{50} (μM) or % inhibition with 100 μM		
IBMX (non Selective)	20 ± 3 (*)	66.5%
Rolipram (PDE 4)	0.6 ± 0.2 (*)	0.7
Specific Activity (nmole/min/mg)	8-12 (**)	45.6
cGMP (2 μM)	< 4% (*)	< 30%

(1) Other published data; (2) This work; (*) Shakur *et al.*, 1993 for recombinant Met[26]RD1; and (‡) Thompson *et al.*, 1988; and Conti *et al.*, 1995 for native PDE 4; and (**) Huston *et al.* 1996 for crude PDE4A4 expressed in COS7 cells. Samples used in these different analyses were crude lysates from large scale expression preparations. Values either represent mean values or mean values with standard deviation (SD).

Purification protocols using ion exchange chromatography, have been used as first step in the purification procedure to try and provide PDE enrichment and a certain degree of purification prior to loading on antibody column (see later in this section). Q-Sepharose chromatography of small scale and large scale expression of Met[26]RD1 using SFV, produced a single peak of activity that eluted with 0.4 M NaCl (figure 6.9). The activity recovered from Q-Sepharose column was sensitive to degradation as multiple bands were found when analysing the eluted fraction on Western blots using antiserum raised against GST-Met[26]RD1 fusion protein produced in *E.coli* (Chapter 4). Furthermore, substantial loss of the eluted activity was observed when storing the fraction at 4°C overnight or -20°C. These findings were in agreement with the reported data for PDE 4 instability during purification attempts reviewed by Conti and Swinnen, 1990.

Following Q-Sepharose chromatography, fractions containing PDE activity were loaded on a GST-Met^{26}RD1 polyclonal antibody column.78 % of the bound PDE activity was eluted with high concentrations of $MgCl_2$. Some separation of the full length Met^{26}RD1 protein from its proteolytic fragments was achieved. The optimisation of this procedure could help to produce a homogenous preparation of the protein for kinetic analysis. The majority of the activity was lost during the removal of $MgCl_2$ by dialysis. The loss of activity was attributed to the loss of the protein possibly through sticking to the dialysis tubing. Complete analysis (i.e. Kinetic analysis) was not possible due to the loss of the protein therefore results of this study were used as a guide for future purification procedures performed on this protein.

Studies on the association state of the expressed Met^{26}RD1 using size exclusion chromatography (figure 6.10) were performed and have shown that Met^{26}RD1 protein exists as a monomeric protein with a molecular weight of 65 kDa. This association state was as reported by Giorgi *et al.*, 1992 for other low K_m PDEs. However, other investigators have reported PDE 4 isoenzymes existing as dimeric molecules or complex oligomeric structures (Conti and Swinnen, 1990). More extensive analysis such as ultracentrifugation would confirm the authenticity of the monomeric Met^{26}RD1 association state.

In conclusion, Met^{26}RD1 was expressed successfully in BHK-21 cells using Semliki Forest Virus in amounts which could be crystallised and analysed by X-ray crystallography. Kinetic and Western blot analyses have shown the authenticity of this recombinant protein, confirming the belonging of the protein to type 4 family of Phosphodiesterase enzymes. Additionally the ground work has been performed for a one step purification method using immunoaffinity chromatography to enable the purification of the protein to homogeneity.

Chapter 7

General Discussion

7.1 Introduction

Phosphodiesterase 4 (PDE4) which has the role of regulating the levels of cAMP in cells has been considered as a clinical target for the treatment of many biological disorders such as asthma and other inflammatory disorders. The design of potential therapeutics will be helped by the structural analysis of phosphodiesterases.

To date, there have been limited reports on expression systems capable of producing milligram quantities of full length PDE4 isoenzymes. This has been due to the protein's paucity and susceptibility to proteolysis. The production of mg quantities of the catalytic domain of human PDE4B2 and the purification to >95% homogeneity was reported by Luther and co-workers (Rocque *et al.*, 1997), notably from the large scale baculovirus expression. The three-dimensional structure of the catalytic domain is found to be highly conserved between all members of the PDE families and was solved recently to 1.77 angstrom for human PDE4B2 (Xu *et al.*, 2000). This structure revealed the presence of a cluster of two metal atoms, providing information on the mechanism of action of PDEs and the basis for specificity for cAMP and cGMP. Other cyclic nucleotide phosphodiesterases have been crystallised and analysed by X-ray crystallography. For instance, the crystal structure of the 1' ,2'- cyclic phosphodiesterase (CPDase) from *Arabidopsis thaliana*, an enzyme that is involved in the tRNA splicing pathway, was determined to 2.5 angstrom resolution (Hofmann *et al.*, 2000). This enzyme hydrolyses the ADP-ribose 1' ,2'-cyclic phosphate to 2'-phosphate which is similar to the hydrolysis of AMP-ribose 3' ,5'-cyclic phosphate to 5'-phosphate performed by cyclic nucleotide phosphodiesterases studied in this thesis. Although CPDase is reported to have different structural folding to the catalytic domain of PDE4, it is interesting to find that CPDase enzymes contain two tetrapeptide motifs of His-X-Thr/Ser-X (X generally represent hydrophobic amino acids) which are implicated in catalytic activity of the enzyme that are similar to the His-Asn-X-X-His and His-Asp-X-X-His motif found in catalytic domains of

PDE4A (Omburo *et al.*, 1998). This similarity could indicate the presence of an evolutionary link between proteins that are involved in RNA and nucleotide metabolism.

The conformational state of the catalytic domain of cyclic nucleotide phosphodiesterase enzymes has been predicted to be regulated by N terminus regions unique to the different gene families. For example, calmodulin-binding domains in PDE1; two non-catalytic cyclic-nucleotide binding domains (GAF domains) in PDE2, 5, 6, 10, and 11; and two up-stream conserved regions (UCR1 and UCR2) in PDE4. The physiological nature of this regulation has not been elucidated due to limited structural studies performed on these regions alone or complexed with the catalytic domain. However, some structural information has been recently determined which have provided vital tools to the study of PDE regulation. For instance, the crystal structure of the *Saccharomyces cerevisiae* YKG9 protein GAF domain was determined at 1.9 angstrom resolution (Ho *et al.*, 2000). This protein which was found to be a mixture of antiparallel β-sheets and α helices, shares similarities to GAF domains present in PDEs including PDE2, 5, 6, 10 and 11 as well as PAS domains (photoactive yellow protein 3PYP; Borgstahl *et al.*, 1995) present in PDE8. Thus providing a three-dimensional template for modelling the GAF domains in PDEs with the eventual elucidation of their mechanism of action. Furthermore, crystal structure of rod transducin alpha x GDP x AlF4- in complex with the effector molecule PDEgamma and the GTPase-activating protein RGS9 has been determined to 2.0 angstrom (Slep *et al.*, 2001). This structure revealed insight into effector binding to a nucleotide dependent site present on the alpha (t) sequesters PDEgamma residues implicated in PDE inhibition, and potentiates recruitment of RGS9 for hydrolytic transition state stabilisation and concomitant signal termination.

Met^{26}RD1 a rat PDE4A1, is a supershort form of PDE4 which consists of the catalytic domain as well as the truncated form of up-stream conserved region 2 (UCR2) (figure 1.5). N terminus regions have been predicted to be involved in the regulation of conformational state of PDE4 isoenzymes which is important for activity, rolipram inhibition, as well as other processes such as phosphorylation. Structural studies on this clone would provide clues to better understand the physiological nature of this regulation and its consequence on activity and rolipram inhibition. Thus, the main objective of this project was to develop an expression system capable of producing full length soluble active rat PDE4A1

(Met^{26}RD1) for the ultimate goal of crystallisation and structural evaluation by X-ray crystallography.

The main achievement of this project was the development of a Semliki Forest Virus mammalian expression system capable of producing Met^{26}RD1 protein possessing correct kinetic properties with the potential of scale up for large scale protein production. Furthermore, the use of the SFV expression system in the production of PDE4 described in this thesis represents the only report to date, that uses a mammalian cell-based expression system in the large scale production of PDEs. Though it is similar to insect expression systems. Another significant achievement was the production of a polyclonal antibody recognising Met^{26}RD1 protein specifically and with high affinity. The absence of commercial antibodies for PDE4, made antibody production necessary and very highly valuable in the analysis of Met^{26}RD1 recombinant protein described in Chapter 6.

7.2 Bacterial Expression Of Met^{26}RD1

Bacterial expression systems using *Escherichia coli* (*E. coli*) are most commonly and routinely used for the production of milligram amounts of proteins. To date there have been no reports in the use of bacterial systems in the production of mg quantities of PDE4. However, there have been numerous reports in the use of bacterial systems to express a number of PDE4 isoforms for the purpose of biochemical analysis or PDE antigen production some of which appeared to have the potential for scale-up. These reasons combined prompted the use of bacterial systems in the production of Met^{26}RD1 for structure analysis.

Met^{26}RD1 gene was expressed in JM109 (DE3) bacterial cells as a Glutathione S-transferase (GST) fusion protein. Expression studies revealed that GST-Met^{26}RD1 construct was expressed efficiently however, the majority of the expressed protein was insoluble even when expressed at ambient temperature. The soluble GST-Met^{26}RD1 expressed, showed poor activity and poor inhibition by rolipram a PDE4 specific inhibitor even following purification using a glutathione affinity column. This reduced activity and inhibition to rolipram were thought to be partly caused by the misfolding of the fusion protein and partly by the extensive proteolytic degradation of the protein. The proteolytic

fragments generated were mapped to regions in the catalytic domain important for both catalytic activity and rolipram binding and to regions 4 kDa from N-terminus of Met^{26}RD1. Cleavage at the catalytic domain was thought to be the cause of the poor activity and lack of response to rolipram.

With the absence of any commercial PDE4 antibodies, the production of antibodies recognising Met^{26}RD1 was considered to be necessary to help characterise the protein when expressed in mammalian cells (Chapter 6). GST-Met^{26}RD1 found in inclusion bodies was utilised for antibody production. The antibody produced recognised the mammalian expressed Met^{26}RD1 protein specifically and with high affinity. The high specificity of the antibody was a consequence of GST-Met^{26}RD1 antigen purification before injection into rabbits. The purification of GST-Met^{26}RD1 was considered to be necessary to remove other bacterial proteins present in the inclusion bodies that could elicit immunological responses higher than those elicited by GST-Met^{26}RD1.

To improve solubility of GST-Met^{26}RD1 expressed in bacteria, the *Met^{26}RD1* gene could be expressed by linking it to other fusion proteins, such as a maltose binding protein or a His tag at its N- or C-terminals. The binding of either of these proteins may help the folding of Met^{26}RD1 protein in bacterial cells. Another approach in improving the solubility of Met^{26}RD1 is the refolding of the protein *in vitro*. Indeed this could be possible as indicated by the recent publication by Richter *et al.*, 2000, that reported the refolding and purification of His tagged human recombinant PDE4A expressed in *E. coli.* Inclusion bodies were solubilised by guanidine hydrochloride and proteins were refolded by rapid dilution into refolding buffer.

7.3 Mammalian Expression Of Met^{26}RD1

Mammalian expression systems used in expression of PDEs have been reported (Salanova *et al.*, 1998) to be the most optimal expression systems as PDE proteins recovered have properties similar or identical to those of native proteins. However, these systems which include transient expression of PDE4 revealed low level of expression leading to the requirement of substantial purification to obtain homogenous preparation of PDE4. The average levels of expression were reported to be in the range of 0.5-5 nmole/ min/ mg of

protein which was 10-50 times higher than levels obtained from cell lines, but 10% lower than levels obtained from insect cells (Table 6.1). Consequently, mammalian expression systems have not been utilised in the large scale production of PDE4 proteins.

Chapter 6 described the use of a novel mammalian expression system for expression of $Met^{26}RD1$ based on the Semliki Forest Virus (SFV) replicon developed by Liljestrom and Garoff in the early 1990s. This system has the advantage of high levels of expression accomplished from the extremely efficient 26S promoter which gives rise to high numbers of RNA copies (up to 200 000 copies) per infected cell leading to high levels of expression (Wurm and Bernard, 1999). Indeed, this was the case as approximately 46 nmole/ min of PDE activity was obtained per milligram of $Met^{26}RD1$ protein in this project. This suggested nearly ten fold increase in expression levels compared to previously reported transient mammalian expressions of PDE4 (Table 6.1). Furthermore, these expression levels were as high as those obtained from baculovirus expression systems of PDE4A isoforms (57.4 nmole/ min /mg, Table 6.1) (Amegadzie *et al.*, 1995) making this system a strong competitor to the baculovirus expression system.

The SFV expression system initially optimised using pSFV-3 carrying the *β-galactosidase* reporter gene described in Chapter 5, produced 0.1-0.3 mg of the $Met^{26}RD1$ protein per 10^7 cells. The expressed protein exhibited correct kinetic properties consistent with previously published data. However, some proteolytic fragments were identified to be approximately 62 kDa in size. The degradation appeared to be not as severe as previously observed in bacterial expression. The cleavage sites were estimated to be present at the N- or C-terminus of the protein rather than in internal regions of the protein as these proteolytic fragments differed by 3 kDa from the 65 kDa full length $Met^{26}RD1$ protein. Although accurate molecular weights of these proteolytic fragments were not identified, it is estimated that the SFV expressed $Met^{26}RD1$ could possibly be cleaved at the N terminus of the protein similar to that observed for the $Met^{26}RD1$ expressed in bacteria as discussed earlier (Chapter 3; figure 3.1). However to confirm this theory these proteolytic fragments should be sequenced and analysed by Mass spectroscopy to reveal the sequence and molecular sizes of these fragments. The removal of these proteolytic fragments is important not only for the production of a homogenous preparation but for the production of the full length sequence of $Met^{26}RD1$ containing both the N-terminus C-terminus

regions.

The availability of an antibody recognising $Met^{26}RD1$ protein with high specificity and affinity enabled the preparation of an 'in-house' GST-$Met^{26}RD1$ antibody affinity column. A preliminary two-step purification protocol was developed and optimised with a 78% recovery of total PDE activity (Chapter 6) from antibody affinity column by elution with 3.5 M $MgCl_2$. However, there was no activity following dialysis to remove the high concentrations of salt. The lack of activity was attributed to the loss of protein sticking to the dialysis tubing. In a scaled up preparation the loss of protein is less likely to have a significant impact on the level of activity. Alternative methods to dialysis such as chromatography procedures using resins such as G-25 Sephadex resin which have the capability of separating salt molecules from larger protein molecules, could be used in future preparations to remove salt from $Met^{26}RD1$ proteins.

7.4 Future Work

In order to obtain sufficient material for crystallographic study of $Met^{26}RD1$, I would now perform the following:

- Isolation of the proteolytic fragments produced during expression of $Met^{26}RD1$ in SFV expression system by 2D gel electrophoresis and sequencing of the extracted fragments followed by analysis by Mass Spectroscopy to identify their molecular weights. These studies should reveal sites at which $Met^{26}RD1$ was cleaved by the proteolytic enzymes present in SFV expression preparations.

- Once the sequence and locations of the proteolytic cleavage site were identified, mutations of these sites may prevent degradation by proteolytic enzymes in future expression studies.

- Analysis of such mutants for activity and inhibition to rolipram to make sure that mutation did not alter the catalytic activity and sensitivity to rolipram.

- Scale up of $Met^{26}RD1$ expression using optimised SFV parameters described in the

project to produce milligram quantities of the protein. The recent publication by Blasey *et al.*, 2000 on the scale up of 5-HT3 receptor expressed in BHK-21 cells by SFV system suggests that > 10 L volume bioreactor may be suitable for large scale $Met^{26}RD1$ protein production.

- Optimisation of purification strategy using preliminary purification data described in Chapter 6 to produce an homogenous preparation for crystallisation experiments.

Appendix 1

RD1 Protein Sequence Published by Davis *et al.*, 1989; Smith *et al.*, 1996. (*) represents the start codon for Met[26]RD1. Underlined sequences represent location of helices. Bold underlined sequence represents the location of the hairpin. H= helix.

```
                                *
MPLVDFFCET  CSKPWLVGWW  DQFKRMLNRE  LTHLSEMSRS  GNQVSEYISN 50

TFLDKQNEVE  IPSPTPRQRA  FQQPPPSVLR  QSQPMSQITG  LKKLVHTGSL 100

NTNVPRFGVK  TDQEDLLAQE  LENLSKWGLN  IFCVSEYAGG  RSLSCIMYTI 150
   H0          H1          H2          H3

FQERDLLKKF  HIPVDTMMMY  MLTLEDHYHA  DVAYHNSLHA  ADVLQSTHVL 200
     H4          H5                              H6

LATPALDAVF  TDLEILAALF  AAAIHDVDHP  GVSNQFLINT  NSELALMYND 250
                H7                      H8          H9

ESVLENHHLA  VGFKLLQEEN  CDIFQNLSKR  QRQSLRKMVI  DMVLATDMSK 300
       H10                                 H11

HMTLLADLKT  MVETKKVTSS  GVLLLDNYSD  RIQVLRNMVH  CADLSNPTKP 350
     H12         Hairpin             H13

LELYRQWTDR  IMAEFFQQGD  RERERGMEIS  PMCDKHTASV  EKSQVGFIDY 400
            H14                                 H15a

IVHPLWETWA  DLVHPDAQDI  LDTLEDNRDW  YHSAIRQSPS  PPLEEEPGGL 450
       H15b                H16

GHPSLPDKFQ  FELTLEEEEE  EDSLEVPGLP  TTEETFLAAE  DARAQAVDWS 500
   H17

KVKGPSTTVV  EVAERLKQET  ASAYGAPQES  MEAVGCSFSP  GTPILPDVRT 550

LSSSEEAPGL  LGLPSTAAEV  EAPRDHLAAT  RACSACSGTS  GDNSAIISTP 600

GRWGSGGDPA 610
```

Appendix 2

RD1 (rat dunce 1) DNA sequence as published by Davis *et al.*, 1989 (EMBL/GenBank database, Accession number J04554). The start of $Met^{26}RD1$ is indicated by the symbol (*). Sequences shown in bold represent primer annealing positions and sequences shown underlined represent sequences in pGEX-3X-$Met^{26}RD1$ and pSFV-1$Met^{26}RD1$ constructs described in Chapters 3 and 6 respectively that have been sequenced using ABI sequencer in which the methodology is described in Chapter 2.

gggactcggc caaacctacc ttacctgtgc gccagcccag agctaagctt ccatcatgcc

tctggttgac ttcttctgcg agacctgctc caagccctgg ctggtgggct ggtgggacca

* RD1f Primer ⟶

gttcaaaagg **atgctgaacc gtgagctcac** acacctgtcg gaaatgagca ggtcaggaaa

ccaggtctca gagtacattt ccaacacatt cctggacaag cagaatgaag tggagatccc

ctcacccaca cctcggcaga gagccttcca gcagcccccg ccgtcagtgc tgcgacagtc

ccagcccatg tctcagatca cagggctgaa aaagctggta cacactggaa gcttgaacac

⟵ S1B Primer

caacgtccca cggtttgga**g tcaagacaga tcaagaggac** ctcttagcac aagaactgga

gaacttgagc aaatggggcc tgaacatctt ttgtgtgtcg gagtacgctg gaggccgctc

actcagctgt atcatgtata cgatattcca ggagcgggac ctactgaaga aattccacat

ccctgtggac accatgatga tgtacatgct gaccctggag gaccactacc atgccgacgt

ggcctaccac aacagcctgc acgcagcgga tgtgctgcag tccacacacg tgctgctggc

cacgcccgca ctggacgctg tgttcacaga cctggagatt cttgctgccc tcttcgctgc

tgccatccac gatgtggacc accctggcgt ctccaaccag ttcctaatca acaccaattc

ggagctggcg ttgatgtaca acgatgagtc tgtgcttgag aaccaccacc tggctgtggg

attcaagctg ctgcaagaag agaactgcga catcttccag aacctcagca agcgccagcg

gcagagcctg cgcaagatgg tcatcgacat ggtgctggcc acagacatgt ccaaacacat

gaccctcctg gctgacctga agactatggt ggagacgaag aaagtgacca gctccggagt

tctcttgctg gacaactact ctgaccgtat ccaggtcctc aggaacatgg tgcactgtgc

agacctcagc aatcccacca agcccctgga gctgtaccga cagtggaccg accgcatcat

ggctgagttc ttccagcagg gcgaccgaga acgggagcgt ggaatggaga tcagccccat

gtgcgacaag cacacagcct ctgtggagaa gtctcaggtg ggcttcatcg actacattgt

tcatccattg tgggagacat gggcagatct cgtccacccg gatgcccaag acatcctgga

cacgctggaa gacaaccggg actggtacca cagtgccatt cggcagagtc cttccccacc

cctggaagag gagccagggg ggcttggcca tccgtccctg cctgacaagt tccaatttga

gctcaccttg gaggaagagg aggaagagga ttccttggag gttccaggat tgcctaccac

tgaggaaacc ttcctggctg cagaggatgc cagagctcaa gctgtggact ggtcaaaggt

S1F Primer ⟶

caaaggcccg agcact**acag tggtggaagt ggcagag**cgc ttgaagcagg agaccgcctc

agcatatggt gctcctcagg agtccatgga ggctgtaggc tgttccttca gccctgggac

ccctattctg cctgacgtga ggaccctatc ctcctcagag gaggccccag gcctcctggg

cctcccctcc acggcggcag aggtggaggc cccaagagac catctggctg ccacgagggc

ttgttctgcc tgctctggga cctcaggaga caattctgcc atcatctcta ctccaggcag

⟵ RD1b Primer

gtgggggtca **ggcggagacc ctgcctgatc** cttttttccct tcacccttgg gtcctccctc

ctccccacac ttcccactca ccacagaccg cctcagcgac tcctggccct cctgagaaaa

aagaaaacag aaaagtgggg ttttttttctc ttttcttttt tttaaccctt tcccctctgc

ccttgtccac agggcctttt tgttgaggtg gggtatgggg agccaggaac tgaagtcccc

aaaaaaaggg attttatttt ttgaatttta attgtaaagt ttttagaaaa agaacaaaaa

gaaaaaaaaa aaaagaatga aacacatcag ctgtagatgc tc

References

Ahmad, F., Cong, L.N., Holst, L.S., Wang, L.M., Landstrom, T.R., Pierce, J.H., Quon, M.J., Degerman, E., and Manganiello, V.C. (2000).Cyclic nucleotide phosphodiesterase 3B is a downstream target of protein kinase B and may be involved in regulation of effects of protein kinase B on thymidine incorporation in FDCP2 cells. *J. Immunol.* **164**, 4678-4688.

Ahn, H.S., Crim, W., Pitts, B., and Sybertz, E. (1992). Calcium-calmodulin-stimulated and cyclic GMP-specific phosphodiesterases. *Adv. Second Messenger Phosphoprotein Res.* **25**, 271-286.

Allet, B., Hochman, A., Martinou, I., Berger, A., Missotten, M., Antonsson, B., Sadoul, R., Martinou, J. C., and Bernasconi, L. (1996). Dissecting processing and apoptoctic activity of a cystein protease by mutant analysis. *J. Cell Biol.* **135**, 479-486.

Alousi, A.A., Farah, A.E., Lesher, G.Y., and Opalka, C.J. (1979). Cardiotonic activity of amrinone-Win 40680 [5-amino-3,4'-bipyridin-6(1H)-one]. *Circulation Res.* **45**, 666-677.

Alousi, A.A., Canter, J.M., Montenaro, M.J., Fort, D.J., and Ferrari, R.A. (1983). Cardiotonic activity of milrinone, a new and potent cardiac bipyridine, on the normal and failing heart of experimental animals. *J. Cardiovasc. Pharmacol.* **5**, 792-803.

Alvarez, R., Sette, C., Yang, D., Eglen, R.M., Wilhelm, R., Shelton, E.R., and Conti, M. (1995). Activation and selective inhibition of a cyclic AMP-specific phosphodiesterase, PDE-4D3. *Mol. Pharmacol.* **48**, 616-622.

Amegadzie, B.Y., Hanning, C.R., McLaughlin, M.M., Burman, M., Cieslinski, L.B., Livi, G.P., and Trophy, T.J. (1995). Characterization of two human cAMP-specific phosphodiesterase subtypes expressed in baculovirus infected insect cells. *Cell Biol. Int.* **19**, 477-484.

Aravind, L., and Ponting, C.P. (1997). The GAF domain: an evolutionary link between diverse phototransducing proteins. *Trends Biochem. Sci.* **22**, 458-459.

Baecker, P.A., Obernolt, R., Bach, C., Yee, C., and Shelton, E.R. (1994). Isolation of a cDNA encoding a human rolipram-sensitive cyclic AMP phosphodiesterase (PDE IVD). *Gene* **138**, 253-256.

Baillie, G.S., MacKenzie, S.J., McPhee, I., and Houslay, M.D. (2000). Sub-family selective actions in the ability of Erk2 MAP kinase to phosphorylate and regulate the activity of PDE4 cyclic AMP-specific phosphodiesterases. *Br. J. Pharmacol.* **131**, 811-819.

Barber, R., and Butcher, R.W. (1980). The turnover of cyclic AMP in cultured fibroblasts. *J. Cyclic Nucleotide Res.* **6**, 3-14.

Barber, R., and Butcher, R.W. (1981). The quantitative relationship between intracellular concentrations and egress of cyclic AMP from cultured cells. *Mol. Pharmacol.* **19**, 38-43.

Barnes, P.J. (1995). Cyclic nucleotides and phosphodiesterases and airway function. *Eur. Respir. J.* **8**, 457-462.

Beard, M.B., Olsen, A.E., Jones, R.E., Erdogan, S., Houslay, M.D., and Bolger, G.B. (2000). UCR1 and UCR2 domains unique to the cAMP-specific phosphodiesterase family form a discrete module via electrostatic interactions. *J. Biol. Chem.* **275**, 10349-10358.

Beavo, J.A. (1988). Multiple isoenzymes of cyclic nucleotide phosphodiesterase. *Adv. In Second Messenger & Phosphodiesterase Research* **22**, 1-38.

Beavo, J.A. (1990) in Molecular Pharmacology of Cell Regulation (Beavo, J.A. and Houslay, M.D. eds), *vol.* 2, 3-15, John Wiley and Sons Ltd., Chichester and New York.

Beavo, J.A., and Reifsnyder, D.H. (1990). Primary sequence of cyclic nucleotide phosphodiesterase isoenzymes and the design of selective inhibitors. *Trends Pharmacol. Sci.* **11**, 150-155.

Beavo, J.A., Conti, A., and Heaslip, R.J. (1994). Multiple cyclic nucleotide phosphodiesterases. *Mol. Pharmacol.* **46**, 399-405.

Beavo, J.A., (1995). Cyclic nucleotide phosphodiesterases: functional implications of multiple isoforms. *Physiol. Rev.* **75**, 725-748.

Beebe, S.J., Redmon, J.B., Blackmore, P.F., and Corbin, J.D. (1985). Discriminative insulin antagonism of stimulatory effects of various cAMP analogs on adipocyte lipolysis and hepatocyte glycogenolysis. *J. Biol. Chem.* **260**, 15781-15788.

Beebe, S.J., and Corbin, J.D. (1986). Cyclic nucleotide-dependent protein kinases. *The Enzymes* (Anonymous, ed) pp. 43-111., Academic Press, New York.

Beese, L.S., and Steitz, T.A. (1991).Structural basis for the 3'-5' exonuclease activity of *Escherichia coli* DNA polymerase I: a two metal ion mechanism. *EMBO J.* **10**, 25-35.

Beltman, J., Sonnenburg, W.K., and Beavo, J.A. (1993). The role of protein phosphorylation in the regulation of cyclic nucleotide phosphodiesterases. *Mol. Cellular Biochem.* **127/128**, 239-253.

Bentley, J.K., and Beavo, J.A. (1992). Regulation and function of cyclic nucleotides. *Curr. Opn. Cell Biol.* **4**, 233-240.

Bentley, J.K., Kadlecek, A., Sherbert, C.H., Sonnenburg, W.K., Charbonneau, H., Novack, J.P., and Beavo, J.A. (1992). Molecular cloning of cDNA encoding a '63-kDa' calmodulin-stimulated phosphodiesterase from bovine brain. *J. Biol. Chem.* **267**, 18676-18682.

Berglund, P., Sjoberg, M., Garoff, H., Atkins, G.J., Sheahan,, B.J., and Liljestrom, P. (1993). Semliki Forest Virus expression system: Production of conditionally infectious recombinant particles. *Bio/Technology* **11**, 916-920.

Bernard, A.R., and Blasy, H.D. (1999). Transient expression systems. In Flickinger, M.C. and Drews, S.W. (eds.). The Encyclopedia of Bioprocess Technology: Fermentation, Biocatalysis and Bioseparation. (pp. 2580-2597) John Wiley and Sons.

Bikker, H., Baas, F., and Vijlder, J-J.M. (1997). Molecular analysis of mutated thyroid peroxidase detected in patients with total iodide organification defect. *J. Clin. Endocrinol. Metab.* **82**, 649-653.

Blasey, H.D., Aubry, J.P., Mazzei, G.J., and Bernard, A.R. (1996). Large scale transient expression with COS cells. *Cytotechnology* **18**, 183-192.

Blasey, H.D., Lundstrom, K., Tale, S., and Bernard, A.R. (1997). Recombinant protein production using Semliki Forest virus system. *Cytotechnology* **24**, 65-72.

Blasey, H.D., Brethon, B., Hovius, R., Vogel H, H., Tairi, A.P., Lundstrom, K., Rey, L., and Bernard, A.R. (2000). Large scale transient 5-HT_3 receptor production with the Semliki Forest Virus Expression System. *Cytotechnology* **32**, 199-208.

Bolger, G., Michacli, T., Martins, T., St John, T., Steiner, B., Rodgers, L., Riggs, M., Wichael, M., and Ferguson, K. (1993). A family of human phosphodiesterase homologous to the dunce learning and memory gene product of *Drosophila melanogaster* are potential targets for antidepressant drugs. *Mol. Cell Biol.* **13,** 6558-6571.

Bolger, G.B. (1994). Molecular biology of cyclic AMP specific nucleotide phosphodiesterase: A diverse family of regulatory enzymes. *Cellular Signaling* **8**, 851-859.

Bolger, G.B., Rodgers, L., and Riggs, M. (1994). Differential CNS expression of alternative mRNA isoforms of the mammalian genes encoding cAMP-specific phosphodiesterases. *Gene* **149**, 237-244.

Boolell, M., Allet, M.J., Ballard, S.A., Gepi-Attee, S., Muirhead, G.J., Naylor, A.M., Osterloh, I.H., and Gingell, C. (1996). Sildenafil: an orally active type 5 cyclic GMP-specific phosphodiesterase inhibitor for the treatment of penile erectile dysfunction. *Int. J. Impot. Res.* **8**, 47-52.

Borgstahl, G.E.O., Williams, D.R., and Getzoff, E.D. (1995). 1.4 Å structure of photoactive yellow protein, a cytosolic photoreceptor: unusual fold, active site and chromophore. *Biochem.* **34**, 6278-6287.

Bradford, M.M. (1976). A rapid and sensitive method for the quantitation of microgram quantities of protein utilizing the principle of protein-dye binding. *Anal. Biochem.* **72**, 248-254.

Burnette, W.N. (1981). Western blotting: electrophoresis transfer of proteins from sodium dodecyl sulphate-polyacrylamide gels to unmodified nitrocellulose and radiographic detection with antibody and radio iodinated protein A. *Anal. Biochem.* **112**, 195-203.

Butcher, R.W., and Sutherland, E.W. (1962). Adenosine 3', 5'-phosphate in biological material. *J. Biol. Chem.* **237**, 1244-1250.

Charbonneau, H., Beier, N., Walsh, K.A., and Beavo, J.A. (1986). Identification of a conserved domain among cyclic nucleotide phosphodiesterases from diverse species. *Proc. Natl. Acad. Sci. USA* **83**, 9308-9317.

Charbonneau, H., Kumar, S., Novack, J.P., Blumenthal, D.K., Griffin, P.R., Shabanowitz, J., Hunt, D.F., Beavo, J.A., and Walsh, K.A. (1991). Evidence for domain organisation within the 61-kDa calmodulin dependent cyclic nucleotide phosphodiesterase from bovine brain. *Biochem.* **30**, 7940-7947.

Ciccarone, V. Jessee, J., Berglund, P., and Liljestrom, P. (1993). PSFV Eukaryotic expression vector: A novel protein expression system. *Focus* **15**, 103-105.

Cik, M., Chazot, P. L., and Stephenson, F. A. (1993). Optimal expression of cloned NMDAR1/NMDAR2A heteromeric glutamate receptors: a biochemical characterization. *Biochem. J.* **296**, 877-883.

Cohen, P.T., Brewis, N.D., Hughes, V., and Mann, D.J. (1990). Protein serine/threonine phosphatases; an expanding family. *FEBS lett.* **268**, 355-359.

Colicelli, J., Birchmeier, C., Michaelli, T., O'Neill, K., Riggs, M., and Wigler, M. (1989). Isolation and characterization of a mammalian gene encoding a high-affinity cAMP phosphodiesterase. *Proc. Natl. Acad. Sci. USA* **86**, 3599-3603.

Conti, M., Jin, S.L.C., Monaco, I., Repaske, D.R., and Swinnen, J.V. (1991). Hormonal regulation of cyclic nucleotide phosphodiesterases. *Endocrine Rev.* **12**, 218-234.

Conti, M., Iona, S., Cuomo, M., Swinnen, J.V., Odeh, J., and Svoboda, M.E. (1995). Characterization of a hormone-inducible, high affinity adenosine 3'-5'-cyclic monophosphate phosphodiesterase from the rat Sertoli cell. *Biochemistry* **34**, 7979-7987.

Conti, M., and Jin, L.C. (1999). The molecular biology of cyclic nucleotide phosphodiesterases. *Prog. Nucleic Acid Res.* **63**, 1-38.

Corbin, J.D., and Francis, S.H. (1999). Cyclic GMP phosphodiesterase-5: target of sildenafil. *J. Biol. Chem.* **274**, 13729-13732.

Couffinhal, T., Kearney, M., Sullivan, A., Silver, M., Tsurumi, Y., and Isner, J.M. (1997). Histochemical staining following *LacZ* gene transfer underestimates transfection efficiency. *Hum. Gene Ther.* **8**, 929-934.

Cull, M., and McHenry C.S. (1990). Preparation of extracts from prokaryotes. *Methods Enzymol.* **182**, 147-153.

D'Amours, M.R., and Cote, R.H. (1999). Regulation of photoreceptor phosphodiesterase catalysis by its non-catalytic cGMP-binding sites. *Biochem. J.* **340**, 863-869.

Davis, C.W. (1984). Assessment of selective inhibition of rat cerebral cortical calcium independent and calcium dependent phosphodiesterase in crude extracts using deoxycyclic AMP and potassium ions. *Biochem. Biophys. Acta.* **797**, 354-362.

Davis, R.L., and Kauvar, L.M. (1984). *Drosophila* cyclic nucleotide phosphodiesterases. *Adv. Cyclic Nucleotide Protein Phosphorylation Res.* **16**, 393-402.

Davis, R.L., Takayasu, H., Eberwine, M., and Myres, J. (1989). Cloning and characterization of mammalian homologs of the *Drosophila dunce+* gene. *Proc. Natl. Sci. USA* **86**, 3604-3608.

Davis, R.L. (1990). Molecular genetics of the cyclic nucleotide phosphodiesterases. Cyclic Nucleotide Phosphodiesterases: Structure, regulation and drug action (Beavo, J.A. and Houslay, M.D., *eds*) pp. 227-242.

Degerman, E., Belfrage, P., and Manganiello, V.C. (1997). Structure, localization, and regulation of cGMP-inhibited phosphodiesterase (PDE3). *J. Biol. Chem.* **272**, 6823-6826.

De Mazancourt, P., and Giudicelli, Y. (1988). Brain low K_m cAMP phosphodiesterase. *Methods Enzymol.* **159**, 766-772.

DiCiommo, D.P., and Bremner, R. (1998). Rapid, high level protein production using DNA-based Semliki Forest Virus Vectors. *J. Biol. Chem.* **273**, 18060-18066.

Dousa, T.P. (1998). Signalling role of PDE isozymes in pathobiology of glomerular mesangial cells. Studies *in vitro* and *in vivo*. *Cell Biochem. Biophys.* **29**, 19-34.

Dousa, T.P. (1999). Cyclic-3',5'-nucleotide phosphodiesterase isozymes in cell biology and pathophysiology of the kidney. *Kidney Int.* **55**, 29-62.

Drewett, J.G., and Garbers, D.L. (1994). The family of guanylyl cyclase receptors and their ligands. *Endocrine Rev.* **15(2)**, 135-162.

Dwarki, V.J., Montminy, M., and Verma, I.M. (1990). Both the basic region and the 'leucine zipper' domain of the cyclic AMP response element binding (CREB) protein are essential for transcriptional activation. *EMBO J.* **9**, 225-232.

Engels, P., Sullivan, M., Muller, T., and Lubbert, H. (1995). Molecular cloning and functional expression in yeast of a human cAMP-specific phosphodiesterase subtype (PDE IV-C). *FEBS Lett.* **358**, 305-310.

Fawcett, L., Baxendal, R., Stacey, P., McGrouther, C., Harrow, I., Soderling, S., Hetman, J., Beavo, J.A., and Phillips, S.C. (2000). Molecular cloning and characterization of a distinct human phosphodiesterase gene family: PDE11A. *Proc. Natl. Acad. Sci. USA* **97**, 3702-3707.

Fougier, S., Nemoz, G., Prigent, A. F., Marivent, M., Bourguignon, C., Wermuth, C., and Pacheco, H. (1986). Purification of cyclic AMP-specific phosphodiesterase from rat heart by affinity chromatography on immobilised rolipram. *Biochem. Biophys Res. Commun.* **138**, 205-214.

Francis, S.H., Colbran, J.L., McAllister-Lucas, L.M., and Corbin, J.D. (1994). Zinc interactions and conserved motifs of the cGMP-binding cGMP-specific phosphodiesterase suggest that it is a zinc hydrolase. *J. Biol. Chem.* **269**, 22477-22480.

Freund, J., and McDermott, K. (1942). Sensitization to horse serum by means of adjuvants. *Proc. Soc. Exp. Biol. Med.* **49**, 548-553.

Freund, J. (1956). The mode of action of immunologic adjuvants. *Adv. Tuberc. Res.* **71**, 130-148.

Fujishige, K., Kotera, J., Michibata, H., Yuasa, K., Takebayashi, S., Okumura, K., and Omori, K. (1999). Cloning and Characterization of a Novel Human Phosphodiesterase That Hydrolyzes Both cAMP and cGMP (PDE10A). *J. Biol. Chem.* **274**, 18438-18445.

Fujishige, K., Kotera, J., Yuasa, K., and Omori, K. (2000). The human phosphodiesterase PDE10A gene genomic organization and evolutionary relatedness with other PDEs containing GAF domains. *Eur. J. Biochem.* **267**, 5943-5951.

Garbers, D.L., and Lowe, D.G. (1994). Guanylyl cyclase receptors. *J. Biol. Chem.* **269**, 30741-30744.

Geoffroy, V, Fouque, F., Nivet, V., Clot, J.P., Lugnier, C., Desbuquois, B., and Benelli, C. (1999). Activation of a cGMP-stimulated cAMP phosphodiesterase by protein kinase C in a liver Golgi-endosomal fraction. *Eur. J. Biochem.* **259**, 892-900.

Gettys, T.W., Blackmore, P.F., Redmon, J.B., Beebe, S.J., and Corbin, J.D. (1987). Short term regulation of cAMP by accelerated degradation in rat tissue. *J. Biol. Chem.* **262**, 333-339.

Gilman, A.G. (1984). G-proteins and dual control of adenylate cyclase. *Cell* **36**, 577-579.

Giorgi, M., Piscitelli, D., Rossi, P., and Geremia, R. (1992). Purification and characterization of a low K_m 3' :5' cyclic adenosine phosphodiesterase from post-meiotic male mouse germ cells. *Bio-chim Biophys. Acta* **1121**, 178-182.

Goldfarb, A.R., Saidel, L.J., and Mosovich, E. (1951). The ultraviolet absorption spectra of proteins. *J. Biol. Chem.* **193**, 397-404.

Gorrie, G.H., Vallis, Y., Stephenson, A., Whitfield, J., Browning, B., Smart, T.G., and Moss, S.J. (1997). Assembly of GABAA receptors composed of alpha1 and beta2 subunits in both cultured neurons and fibroblasts. *J. Neurosci.* **17**, 6587-6596.

Graham, F.L., and Van der Em, A.J. (1973). A new technique for the assay of infectability of human adenovirus 5 DNA. *Virology* **52**, 456-467.

Granovsky, A.E., Natochin, M., McEntaffer, R.L., Haik, T.L., Francis, S.H., Corbin, J.D., and Artemyev, N.O. (1998). Probing domain functions of chimeric PDE6alpha'/PDE5 cGMP-phosphodiesterase. *J. Biol. Chem.* **273**, 24485-24490.

Griswood, R.W., Eden, R.J., Owen, D.A., and Taylor, E.M.(1986). Pharmacological studies with SK&F 94120, a novel positive inotropic agent with vasodilator activity. *J. Pharmacol.* **38**, 452-459.

Hagiwara, M., Endo, T., and Hidaka, H. (1984). Effects of vinpocetine on cyclic nucleotide metabolism in vascular smooth muscle. *Biochem. Pharmacol.* **33**, 453-457.

Harlow, E., and Lane, D. (1988) in Antibody: A laboratory manual (Harlow, E., and Lane, D., eds) Cold Spring Harbor laboratory.

Harrison, S.A., Reifsnyder, D.H., Gallis, B., Cadd, G.G., and Beavo, J.A. (1986). Isolation and characterization of bovine cardiac muscle cGMP-inhibited phosphodiesterase: A receptor for new cardiotonic drugs. *Mol. Pharmacol.* **29**, 506-514.

Hashimoto, Y., Sharma, R.K., and Soderling, T.S. (1989). Regulation of Ca^{2+}/ calmodulin-dependent cyclic nucleotide phosphodiesterase by the autophosphorylated form of Ca^{2+}/ calmodulin-dependent protein kinase II. *J. Biol. Chem.* **264**, 10884-10887.

Helenius, A., Kartenbeck, J., Simons, K., and Fries, E. (1980). On the entry of Semliki forest virus into BHK-21 cells. *J. Cell Biol.* **84**, 404-420.

Henkel-Tigges, J., and Davis, R.L. (1990). Rat homologs of the *Drosophila dunce* gene code for cAMP phosphodiesterase sensitive to rolipram and Ro 20-1724. *Mol. Pharmacol.* **37**, 7-10.

Ho, Y.J., Burden, L.M., and Hurley, J.H. (2000). Structure of the GAF domain, a ubiquitous signaling motif and a new class of cyclic GMP receptor. *EMBO J.* **19**, 5288-5299.

Hoffmann, R., Wilkinson, I.R., McCallum, J.F., Engels, P., and Houslay, M.D. (1998). cAMP-specific phosphodiesterase HSPDE4D3 mutants which mimic activation and changes in rolipram inhibition triggered by protein kinase A phosphorylation of Ser-54: generation of a molecular model. *Biochem. J.* **333**, 139-149.

Hofmann, A., Zdanov, A., Genschik, P., Ruvinov, S., Filipowicz, W., and Wlodawer, A. (2000). Structure and mechanism of activity of the cyclic phosphodiesterase of APP>p, a product of the tRNA splicing reaction. *EMBO J.* **19**, 6207-6217.

Horton, Y.M., Sullivan, M., and Houslay, M.D. (1995). Molecular cloning of a novel splice variant of human type IVA (PDE-IVA) cyclic AMP phosphodiesterase and localization of the gene to the p13.2-q12 region of human chromosome 19. *Biochem. J.* **308**, 683-691.

Houslay, M.D. (1998). Adaptation in cyclic AMP signalling processes: a central role for cyclic AMP phosphodiesterases. *Seminars Cell & Dev. Biol.* **9**, 161-167.

Houslay, M.D., Sullivan, M., and Bolger, G.B. (1998). The multienzyme PDE4 cyclic adenosine monophosphate-specific phosphodiesterase family: intracellular targeting, regulation, and selective inhibition by compounds exerting anti-inflammatory and antidepressant actions. *Adv. Pharmacol.* **44**, 225-342.

Houslay, M.D. (2001). PDE4 cAMP-Specific Phosphodiesterases. *Prog. Nucleic Acid Res. Mol. Biol.* **69**, 249-315.

Hurwitz, R.L., Hansen, R.S., Harrison, S.A., Martins, T.J., Mumby, M.C., and Beavo, J.A. (1984). Immunologic approaches to the study of cyclic nucleotide phosphodiesterases. *Adv. Cyclic nucleotide and protein phosphorylation Research* **16**, 89-105.

Hurwitz, R.L., Bunt-Milam, A.H., Chang, M.L., and Beavo, J.A. (1985). cGMP phosphodiesterases in rod and cone outer segments of the retina. *J. Biol. Chem.* **260**, 568-573.

Huston, E., Pooley, L., Julien, P., Scotland, G., McPee, I., Sullivan, M., Bolgar, G., and Houslay, M. (1996). The human cyclic AMP-specific phosphodiesterase PDE-46 (HSPDE4A4B) expressed in transfected COS7 cells occurs as both particulate and cytosolic species that exhibit distinct kinetics of inhibition by the antidepressant rolipram. *J. Biol. Chem.* **271**, 31334-31344.

Ikonen, E., Parton, R.G., Hunziker, W., Simons, K., and Dotti, C.G. (1993). Transcytosis of the polymeric immunoglobuline receptor in cultured hippocampal neurons. *Curr. Biol.* **3**, 635-643.

Jacobitz, S., McLaughlin, M.M., Livi, G.P., Burman, M., and Torphy, T.J. (1996). Mapping the functional domains of human recombinant phosphodiesterase 4A: structural requirements for catalytic activity and rolipram binding. *Mol. Pharmacol.* **50**, 891-899.

Jacobitz, S., Ryan, M.D., McLaughlin, M.M., Livi, G.P., DeWolf, W.E., and Torphy, T.J. (1997). Role of conserved histidines in catalytic activity and inhibitor binding of human recombinant phosphodiesterase 4A. *Mol. Pharmacol.* **51**, 999-1006.

Jin, S.L., Swinnen, J.V., and Conti, M. (1992). Characterization of the structure of a low K_m, rolipram-sensitive cAMP phosphodiesterase. Mapping of the catalytic domain. *J. Biol. Chem.* **267**, 18929-18939.

Juilfs, D., Fulle, H.J., Zhao, A.Z., Houslay, M.D., Garbers, D., and Beavo, J.A. (1997). A subset of olfactory neurons that selectively express cGMP-stimulated phosphodiesterase (PDE2) and guanylyl cyclase-D define a unique olfactory signal transduction pathway. *Proc. Natl. Acad. Sci. U.S.A.* **94**, 3388-3395.

Kakkar, R., Raju, R.V., and Sharma, R.K. (1999). Calmodulin-dependent cyclic nucleotide phosphodiesterase (PDE1). *Cell Mol. Life Sci.* **55 (8-9)**, 1164-1186.

Kane, J.F., and Hartly, D.L. (1989). Formation of recombinant proteins inclusions in *Escherichia coli*. *Tibtech.* **6**, 95-101.

Kenan, Y., Murata, T., Shakur, Y., Degerman, E., and Manganiello, V.C. (2000). Functions of the N-terminal region of cyclic nucleotide phosphodiesterase 3 (PDE 3) isoforms. *J. Biol. Chem.* **275**, 12331-12338.

Kielian, M. (1995). Membrane fusion and the alphavirus life cycle. *Adv. Virus Res.* **46**, 113-151.

Kincaid, R.L., Stith-Coleman, I.E., and Vaughan, M. (1985). Proteolytic activation of calmodulin-dependent cyclic nucleotide phosphodiesterase. *J. Biol. Chem.* **260**, 9009-9015.

Koesling, D., and Friebe, A. (1999). Soluble guanylyl cyclase: structure and regulation. *Rev. Physiol. Biochem. Pharmacol.* **135**, 41-65.

Kohler, G., and Milstein, C. (1975). Continuous cultures of fused cells secreting antibody of predefined specificity. *Nature* **256**, 495.

Komas, N., Movsesian, M., Kedev, S., Degerman, E., Belfrage, P., and Manganiello, V.C. (1996). In Handbook of Pharmacology: Phosphodiesterase Inhibitors (Schudt, C., Dent, G., and Rabe, K.F., eds) pp. 89-109, Academic Press, London.

Kotera, J., Yanaka, N., Fujishige, K., Imai, Y., Akatsuka, H., Ishizuka, T., Kawashima, K., and Omori, K. (1997). *Eur. J. Biochem.* **249**, 434-442.

Kotera, J., Fujishige, K., Akatsuka, H., Imai, Y., Yanaka, N., and Omori, K. (1998). Novel alternative splice variants of cGMP-binding cGMP-specific phosphodiesterase. *J. Biol. Chem.* **273**, 26982-26990.

Kotera, J., Fujishige, K.,Imai, Y., Kawai, E., Michilbata, H., Akatsuka, H., Yanaka, N., and Omori, K. (1999a). Genomic origin and transcriptional regulation of two variants of cGMP-binding cGMP-specific phosphodiesterases. *Eur. J. Biochem.* **262**, 866-873.

Kotera, J., Fujishige, K., Yuasa, K., and Omori, K (1999b). Characterization and Phosphorylation of PDE10A2, a Novel Alternative Splice Variant Of Human Phosphodiesterase That Hydrolyzes cAMP and cGMP. *Biochem. Biophys. Res. Comm.* **261**, 551-557.

Kovala. T., Sanwal, B.D., and Ball, E.H. (1997). Recombinant expression of a type IV, cAMP-specific phosphodiesterase: Characterization and structure-function studies of deletion mutants. *Biochem.* **36**, 2968-2976.

Kozak, M. (1992). Regulation of translation in eukaryotic systems. *Ann. Rev. Cell Biol.* **8**, 197-225.

Kraulis, P.J. (1991). MOLSCRIPT: A program to produce both detailed and schematic plots of protein structures. *J. of Applied Crystallography* **24**, 946-950.

Krupinski, J. (1991). The adenylyl cyclase family. *Mol. Cell. Biochem.* **104**, 73-79.

Laemmli, U.K. (1970). Cleavage of structural proteins during the assembly of the head of bacteriophage T4. *Nature* **227,** 680-685.

Lagnado, L., and Baylor, D. (1992). Signal flow in visual transduction. *Neuron* **8**, 995-1002.

Laliberte, F., Han, Y., Govindarajan, A., Giroux, A., Liu, S., Bobechko, B., Lario, P., Bartlett, A., Gorseth, E., Gresser, M., and Huang, Z. (2000). Conformational difference between PDE4 apoenzyme and holoenzyme. *Biochemistry* **39**, 6449-6458.

Lario, P.I., Bobechko, B., Bateman, K., Kelly, J., Verielink, A., and Huang, Z. (2001). Purification and characterization of the human PDE4A catalytic domain (PDE4A330-723) expressed in Sf9 cells. *Arch. Biochem. Biophys.* **394**, 54-60.

Latorre, R., Bacigalupo, J., Delgado, R., and Labarca, P. (1991). Four cases of direct ion channel gating by cyclic nucleotides. *J. Bioenerg. Biomemb.* **23**, 577-597.

LaVallie, E.R., DiBlasio, E.A., Kovacic, S., Grant, K.L., Schendel, P.F., and McCoy, J.M. (1993). A thioredoxin gene fusion expression system that circumvents inclusion body formation in *E.coli* cytoplasm. *BioTechnology* **11**, 187-193.

Li, L., Yee, C., and Beavo, J.A. (1999). CD3- and CD28-dependent induction of PDE7 required for T cell activation. *Science* **283**, 848-851.

Liljestrom, P., and Garoff, H. (1991). A new generation of animal cell expression vectors based on the Semliki Forest Virus replicon. *Bio/Technology* **9**, 1356-1361.

Liljestrom, P., Lusa, S., Huylebroeck, D., and Garoff, H. (1991). *In vitro* mutagenesis of a full-length cDNA clone of Semliki Forest virus: the small 6,000 molecular-weight membrane protein modulates virus release. *J. Virol.* **65**, 4107-4113.

Liljestrom, P., and Garoff, H. (1994). Expression of proteins using Semliki Forest virus vectors, pp. 16.20.11 1-16.20.16. *In*: Current Protocols in Molecular Biology, *vol.* 2 (F.M. Ausubel, R. Brent, R.E. Kingston, D.D. Moore, J.A. Smith, J.G. Seidman and K. Struhl, eds). Greene Publishing Associates and Wiley interscience, New York.

Light, D.B., Corbin, J.D., and Stanton, B.A. (1990). Dual ion-channel regulation by cyclic GMP and cyclic GMP-dependent protein kinase. *Nature* **344**, 336-339.

Livi, G.P., Kmetz, P., McHale, M.M., Cieslinski, L.B., Sathe, G.M., Taylor, D.P., Davis, R.L., Trophy, T.J., and Balcarek, J.M. (1990). Cloning and expression of cDNA for human low-k_m rolipram-sensitive cyclic AMP phosphodiesterase. *Mol. Cell Biol.* **10**, 2678-2686.

Lochhead, A., Nekrasova, E., Arshavsky, V., and Pyne, N.J. (1997). The regulation of the cGMP-binding cGMP phosphodiesterase by proteins that are immunologically related to gamma subunit of the photoreceptor cGMP phosphodiesterase. *J. Biol. Chem.* **272**, 18397-18403.

Londesborough, J. (1985). Evidence that the peripheral cyclic AMP phosphodiesterase of rat liver plasma membranes is a metalloenzyme. *Biochem. J.* **225**, 143-147.

Lugnier, C., Keravis, T., and Eckly-Michel, A. (1999). Cross talk between NO and cyclic nucleotide phosphodiesterases in the modulation of signal transduction in blood vessel. *J. Physiol. Pharmacol.* **50**, 639-652.

Lundstrom, S., Mills, A., Buell, G., Allet, E., Adami, N., and Liljestrom, P. (1994). High-level expression of the human neurokine-1 receptor in mammalian cell lines using the Semliki Forest virus expression system. *J. Biochem.* **224**, 917-921.

Lundstrom, S., Mills, A., Allet E., Ceszkowski, K., Agudo, G., Chollet, A., and Liljestrom, P. (1995). High level of expression of G-protein-coupled receptors with the aid of Semliki Forest virus expression system. *J. Recept. Signal Transduct. Res.* **15**, 23-32.

Lundstrom, K., Vargas, A., and Allet, B. (1995). Functional activity of a biotinylated human neurokine-1 receptor fusion expressed in the Semliki Forest virus system. *Biochem. Biophys. Res. Commun.* **208**, 260-266.

Lundstrom, K., Michel, A., Blasey, H.D., Bernard, A.R., Hovius, R., Vogel, H., and Suprenant, A. (1997). Expression of ligand-gated ion channels with the Semliki Forest virus expression system. *J. Recept. Signal Transduct. Res.* **17**, 115-126.

Lundstrom, K. (1999). Alphavirus as tools in neurobiology and gene therapy. *J. Recept. Signal Transduct. Res.* **19**, 673-686.

Lusa, S., Garoff, H., and Liljestrom, P. (1991). Fate of the 6K membrane protein of Semliki Forest virus during virus assembly. *Virology* **185**, 843-846.

MacKenzie, S.J., Baillie, G.S., McPhee, I., Bolger, G.B., and Houslay, M.D. (2000). ERK2 mitogen-activated protein kinase binding, phosphorylation, and regulation of the PDE4D cAMP-specific phosphodiesterases. The involvement of COOH-terminal docking sites and NH2-terminal UCR regions. *J. Biol. Chem.* **275**, 16609-16617.

MacPhee, C.H., Harrison, S.A., and Beavo, J.A. (1986). Immunological identification of the major platelet low K_m cAMP phosphodiesterase: Probable target for anti-thrombotic agents. *Proc. Natl. Acad. Sci. USA* **83**, 6660-6663.

MacPhee, C.H., Riefsnyder, D.H., Moore, T.A., Lerea, K.M., and Beavo, J.A. (1988). Phosphorylation results in activation of a cAMP phosphodiesterase in human Platelets. *J. Biol. Chem.* **263**, 10353-10358.

Makrides, S.C.(1996). Strategies for achieving high-level expression of genes in *Escherichia coli*. *Microbiol. Rev.* **60**, 512-538.

Malherbe, P., Kratzeisen, C., Lundstrom, K., Richards, J.G., Faull, R.L.M., and Mutel, V. (1999). Cloning and functional expression of alternative spliced variant of human metabotropic glutamate receptor 8. *Mol. Brain Res.* **67**, 201-210.

Manganiello, V.C., Taira, M., Degerman, E. and Belfrage, P. (1995). Type III cGMP-inhibited cyclic nucleotide phosphodiesterases (PDE3 gene family). *Cell Signaling* **7**, 445-455.

Marchmont, R.J., and Houslay, M.D. (1980a). A peripheral and an intrinsic enzyme constitute the cyclic AMP phosphodiesterase activity of rat liver plasma membranes. *Biochem. J.* **187**, 381-392.

Marchmont, R.J., and Houslay, M.D. (1980b). Insulin trigger, cyclic AMP-dependent activation and phosphorylation of a plasma membrane cyclic AMP phosphodiesterase. *Nature* **286**, 904-906.

Marchmont, R.J., Ayad, S.R., and Houslay, M.D. (1981). Purification and properties of the insulin-stimulated cyclic AMP phosphodiesterase from rat liver plasma membranes. *Biochem. J.* **195**, 645-652.

Marsh, M., and Helenius, A. (1989). Virus entry into animal cells. *Adv. Virus Res.* **36**, 107-151.

Marshall, F.H., Patel, K., Lundstrom, K., Camacho, J., Foord, S.M., and Lee, M.G. (1997). Characterization of (3H)-prostaglandin E-2 binding to prostaglandin EP-4 receptors expressed with Semliki Forest virus. *Br. J. Pharmacol.* **121**, 1673-1678.

Marston, F.A.O., Lowe, P.A., Doel, M.T., Schoemaker, S.W., and Angal, S. (1984). Purification of calf prochymosin (prorennin) synthesized in *Escherichia coli*. *Bio/Technolog* **2**, 800-804.

Martins, T.J., Mumby, M.C., and Beavo, J.A. (1982). Purification and characterization of a cyclic GMP-stimulated cyclic nucleotide phosphodiesterase from bovine tissue. *J. Biol. Chem.* **257**, 1973-1979.

McAllister-Lucas, L.M., Haik, T.L., Colbran, J.L., Sonnenburg, W.K., Seger, D., Turko, I.V., Beavo, J.A., Francis, S.H., and Corbin, J.D. (1995). An essential aspartic acid at each of two allosteric cGMP-binding sites of a cGMP-specific phosphodiesterase. *J. Biol. Chem.* **270**, 30671-30679.

McCutchan, J., and Pagano, J.S. (1968). Enhancement of the infectability of simian virus 40 deoxyribonucleic acid with diethylaminoethyl-dextran. *J. Natl. Cancer Inst.* **41**, 351-356.

McLaughlin, M.M., Cieslinski, L.B., Burman, M., Trophy, T.J., and Livi, G.P. (1993). A low-K_m, rolipram-sensitive, cAMP-specific phosphodiesterase from human brain. Cloning and expression of cDNA, biochemical characterization of recombinant protein, and tissue distribution of mRNA. *J. Biol. Chem.* **268**, 6470-6476.

McPhee, I., Yarwood, S.J., Huston, E., Scotland, G., Beard, M.B., Ross, A.H., Houslay, E.S., and Houslay, M.D. (1999). Association with the SRC family tyrosyl kinase LYN triggers a conformational change in the catalytic region of human cAMP-specific phosphodiesterase HSPDE4A4B. Consequences for rolipram inhibition. *J. Biol. Chem.* **274**, 11796-11810.

Meacci, E., Taira, M., Moos, M., Jr., Smith, C.J., Movsesian, M.A., Degerman, E., Belfrage, P., and Manganiello, V.C. (1992). Molecular cloning and expression of human myocardial cGMP-inhibited cAMP phosphodiesterase. *Proc. Natl. Acad. Sci. U.S.A.* **89**, 3721-3725.

Michibata, H., Yanaka, N., Kanoh, Y., Okumura, K., and Omori, K. (2001). Human Ca^{2+}/ calmodulin-dependent phosphodiesterase PDE1A: novel splice variants, their specific expression, genomic organisation, and chromosomal localization. *Biochem. Biophys. Acta.* **1517**, 278-287.

Milatovich, A., Bolger, G., Michaeli, T., and Francke, U. (1994). Chromosome localizations of genes for five cAMP-specific phosphodiesterases in man and mouse. *Som. Cell Mol. Genet.* **20**, 75-86.

Monaco, L., Vicini, E., and Conti, M. (1994). Structure of two rat genes coding for closely related rolipram-sensitive cAMP phosphodiesterases. Multiple mRNA variants originate from alternative splicing and multiple start sites. *J. Biol. Chem.* **269**, 347-357.

Monasyrskaia, K., Goepfert, F., Hochstrasser, R., Acuna, G., Leighton, J., Pink, J.P., and Lundstrom, K. (1999). Expression and intracellular localisation of odorant receptors in mammalian cell lines using Semliki Forest virus vectors. *J. Recept. Signal Transduct Res.* **19**, 687-701.

Moore, J.B., Combs, D.W., and Tobia, A.J. (1991). Bemoradan- A novel inhibitor of the rolipram-insensitive cyclic AMP phosphodiesterase from canine heart tissue. *Biochem. Pharmacol.* **42**, 679-683.

Mou, H., Grazio, H.J. 3d, Cook, T.A., Beavo, J.A., and Cote, R.H. (1999). cGMP binding to noncatalytic sites on mammalian rod photoreceptor phosphodiesterase is regulated by binding of its gamma and delta subunits. *J. Biol. Chem.* **274**, 18813-18820.

Muller, T., Engels, P., and Fozard, J.R. (1996). Subtypes of the type 4 cAMP phosphodiesterases: structure, regulation and selective inhibition. *TIPS* **17**, 294-298.

Murashima, S., Tanaka, T., Hockman, S., and Manganiello, V. (1990). Characterization of particulate cyclic nucleotide phosphodiesterase from bovine brain: Purification of a distinct cGMP-stimulated isoenzyme. *Biochemistry* **29**, 5285-5292.

Murray, K.J. (1992). Methods in Cyclic Nucleotide Research in Neuromethodes (Boulton, A., Baker, G., and Taylor, C. Eds) *vol.* 20, 313-368, The Humana Press inc.

Murray, K.J., and England, P.J. (1992). Inhibitors of cyclic nucleotide phosphodiesterases as therapeutic agents. *Biochem. Soc. Trans.* **20**, 460-464.

Nairn, A.C., Hemmings, H.C., and Greengard, P. (1985). Protein kinases in the brain. *Ann. Rev. Biochem.* **54**, 931-976.

Nicholson, C.D., Challiss, R.A., and Shahid, M. (1991). Differential modulation of tissue function and therapeutic potential of selective inhibitors of cyclic nucleotide phosphodiesterase isoenzymes. *TiPs* **12**, 19-27.

Nicholson, C.D., and Shahid, M. (1994).Inhibitors of cyclic nucleotide phosphodiesterases isoenzymes- their potential utility in the treatment of asthma. *Pulm. Pharm.* **7**, 1-17.

Novack, J.P., Charbonneau, H., Bentley, J.K., Walsh, K.A., and Beavo, J.A. (1991). Sequence comparison of the 63-, 61- and 59-kDa calmodulin dependent cyclic nucleotide phosphodiesterases. *Biochem.* **30**, 7940-7947.

Obernolte, R., Bhakta, S., Alvarez, R., Bach, C., Zuppan, P., Mulkins, M., Jarnagin, K., and Shelton, E.R. (1993). The cDNA of a human lymphocyte cyclic-AMP phosphodiesterase (PDE IV) reveals a multigene family. *Gene* **129**, 239-247.

Omburo, G.A., Brickus, T., Ghazaleh, F.A., and Colman, R.W. (1995). Divalent metal cation requirement and possible classification of cGMP-inhibited phosphodiesterase as a metallohydrolase. *Arch. Biochem. Biophys.* **323**, 1-5.

Omburo, G.A., Jacobitz, S., Torphy, T.J., and Colman, R.W. (1998). Critical role of conserved histidine pairs HNXXH and HDXXH in recombinant human phosphodiesterase 4A. *Cell Signal.* **10**, 491-497.

O'Neil, K.T., and Degrado, W.F. (1985). A predicted structure of calmodulin suggests an electrostatic basis for its function. *Proc. Natl. Acad. Sci. USA* **82**, 5954-5958.

Owens, R.J., Catteral, C., Batty, D., Jappy, J., Russell, A., Smith, B., O'Connel, J., and Perry, M. (1997). Human phosphodiesterase 4A: characterization of full-length and truncated enzymes expressed in COS cells. *Biochem. J.* **326**, 53-60.

Palfreyman, M.N., and Souness, J.E. (1996). Phosphodiesterase type IV inhibitors. *Prog. Med. Chem.* **33,** 1-52.

Patel, M., Harris, C., and Lundstrom, K. (1997). Binding of (1251) AB-MECA to the human cloned adenosine A-3 receptor using the Semliki Forest virus expression system. *Drug Dev. Res.* **40**, 35-40.

Pilla, R., Kytle, K., Reyes, A., and Colicelli, J., (1993). Use of a yeast expression system for the isolation and analysis of drug-resistant mutants of a mammalian phosphodiesterase. *Proc. Natl. Acad. Sci. U.S.A.* **90**, 11970-11974.

Pooley, L., Shakur, Y., Rena, G., and Houslay, M.D. (1997). Intracellular localization of the PDE4A cAMP-specific phosphodiesterase splice variant RD1 (RNPDE4A1A) in stably transfected human thyroid carcinoma FTC cell lines. *Biochem. J.* **321**, 177-185.

Richter, W., Hermsdorf, T., Lilie, H., Egerland, U., Rudolph, R., Kronbach, T., and Dettmer, D. (2000). Refolding, purification, and characterization of human recombinant PDE4A constructs expressed in *Escherichia coli*. *Protein Expression and Purification* **19**. 375-385.

Rocque, W.J., Holmes, W.D., Patel, I.R., Dougherty, R.W., Ittoop, O., Overton, L., Hoffman, C.R., Wisely, G.B., Willard, D.H., and Luther, M.A. (1997). Detailed characterization of a purified type 4 phosphodiesterase, HSPDE4B2B: differentiation of high- and low-affinity (R)-rolipram binding. *Protein Expr. Purif.* **9**, 191-202.

Rosman, G.J., Martins, T.J., Sonnenburg, W.K., Beavo, J.A., Ferguson, K., and Loughney, K. (1997). Isolation and characterization of human cDNAs encoding a cGMP-stimulated 3',5'-cyclic nucleotide phosphodiesterase. *Gene* **191**, 89-95.

Rossi, P., Giorgi, M., Geremia, R., and Kincaid, R.L. (1988). Testis-specific calmodulin-dependent phosphodiesterase. *J. Biol. Chem.* **263**, 15521-15527.

Rybalkin, S.D., and Beavo, J.A. (1996). Multiplicity within cyclic nucleotide phosphodiesterases. *Biochem. Soc. Trans.* **24**, 1005-1009.

Sanes, J.R., Rubenstein, J.L., and Nicolas, J,F. (1986). Use of a recombinant retrovirus to study post-implantation cell lineage in mouse embryos. *EMBO J.* **5**, 3133-3142.

Schein, C.H., and Noteborn, M.H.M. (1988). Formation of soluble recombinant proteins is favoured by lower growth temperature. *BioTechnology* **6**, 291-294.

Schmid S, Fuchs R, Kielian M, Helenius A, and Mellman I. (1989). Acidification of endosome subpopulations in wild-type Chinese hamster ovary cells and temperature-sensitive acidification-defective mutants. *J Cell Biol.* **108**,1291-1300.

Schramm, M., and Selinger, Z. (1984). Message transmission: receptor controlled adenylate cyclase system. *Science* **225**, 1350-1356.

Scotland, G., and Houslay, M.D. (1995). Chimeric constructs show that the unique N-terminal domain of the cyclic AMP phosphodiesterase RD1 (RNPDE4A1A; rPDE-IVA1) can confer membrane association upon the normally cytosolic protein chloramphenicol acetyltransferase. *Biochem. J.* **308**, 673-681.

Seeholzer,S.H., Cohn, M., Putkey, J.A., Means, A.R., and Crespi, H.L. (1986). NMR studies of a complex of deuterated calmodulin with melittin. *Proc. Natl. Acad. Sci USA* **83**, 3634-3638.

Sette, C., Iona, S., and Conti, M. (1994a). The short-term activation of a rolipram-sensitive, cAMP-specific phosphodiesterase by thyroid-stimulating hormone in thyroid FRTL-5 cells is mediated by a cAMP-dependent phosphorylation. *J. Biol. Chem.* **269**, 9245-9252.

Sette, C., Vicini, E., and Conti, M. (1994b). The rat PDE3/IVd phosphodiesterase gene codes for multiple proteins differentially activated by cAMP-dependent protein kinase. *J. Biol. Chem.* **269**, 18271-18274.

Sette, C., and Conti, M. (1996). Phosphorylation and activation of a cAMP-specific phosphodiesterase by the cAMP-dependent protein kinase. Involvement of serine 54 in the enzyme activation. *J. Biol. Chem.* **271**, 16526-16534.

Shabb, J.B., and Corbin, J.D. (1992). Cyclic nucleotide-binding domains in proteins having diverse functions. *J. Biol. Chem.* **267**, 5723-5726.

Shahid, M., Van Amsterdam, R.G.M., De Boer, J., Ten Berge, R.E., Nicholson, C.D., and Zaagsma, J. (1991). The presence of five nucleotide phosphodiesterase isoenzyme activity in bovine tracheal smooth muscle and the functional effects of selective inhibitors. *Br. J. Pharamacol.* **104**, 471-477.

Shakur, Y., Pryde, J.G., and Houslay, M.D. (1993). Engineered deletion of the unique N-terminal domain of the cyclic AMP-specific phosphodiesterase RD1 prevents plasma membrane association and the attainment of enhanced thermostability without altering its sensitivity to inhibition by rolipram. *Biochem. J.* **292**, 677-686.

Shakur, Y., Wilson, M., Pooley, L., Lobban, M., Griffiths, S.L., Campbell, A.M., Beattie, J., Daly, C., and Houslay, M.D. (1995). Identification and characterization of the type-IVA cyclic AMP-specific phosphodiesterase RD1 as a membrane-bound protein expressed in cerebellum. *Biochem. J.* **306**, 801-809.

Shakur, Y., Takeda, K., Kenan, Y., Yu, Z.-X., Rena, G., Brandt, D., Houslay, M.D., Degerman, E., Ferrans, V.J., and Mangeniello, V.C. (2000). Membrane localization of cyclic nucleotide phosphodiesterase 3 (PDE3). Two N-terminal domains are required for the efficient targeting to, and association of, PDE3 with endoplasmic reticulum. *J. Biol. Chem.* **275**, 38749-38761.

Sharma, R.K., Wang, T.H., Wirch, E., and Wang, J.H. (1980). Purification and properties of bovine brain calmodulin-dependent cyclic nucleotide phosphodiesterase. *J. Biol. Chem.* **255**, 5916-5923.

Sharma, R.K., Adachi, A.M., Adachi, K., and Wang, J.H. (1984). Demonstration of bovine brain calmodulin-dependent cyclic nucleotide phosphodiesterase isoenzyme by monoclonal antibodies. *J. Biol. Chem.* **259**, 9248-9254.

Sharma, R.K., and Wang, J.H. (1986). Calmodulin and Ca^{2+}-dependent phosphorylation and dephosphorylation of 63-kDa subunit-containing bovine brain calmodulin stimulated cyclic nucleotide phosphodiesterase isoenzyme. *J. Biol. Chem.* **261**, 1322-1328.

Sheer, A., Bjorklof, K., Cotecchia, S., and Lundstrom, K. (1999). Co-expression of the α1B-adrenergic receptor and G protein subunit in mammalian cell lines using Semliki Forest virus expression system. *J. Recept. Signal Transduct. Res.* **19**, 369-378.

Sheth, S.B., and Colman, R.W. (1995). Platelet cAMP and cGMP Phosphodiesterases. *Platelets* **6**, 61-70.

Slep, K.C., Kercher, M.A., He, W., Cowan, C.W., Wensel, T.G., and Sigler, P.B. (2001). Structural determination for regulation of phosphodiesterase by a G protein at 2.0 Å. *Nature* **409**, 1071-1077.

Smith, D.B., and Johnson, K.S. (1988). Single step purification of polypeptides expressed in *E.coli* as fusions with glutathione S-transferase. *Gene* **67**, 31-40.

Smith, K.J., Scotland, G., Beattie, J., Trayer, I.P., and Houslay, M.D. (1996). Determination of the structure of the N-terminal splice region of the cyclic AMP-specific phosphodiesterase RD1 (RNPDE4A1) by 1H NMR and identification of the membrane association domain using chimeric constructs. *J. Biol. Chem.* **271**, 16703-16711.

Soderling, S.H., Bayuga, S.J., and Beavo, J.A. (1999). Isolation and characterization of a dual-substrate phosphodiesterase gene family: PDE10A. *Proc. Natl. Acad. Sci. USA* **96**, 7071-7076.

Soderling, S.H., and Beavo, J.A. (2000). Regulation of cAMP and cGMP signaling: new phosphodiesterases and new functions. *Curr. Opin. Cell. Biol.* **12**, 174-179.

Sonnenburg, W.K., and Beavo, JA. (1994). Cyclic GMP and regulation of cyclic nucleotide hydrolysis. *Adv. Pharmacol.* **26**, 87-114.

Sonnenburg, W.K., Mullaney, P.J., and Beavo, J.A. (1991). Molecular cloning of a cyclic GMP-stimulated cyclic nucleotide phosphodiesterase cDNA. Identification and distribution of isozyme variants. *J. Biol. Chem.* **266**, 17655-17661.

Sonnenburg, W.K., Seger, D., Kwak, K.S., Huang, J., Charbonneau, H., and Beavo, J.A. (1995). Identification of inhibitory and calmodulin-binding domains of the phosphodiesterase1A1 and phosphodiesteraseA2 calmodulin-stimulated cyclic phosphodiesterases. *J. Biol. Chem.* **270**, 30989-31000.

Sonnenburg, W.K., Rybalkin, S.D., Bornfeldt, K.E., Kwak, K.S., Rybalkina, I.G., and Beavo, J.A. (1998). Identification, quantitation, and cellular localization of PDE1 calmodulin-stimulated cyclic nucleotide phosphodiesterases. *Methods* **14**, 3-19.

Souness, J.E., Maslen, C., and Scott, L.C. (1992). Effects of solubilization and vanadate/glutathione complex on inhibitor potencies against eosinophil cyclic AMP-specific phosphodiesterase. *FEBS Lett.* **302**, 181-184.

Spence, S., Rena, G., Sweeney, G., and Houslay, M.D. (1995). Induction of Ca^{2+}/calmodulin-stimulated cyclic AMP phosphodiesterase (PDE1) activity in Chinese hamster ovary cells (CHO) by phorbol 12-myristate 13-acetate and by the selective overexpression of protein kinase C isoforms. *Biochem. J.* **310**, 975-982.

Stables, J., Rees, S., Lundstrom, K., Livingstone, D., and Lee, M.G. (1997). High level expression of the human 5-$HT_{1D\alpha}$ receptor using the Semliki Forest virus expression system. *Ann. NY. Acad. Sci.* **812**, 229-230.

Stryer, L. (1991). Visual excitation and recovery. *J. Biol. Chem.* **266**,10711-10714.

Sullivan, M., Rena, G., Begg, F., Gordon, L., Olsen, A.S., and Houslay, M.D. (1998). Identification and characterization of the human homologue of the short PDE4A cAMP-specific phosphodiesterase RD1 (PDE4A1) by analysis of the human HSPDE4A gene locus located at chromosome 19p13.2. *Biochem. J.* **333**, 693-703.

Sullivan, M., Olsen, A.S., and Houslay, M.D. (1999). Genomic organisation of the human cyclic AMP-specific phosphodiesterase PDE4C gene and its chromosomal localisation to 19p13.1, between RAB3A and JUND. *Cell. Signal.* **11**, 735-742.

Sutherland, E.W., and Rall, T.W. (1958). Fractionation and characterization of a cyclic adenosine nucleotide formed by tissue particles. *J. Bio. Chem.* **232**, 1077-1091.

Sutherland, E.W., Rall, T.W., and Menon, T. (1962). Adenyl cyclase. I. Distribution, preparation, and properties. *J. Biol. Chem.* **237**, 1220-1227.

Swinnen, J.V., Joseph, D.R., and Conti, M. (1989b). The mRNA encoding a high-affinity cAMP phosphodiesterase is regulated by hormones and cAMP. *Proc. Natl. Acad. Sci. USA* **86**, 8197-8201.

Swinnen, J.V., Joseph, D.R., and Conti, M. (1989a). Molecular cloning of rat homologues of the *Drosophila melanogaster* dunce cAMP phosphodiesterase: Evidence for a family of genes. *Proc. Natl. Acad. Sci. USA* **86**, 5325-5329.

Swinnen, J.V., D'Souza, B., Conti, M., and Ascoli, M. (1991). Properties and hormonal regulation of two structurally related cAMP phosphodiesterases from the rat sertoli cell. *J. Biol. Chem.* **266**, 14383-14389.

Szpirer, C., Szpirer, J., Riviere, M., Swinnen, J., Vicini, E., and Conti, M. (1995). Chromosomal localization of the human and rat genes (PDE4D and PDE4B) encoding the cAMP-specific phosphodiesterases 3 and 4. *Cytogenet. Cell Genet.* **69**, 11-14.

Taira, M., Hockman, S., Calvo, J., Taira, M., Belfrage, P., and Manganiello, V.C. (1993). Molecular cloning of the rat adipocyte hormone-sensitive cyclic GMP-inhibited cyclic nucleotide phosphodiesterase. *J. Biol. Chem.* **268**, 18573-18579.

Takemoto, D.J., and Cunnick, J.M. (1990). Visual transduction in rod outer segment. *Cell Signaling* **2**, 99-104.

Tenor, H., Bartel, S., and Krause, E. (1987). Cyclic nucleotide phosphodiesterase activity in the rat myocardium: evidence of four different phosphodiesterase subtypes. *Biomed. Biochem. Acta* **10**, S749-S753.

Thomas, M.K., Francis, S.H., and Corbin, J.D. (1990a). Substrate- and kinase-directed regulation of phosphorylation of a cGMP-binding phosphodiesterase by cGMP. *J. Biol. Chem.* **265**, 14971-14978.

Thomas, M.K., Francis, S.H., and Corbin, J.D. (1990b). Characterization of a purified bovine lung cGMP-binding cGMP phosphodiesterase. *J. Biol. Chem.* **265**, 14964-14970.

Thomas, M.K., Francis, S.H., Beebe, S.J., Gettys, T.W., and Corbin, J.D. (1992). Partial mapping of cyclic nucleotide sites and studies of regulatory mechanisms of phosphodiesterases using cyclic nucleotide analogues. *Adv. Second Messenger Phosphoprotein Res.* **25**, 45-53.

Thompson, W.J., and Appleman, M.M. (1971). Multiple cyclic nucleotide phosphodiesterase activities from rat brain. *Biochem.* **10**, 311-316.

Thompson, W.J., Epstein, P.M., and Strada, S.J. (1979). Purification and characterization of high-affinity cyclic adenosine monophosphate phosphodiesterase from dog kidney. *Biochem.* **18**, 5228-5237.

Thompson, W.J., Shen, C.C., and Strada, S.J. (1988). Preparation of dog kidney high-affinity cAMP phosphodiesterase. *Methods Enzymol.* **159**, 760-766.

Torphy, T.J., and Cieslinski, L.B. (1990). Characterization and selective inhibition of cyclic nucleotide phosphodiesterase isoenzymes in canine smooth muscle. *Mol. Pharmacol.* **37**, 206-214.

Torphy, T.J., and Undem, B.J. (1991). Phosphodiesterase inhibitors: new opportunities for the treatment of ashma. *Thorax* **46**, 512-523.

Torphy, T.J., Barnett, M.S., Hay, D.W.P., and Underwood, D.C. (1994). Phosphodiesterase IV inhibitors as therapy for eosinophil-induced lung injury in asthma. *Environ. Health Prespectives* **102**, 79-84.

Trembley, J., Lachance, B., and Hamet, P. (1985). Activation of cGMP-binding and cAMP-specific phosphodiesterase of rat Platelets by a mechanism involving cAMP-dependent phosphorylation. *J. Cyclic Nucleotide Protein Phosphorylation Res.* **10**, 397-411.

Trong, H.L., Beier, N., Sonnenburg, W.K., Stroop, S.D., Walsh, K.A., Beavo, J.A., and Charbonneau, H. (1990). Amino acid sequence of the cyclic GMP stimulated cyclic nucleotide phosphodiesterase from bovine heart. *Biochem.* **29**, 10280-10288.

Ulmanen, I., Peranen, J., Tenhunen, J., Tilgmann, C., Karhunen, T., Panula, P., Bernasconi, L., Aubry, J.P. and Lundstrom, K. (1997). Expression and intracellular localization of catechol-o-methyltransferase in transfected mammalian cells. *Eur. J. Biochem.* **243**, 452-459.

Wachtel, H. (1983). Potential antidepressant activity of rolipram and other selective cyclic adenosine 3', 5'-monophosphate phosphodiesterase inhibitors. *Neuropharmacol.* **22**, 267-272.

Wang, J.H., Sharma, R.K., and Mooiborek, M.J. (1990). Calmodulin-stimulated Cyclic Nucleotide Phosphodiestaerse. *Cyclic nucleotide Phosphodiesterase: Structure, Function and Drug Action* (Beavo, J.A. and Houslay, M.D., eds) pp. 19-60, John Wiley and Sons Ltd., Chichester and New York.

Wang, P., Myers, J.G., Wu, P., Cheewatrakoolpong, B., Egan, R.W., and Billah, M.M. (1997). Expression, purification, and characterization of human cAMP-specific phosphodiesterase (PDE4) subtypes A, B, C, and D. *Biochem. Bioph. Research Comm.* **234**, 320-324.

Warburg, O., and Christian, W. (1941). Isolierung und Kristallisation des Garungsferments Enolase. *Biochem. Z.* **310**, 384-421.

Weishaar, R.E., Kobylarz-Singer, D.C., Quade, M.M., Steffen, R.P., and Kaplan, H.R. (1987). Multiple molecular forms of phosphodiesterase and the regulation of cardiac muscle contractility. *J. Nucleotide Protein Phosphorylation Res.* **11**, 513-527.

Werner, P., Kawashima, E., Reid, J., Hussy, N., Lundstrom, K., Buell, G., Humbert, Y., and Jones, K.A. (1994). Organisation of the mouse 5-HT3 receptor gene and functional expression of two splice variants. *Brain Res. Mol. Brain. Res.* **26**, 233-241.

Wilson, M., Sullivan, M., Brown, N., and Houslay, M.D. (1994). Purification, characterization and analysis of rolipram inhibition of a human type-IVA cyclic AMP-specific phosphodiesterase expressed in yeast. *Biochem. J.* **304**, 407-415.

Wurm, F., and Bernard, A.R. (1999) Large-scale transient expression in mammalian cells for recombinant protein production. *Curr. Opin. Biotechnol.* **10**,156-159.

Wyatt, T.A., Naftilan, A.J., Francis, S.H., and Corbin, J.D. (1998). ANF elicits phosphorylation of the cGMP phosphodiesterase in vascular smooth muscle cells. *Am. J. Physiol.* **274**, H448-H455.

Xu, R.X., Hassell, A.M., Vanderwall, D., Lambert, M.H., Holmes, W.D., Luther, M.A., Rocque, W.J., Milburn, M.V., Zhao, Y., Ke, H., and Nolte, R.T. (2000). Atomic structure of PDE4: insights into phosphodiesterase mechanism and specificity. *Science* **288**, 1822-1825.

Yamamoto, T., Yamamoto, S., Osborne, J., Manganiello, V.C., Vaughan, M., and Hidaka, H. (1983). Complex effects of inhibitors on cyclic GMP-stimulated cyclic nucleotide phosphodiesterase. *J. Biol. Chem.* **258**, 14173-14177.

Yamamoto, T., Lieberman, F., Osborne, J.C., Manganiello, V.C., Vaughan, M., and Hidaka, H. (1984). Selective inhibition of two soluble adenosine cyclic 3', 5'-phosphate phosphodiesterases partially purified from calf liver. *Biochem.* **23**, 670-675.

Yan, C., Zhao, A.Z., Bentley, J.K., and Beavo, J.A. (1996). The calmodulin-dependent phosphodiesterase gene PDE1C encodes several functionally different splice variants in a tissue-specific manner. *J Biol. Chem.* **271**, 25699-25706.

Yarfitz, S., and Hurley, J.B. (1994). Transduction mechanisms of vertebrate and invertebrate photoreceptors. *J. Biol. Chem.* **269**, 14329-14332.

Yarwood, S.J., Steele, M.R., Scotland, G., Houslay, M.D., and Bolger, G.B. (1999). The RACK1 signalling scaffold protein selectively interacts with the cAMP-specific phosphodiesterase PDE4D5 isoform. *J. Biol. Chem.* **274**, 14909-14917.

Yuasa, K., Kotera, J., Fujishige, K., Michibata, H., Sasaki, T., and Omori, K. (2000). Isolation and Characterization of Two Novel Phosphodiesterase PDE11A Variants Showing Unique Structure and Tissue-Specific Expression. *J. Biol. Chem.* **275**, 31469-31479.

Zhang, W., and Colman, R.W. (2000). Conserved amino acids in metal-binding motifs of PDE3A are involved in substrate and inhibitor binding. *Blood* **95**, 3380-3386.